New Perspectives on Functional Assessment in Musculoskeletal Research and Orthopedic Surgery

Sjoerd Kolk

ISBN
978-94-6295-862-3

Cover
Stefanie van den Herik

Design & Lay-out
Sjoerd Kolk

Printed by
ProefschriftMaken

The work presented in this thesis was carried out within the Radboud Institute for Health Sciences.

New Perspectives on Functional Assessment in Musculoskeletal Research and Orthopedic Surgery

Proefschrift

ter verkrijging van de graad van doctor
aan de Radboud Universiteit Nijmegen
op gezag van de rector magnificus prof. dr. J.H.J.M. van Krieken,
volgens besluit van het college van decanen
in het openbaar te verdedigen op

dinsdag 10 april 2018,

om 14:30 uur precies

door

Sjoerd Kolk

geboren op 23 oktober 1985

te Enschede

Promotoren
Prof. dr. ir. N. Verdonschot
Prof. dr. A.C.H. Geurts

Copromotor
Dr. V. Weerdesteyn

Manuscriptcommissie
Prof. dr. M. Gotthardt
Prof. dr. T. Scheerlinck *(Vrije Universiteit Brussel, België)*
Prof. dr. ir. J. Harlaar *(Technische Universiteit Delft)*

Contents

Chapter 1

General Introduction and Outline

Motivation

The musculoskeletal system is essential for human movement. It is very versatile, allowing most people to walk, run, or dance seemingly effortlessly. These and other activities of daily living that most of us take for granted can be much more difficult to perform when disease compromises the functioning of the musculoskeletal system. The ability to perform more basic but very common activities of daily living such as walking, negotiating stairs, and getting up from a seated position in a pain-free manner, is important for many aspects of life, including general mobility, societal participation, and ultimately, quality of life. Indeed, besides pain, a reduced ability to move around independently is one of the most important reasons for patients to undergo orthopedic surgery (Wright et al. 1994). The work in this thesis focuses on walking and other related activities of daily living that are primarily performed by the lower limbs in different types of patients, spanning a range of diseases, levels of severity, and associated surgical interventions. From least severe to most severe, these include primary osteoarthritis of the hip, secondary osteoarthritis due to hip dysplasia, and sarcoma (a malignant tumor) in the lower limb. Patients suffering from any of these diseases present their own specific problems and have their own specific treatment options, which include conservative treatment and surgical interventions. Conservative treatment consists of, for example, pain medication and lifestyle advice to alleviate the symptoms as much as possible. However, when these treatment options are exhausted or undesired, surgical interventions to treat the disease are considered a more viable alternative. These interventions vary in their degree of effectiveness and complexity. One of the most ubiquitous is total hip arthroplasty (Charnley 1961). Although this operation is widely used and generally very successful at relieving pain and restoring mobility (Learmonth et al. 2007), it is not completely clear to what degree the operation restores normal biomechanics during activities of daily living. This unclarity about the restoration of normal biomechanics is also true in the case of triple innominate osteotomy (Steel 1973), which is a more extensive surgical intervention to treat secondary osteoarthritis of the hip due to dysplasia. An even more extensive surgical intervention with a far less firmly established functional outcome is limb salvage surgery for osteosarcoma and soft-tissue sarcoma (Veth et al. 1995). Since each tumor is unique, each patient likewise represents a unique challenge for the orthopedic oncologist. Predicting the functional outcome of patients suffering from sarcoma is part of the decision-making process between lower limb amputation and limb salvage surgery, and is also important for informing the patient at the pre-operative stage.

Musculoskeletal models and their validation

To study, to predict, and to eventually improve the outcomes of orthopedic interventions, musculoskeletal models are a useful tool (e.g., Delp et al. 1994b; Fluit 2015; Hicks et al. 2007). Musculoskeletal models have the potential to aid in clinical decision making in several ways. These include, for example, predicting the effects of tendon transfers (Piazza et al. 2003; Reinbolt et al. 2009), joint replacement (Delp et al. 1994a; Piazza et al. 2001), and to predict patterns of bone-implant micromotions (van der Ploeg et al. 2012), which may cause aseptic loosening in primary joint replacements (Ulrich et al. 2008). Traditionally, musculoskeletal models are constructed based on anatomical measurements stemming

from one (Carbone et al. 2015; Klein Horsman et al. 2007) or several (Duda et al. 1996; White et al. 1989) cadaver specimens. This is commonly called a generic model, which is simply scaled linearly to represent a subject based on anthropometric measurements, such as body length and weight. This way of working does not take into account the variability that is present in musculoskeletal geometry (Duda et al. 1996; White et al. 1989), which is particularly relevant when studying complex biomechanical problems. Therefore, subject-specific models, for example based on extensive medical imaging data, are necessary to form an accurate representation of each subject's anatomy (Lenaerts et al. 2009; Scheys et al. 2008; Taddei et al. 2012). Since a trend towards increased use of subject-specific models appears to be going on, the need increases to validate their subject-specific predictions (Lund et al. 2012). Some of the most critical predictions that need to be validated from the models are the muscle forces, since these ultimately dictate a given movement of the subject and the resulting loads on the joints. However, measuring muscle forces in vivo is not easy to do, since invasive measurements would need to be performed. Indirect measurements such as electromyography are a more viable alternative, but this technique has many inherent limitations, including the limited number of muscles that can be measured simultaneously, the inability to measure deep-lying muscles, and the fact that muscle activity from only a small area of a muscle can be measured. A more comprehensive validation technique is, therefore, highly desirable. Especially if musculoskeletal models are ever to be used on a broader scale, for example in assisting surgical planning in a clinical setting rather than in a research setting, the need to expand our knowledge of the construction of these models and the need for their validation is clear. This was recognized and made one of the primary focus points in the TLEMsafe project.

The TLEMsafe project

The work presented in this thesis was part of a large international research project called TLEMsafe ('Twente Lower Extremity Model' to be used for 'safe' surgery). This project aimed to research and improve the functional outcome of complex orthopedic surgical interventions by using state-of-the-art musculoskeletal models. The workflow of the project is shown schematically in Figure 1.1. The conceptual idea is that a highly personalized musculoskeletal model should be able to predict whether a patient would, for instance, be able to walk after an extensive orthopedic intervention on the lower limb. The original TLEM model, consisting of a full anatomical dataset of the lower limb based on a single cadaver specimen, was used as a starting point in the project (Klein Horsman et al. 2007). The generic TLEM was made subject-specific for each participating patient and healthy subject in the TLEMsafe project, based on anatomical data extracted from an MRI scan and functional measurements. The MRI scan was made at the Radboud University Medical Center, using a protocol that was specifically designed to allow for the easiest distinction of muscle boundaries (Scheys 2009). From the MRI scan, muscle volumes, bone geometries, joint rotation centers, and muscle attachment points were extracted by Materialise using Mimics (Materialise N.V., Leuven, Belgium). These subject-specific anatomical data were used by the University of Twente and AnyBody to create subject-specific musculoskeletal models in the AnyBody Modeling System (AnyBody A/S, Aalborg, Denmark). As input to the inverse-dynamics-based models, motion capture data and measurements of lower limb

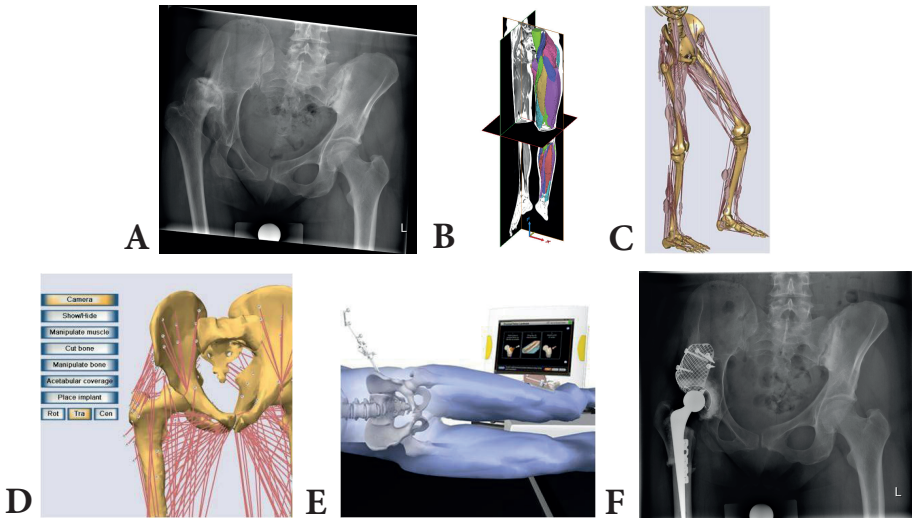

Figure 1.1. The workflow of the TLEMsafe project for a patient suffering from hip dysplasia with high luxation. A) Pre-operative data are collected, including an MRI scan, motion-capture and strength tests. B) Patient-specific data (bone shapes, joint locations, muscle volumes and muscle attachment sites) are extracted semi-automatically from the MRI scan. C) A musculo-skeletal model is built specifically for this patient. D) The functional effects of several operative plans are predicted using the model. E) The most optimal surgical plan is executed as planned with the help of a navigation system. F) The optimal reconstruction has decreased the risk of complications and yielded an optimal functional outcome.

strength were essential. These were collected at the Radboud University Medical Center, and a large part of them form the basis of the work presented in this thesis. Using a surgical pre-planning interface developed by the Warsaw University of Technology, participating surgeons were able to pre-plan several surgical scenarios (e.g., different bone resections, muscle transfers, surgical approaches) in the musculoskeletal models, and to choose the most optimal one in terms of functional outcome. The functional effects of each scenario were predicted by new musculoskeletal modeling algorithms, developed at the University of Twente (Fluit 2015). If desired by the surgeon, the pre-planned optimal surgical scenario could be loaded into a navigation system provided by Brainlab (Brainlab A/G, Munich, Germany) to allow for executing the surgery exactly as it was planned. This thesis is part of the TLEMsafe project and focuses on step A (Figure 1.1), collecting data of healthy subjects and patients as input for the construction of musculoskeletal models and their validation, and step F (Figure 1.1), measuring the functional outcome of interventions in an objective way.

The rest of this introductory chapter first describes the knowledge gaps of the functional outcome of contemporary surgical treatment for several diseases of the musculoskeletal system (osteoarthritis of the hip, hip dysplasia, and sarcoma in the lower limb). These three diseases were chosen because they each represent specific levels of anatomical complexity, expected functional outcome, and differ in the expected subject specificity required from

musculoskeletal models to model the functional outcome of their associated surgical interventions. This was intended to lead to more knowledge about which biomechanical aspects, and which aspects of functional outcome the project needed to focus on in terms of musculoskeletal validation. After introducing the diseases, this chapter introduces a new measurement technique for assessing muscle activity in the entire lower limb during walking. Besides providing the opportunity to obtain valuable insight on a fundamental level into the functioning of the musculoskeletal system, this technique could be used to validate musculoskeletal models in a pre-operative assessment of a patient who is a candidate for orthopedic surgery, or in quantifying and specifying the functional effects of orthopedic interventions in more detail.

Total hip arthroplasty for osteoarthritis

Osteoarthritis of the hip is a leading cause of disability. It is a more frequent cause of activity limitation than heart disease, cancer, or diabetes, is the second most frequently reported chronic condition, and the third leading cause of work limitation (Orthoworld Annual Report 2014). This disease is often treated by total hip arthroplasty (Figure 1.2). Almost 21.000 total hip arthroplasties are performed each year in the Netherlands (Otten et al. 2010); with the number of surgeries still increasing worldwide. From 2000 to 2009, it grew by 73% (123% for patients aged 45 to 64 years, 54% for ages 65 to 84 years) (Orthoworld Annual Report 2014). This indicates that the patients who undergo total hip arthroplasty are becoming younger at the time of surgery. This is partly due to the increased longevity of the implants, which allows the operation to take place at a younger age. Younger patients are generally more active than older patients, which infers that the demands that the total hip arthroplasty patient population places on the functional outcome of this intervention are higher than ever before. Fortunately, total hip arthroplasty is one of the most successful medical interventions in the world, and has even been called 'The operation of the century'

Figure 1.2. In total hip replacement, the proximal femur and the acetabulum are replaced by artificial parts. This typically relieves pain and restores range of motion, thereby increasing the quality of life of the patient.

(Learmonth et al. 2007). The modern inception of the total hip arthroplasty has been performed since it was introduced by Sir John Charnley in the early 1960s (Charnley 1961). Since then, several improvements have been made in the design of the implants, such as improved materials for the cup liner and surface coatings for uncemented implants; and the surgical technique, such as minimally invasive approaches. Although the clinical results of total hip arthroplasty (such as relief of pain and restoration of range of movement), and radiographic placement have been researched in excruciating detail, most of this research has been performed using clinical scoring systems such as the Merle d'Aubigné and Postel score (D'Aubigne et al. 1954) and the Harris hip score (Harris 1969). Such scoring systems provide a convenient way of assessing the functional outcome, but they are inherently subjective, and do not include objective measurements of human functioning. As complementary tools to the scoring systems, quantitative measurement techniques such as gait analysis can be used to provide additional insight into the patient's level of functioning after the operation (Lindemann et al. 2006; Nantel et al. 2009; Rosler et al. 2000). 'Gait analysis' is a term that encompasses any combination of the analysis of spatiotemporal, kinematic, and kinetic parameters. Spatiotemporal parameters include aspects such as walking speed, stride length, step length, and single and double support time (Perry et al. 2010). Kinematic parameters describe the motion of the body segments during the gait cycle, e.g., the frontal hip joint angle and the sagittal knee joint angle. Kinetic parameters are the forces, moments, and powers that are involved in the gait cycle. Although by 'gait analysis' authors commonly mean the analysis of walking (i.e. the gait cycle), the same analysis methodology can also be applied to other related activities of daily living such as stair negotiation and stepping over an obstacle. Regardless of the movement, this type of quantitative research into the functional outcome of total hip arthroplasty has been relatively scarce, and several discrepant findings have been reported in the literature. Although authors have attempted to summarize the published literature on walking (Ewen et al. 2012; Sinha et al. 2011), an extensive overview that also includes other functional movements (e.g., stair negotiation, stepping over an obstacle), takes into account factors such as differences in walking speed between study groups, and comparisons between the operated and the non-operated limb, has thus far been lacking.

Triple innominate osteotomy and total hip arthroplasty for hip dysplasia

Hip dysplasia is congenital or developmental in nature. The disease is characterized by a shallow, obliquely-oriented acetabulum and a malposition of the proximal femur (Figure 1.3). When such a joint is loaded, as is the case during activities of daily living, an increased rate of wear is experienced due to the relatively small weight-bearing area that has to carry the same body weight as any other healthy person (Hsin et al. 1996). As the disease progresses, the pain that the wear causes can severely limit patients in their daily activities. To address these problems, orthopedic surgeons have several options. In some patients, conservative treatment with pain medication and lifestyle advice is warranted, whereas in others with more advanced stages of the disease (including luxation of the hip), a total hip arthroplasty with femoral shortening may be the best option. In these most severely affected patients, the objectives of the surgery are to relieve pain, and to reduce as much as possible the biomechanical problems associated with the disease. These include restoring the limb

length discrepancy, the hip joint's center of rotation and range of motion, and the force generating capacity of mainly the abductor muscles (Lai et al. 2001; Marangoz et al. 2010). Reports on the gait characteristics and post-operative muscle strength of these patients have been scarce, and most studies reported only spatiotemporal or kinematic gait parameters (Kyriazis et al. 2002; Marangoz et al. 2010).

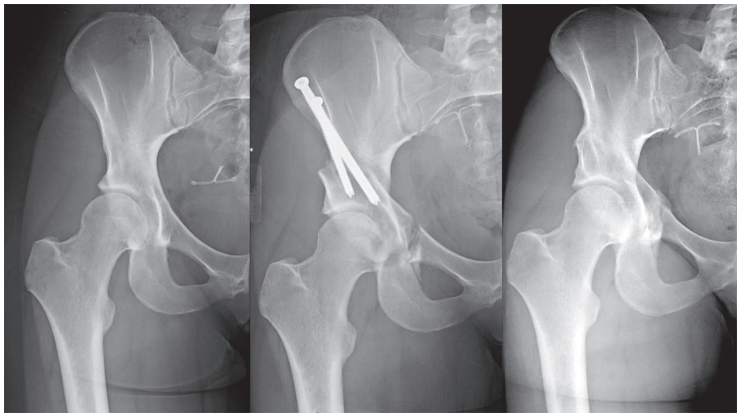

Figure 1.3. *Left:* X-ray of a dysplastic hip, showing insufficient coverage. *Middle:* Post-operative X-ray of a triple innominate osteotomy. The area around the acetabulum has been osteotomized in three locations, allowing its rotation in the coronal plane, and improving the coverage over the femoral head. *Right:* X-ray of a successful triple osteotomy. The acetabulum provides enough coverage to relieve pain and this allows the patient to return to daily activities.

Additionally, there are also patients who suffer from too much pain for conservative treatment, but who are too young for a total hip arthroplasty and who show no or low-grade osteoarthritis (de Kleuver et al. 1997; Janssen et al. 2009). For those patients, triple innominate osteotomy is a surgical procedure that can offer a solution (Steel 1973; Tonnis et al. 1981). The aim of this type of surgery is to improve the acetabular coverage over the femoral head (Figure 1.3). The improved coverage spreads the forces of the body's weight over a larger surface area, thereby reducing the local pressure, pain, and further joint degeneration. In spite of these seemingly great advantages, functional outcome is also an important factor to take into account when evaluating the results of the surgery, since the patients are generally young adults who enjoy an active lifestyle. Similarly to functional analyses in total hip arthroplasty, functional outcome of triple innominate osteotomy is most commonly measured with clinical scoring systems. Whereas clinical results of this operation are generally reported as 'good', 'excellent', or 'improved compared to before the operation' (de Kleuver et al. 1997; Hsin et al. 1996; Janssen et al. 2009), studies that use complimentary quantitative measurements such as gait analysis and measurements of residual muscle strength after the operation, are lacking. Since several treatment options exist for the group of patients eligible for triple innominate osteotomy, studies into the functional outcome of the operation would allow comparing it quantitatively to the outcome of other treatment options.

Limb salvage surgery for sarcoma in the lower limb

Osteosarcoma and soft-tissue sarcoma are malignant tumors that occur most frequently in the lower limb (Figure 1.4). When these occur, (large) segments of bone and soft tissue need to be surgically removed to prevent the cancerous cells from spreading to other parts of the body. Amputation was often the only viable option until the 1980s, when limb salvage surgery came into more frequent use, combined with vastly improved staging techniques, chemotherapy, and reconstructive prostheses (Veth et al. 2003). Nowadays, the vast majority of patients (70-85%) that suffer from sarcoma can be treated with limb salvage surgery (Veth et al. 2003). The decision on whether to amputate or perform limb salvage surgery is based on several factors, such as tumor size, location, and the anticipated level of functional outcome (Robert et al. 2010). The expected functional outcome is, thus, an important aspect that is taken into consideration in the pre-operative decision making process. The importance of functional outcome is further highlighted by its strong relation to quality of life after the operation (Robert et al. 2010). However, it is not known how well surgeons are able to predict the functional outcome of limb salvage surgery. If they are not able to predict the functional outcome of limb salvage surgery, there may be a need for the development of tools (e.g., patient-specific musculoskeletal models) that can help the surgeon in his/her decision making process before the surgery. For instance, a personalized musculoskeletal model may be able to predict whether enough muscle strength will remain for the patient to be able to extend the leg and stand on it, or to estimate whether a patient can walk or not after the operation (Fluit 2015).

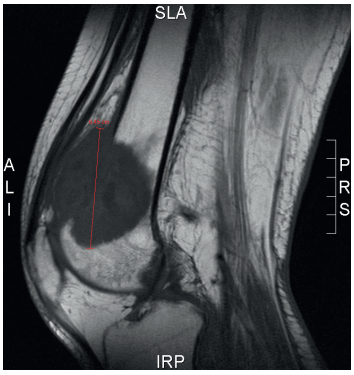

Figure 1.4. MRI scan of a patient with osteosarcoma in the distal femur region (dark area).

Positron emission tomography

Positron emission tomography (PET) is an imaging technique with which the location of a tracer molecule in the body can be detected (Cherry et al. 2012) (Figure 1.5). The most commonly used PET tracer, and the one used in the work reported in this thesis, is the fluorinated analogue of glucose, [^{18}F]-fluorodeoxyglucose (FDG). In this molecule, one of

the OH groups has been replaced by [^{18}F]Fluorine. The chemical alteration does not affect the molecule's ability to enter cells in the same way as regular glucose, but it does prevent the completion of its metabolic pathway. After phosphorylation, FDG-6-phosphate does not undergo glycolysis, and becomes trapped in the intracellular space (Shimada et al. 2009). This trapping property, combined with [^{18}F]'s relatively long half-life of 110 minutes, makes it an ideal tracer to measure cumulative activity in the region of interest using PET. The FDG-PET technique has many clinical applications, such as mapping metabolically active regions of the brain (Kirshner 2014) and detecting and staging cancerous tumors (Gallamini et al. 2014). The common denominator in these applications is that the tissue of interest exhibits an increased uptake of glucose (and FDG) to generate ATP in the cells. This principle also applies to activated muscles; the FDG uptake is closely correlated with the exercise intensity. For example, Pappas et al. studied subjects who performed an elbow flexion exercise, and found that a fivefold increase in the lifted weight (from 2 pounds to 10 pounds) led to an increase in FDG uptake in the biceps brachii, by a factor of 4.94 (Pappas et al. 2001). This correlation between activation and FDG uptake is one of the cornerstones that makes FDG-PET a suitable method to study muscle activity during exercise. Pappas et al. also found that, in contrast to common biomechanical assumptions, the level of activity within the muscle varied considerably (Pappas et al. 2001). This spatial variation enables the study of region-specific activation of muscles, but also necessitates the use of three-dimensional analyses of the FDG uptake in muscles. Since Fujimoto et al. first started using the FDG-PET technique for measuring muscle activity during running in the late 1990s (Fujimoto et al. 1996), the technique has been applied to measure muscle activity during a range of activities including walking (Oi et al. 2003; Shimada et al. 2009; Shimada et al. 2007), cycling (Fujimoto et al. 2003; Gondoh et al. 2009), and even double poling (Bojsen-Moller et al. 2010).

The work in this thesis focuses on walking, since it is one of the most important activities of daily living. Knowledge about how each individual muscle contributes to walking can be useful for several purposes, including rehabilitation, medical education, and validating

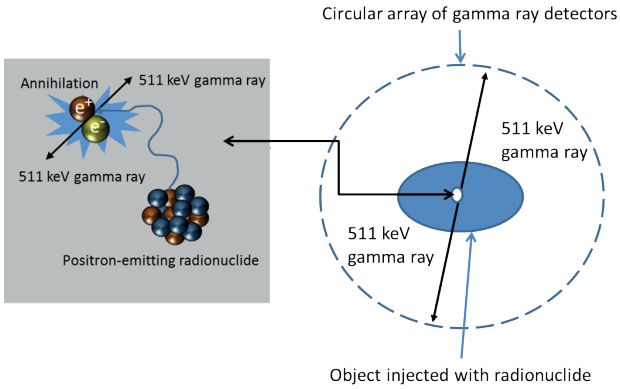

Figure 1.5. Illustration of the fundamental principle of positron emission tomography. The PET scanner detects pairs of gamma rays emitted indirectly by a positron-emitting radionuclide tracer, which is introduced into the body on a biologically active molecule. The three-dimensional images of the tracer's concentration within the body are then reconstructed by computer analysis.

musculoskeletal models. However, until FDG-PET was first used for measuring muscle activity in the late 1990's (Fujimoto et al. 1996), it was difficult to measure the muscle activities of all the muscles of the lower limb simultaneously, because existing measurement techniques (such as electromyography) suffered from limitations. FDG-PET holds several key advantages over electromyography. First, FDG-PET can measure the activity of all muscles in the lower limb simultaneously, whilst electromyography is limited by the number of applied electrodes. Second, deep-lying muscles can be measured more easily than with electromyography, as the latter requires insertion of invasive needle electrodes. Third, the activity in the entire muscle can be measured in three dimensions, whereas electromyography only provides information about a small muscle region, which might not be representative for the activity in the entire muscle (Hodson-Tole et al. 2013; Holtermann et al. 2005; Pappas et al. 2001).

The problems associated with measuring muscle activity with electromyography have thus far only been partly overcome by authors who used FDG-PET. Several authors limited their analyses to measuring muscle FDG uptake in only one or a few discrete slices of the PET scan, rather than analyzing the entire muscle (Oi et al. 2003; Rudroff et al. 2014; Shimada et al. 2009; Shimada et al. 2007). Therefore, their results might not be representative for the activity of the entire muscle (Hodson-Tole et al. 2013; Holtermann et al. 2005; Pappas et al. 2001; Staudenmann et al. 2009). Furthermore, they did not report muscle activity of the muscles that were not present in the discrete slices. As for asymmetries in activity between the muscles in the dominant and those in the non-dominant lower limb, some authors have examined these using FDG-PET (Rudroff et al. 2014). However, they only performed a slice-based analysis on a limited number of muscles. Finally, although region-specific activation within muscles has been studied using FDG-PET, the literature in this area is limited in two ways: region-specific activation has only been reported during simple isometric contractions (Kalliokoski et al. 2007; Pappas et al. 2001), and studies that performed more complicated tasks such as cycling (Heinonen et al. 2012) or walking (Kindred et al. 2015) only reported glucose uptake heterogeneity of the entire muscle rather than distinguishing between areas of high and low uptake. In part, the limitations of the mentioned literature are due to the very labor-intensive manual work that is involved in measuring muscle glucose consumption from PET scans. Since PET scans of muscle activity do not contain anatomical information about the locations of muscles, the muscle regions-of-interest (of typically about a dozen muscles per slice) need to be drawn manually, referring to a concurrently made CT or MRI scan. This tedious manual contour-drawing process needs to be repeated hundreds of times, as scans of the entire lower limb typically consist of hundreds of slices. Then, the process would need to be repeated for each participant in the study. It is in this area where automatic muscle segmentation methods would have a tremendous benefit.

Aims and research questions

This thesis has two main aims. The first aim is to provide insight into the current status and challenges regarding functional outcome after the major orthopedic interventions described in this introduction. This aim is addressed in **part I** (chapters 2-4) of the thesis, guided by the following research questions:

1) What is the current level of functional outcome after total hip arthroplasty, assessed with objective measurement methods, during gait and gait-related activities of daily living?

2) To what extent is the functional outcome in terms of gait and lower limb strength after triple innominate osteotomy and total hip arthroplasty with femoral shortening similar to healthy controls and comparable between the limbs?

3) Are orthopedic oncologists able to accurately predict the functional effects of limb salvage surgery in the lower limb?

The second aim is to explore the possibilities of FDG-PET in providing fundamental insight into the musculoskeletal system, and its potential as a supporting technique to help in solving some of the identified challenges surrounding functional outcome. This aim is addressed in **part II** (chapters 5-7) of the thesis, using the following research questions:

4) Which muscles in the lower limb are of primary importance during walking?

5) Are the muscles in the lower limb symmetrically active during walking?

6) Is muscle activity homogeneous or region-specific during walking?

7) Can FDG-PET be used to validate healthy subject-specific musculoskeletal models?

Outline

In **chapter 2**, we present a systematic review in which we mapped the differences between patients after total hip arthroplasty and healthy controls, and between the operated and non-operated limbs during gait and gait-related activities of daily living. In **chapter 3a**, we present a retrospective, controlled cohort study in which we investigated differences in gait and muscle strength between patients who had undergone triple innominate osteotomy and healthy controls, and between the operated and the non-operated leg. In **chapter 3b**, we examined the gait and strength of patients after total hip arthroplasty with femoral shortening for congenital hip dysplasia. In **chapter 4**, we investigated whether independent orthopedic oncologists were able to predict the functional effects of limb salvage surgery in the lower limb in a nationwide study. In **chapter 5**, we used FDG-PET in combination with three-dimensional muscle segmentations to determine the contribution of each muscle of the lower limb to walking in healthy subjects. In **chapter 6**, we employed the FDG-PET technique to detect asymmetries in muscle activity between the dominant and the non-dominant lower limb, and examined whether muscle activity is homogeneous throughout each muscle, or whether it is region-specific in healthy subjects. In **chapter 7**, we used advanced modeling techniques to generate subject-specific musculoskeletal models. The predicted muscle activities were compared to those previously obtained using FDG-PET. The thesis concludes with a summary and general discussion of the findings (**chapter 8**), in which we interpret the findings of this thesis, and provide directions for future research.

References

Bojsen-Moller, J., T. Losnegard, J. Kemppainen, T. Viljanen, K. K. Kalliokoski, and J. Hallen. 2010. Muscle use during double poling evaluated by positron emission tomography, J Appl Physiol (1985), 109: 1895-1903.

Carbone, V., R. Fluit, P. Pellikaan, M. M. van der Krogt, D. Janssen, M. Damsgaard, L. Vigneron, T. Feilkas, H. F. Koopman, and N. Verdonschot. 2015. TLEM 2.0 - a comprehensive musculoskeletal geometry dataset for subject-specific modeling of lower extremity, J Biomech, 48: 734-741.

Charnley, J. 1961. Arthroplasty of the hip. A new operation, Lancet, 1: 1129-1132.

Cherry, S.R., J.A. Sorenson, and M.E. Phelps. 2012. Physics in Nuclear Medicine (Saunders: Philadelphia, PA).

D'Aubigne, R. M., and M. Postel. 1954. Functional results of hip arthroplasty with acrylic prosthesis, J Bone Joint Surg Am, 36-A: 451-475.

de Kleuver, M., M. A. Kooijman, P. W. Pavlov, and R. P. Veth. 1997. Triple osteotomy of the pelvis for acetabular dysplasia: results at 8 to 15 years, J. Bone Joint Surg. Br., 79: 225-229.

Delp, S. L., A. V. Komattu, and R. L. Wixson. 1994a. Superior displacement of the hip in total joint replacement: effects of prosthetic neck length, neck-stem angle, and anteversion angle on the moment-generating capacity of the muscles, Journal of orthopaedic research : official publication of the Orthopaedic Research Society, 12: 860-870.

Delp, S. L., D. A. Ringwelski, and N. C. Carroll. 1994b. Transfer of the rectus femoris: effects of transfer site on moment arms about the knee and hip, J Biomech, 27: 1201-1211.

Duda, G. N., D. Brand, S. Freitag, W. Lierse, and E. Schneider. 1996. Variability of femoral muscle attachments, J Biomech, 29: 1185-1190.

Ewen, A. M., S. Stewart, A. St Clair Gibson, S. N. Kashyap, and N. Caplan. 2012. Post-operative gait analysis in total hip replacement patients-a review of current literature and meta-analysis, Gait Posture, 36: 1-6.

Fluit, R. 2015. Functional outcome prediction after surgery: a bridge too far?, University of Twente.

Fujimoto, T., M. Itoh, H. Kumano, M. Tashiro, and T. Ido. 1996. Whole-body metabolic map with positron emission tomography of a man after running, Lancet, 348: 266.

Fujimoto, T., J. Kemppainen, K. K. Kalliokoski, P. Nuutila, M. Ito, and J. Knuuti. 2003. Skeletal muscle glucose uptake response to exercise in trained and untrained men, Med Sci Sports Exerc, 35: 777-783.

Gallamini, A., C. Zwarthoed, and A. Borra. 2014. Positron Emission Tomography (PET) in Oncology, Cancers (Basel), 6: 1821-1889.

Gondoh, Y., M. Tashiro, M. Itoh, M. M. Masud, H. Sensui, S. Watanuki, K. Ishii, H. Takekura, R. Nagatomi, and T. Fujimoto. 2009. Evaluation of individual skeletal muscle activity by glucose uptake during pedaling exercise at different workloads using positron emission tomography, J Appl Physiol, 107: 599-604.

Harris, W. H. 1969. Traumatic arthritis of the hip after dislocation and acetabular fractures: treatment by mold arthroplasty. An end-result study using a new method of result evaluation, J. Bone Joint Surg. Am., 51: 737-755.

Heinonen, I., S. V. Nesterov, J. Kemppainen, T. Fujimoto, J. Knuuti, and K. K. Kalliokoski. 2012. Increasing exercise intensity reduces heterogeneity of glucose uptake in human skeletal muscles, PLoS One, 7: e52191.

Hicks, J., A. Arnold, F. Anderson, M. Schwartz, and S. Delp. 2007. The effect of excessive tibial torsion on the capacity of muscles to extend the hip and knee during single-limb stance, Gait Posture, 26: 546-552.

Hodson-Tole, E. F., I. D. Loram, and T. M. Vieira. 2013. Myoelectric activity along human gastrocnemius medialis: different spatial distributions of postural and electrically elicited surface potentials, J

Electromyogr Kinesiol, 23: 43-50.
Holtermann, A., K. Roeleveld, and J. S. Karlsson. 2005. Inhomogeneities in muscle activation reveal motor unit recruitment, J Electromyogr Kinesiol, 15: 131-137.
Hsin, J., R. Saluja, R. E. Eilert, and J. D. Wiedel. 1996. Evaluation of the biomechanics of the hip following a triple osteotomy of the innominate bone, J. Bone Joint Surg. Am., 78: 855-862.
Janssen, D., K. Kalchschmidt, and B. D. Katthagen. 2009. Triple pelvic osteotomy as treatment for osteoarthritis secondary to developmental dysplasia of the hip, Int. Orthop., 33: 1555-1559.
Kalliokoski, K. K., J. Bojsen-Moller, M. Seppanen, J. Johansson, M. Kjaer, M. Teras, and S. P. Magnusson. 2007. Contraction-induced [18F]-fluoro-deoxy-glucose uptake can be measured in human calf muscle using high-resolution PET, Clin Physiol Funct Imaging, 27: 239-241.
Kindred, J. H., N. B. Ketelhut, and T. Rudroff. 2015. Glucose uptake heterogeneity of the leg muscles is similar between patients with multiple sclerosis and healthy controls during walking, Clin Biomech (Bristol, Avon), 30: 159-165.
Kirshner, H. S. 2014. Frontotemporal dementia and primary progressive aphasia, a review, Neuropsychiatr Dis Treat, 10: 1045-1055.
Klein Horsman, M. D., H. F. Koopman, F. C. van der Helm, L. P. Prose, and H. E. Veeger. 2007. Morphological muscle and joint parameters for musculoskeletal modelling of the lower extremity, Clin Biomech (Bristol, Avon), 22: 239-247.
Kyriazis, V., and C. Rigas. 2002. Temporal gait analysis of hip osteoarthritic patients operated with cementless hip replacement, Clin Biomech (Bristol, Avon), 17: 318-321.
Lai, K. A., C. J. Lin, I. M. Jou, and F. C. Su. 2001. Gait analysis after total hip arthroplasty with leg-length equalization in women with unilateral congenital complete dislocation of the hip--comparison with untreated patients, Journal of Orthopaedic Research, 19: 1147-1152.
Learmonth, I. D., C. Young, and C. Rorabeck. 2007. The operation of the century: total hip replacement, Lancet, 370: 1508-1519.
Lenaerts, G., W. Bartels, F. Gelaude, M. Mulier, A. Spaepen, G. Van der Perre, and I. Jonkers. 2009. Subject-specific hip geometry and hip joint centre location affects calculated contact forces at the hip during gait, J Biomech, 42: 1246-1251.
Lindemann, U., C. Becker, I. Unnewehr, R. Muche, K. Aminin, H. Dejnabadi, T. Nikolaus, W. Puhl, K. Huch, and K. E. Dreinhofer. 2006. Gait analysis and WOMAC are complementary in assessing functional outcome in total hip replacement, Clin. Rehabil., 20: 413-420.
Lund, M. E., M. de Zee, M. S. Andersen, and J. Rasmussen. 2012. On validation of multibody musculoskeletal models, Proc Inst Mech Eng H, 226: 82-94.
Marangoz, S., B. Atilla, H. Gok, G. Yavuzer, S. Ergin, A. M. Tokgozoglu, and M. Alpaslan. 2010. Gait analysis in adults with severe hip dysplasia before and after total hip arthroplasty, Hip Int, 20: 466-472.
Nantel, J., N. Termoz, P. A. Vendittoli, M. Lavigne, and F. Prince. 2009. Gait patterns after total hip arthroplasty and surface replacement arthroplasty, Arch. Phys. Med. Rehabil., 90: 463-469.
Oi, N., T. Iwaya, M. Itoh, K. Yamaguchi, Y. Tobimatsu, and T. Fujimoto. 2003. FDG-PET imaging of lower extremity muscular activity during level walking, J Orthop Sci, 8: 55-61.
Orthoworld Annual Report, . 2014. Orthoworld Annual Report (Orthoworld: Chagrin Falls, Ohio).
Otten, R., P. M. van Roermund, and H. S. Picavet. 2010. [Trends in the number of knee and hip arthroplasties: considerably more knee and hip prostheses due to osteoarthritis in 2030], Ned Tijdschr Geneeskd, 154: A1534.
Pappas, G. P., E. W. Olcott, and J. E. Drace. 2001. Imaging of skeletal muscle function using (18)FDG PET: force production, activation, and metabolism, J Appl Physiol (1985), 90: 329-337.
Perry, Jacquelin, and Judith M. Burnfield. 2010. Gait analysis : normal and pathological function (SLACK: Thorofare, NJ).
Piazza, S. J., R. L. Adamson, M. F. Moran, J. O. Sanders, and N. A. Sharkey. 2003. Effects of tensioning errors in split transfers of tibialis anterior and posterior tendons, The Journal of bone and joint

surgery. American volume, 85-A: 858-865.
Piazza, S. J., and S. L. Delp. 2001. Three-dimensional dynamic simulation of total knee replacement motion during a step-up task, Journal of biomechanical engineering, 123: 599-606.
Reinbolt, J. A., M. D. Fox, M. H. Schwartz, and S. L. Delp. 2009. Predicting outcomes of rectus femoris transfer surgery, Gait & Posture, 30: 100-105.
Robert, R. S., G. Ottaviani, W. W. Huh, S. Palla, and N. Jaffe. 2010. Psychosocial and functional outcomes in long-term survivors of osteosarcoma: a comparison of limb-salvage surgery and amputation, Pediatr Blood Cancer, 54: 990-999.
Rosler, J., and C. Perka. 2000. The effect of anatomical positional relationships on kinetic parameters after total hip replacement, Int. Orthop., 24: 23-27.
Rudroff, T., J. H. Kindred, P. J. Koo, R. Karki, and J. R. Hebert. 2014. Asymmetric glucose uptake in leg muscles of patients with Multiple Sclerosis during walking detected by [18F]-FDG PET/CT, NeuroRehabilitation, 35: 813-823.
Scheys, L. 2009. Personalized musculoskeletal modeling based on magnetic resonance images: use for biomechanical analysis of gait, K.U. Leuven.
Scheys, L., A. Van Campenhout, A. Spaepen, P. Suetens, and I. Jonkers. 2008. Personalized MR-based musculoskeletal models compared to rescaled generic models in the presence of increased femoral anteversion: effect on hip moment arm lengths, Gait Posture, 28: 358-365.
Shimada, H., Y. Kimura, S. R. Lord, K. Oda, K. Ishii, T. Suzuki, and K. Ishiwata. 2009. Comparison of regional lower limb glucose metabolism in older adults during walking, Scand J Med Sci Sports, 19: 389-397.
Shimada, H., Y. Kimura, T. Suzuki, T. Hirata, M. Sugiura, Y. Endo, K. Yasuhara, K. Shimada, K. Kikuchi, M. Hashimoto, M. Ishikawa, K. Oda, K. Ishii, and K. Ishiwata. 2007. The use of positron emission tomography and [18F]fluorodeoxyglucose for functional imaging of muscular activity during exercise with a stride assistance system, IEEE Trans Neural Syst Rehabil Eng, 15: 442-448.
Sinha, A., R. Twycross-Lewis, C. Small, D. Morrissey, and N. Maffulli. 2011. Motion analysis as an outcome measure for hip arthroplasty, Surgeon, 9: 284-291.
Staudenmann, D., I. Kingma, A. Daffertshofer, D. F. Stegeman, and J. H. van Dieen. 2009. Heterogeneity of muscle activation in relation to force direction: a multi-channel surface electromyography study on the triceps surae muscle, J Electromyogr Kinesiol, 19: 882-895.
Steel, H. H. 1973. Triple osteotomy of the innominate bone, J. Bone Joint Surg. Am., 55: 343-350.
Taddei, F., S. Martelli, G. Valente, A. Leardini, M. G. Benedetti, M. Manfrini, and M. Viceconti. 2012. Femoral loads during gait in a patient with massive skeletal reconstruction, Clin Biomech (Bristol, Avon), 27: 273-280.
Tonnis, D., K. Behrens, and F. Tscharani. 1981. [A new technique of triple osteotomy for turning dysplastic acetabula in adolescents and adults (author's transl)], Z. Orthop. Ihre Grenzgeb., 119: 253-265.
Ulrich, S. D., T. M. Seyler, D. Bennett, R. E. Delanois, K. J. Saleh, I. Thongtrangan, M. Kuskowski, E. Y. Cheng, P. F. Sharkey, J. Parvizi, J. B. Stiehl, and M. A. Mont. 2008. Total hip arthroplasties: what are the reasons for revision?, Int Orthop, 32: 597-604.
van der Ploeg, B., M. Tarala, J. Homminga, D. Janssen, P. Buma, and N. Verdonschot. 2012. Toward a more realistic prediction of peri-prosthetic micromotions, J Orthop Res, 30: 1147-1154.
Van Der Veldt, Astrid, Egbert Smit, and Adriaan Anthonius Lammertsma. 2013. Positron emission tomography as a method for measuring drug delivery to tumors in vivo: the example of [11C] docetaxel, Frontiers in Oncology, 3.
Veth, R. P., Q. G. van Hoesel, J. P. Bokkerink, J. Hoogenhout, and M. Pruszczynski. 1995. The art of limb salvage in musculoskeletal oncology, Crit Rev Oncol Hematol, 21: 77-103.
Veth, R., Hoesel R. van, M. Pruszczynski, J. Hoogenhout, B. Schreuder, and T. Wobbes. 2003. Limb salvage in musculoskeletal oncology, Lancet Oncol, 4: 343-350.
White, S. C., H. J. Yack, and D. A. Winter. 1989. A three-dimensional musculoskeletal model for gait

analysis. Anatomical variability estimates, J Biomech, 22: 885-893.
Wright, J. G., S. Rudicel, and A. R. Feinstein. 1994. Ask patients what they want. Evaluation of individual complaints before total hip replacement, J Bone Joint Surg Br, 76: 229-234.

Part I

New Perspectives on Functional Assessment
in Orthopedic Surgery

Chapter 2

Gait and gait-related activities of daily living after total hip arthroplasty: a systematic review

Published as:

Kolk, S., Minten, M.J., van Bon, G.E., Rijnen, W.H., Geurts, A.C., Verdonschot, N., Weerdesteyn, V. 2014. Gait and gait-related activities of daily living after total hip arthroplasty: a systematic review, Clinical Biomechanics, 29: 705-718.

Abstract

Background: Differences in the performance of gait and gait-related activities of daily living are known to persist after total hip arthroplasty compared to healthy controls, but the specific underlying deficits (spatiotemporal, kinematics and kinetics) are not completely understood. This review aimed to map the differences between patients and controls, and between the operated and non-operated limbs during various activities of daily living.

Methods: A computerized search with broad search terms was performed in the MEDLINE database. Primary inclusion criteria were: primary osteoarthritis as indication, comparison with healthy controls or comparison between the operated and the non-operated limbs, and follow-up period at least six months after surgery.

Results: The literature search yielded 2177 citations, of which 35 articles were included. Compared to controls, reductions were identified in the operated hip in sagittal range of motion, peak extension, sagittal power generation, abduction moment and external rotation moment. During stair ascent, these reductions did not become more apparent, although deficits in hip kinetics in all three planes were found. Walking speed and step length were reduced compared to controls at longer-term follow-up, but not at short-term follow-up.

Conclusions: The hip abduction moment deficit was present both in level walking and in stair ascent in total hip arthroplasty patients compared to controls. Reduced sagittal hip power generation and external rotation moment were also found, of which the clinical relevance remains to be established. Due to a low number of studies, many of the longer-term effects of THA on gait and gait-related ADL are not yet accurately known.

Introduction

Total hip arthroplasty (THA) is a surgical procedure commonly performed in patients with osteoarthritis. Even though THA is very successful in achieving its primary objective of relieving pain (Bennett et al. 2009), functional limitations may persist after surgery (Johanson et al. 1992; Laupacis et al. 1993). The ability to successfully perform common activities of daily living (ADL) is important for safe mobility, societal participation, and ultimately, quality of life. It is not surprising that besides pain, limitations in ADL (e.g., reduced ability to walk and to negotiate stairs) are important complaints in patients before THA (Wright et al. 1994). After THA, the ability to perform ADL generally improves (Foucher et al. 2008; Lamontagne et al. 2012; Shrader et al. 2009), but some activities such as stair climbing and rising from a chair may still be challenging (Foucher et al. 2008; Talis et al. 2008).

The outcome of THA is traditionally measured with clinical scoring systems such as the Merle d'Aubigné and Postel score (D'Aubigne et al. 1954) and the Harris hip score (Harris 1969). These scoring systems are subjective, and do not include objective measurements of human functioning. Thus, in order to obtain a complimentary objective evaluation of function after hip surgery, it is necessary to employ quantitative measurement techniques such as gait analysis (Lindemann et al. 2006; Nantel et al. 2009; Rosler et al. 2000; Saleh et al. 1985). Such instrumented methods can also be employed to measure other ADL, such as stair negotiation, chair rising and sitting, and stepping over obstacles.

Walking after THA has been extensively investigated. Generally, walking is known to improve after THA, but does not reach a level that would be considered normal (Bennett et al. 2009; Bennett et al. 2006; Foucher et al. 2007; Perron et al. 2000). Ewen et al. summarized the findings of seven studies in this area in a review and meta-analysis, and found reductions in walking velocity, stride length, sagittal hip range of motion (RoM) and hip abduction moment, whilst hip flexion and extension moments were increased compared to healthy controls (Ewen et al. 2012). In spite of those comprehensive findings, many kinematic and kinetic parameters were not included. Moreover, several interesting studies have been published since and a number of relevant issues remained unaddressed.

First, walking at self-selected comfortable speed arguably does not reflect a patient's full motor capacity. Other functional tasks may be more suitable to test performance at higher capacity levels and thereby identify possible functional limitations. Other gait-related ADL (e.g., stair negotiation) may place different or higher demands on the operated limb compared to level walking (Aqil et al. 2013; Chamnongkich et al. 2012; Foucher et al. 2008; Lamontagne et al. 2012; Shrader et al. 2009). Yet, research into other ADL besides level walking has been scarce in patients who underwent THA (Aqil et al. 2013; Benedetti et al. 2010; Chamnongkich et al. 2012; Foucher et al. 2008; Lamontagne et al. 2011a; Lamontagne et al. 2009, 2012; Lamontagne et al. 2011b; Majewski et al. 2005; Perron et al. 2003; Queen et al. 2013; Shrader et al. 2009; Stansfield et al. 2002; Talis et al. 2008; Vissers et al. 2011), and the findings have not previously been categorized, interpreted or summarized.

Second, many studies comparing gait characteristics between THA patients and controls did not match walking speeds between the groups. As walking speed influences kinematic

and kinetic gait parameters (McCrory et al. 2001; Mockel et al. 2003; Perron et al. 2000), previously reported differences after THA might have in fact been epiphenomena of a reduced walking speed. Several recent papers, therefore, reported group comparisons at matched or imposed walking speeds, whereas other studies investigated differences in gait parameters between the operated and the non-operated limbs. The latter methodology may reveal compensatory strategies implemented by the non-operated limb.

The primary goal of this review was to provide an overview of the differences in spatiotemporal, kinematic and kinetic parameters between patients who underwent THA more than six months ago and healthy controls, and between the operated and non-operated limbs of the patients during gait and gait-related ADL. The secondary goal was to define areas to be focused on in rehabilitation protocols as well as in future research.

Methods

Eligibility criteria

Studies were eligible if they 1) included THA patients with primary osteoarthritis as the indication for surgery, 2) reported spatiotemporal and/or kinematic and/or kinetic parameters during gait or gait-related ADL, 3) compared the results with a control group of healthy subjects or compared the operated limb with the non-operated limb, and 4) had a follow-up period of at least six months post surgery. Our argument for the latter criterion was that most improvement in gait is generally reported to be achieved within that time frame, which was based on a preliminary literature search before the review was performed (Casartelli et al. 2013; Lavigne et al. 2010; Nantel et al. 2009; Perron et al. 2000; Rasch et al. 2010). Furthermore, most rehabilitation programmes end at six months or sooner, after which the rate of recovery is presumed to decrease (Nantel et al. 2009; Perron et al. 2000; Sicard-Rosenbaum et al. 2002).

Studies were excluded if the control group was not comparable with regard to age (within ten years). In addition, the language of the publication had to be English, Dutch or German. Furthermore, comments, guidelines, abstracts, protocols and review studies were excluded. Selection of studies was unconstrained regarding subject age and sex, type of implant used and surgical approach.

Literature search

A computerized literature search was conducted in the MEDLINE database on July 8th, 2013. The search strategy was based on medical subject headings (MeSH) terms, words in the title or abstract, and Boolean operators, and was phrased as follows:

(Postoperative Period [MeSH] OR Posture [MeSH] OR Postural Balance [MeSH] OR Movement [MeSH] OR chair [tiab] OR sit [tiab] OR sitting [tiab] OR Stair [tiab] OR Gait [tiab] OR Stairs [tiab] OR obstacle [tiab] OR obstacles [tiab] OR barrier [tiab] OR barriers [tiab]) AND (hip arthroplast*[tiab] OR Total Hip[tiab] OR Hip Replacement[tiab] OR

Hip Prosthesis[tiab] OR "Arthroplasty, Replacement, Hip"[Mesh]).

These broad search terms were used to minimize the chance of missing relevant articles. Additionally, the reference lists of eligible articles were scanned for potentially relevant articles, missed by the computerized search.

Selection procedure

The titles and abstracts of the studies found by the literature search and the scanning of reference lists were screened on possible eligibility for inclusion by SK, MM and GB. In the case of disagreement about inclusion, an independent reviewer, VW, was consulted. The study was discussed until complete consensus was reached.

Data extraction

A predefined data extraction form was used to aid in extracting data from included papers. This form included data fields of follow-up period, surgical approach, number of patients and controls, age of patients and controls, and reported outcome measures.

Primary outcomes

The primary outcome measures investigated in this review were spatiotemporal, kinematic and kinetic parameters during gait and gait-related ADL. If a parameter was reported in fewer than three studies, we chose not to include it in this review. Spatiotemporal parameters were walking speed, stride length, cadence, step length, stance duration, single support time, double support time, step width and cycle duration. Kinematic parameters comprised hip RoM in the sagittal plane, peak hip flexion and extension angles, hip RoM in the frontal plane, peak hip abduction and adduction angles, and pelvic tilt RoM. Kinetic parameters were peak hip flexion and extension moment, peak hip power generation and absorption in the sagittal plane, peak hip abduction and adduction moment, peak hip external and internal rotation moment, and total hip power generation.

Results

Study inclusion

The study screening and inclusion process are shown in Figure 2.1. Of the 35 included articles, 28 investigated gait and seven investigated stair negotiation. Sit-to-stand/stand-to-sit and ramp ascent/descent were each investigated by one study. The study characteristics are listed in Table 2.1. Some studies performed subgroup analyses for patients operated on by different surgical approaches (Kiss et al. 2012; Varin et al. 2013), implant varus/valgus angles (Hodge et al. 1991), or follow-up times (Berman et al. 1991; Kiss et al. 2012; Lavigne et al. 2010). In those cases, the findings were split accordingly and treated as separate results. Some studies used data from the same patient cohort (e.g., Lamontagne et al. 2011a; Lamontagne et al. 2009), in which case the findings were combined.

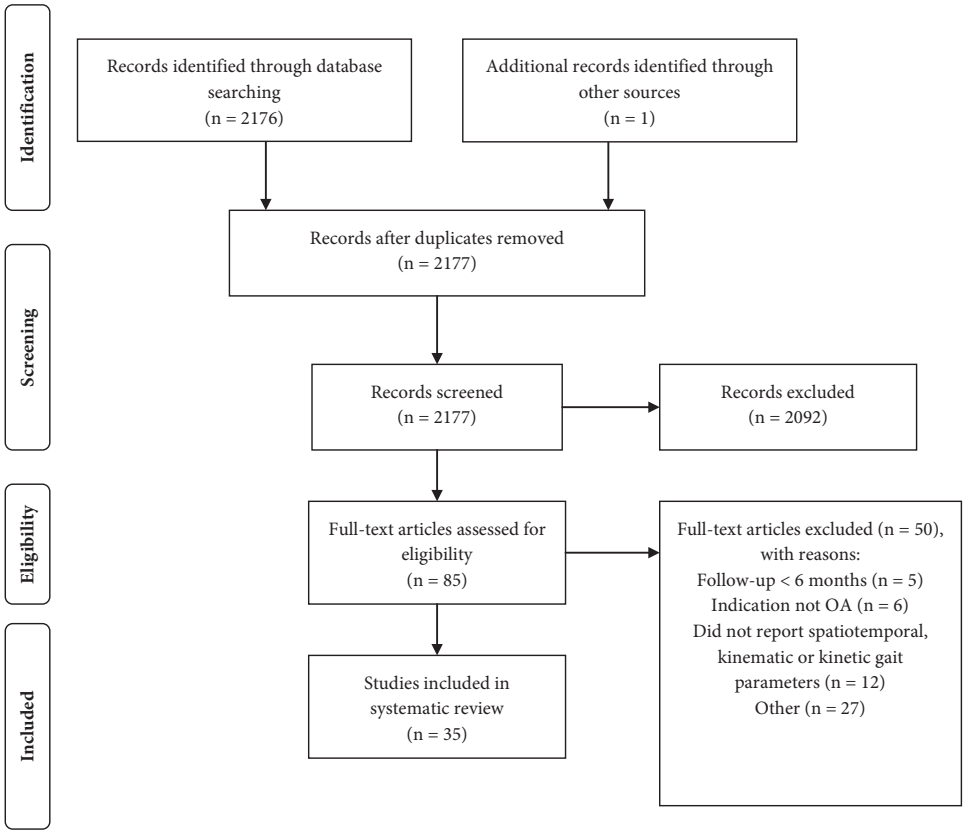

Figure 2.1. Flow chart of the literature search and study inclusion, according to PRISMA guidelines (Moher et al. 2009).

Gait

Findings regarding gait are listed in Table 2.2 and Table 2.3.

Spatiotemporal characteristics

Generally, studies that allowed self-selected walking speed found it was lower in patients than in controls (Beaulieu et al. 2010; Bennett et al. 2008; Guedes et al. 2011; Leuchte et al. 2007; Loizeau et al. 1995; Mont et al. 2007; Perron et al. 2000; Talis et al. 2008) or not different between the groups (Berman et al. 1991; Casartelli et al. 2013; Lavigne et al. 2010 (at 6m post-OR); Nantel et al. 2009; Sicard-Rosenbaum et al. 2002; Tanaka 1998; Tateuchi et al. 2011; Varin et al. 2013). Stride length was also either smaller (Beaulieu et al. 2010; Bennett et al. 2008; Hodge et al. 1991 (varus group); Loizeau et al. 1995; Perron et al. 2000), or similar to controls (Hodge et al. 1991 (valgus group); Nantel et al. 2009; Sicard-Rosenbaum et al. 2002; Tateuchi et al. 2011). The results for all other spatiotemporal parameters tended to yield outcomes that did not differ between THA and control groups. Studies that compared the operated with the non-operated limb did not yield consistent results.

Kinematics

Hip RoM in the sagittal plane was reduced in almost all studies compared to healthy controls (Beaulieu et al. 2010; Bennett et al. 2008; Foucher et al. 2007; Kiss et al. 2012; Madsen et al. 2004; Perron et al. 2000; Varin et al. 2013) as well as compared to the non-operated limb (Benedetti et al. 2010; Kiss et al. 2012). Peak hip extension was consistently reduced compared to controls (Beaulieu et al. 2010; Bennett et al. 2008; Perron et al. 2000; Sander et al. 2011; Tanaka 1998; Varin et al. 2013). Peak hip flexion was most often similar to controls (Bennett et al. 2008; Kiss et al. 2012; Tanaka 1998; Tateuchi et al. 2011), but was reduced in some studies (Beaulieu et al. 2010; Kiss et al. 2012 (anterolateral group)). Pelvic tilt RoM was mostly not different between patients and controls (Beaulieu et al. 2010; Bennett et al. 2008; Kiss et al. 2012; Varin et al. 2013).

Kinetics

Peak hip abduction moment was reduced in almost all studies (Beaulieu et al. 2010; Foucher et al. 2007; Foucher et al. 2011; Mont et al. 2007; Perron et al. 2000; Varin et al. 2013), and peak hip external rotation moment was reduced across all reporting studies (Beaulieu et al. 2010; Foucher et al. 2007; Foucher et al. 2011; Perron et al. 2000; Varin et al. 2013). Peak hip flexion moment did not differ between patients and controls in almost all studies (Foucher et al. 2007; Foucher et al. 2011; Hodge et al. 1991 (valgus group); Tanaka 1998; Tateuchi et al. 2011; Varin et al. 2013); the same was true for the extension moment (Foucher et al. 2007; Foucher et al. 2011; Hodge et al. 1991 (valgus group); Mont et al. 2007; Nantel et al. 2009; Tanaka 1998; Tateuchi et al. 2011; Varin et al. 2013). Peak sagittal hip power generation was either reduced (Perron et al. 2000; Tateuchi et al. 2011; Varin et al. 2013), or similar compared to controls (Nantel et al. 2009; Varin et al. 2013). Sagittal hip power absorption findings were ambiguous, being lower (Loizeau et al. 1995; Perron et al. 2000; Tateuchi et al. 2011), similar (Beaulieu et al. 2010; Varin et al. 2013) or higher (Nantel et al. 2009) than controls.

Relation kinematics and kinetics with walking speed

Some studies matched walking speeds between patients and controls during the measurement (Hodge et al. 1991; Kiss et al. 2012) or in the analysis (Foucher et al. 2007; Foucher et al. 2011; Perron et al. 2000). In those studies, the previously identified reduction of sagittal hip RoM was found almost as consistently as when walking speed was not taken into consideration. Thus, the sagittal hip RoM deficit did not appear to be speed-related. With respect to gait kinetics, these studies yielded similar results to those described above. Particularly the reduced peak hip abduction moment and peak hip external rotation moment in the THA groups persisted in studies that matched walking speeds (Foucher et al. 2007; Foucher et al. 2011; Perron et al. 2000).

Table 2.1 Characteristics of included studies

Publication	Follow-up (months)	Number of subjects, age (years)	Approach	Self-selected or imposed walking speed	Remarks
Beaulieu et al. 2010	10.6	THA: 20, 66.2 (6.7) CON: 20, 63.5 (4.4)	LAT	Self-selected, but ANCOVAs used to correct for differences in walking speed between groups.	Patient group same as lateral group in Varin et al. (2013); additional results from that study (cadence, peak hip power generation and absorption, peak hip flexion and extension moment) were added to the results of this study.
Benedetti et al. 2010a	16 (12–30)	THA: 20, 71 (49–80)	LAT	Self-selected	Operated limb was on average 11 mm longer than the non-operated limb.
Bennett et al. 2008	120	THA: 134, 71.5 (54–85) CON:10, 64 (3.6)	POST	Self-selected	
Bennett et al. 2009	120	THA: 139, 71.1 (54.4–92.8) CON: 10, 64 (59.2–68.5)	POST	Self-selected	
Berman et al. 1991	5–8, 9–12, 13–18	THA: 21, NS CON: 91, NS	AL	Self-selected	No demographic data given. Only group I was used because that group had unilateral OA.
Bhargava et al. 2007	6–51	THA: 20, 51.6 CON: NS, 'age-matched'	POST	Self-selected	
Bouffard et al. 2011	12	THA: 12, 50.8 (6.1) CON: 11, 45.7 (8.2)	POST	Self-selected	
Casartelli et al. 2013	6	THA: 26, 65 (8) CON: 26, 62 (10)	14 POST, 12 ANT	Self-selected, but walking speed was used as covariate.	

Foucher et al. 2007a	14 (3)	THA: 28, 63.6 (7.1) CON: NS, 57.6 (7.7)	13 LAT, 15 POST	'Slow', 'normal', and 'fast' trials were recorded, then trial closest to 1 m/s was analysed.	
Foucher et al. 2008a	14 (3)	THA: 15, 63.4 (7) CON: 15, 56.2 (5.6)	10 POST, 5 LAT	Self-selected	
Foucher et al. 2011a	12	THA: 26, 60 (42–79) CON: 25, 54 (6)	13 MI ANT, 13 MI two-incision approach	Self-selected, but walking trials were matched for speed between groups.	Pooled results from surgical approach groups are used here, as was done in the original article. No significance outcomes provided for comparisons with controls at 6 months, therefore those results are not used here.
Guedes et al. 2011	31.2 (15.2)	THA: 23, 72.0 (6.5) CON: 23, 70.1 (5.9)	PL	Self-selected, speed corrected by leg length.	
Hodge et al. 1991a	30 (15–54) (valgus), 33 (12–58) (varus)	THA: 10, 63.9 (54–76) (valgus) and 66.4 (54–76) (varus) CON: 10, 64.9 (59–75)	NS	'Self-selected normal walking speed of approximately 1 m/s'.	
Kiss et al. 2012	6 and 12	THA: 40, 71.3 (3.7) (DL), 70.1 (1.4) (AL) CON: 40, 70.8 (3.1)	DL	Imposed at 0.56 m/s	
Leuchte et al. 2007	6	THA: 32, 61.2 CON: 30, 59.5 (9.1)	16 AL, 16 trans-gluteal	Self-selected	MIS group and standard group grouped together by the original authors, because outcomes were not different.

Lamontagne et al. 2009 and 2011a	10.6	THA: 20, 66.2 (6.7) CON: 20, 63.5 (4.4)	LAT	Self-selected	Exactly the same patient and control groups in these two studies, therefore the results were pooled and used here integrally. The lower peak hip internal rotation moment during ascent was obtained from Lamontagne 2011b.
Lamontagne et al. 2011b	9.6 (3.7)	THA: 20, 60.5 (6.0) CON: 20, 63.5 (4.4)	ANT	Self-selected	Same LAT group and control group as Lamontagne et al. 2011a. Results of LAT group therefore were summarized under Lamontagne 2011a and Lamontagne 2009.
Lamontagne et al. 2012	10.6	THA: 20, 66.2 (6.7) CON: 20, 63.5 (4.4)	LAT		
Lavigne et al. 2010	6 and 12	THA: 21, 49.8 (33–62) CON: 14, 44.4 (31–56)	POST	Self-selected	
Loizeau et al. 1995	45.6 (30)	THA: 4, 67.3 (8.0) CON: 4, 58.9 (8.9)	NS	Self-selected	
Madsen et al. 2004	6	THA: 20, 62 (8) CON: 9, 54 (9.5)	10 AL, 10 PL	Self-selected	Age has been calculated from a combination of 2 groups.
McCrory et al. 2001	2–53	THA: 27, 59.7 (13.8) CON: 35, 27.5 (5.7)	NS	Self-selected	Excluded from our patient–control comparisons because of 32 year age difference between groups; included on basis of comparison operated vs. non-operated limb.
Mont et al. 2007	12 (6–15)	THA: 15, 58 (44–68) CON: 30, 'age-matched'	AL	Self-selected	
Nantel et al. 2009	6	THA: 10, 49.0 (7.5) CON: 10, 48.6 (6.0)	POST	Self-selected	Took a range instead of a peak for torque and power values.

Perron et al. 2000	11 (4)	THA: 18, 65.6 (6.0) CON: 15, 65.5 (6.5)	9 AL, 9 POST	Self-selected. Additionally, performed speed-matched sub-analysis.	Peak hip extension moment and peak sagittal hip power absorption became similar to controls when speeds were matched between groups.
Queen et al. 2013	18	THA: 10, 58.5 (12.0) CON: 15, 49.2 (7.1)	POST	Self-selected	THA group significantly older and heavier than control group. No differences were found between operated and non-operated limbs, but this was not elucidated.
Rasch et al. 2010	6 and 24	THA: 20, 67 (7)	POST	Self-selected	
Sicard-Rosenbaum et al. 2002	23.6 (9.0–61.2)	THA: 15, 59.9 (14.9) CON: 15, 60.2 (15.0)	NS	Self-selected	Indication: 10 osteoarthritis, 5 fractures.
Stansfield et al. 2002	18.6 (4.1)	THA: 5, 52.6 (6.6) CON: 5, 49.4 (5.0)	NS	Self-selected	Only results compared to healthy controls are reported here.
Talis et al. 2008	19	THA: 27, 56 (10) CON: 27, 55 (9)	NS	Self-selected	Investigated weight bearing distributions during sit-to-stand, but this is not an outcome measure in this review. Only results for gait are used here.
Tanaka 1998	12-85	THA: 40, 60.8 (41–77) CON: 56, NS	NS	Self-selected	Age and follow-up time are given for the total group of 85 patients, of which only the results of 40 unilateral cases are used here.
Tateuchi et al. 2011	35 (10–56)	THA: 12, 63.2 (7.2) CON: 12, 63.4 (5.1)	NS	Self-selected	Had a bilateral and a unilateral THA group; only results from the unilateral group are used here.

Varin et al. 2013	10	THA: 20, 60.5 (6.0) CON: 20, 63.5 (4.4)	ANT	Self-selected, but final ANOVAs weighted by linear least squares regression.	Hip internal and external rotation measured at ipsilateral foot off. The group that was operated on by lateral approach is the same as that used in Beaulieu 2010, therefore the findings were combined and reported as though coming from Beaulieu 2010.
Vissers et al. 2011	6	THA: 30, 60.3 (13.0) CON: 30, 60.1 (12.9)	PL	Self-selected	Measurements with accelerometers worn during daily life.

General abbreviations: THA: total hip arthroplasty, CON: healthy controls, NS: not stated, NA: not applicable.
Approach abbreviations: AL: anterolateral, ANT: anterior, DL: direct lateral, LAT: lateral, MI: minimally invasive, PL: posterolateral, POST: posterior.
[a] Reported external moments rather than internal moments, e.g., an external abduction moment was an internal adduction moment. In this review, we report internal moment data, therefore all external moments have been 'reversed' to resemble internal moments.

Effects of follow-up time on outcome measures

To determine the influence of follow-up time on the outcome measures, we compared the studies with the shortest follow-up (six to nine months) to those with the longest follow-up (more than 24 months). Of the 23 studies in Table 2.2, eight studies had a follow-up period of six to nine months (Berman et al. 1991; Casartelli et al. 2013; Kiss et al. 2012; Lavigne et al. 2010; Leuchte et al. 2007; Madsen et al. 2004; Nantel et al. 2009; Vissers et al. 2011). In contrast, only one study included patients exclusively after 24 months (Bennett et al. 2008). Five other studies included patients at a range of follow-up periods, but with a mean of 24 months or longer (Guedes et al. 2011; Hodge et al. 1991; Loizeau et al. 1995; Tanaka 1998; Tateuchi et al. 2011). Walking speed was not different from controls in most studies that had a short follow-up period, whereas it was lower than controls in most of the studies that had a follow-up of 24 months or longer. This coincided with a reduction in step length in the long-term follow-up studies (Bennett et al. 2008; Tanaka 1998), which was generally not found in the short-term follow-up studies (Casartelli et al. 2013; Kiss et al. 2012 (anterolateral group); Lavigne et al. 2010). Cadence and sagittal hip RoM did not appear to depend on the follow-up period: cadence was similar and sagittal hip RoM was reduced compared to controls both at short-term and at long-term follow-ups. Other parameters were too scarcely reported in one or both categories of follow-up to draw solid conclusions. Although walking speed was matched between groups in one short-term follow-up study (Kiss et al. 2012) and in one long-term follow-up study (Hodge et al. 1991), excluding them from the follow-up time comparison would not have yielded different results.

In studies that compared the operated with the non-operated limb, the findings in studies with long-term follow-up were inconsistent, or reported parameters different from those in studies with short-term follow-up, or the parameters were reported too scarcely in either or both follow-up categories to draw solid conclusions.

Stair negotiation and other gait-related ADL

Findings regarding stair negotiation and other gait-related ADL are listed in Table 2.4.

Stair ascent

In stair ascent, sagittal hip RoM was similar between patients and controls across all studies (Foucher et al. 2008; Lamontagne et al. 2011a; Lamontagne et al. 2011b; Queen et al. 2013), but findings regarding its subcomponents (peak hip flexion and extension angles) differed. Queen et al. found higher flexion and lower extension (Queen et al. 2013), whereas Lamontagne et al. found an almost opposite result with similar flexion and increased extension angles (Lamontagne et al. 2011b). However, Lamontagne et al. also measured another cohort of patients and did not identify any differences in the sagittal plane peak angles in those patients (Lamontagne et al. 2011a; Lamontagne et al. 2009). In the frontal plane, hip RoM and peak hip abduction and adduction angles were mostly similar between groups (Lamontagne et al. 2011a; Lamontagne et al. 2011b; Queen et al. 2013).

Table 2.2 Outcomes of reported tests for significance of spatiotemporal, kinematic and kinetic parameters of included studies during gait: total hip arthroplasty patients compared with healthy controls

	Spatiotemporal parameters									Kinematics							Kinetics							
	Walking speed	Stride length	Cadence	Step length	Stance duration/percentage	Single support time/percentage	Double support time/percentage	Step width	Cycle duration	Hip RoM sagittal	Peak hip flexion	Peak hip extension	Hip RoM frontal	Peak hip abduction	Peak hip adduction	Pelvic tilt RoM	Peak hip flexion moment	Peak hip extension moment	Peak sagittal hip power generation	Peak sagittal hip power absorption	Peak hip abduction moment	Peak hip adduction moment	Peak hip external rotation moment	Peak hip internal rotation moment	Total hip power generation
Beaulieu et al. 2010	<	<	=							<	<	<	=	=	<	=	=	=	<	=	<		<		<
Bennett et al. 2008	<	<	=	<	=					<	=	<	<			=									
Berman et al. 1991 (5–8 m follow-up)	=			>	>		>																		
Berman et al. 1991 (9–12 m follow-up)	=			=	=		=																		
Berman et al. 1991 (13–18 m follow-up)	=			=	=		=																		
Bouffard et al. 2011	>		>	=																					
Casartelli et al. 2013	=		=	=	=	=	=	=																	
Foucher et al. 2007										<							=	=			<	=	<	=	
Foucher et al. 2011										=							=	=			<	=	<	=	
Guedes et al. 2011	<		=																						
Hodge et al. 1991 (valgus)		=								=							=	=							

Hodge et al. 1991 (varus)			<										<								<		>										
Kiss et al. 2012 (6 m follow-up) (DL group)				=		<			=		>			<		<		<				>											
Kiss et al. 2012 (12 m follow-up) (DL group)				=		=			=		=			<		<		<				=											
Kiss et al. 2012 (6 m follow-up) (AL group)				=		=			=		=			<		=		=				=											
Kiss et al. 2012 (12 m follow-up) (AL group)				=		=			=		=			=		=		=				=											
Lavigne et al. 2010 (6 m follow-up)		=			=		=																										
Lavigne et al. 2010 (12 m follow-up)		>			>		=																										
Leuchte et al. 2007		<							>			>																					
Loizeau et al. 1995		<		<			<																				<						
Madsen et al. 2004														<					=														
Mont et al. 2007		<																					=			<							
Nantel et al. 2009		=	=				=		=													>	=	=	>	=							
Perron et al. 2000		<	<	<			<								<								<	<	<	<		<					
Sicard-Rosenbaum et al. 2002		=	=	=	=	=	=	=																									
Talis et al. 2008		<																															
Tanaka 1998		=		=	<		<							=	<							=	=			=							
Tateuchi et al. 2011		=	=											=	=							=	=	<	<							
Varin et al. 2013		=		=									<		<			<	=			=	=	=	=	<		<		<		
Vissers et al. 2011				=																													

Symbols '<', '>' and '=' indicate that parameter was significantly smaller (<), significantly larger (>), or not significantly different in the total hip arthroplasty group compared with the healthy control group.
AL group: total hip arthroplasty group operated by anterolateral approach, DL group: total hip arthroplasty group operated by direct lateral approach.

Table 2.3 Outcomes of reported tests for significance of spatiotemporal, kinematic and kinetic parameters of included studies during gait: total hip arthroplasty patients' operated compared with the non-operated limb

	Spatiotemporal parameters								Kinematics							Kinetics							
	Walking speed	Stride length	Cadence	Step length	Stance duration/percentage	Single support time/percentage	Double support time/percentage	Step width	Cycle duration	Hip RoM sagittal	Peak hip flexion	Peak hip extension	Hip RoM frontal	Peak hip abduction	Peak hip adduction	Pelvic tilt RoM	Peak hip flexion moment	Peak hip extension moment	Peak sagittal hip power generation	Peak sagittal hip power absorption	Peak hip abduction moment	Peak hip adduction moment	Peak hip external rotation moment	Peak hip internal rotation moment	Total hip power generation
Benedetti et al. 2010	=		=	=					=	<	=	=					=	=			=			=	
Bennett et al. 2009	=		=	=	=																				
Bhargava et al. 2007					<	<	>																		
Guedes et al. 2011				>	<	<																			
Kiss et al. 2012 (6 m follow-up) (DL group)				<				<		<	<	<													
Kiss et al. 2012 (12 m follow-up) (DL group)				=				=		<	<	<													
Kiss et al. 2012 (6 m follow-up) (AL group)				=				=		<	=	=													
Kiss et al. 2012 (12 m follow-up) (AL group)				=				=		=	=	=													
Loizeau et al. 1995	=				>																				

McCrory et al. 2001		=	
Rasch et al. 2010 (6 m follow-up)	=		=
Rasch et al. 2010 (24 m follow-up)	=		=
Talis et al. 2008		<	

Symbols '<', '>' and '=' indicate that parameter was significantly smaller (<), significantly larger (>), or not significantly different in the operated limb compared with the non-operated limb.
AL group: total hip arthroplasty patient group operated by anterolateral approach, DL group: total hip arthroplasty patient group operated by direct lateral approach.

Table 2.4 Outcomes of reported tests for significance of spatiotemporal, kinematic and kinetic parameters of included studies during stair negotiation and other gait-related activities of daily living: total hip arthroplasty patients compared with healthy controls and operated limb compared with the non-operated limb

	Spatiotemporal parameters									Kinematics								Kinetics								
	Walking speed	Stride length	Cadence	Step length	Stance duration/percentage	Single support time/percentage	Double support time/percentage	Step width	Cycle duration	Hip RoM sagittal	Peak hip flexion	Peak hip extension	Hip RoM frontal	Peak hip abduction	Peak hip adduction	Pelvic tilt RoM		Peak hip flexion moment	Peak hip extension moment	Peak sagittal hip power generation	Peak sagittal hip power absorption	Peak hip abduction moment	Peak hip adduction moment	Peak hip external rotation moment	Peak hip internal rotation moment	Total hip power generation	
Stair ascent – THA compared to controls																										
Foucher et al. 2008										=								>	=			<	=	=	<	
Lamontagne et al. 2009, 2011a			<							=	=	=	<	=	<	>		=	<			<	=		<	<
Lamontagne et al. 2011b										=	=	>	=	=	=			>	=			=	=	=	=	<
Queen et al. 2013										=	>	<		=	=			=	=			=	=			
Stansfield et al. 2002			<																							
Stair descent – THA compared to controls																										

Lamontagne et al. 2011b							=	<	=	=	=	=		=	=		<	=	=	<	<
Lamontagne et al. 2009, 2011a			<				<	<	=	=	=	=		=	=		=	=		<	=
Queen et al. 2013							=	=	=		=	=		<	=		=	=			
Stansfield et al. 2002			<																		
Stair negotiation – Operated compared to non-operated limb																					
Benedetti et al. 2010 (ascent)	=		=	=		=	=	=	=					=	=		=			<	
Benedetti et al. 2010 (descent)	=		=	<		=	=	=	=					=	=		=			=	
Sit-to-stand and stand-to-sit – THA compared to controls																					
Lamontagne et al. 2012 (sit-to-stand)							<	<		>	>				<			=		=	<
Lamontagne et al. 2012 (stand-to-sit)							<	<		=	>				<			=		>	<
Sit-to-stand and stand-to-sit – Operated compared to non-operated limb																					
Lamontagne et al. 2012 (sit-to-stand)							=	<		>	>				<			>		<	<
Lamontagne et al. 2012 (stand-to-sit)							=	<		>	>				<			=		>	<
Incline and decline walking – THA compared to controls																					
Stansfield et al. 2002 (ramp ascent)	<	=	<																		
Stansfield et al. 2002 (ramp descent)	<	<	<																		

Symbols '<', '>' and '=' indicate that parameter was significantly smaller (<), significantly larger (>), or not significantly different in the total hip arthroplasty group compared with the healthy control group, or in the operated limb compared with the non-operated limb. THA: total hip arthroplasty.

In the patients, hip flexion moment was higher than controls (Foucher et al. 2008; Lamontagne et al. 2011b) or similar (Lamontagne et al. 2011a; Queen et al. 2013), and the extension moment was mostly similar to controls (Foucher et al. 2008; Lamontagne et al. 2011b; Queen et al. 2013). Peak hip abduction moment was lower than controls (Foucher et al. 2008; Lamontagne et al. 2011a) or similar (Lamontagne et al. 2011b; Queen et al. 2013), and adduction moment was similar across all studies (Foucher et al. 2008; Lamontagne et al. 2011a; Lamontagne et al. 2011b; Queen et al. 2013). Peak internal rotation moment was mostly lower (Foucher et al. 2008; Lamontagne et al. 2011a) than controls, as was the total hip power generation (Lamontagne et al. 2011a; Lamontagne et al. 2009; Lamontagne et al. 2011b). The operated limb had a lower peak hip internal rotation moment than the non-operated limb (Benedetti et al. 2010).

Stair descent

Peak hip flexion angle (Lamontagne et al. 2011a; Lamontagne et al. 2011b) and peak internal rotation moment (Lamontagne et al. 2011a; Lamontagne et al. 2009; Lamontagne et al. 2011b) were most often reduced compared to healthy controls. Abduction and adduction moments were mostly similar to controls (Lamontagne et al. 2011a; Lamontagne et al. 2011b; Queen et al. 2013). The operated limb had a shorter stance duration than the non-operated limb (Benedetti et al. 2010).

Incline walking and sit-to-stand

Patients walked slower, and with reduced cadence on a ramp with 10° incline or decline (Stansfield et al. 2002). In sit-to-stand and stand-to-sit, sagittal hip RoM, peak hip flexion, hip extension moment and power generation were lower than in controls (Lamontagne et al. 2012).

Discussion

This review aimed to investigate the underlying deficits during gait and gait-related ADL in patients after THA. Similar to previous work (Ewen et al. 2012), we identified reductions in sagittal hip RoM and hip abduction moment, but additionally found reductions in peak hip extension, sagittal hip power generation, and peak hip external rotation moment in THA patients compared with controls. Most of these findings (sagittal hip RoM, hip abduction moment, hip external rotation moment) could not be attributed to a difference in walking speed, as they persisted in studies that matched walking speed between groups. During stair ascent, the identified impairments did not become more apparent, although deficits in hip kinetics in all three planes were found. In stair descent, differences with healthy controls were found less frequently. Other ADL beside walking and stair negotiation have scarcely been researched in THA patients.

The results from this review indicate that the gait of THA patients is different from healthy controls in several ways. In the sagittal plane, the reduction in hip RoM appeared to be due to the concomitantly reduced hip extension. The hip extension deficit may be caused

by increased passive resistance from the hip flexors (i.e. a flexion contracture), which is relatively prevalent in THA patients (Davis et al. 2007). Alternatively, it may be related to weakness of the hip extensor muscles. However, as we found no consistent reduction in extension moment in THA patients compared to healthy controls, this explanation seems less likely.

Besides the kinematic differences, we also found that the peak sagittal hip power generation was reduced in most studies. Because of the timing of this peak in the pre-swing phase of gait (in which the hip is flexing), this indicates that the flexor muscles may contribute less to gait propulsion in THA patients than in controls. Differences between groups persisted even in studies where walking speed was matched (Perron et al. 2000), or where it was used as a covariate in the analysis (Beaulieu et al. 2010), thus indicating a 'real' reduction in hip flexor activity rather than it being an epiphenomenon of reduced walking speed. A strength deficit may underlie the lower flexor activity, as previous research found that, compared to controls, THA patients had significantly reduced hip flexor strength (Frost et al. 2006). It therefore seems that the hip flexors deserve more attention in rehabilitation, besides the commonly performed hip extensor and abductor strengthening exercises (Hesse et al. 2003; Okoro et al. 2013).

Frontal plane hip kinematics were investigated in only a few studies (Beaulieu et al. 2010; Bennett et al. 2008; Madsen et al. 2004; Varin et al. 2013). This is surprising since some of the clinically most relevant and frequently observed gait deviations in patients before and after THA (Trendelenburg and Duchenne gait) take place in the frontal plane. The reductions in peak hip adduction angle (Beaulieu et al. 2010; Varin et al. 2013) and hip abduction moment (Beaulieu et al. 2010; Foucher et al. 2007; Foucher et al. 2011; Mont et al. 2007; Perron et al. 2000; Varin et al. 2013) may indeed point to a Trendelenburg-type gait pattern. This may be due to persisting muscle weakness that patients had developed in the years before the surgery. This postulation is supported by Arokoski et al., who found significantly reduced hip abduction strength in hip osteoarthritis patients compared to healthy controls (Arokoski et al. 2002). An alternative explanation is damage to the abductor muscles inflicted during certain surgical approaches (e.g., lateral and anterolateral approaches). However, almost all reporting studies in this review found a reduced abduction moment in their patients, including studies that employed the posterior approach, which spares the abductor musculature (Jolles et al. 2006; Madsen et al. 2004).

The reduced peak hip external rotation moment we identified might be due to the operative technique, as the external rotators are partly released in several approaches to the hip, including the common posterior approach (Madsen et al. 2004). However, the studies in which the external rotation moment deficit was found, used other approaches in their patients (Beaulieu et al. 2010; Foucher et al. 2011; Varin et al. 2013), or only used the posterior approach in a subset of their cohort (Foucher et al. 2007; Perron et al. 2000). Thus, the external rotator weakness appears to be independent of surgical approach, and may instead be persisting from before the surgery. This postulation is supported by Hakkinen et al. who found significantly reduced external rotator strength in the operated compared to the non-operated hip of patients before, and at 3, 6 and 12 months after hip resurfacing arthroplasty (Hakkinen et al. 2010). Further research is required to establish the origin and the clinical relevance of this finding.

Differences between the kinematics of the operated and non-operated limbs are an interesting area of study, because it allows compensatory inter-limb strategies to be identified. Such strategies are potentially harmful, as an asymmetric gait pattern may cause abnormal loading, which in turn could jeopardize the prosthesis' fixation (McCrory et al. 2001) or cause secondary complaints in other joints (Foucher et al. 2012). It therefore is surprising that only two studies investigated asymmetries in kinematics or kinetics between the operated and the non-operated hip (Benedetti et al. 2010; Kiss et al. 2012). Those studies found reduced sagittal RoM in the operated hip compared to the non-operated hip, for which compensatory strategies included increasing pelvic rotation, obliquity and tilt (Huang et al. 2011; Kiss et al. 2012; Miki et al. 2004). The larger pelvic motions thereby allow maintenance of normal step length (Huang et al. 2011; Kiss et al. 2012; Wu et al. 2002), which is beneficial for maintaining walking speed, but their long-term consequences are unknown and in need of further study.

The importance of studying the effects of THA on the operated as well as the non-operated limb was underlined by Foucher et al. (2012), who found several significant and relevant differences compared to controls. These included increased abduction and extension moments in the knee contralateral to the operated hip, both before and after the operation (Foucher et al. 2012). The higher knee abduction moment in particular has been linked to the development (Hurwitz et al. 2000) and aggravation of knee osteoarthritis (Andriacchi et al. 2006; Miyazaki et al. 2002). These findings call for further investigations into gait re-training and rehabilitation strategies that aim to establish gait symmetry.

Interestingly, the literature did not provide clear indications for gait deviations to decrease with prolonged time post surgery. In fact, walking speed was similar to controls in most studies that had a short follow-up of six to nine months, whereas it was reduced, in parallel with reductions in step length, in most studies that had a relatively long mean follow-up of 24 months or longer. Furthermore, the results for cadence or sagittal hip RoM were not different between short and long term follow-up periods. However, it is difficult to firmly establish the effects of time post surgery, as the comparison between short-term and long-term follow-up studies is hampered by the small number of studies in each group. Particularly, only a single study included patients exclusively after 24 months. Additionally, several gait parameters (peak hip abduction moment, peak hip external rotation moment) that were identified in this review as being reduced compared to healthy controls at follow-up times less than 24 months were not or scarcely reported in the long-term follow-up studies. Future studies that investigate gait longitudinally at several follow-up times (including a follow-up of two years and more) should address these gaps.

In stair negotiation, we found several differences between patients and controls, but compared to level walking, the differences did not become magnified. In stair ascent, several differences with healthy controls were apparent in the kinetics of the hip in all three planes. In the sagittal plane, two studies found an increased hip flexion moment in THA patients (Foucher et al. 2008; Lamontagne et al. 2011b). This increase may be part of a strategy in which patients make their trunk lean forward during late stance, increasing their feeling of stability and relying less on their reduced hip abductor function (Foucher et al. 2008). In the frontal plane, the peak hip abduction moment was lower (Foucher et al. 2008; Lamontagne

et al. 2011a) or similar compared to controls (Lamontagne et al. 2011b; Queen et al. 2013). Thus, the reduced hip abduction moment in THA patients found in level walking was also found, albeit less consistently, in stair ascent. In addition to the lower hip abduction moment, the reduced internal rotation moment in THA patients (Lamontagne et al. 2011a; Lamontagne et al. 2011b) may be reflective of abductor weakness because, when the hip is flexed, most fibres of the gluteus medius and minimus act as internal rotators (Platzer 1999).

In descent, peak hip flexion was found to be lower than healthy controls in two studies (Lamontagne et al. 2011a; Lamontagne et al. 2011b). This might be indicative of a particular strategy whereby the trunk inclination is reduced and the centre of mass is brought backward, so as to reduce the chance of falling forward (Lamontagne et al. 2011b). It might also be indicative of hip flexor muscle weakness. However, the peak hip flexion moment was not concurrently reduced in the THA patients in the studies that found reduced hip flexion (Lamontagne et al. 2011a; Lamontagne et al. 2011b), which argues against this postulation.

Generally, previous research indicates that the hip joint moments required to negotiate stairs are similar or lower than those required for level walking (Kirkwood et al. 1999; Nadeau et al. 2003; Riener et al. 2002). This implicates that THA patients are not pushed further towards the limits of their capacity in stair negotiation than in level walking, which explains why differences with healthy controls did not become more apparent in stair negotiation than in level walking.

Chair rising and sitting were investigated in only one included study (Lamontagne et al. 2012). Since these are common ADL in THA patients (Morlock et al. 2001), it is surprising that they have been investigated by so few studies. Lamontagne et al. (2012) and Talis et al. (2008) found that both rising and sitting are performed asymmetrically in THA patients. As discussed earlier, asymmetric movement and loading may increase the risk of developing secondary complaints in the contralateral limb. Increasing the strength of the primary muscles responsible for this movement in the operated limb (vastus and gluteus maximus muscles) and retraining THA patients to properly load the operated hip joint may help in improving the patients' recovery (Lamontagne et al. 2012).

This review has some limitations. We examined only peak values for the kinematic and kinetic parameters. The absence of differences in peak values does not necessarily imply that the pattern as a whole is not different. Thus, a patient may still walk or negotiate stairs quite differently compared to a healthy peer. Furthermore, statistically significant results do not always imply clinical relevance. Lastly, the methodological quality of the included studies differed. For instance, in some of the studies that were included in this review, there might have been a reporting bias. It was often described unclearly which gait parameters were statistically compared between THA patients and controls, whilst only the statistically significant parameters were reported.

Conclusions

The available literature showed that THA patients had reduced sagittal hip RoM, peak hip extension, sagittal hip power generation, hip abduction moment, and peak hip external rotation moment during gait compared to controls. The lower hip abduction moment was also found during stair ascent, and appeared to be independent of the surgical approach. Stair ascent and descent did not magnify the deficits found during level walking. Research into other ADL (e.g., sit-to-stand transfers) has been scarce, even though THA patients perform such activities frequently and in a plausibly harmful asymmetric way. Walking speed and step length were reduced compared to controls at longer-term follow-up, which was not observed at short-term follow-up. However, given the low number of studies that had a follow-up of two years or longer, many of the longer-term effects of THA on gait and gait-related ADL are not yet accurately known, which indicates a need for more research.

Acknowledgements

We gratefully acknowledge the financial support of the European Commission (grant FP7-ICT-247860) for the TLEMsafe project (http://www.tlemsafe.eu). The funding agency played no role in design, collection, analysis, interpretation of data, writing process, or in the decision to submit the paper for publication.

References

Andriacchi, T. P., and A. Mundermann. 2006. The role of ambulatory mechanics in the initiation and progression of knee osteoarthritis, Current Opinion in Rheumatology, 18: 514-518.

Aqil, A., R. Drabu, J. H. Bergmann, M. Masjedi, V. Manning, B. Andrews, S. K. Muirhead-Allwood, and J. P. Cobb. 2013. The gait of patients with one resurfacing and one replacement hip: a single blinded controlled study, International Orthopaedics, 37: 795-801.

Arokoski, M. H., J. P. Arokoski, M. Haara, M. Kankaanpaa, M. Vesterinen, L. H. Niemitukia, and H. J. Helminen. 2002. Hip muscle strength and muscle cross sectional area in men with and without hip osteoarthritis, Journal of Rheumatology, 29: 2185-2195.

Beaulieu, M. L., M. Lamontagne, and P. E. Beaule. 2010. Lower limb biomechanics during gait do not return to normal following total hip arthroplasty, Gait and Posture, 32: 269-273.

Benedetti, M. G., F. Catani, E. Benedetti, L. Berti, A. Di Gioia, and S. Giannini. 2010. To what extent does leg length discrepancy impair motor activity in patients after total hip arthroplasty?, International Orthopaedics, 34: 1115-1121.

Bennett, D., L. Humphreys, S. O'Brien, C. Kelly, J. F. Orr, and D. E. Beverland. 2008. Gait kinematics of age-stratified hip replacement patients--a large scale, long-term follow-up study, Gait Posture, 28: 194-200.

Bennett, D., L. Humphreys, S. O'Brien, J. Orr, and D. E. Beverland. 2009. Temporospatial parameters of hip replacement patients ten years post-operatively, International Orthopaedics, 33: 1203-1207.

Bennett, D., L. Ogonda, D. Elliott, L. Humphreys, and D. E. Beverland. 2006. Comparison of gait kinematics in patients receiving minimally invasive and traditional hip replacement surgery: a prospective blinded study, Gait and Posture, 23: 374-382.

Berman, A. T., R. H. Quinn, and V. J. Zarro. 1991. Quantitative gait analysis in unilateral and bilateral total hip replacements, Archives of Physical Medicine and Rehabilitation, 72: 190-194.

Casartelli, N. C., J. F. Item-Glatthorn, M. Bizzini, M. Leunig, and N. A. Maffiuletti. 2013. Differences in gait characteristics between total hip, knee, and ankle arthroplasty patients: a six-month postoperative comparison, BMC Musculoskelet Disord, 14: 176.

Chamnongkich, S., I. Asayama, T. L. Kinsey, O. M. Mahoney, and K. J. Simpson. 2012. Difference in hip prosthesis femoral offset affects hip abductor strength and gait characteristics during obstacle crossing, Orthopedic Clinics of North America, 43: e48-58.

D'Aubigne, R. M., and M. Postel. 1954. Functional results of hip arthroplasty with acrylic prosthesis, J Bone Joint Surg Am, 36-A: 451-475.

Davis, K. E., M. A. Ritter, M. E. Berend, and J. B. Meding. 2007. The importance of range of motion after total hip arthroplasty, Clin Orthop Relat Res, 465: 180-184.

Ewen, A. M., S. Stewart, A. St Clair Gibson, S. N. Kashyap, and N. Caplan. 2012. Post-operative gait analysis in total hip replacement patients-a review of current literature and meta-analysis, Gait Posture, 36: 1-6.

Foucher, K. C., D. E. Hurwitz, and M. A. Wimmer. 2007. Preoperative gait adaptations persist one year after surgery in clinically well-functioning total hip replacement patients, Journal of Biomechanics, 40: 3432-3437.

Foucher, K. C., D. E. Hurwitz, and M. A. Wimmer. 2008. Do gait adaptations during stair climbing result in changes in implant forces in subjects with total hip replacements compared to normal subjects?, Clin Biomech, 23: 754-761.

Foucher, K. C., and M. A. Wimmer. 2012. Contralateral hip and knee gait biomechanics are unchanged by total hip replacement for unilateral hip osteoarthritis, Gait and Posture, 35: 61-65.

Foucher, K. C., M. A. Wimmer, K. C. Moisio, M. Hildebrand, M. C. Berli, M. R. Walker, R. A. Berger, and J. O. Galante. 2011. Time course and extent of functional recovery during the first postoperative year after minimally invasive total hip arthroplasty with two different surgical

approaches–a randomized controlled trial, Journal of Biomechanics, 44: 372-378.
Frost, K. L., G. E. Bertocci, C. A. Wassinger, M. C. Munin, R. G. Burdett, and S. G. Fitzgerald. 2006. Isometric performance following total hip arthroplasty and rehabilitation, Journal of Rehabilitation Research and Development, 43: 435-444.
Guedes, R. C., J. M. Dias, R. C. Dias, V. S. Borges, L. P. Lustosa, and N. M. Rosa. 2011. Total hip arthroplasty in the elderly: impact on functional performance, Rev Bras Fisioter, 15: 123-130.
Hakkinen, A., H. Borg, H. Kautiainen, E. Anttila, K. Hakkinen, J. Ylinen, and I. Kiviranta. 2010. Muscle strength and range of movement deficits 1 year after hip resurfacing surgery using posterior approach, Disability and Rehabilitation, 32: 483-491.
Harris, W. H. 1969. Traumatic arthritis of the hip after dislocation and acetabular fractures: treatment by mold arthroplasty. An end-result study using a new method of result evaluation, J. Bone Joint Surg. Am., 51: 737-755.
Hesse, S., C. Werner, H. Seibel, S. von Frankenberg, E. M. Kappel, S. Kirker, and M. Kading. 2003. Treadmill training with partial body-weight support after total hip arthroplasty: a randomized controlled trial, Archives of Physical Medicine and Rehabilitation, 84: 1767-1773.
Hodge, W. A., T. P. Andriacchi, and J. O. Galante. 1991. A relationship between stem orientation and function following total hip arthroplasty, Journal of Arthroplasty, 6: 229-235.
Huang, Y. P., S. M. Bruijn, J. H. Lin, O. G. Meijer, W. H. Wu, H. Abbasi-Bafghi, X. C. Lin, and J. H. van Dieen. 2011. Gait adaptations in low back pain patients with lumbar disc herniation: trunk coordination and arm swing, European Spine Journal, 20: 491-499.
Hurwitz, D. E., A. R. Ryals, J. A. Block, L. Sharma, T. J. Schnitzer, and T. P. Andriacchi. 2000. Knee pain and joint loading in subjects with osteoarthritis of the knee, Journal of Orthopaedic Research, 18: 572-579.
Johanson, N. A., M. E. Charlson, T. P. Szatrowski, and C. S. Ranawat. 1992. A self-administered hip-rating questionnaire for the assessment of outcome after total hip replacement, J Bone Joint Surg Am, 74: 587-597.
Jolles, B. M., and E. R. Bogoch. 2006. Posterior versus lateral surgical approach for total hip arthroplasty in adults with osteoarthritis, Cochrane Database Syst Rev: CD003828.
Kirkwood, R. N., E. G. Culham, and P. Costigan. 1999. Hip moments during level walking, stair climbing, and exercise in individuals aged 55 years or older, Physical Therapy, 79: 360-370.
Kiss, R. M., and A. Illyes. 2012. Comparison of gait parameters in patients following total hip arthroplasty with a direct-lateral or antero-lateral surgical approach, Hum Mov Sci, 31: 1302-1316.
Lamontagne, M., M. L. Beaulieu, and P. E. Beaule. 2011a. Comparison of joint mechanics of both lower limbs of THA patients with healthy participants during stair ascent and descent, Journal of Orthopaedic Research, 29: 305-311.
Lamontagne, M., M. L. Beaulieu, D. Varin, and P. E. Beaule. 2009. Gait and motion analysis of the lower extremity after total hip arthroplasty: what the orthopedic surgeon should know, Orthopedic Clinics of North America, 40: 397-405.
Lamontagne, M., M. L. Beaulieu, D. Varin, and P. E. Beaule. 2012. Lower-limb joint mechanics after total hip arthroplasty during sitting and standing tasks, Journal of Orthopaedic Research, 30: 1611-1617.
Lamontagne, M., D. Varin, and P. E. Beaule. 2011b. Does the anterior approach for total hip arthroplasty better restore stair climbing gait mechanics?, Journal of Orthopaedic Research, 29: 1412-1417.
Laupacis, A., R. Bourne, C. Rorabeck, D. Feeny, C. Wong, P. Tugwell, K. Leslie, and R. Bullas. 1993. The effect of elective total hip replacement on health-related quality of life, J Bone Joint Surg Am, 75: 1619-1626.
Lavigne, M., M. Therrien, J. Nantel, A. Roy, F. Prince, and P. A. Vendittoli. 2010. The John Charnley Award: The functional outcome of hip resurfacing and large-head THA is the same: a randomized, double-blind study, Clin Orthop Relat Res, 468: 326-336.
Leuchte, S., A. Luchs, and D. Wohlrab. 2007. [Measurement of ground reaction forces after total

hip arthroplasty using different surgical approaches], Zeitschrift fur Orthopadie und Ihre Grenzgebiete, 145: 74-80.

Lindemann, U., C. Becker, I. Unnewehr, R. Muche, K. Aminin, H. Dejnabadi, T. Nikolaus, W. Puhl, K. Huch, and K. E. Dreinhofer. 2006. Gait analysis and WOMAC are complementary in assessing functional outcome in total hip replacement, Clinical Rehabilitation, 20: 413-420.

Loizeau, J., P. Allard, M. Duhaime, and B. Landjerit. 1995. Bilateral gait patterns in subjects fitted with a total hip prosthesis, Archives of Physical Medicine and Rehabilitation, 76: 552-557.

Madsen, M. S., M. A. Ritter, H. H. Morris, J. B. Meding, M. E. Berend, P. M. Faris, and V. G. Vardaxis. 2004. The effect of total hip arthroplasty surgical approach on gait, Journal of Orthopaedic Research, 22: 44-50.

Majewski, M., H. A. Bischoff-Ferrari, C. Gruneberg, W. Dick, and J. H. Allum. 2005. Improvements in balance after total hip replacement, Journal of Bone and Joint Surgery. British Volume, 87: 1337-1343.

McCrory, J. L., S. C. White, and R. M. Lifeso. 2001. Vertical ground reaction forces: objective measures of gait following hip arthroplasty, Gait and Posture, 14: 104-109.

Miki, H., N. Sugano, K. Hagio, T. Nishii, H. Kawakami, A. Kakimoto, N. Nakamura, and H. Yoshikawa. 2004. Recovery of walking speed and symmetrical movement of the pelvis and lower extremity joints after unilateral THA, Journal of Biomechanics, 37: 443-455.

Miyazaki, T., M. Wada, H. Kawahara, M. Sato, H. Baba, and S. Shimada. 2002. Dynamic load at baseline can predict radiographic disease progression in medial compartment knee osteoarthritis, Annals of the Rheumatic Diseases, 61: 617-622.

Mockel, G., C. Perka, K. Labs, and G. Duda. 2003. The influence of walking speed on kinetic and kinematic parameters in patients with osteoarthritis of the hip using a force-instrumented treadmill and standardised gait speeds, Archives of Orthopaedic and Trauma Surgery, 123: 278-282.

Mont, M. A., T. M. Seyler, P. S. Ragland, R. Starr, J. Erhart, and A. Bhave. 2007. Gait analysis of patients with resurfacing hip arthroplasty compared with hip osteoarthritis and standard total hip arthroplasty, Journal of Arthroplasty, 22: 100-108.

Morlock, M., E. Schneider, A. Bluhm, M. Vollmer, G. Bergmann, V. Muller, and M. Honl. 2001. Duration and frequency of everyday activities in total hip patients, Journal of Biomechanics, 34: 873-881.

Nadeau, S., B. J. McFadyen, and F. Malouin. 2003. Frontal and sagittal plane analyses of the stair climbing task in healthy adults aged over 40 years: what are the challenges compared to level walking?, Clin Biomech, 18: 950-959.

Nantel, J., N. Termoz, P. A. Vendittoli, M. Lavigne, and F. Prince. 2009. Gait patterns after total hip arthroplasty and surface replacement arthroplasty, Archives of Physical Medicine and Rehabilitation, 90: 463-469.

Okoro, T., A. Ramavath, J. Howarth, J. Jenkinson, P. Maddison, J. G. Andrew, and A. Lemmey. 2013. What does standard rehabilitation practice after total hip replacement in the UK entail? Results of a mixed methods study, BMC Musculoskelet Disord, 14: 91.

Perron, M., F. Malouin, and H. Moffet. 2003. Assessing advanced locomotor recovery after total hip arthroplasty with the timed stair test, Clinical Rehabilitation, 17: 780-786.

Perron, M., F. Malouin, H. Moffet, and B. J. McFadyen. 2000. Three-dimensional gait analysis in women with a total hip arthroplasty, Clin Biomech, 15: 504-515.

Platzer, W. 1999. Taschenatlas der Anatomie, Band 1, Bewegungsapparat (Georg Thieme Verlag: Stuttgart).

Queen, R. M., E. T. Newman, A. N. Abbey, T. P. Vail, and M. P. Bolognesi. 2013. Stair ascending and descending in hip resurfacing and large head total hip arthroplasty patients, Journal of Arthroplasty, 28: 684-689.

Rasch, A., N. Dalen, and H. E. Berg. 2010. Muscle strength, gait, and balance in 20 patients with hip

osteoarthritis followed for 2 years after THA, Acta Orthop, 81: 183-188.
Riener, R., M. Rabuffetti, and C. Frigo. 2002. Stair ascent and descent at different inclinations, Gait and Posture, 15: 32-44.
Rosler, J., and C. Perka. 2000. The effect of anatomical positional relationships on kinetic parameters after total hip replacement, International Orthopaedics, 24: 23-27.
Saleh, M., and G. Murdoch. 1985. In defence of gait analysis. Observation and measurement in gait assessment, J. Bone Joint Surg. Br., 67: 237-241.
Sander, K., F. Layher, J. Babisch, and A. Roth. 2011. [Evaluation of results after total hip replacement using a minimally invasive and a conventional approach. Clinical scores and gait analysis], Z Orthop Unfall, 149: 191-199.
Shrader, M. W., M. Bhowmik-Stoker, M. C. Jacofsky, and D. J. Jacofsky. 2009. Gait and stair function in total and resurfacing hip arthroplasty: a pilot study, Clin Orthop Relat Res, 467: 1476-1484.
Sicard-Rosenbaum, L., K. E. Light, and A. L. Behrman. 2002. Gait, lower extremity strength, and self-assessed mobility after hip arthroplasty, Journals of Gerontology. Series A, Biological Sciences and Medical Sciences, 57: M47-51.
Stansfield, B. W., and A. C. Nicol. 2002. Hip joint contact forces in normal subjects and subjects with total hip prostheses: walking and stair and ramp negotiation, Clin Biomech, 17: 130-139.
Talis, V. L., A. A. Grishin, I. A. Solopova, T. L. Oskanyan, V. E. Belenky, and Y. P. Ivanenko. 2008. Asymmetric leg loading during sit-to-stand, walking and quiet standing in patients after unilateral total hip replacement surgery, Clin Biomech, 23: 424-433.
Tanaka, Y. 1998. Gait analysis of patients with osteoarthritis of the hip and the those with total hip arthroplasty, Bio-Medical Materials and Engineering, 8: 187-196.
Tateuchi, H., R. Tsukagoshi, Y. Fukumoto, S. Oda, and N. Ichihashi. 2011. Dynamic hip joint stiffness in individuals with total hip arthroplasty: relationships between hip impairments and dynamics of the other joints, Clin Biomech (Bristol, Avon), 26: 598-604.
Varin, D., M. Lamontagne, and P. E. Beaule. 2013. Does the anterior approach for THA provide closer-to-normal lower-limb motion?, Journal of Arthroplasty, 28: 1401-1407.
Vissers, M. M., J. B. Bussmann, I. B. de Groot, J. A. Verhaar, and M. Reijman. 2011. Walking and chair rising performed in the daily life situation before and after total hip arthroplasty, Osteoarthritis and Cartilage, 19: 1102-1107.
Wright, J. G., S. Rudicel, and A. R. Feinstein. 1994. Ask patients what they want. Evaluation of individual complaints before total hip replacement, J Bone Joint Surg Br, 76: 229-234.
Wu, W., O. G. Meijer, P. C. Jutte, K. Uegaki, C. J. Lamoth, G. Sander de Wolf, J. H. van Dieen, P. I. Wuisman, G. Kwakkel, J. I. de Vries, and P. J. Beek. 2002. Gait in patients with pregnancy-related pain in the pelvis: an emphasis on the coordination of transverse pelvic and thoracic rotations, Clin Biomech, 17: 678-686.

Chapter 3a

Gait and lower limb muscle strength in women after triple innominate osteotomy

Published as:

Kolk, S., Fluit, R., Luijten, J., Heesterbeek, P.J., Geurts, A.C., Verdonschot, N., and Weerdesteyn, V. 2015. Gait and lower limb muscle strength in women after triple innominate osteotomy, BMC Musculoskeletal Disorders, 16: 68.

Abstract

Background: In adult patients with developmental hip dysplasia, a surgical procedure (triple innominate osteotomy) of the pelvic bone can be performed to rotate the acetabulum in the frontal plane, establishing better acetabular coverage. Although common clinical hip scores demonstrate significant improvements after surgery, they provide only overall information about function. The purpose of this study was to quantify the long-term outcome of triple innominate osteotomy in more detail using gait analyses and muscle strength measurements.

Methods: We performed gait analyses at self-selected walking speed as well as isometric hip and knee muscle strength tests in twelve women who had undergone a unilateral triple innominate osteotomy (age: 34±12y, time post surgery: 80±18m). We compared the results to reference values obtained from eight healthy peers (age: 33±10y).

Results: The patients exhibited slight asymmetries in step length (smaller steps) and stance time (longer stance) as well as lower hip abduction moments in the operated limb in early stance compared to the non-operated limb. However, there were no differences in gait compared to healthy controls, even though the patients showed reduced bilateral hip abduction strength compared to controls.

Conclusions: Our results indicate that the patients' gait pattern had generally recovered very well, despite slight asymmetries in spatiotemporal parameters. Subtle deviations in hip abduction moments were observed during gait, whereas hip abduction strength was substantially reduced. Hence, the patients walked at a higher percentage of their maximal capacity. They may, therefore, be prone to fatigue and adopt compensatory gait strategies more quickly than healthy peers when walking long distances.

Background

Developmental dysplasia of the hip is characterized by a shallow, obliquely-oriented acetabulum and malposition of the proximal femur. Together, these anatomical deformations lead to an increased local load because of a decreased weight-bearing area (Hsin et al. 1996). This is painful for patients, can cause secondary osteoarthritis, and limits patients in their daily activities. To relieve the symptoms, a surgical procedure (Triple Innominate Osteotomy; TIO) can be performed (Steel 1973; Tonnis et al. 1981). In this surgery, the acetabulum is rotated in the frontal plane to increase its coverage over the femoral head (de Kleuver et al. 1997). This procedure reduces pain and further joint degeneration and, thereby, greatly improves the quality of life of patients (Faciszewski et al. 1993). In addition to pain relief and radiographic improvement, functional outcome is also important in determining the success of hip dysplasia surgery.

Most patients who underwent TIO achieve good to excellent functional results based on clinical functional scores (de Kleuver et al. 1997; Guille et al. 1992; Nakamura et al. 1998). However, drawbacks of these scoring systems are that they are subjective (Learmonth et al. 2007), may have ceiling effects (Wamper et al. 2010), and only provide information about the overall level of function. They do not allow one to assess which joints or muscle groups underlie functional abnormalities. Thus, in order to obtain a quantitative and objective evaluation of function after TIO, it is necessary to employ more detailed and quantitative measurement techniques such as gait analysis (Kolk et al. 2014; Lindemann et al. 2006; Nantel et al. 2009; Rosler et al. 2000). In addition to gait analysis, muscle strength measurements are valuable to assess the biomechanical properties of the operated limb (Lin et al. 2007).

To our knowledge, there have been no reports on the impact of TIO at such a detailed functional level. The information obtained from gait analysis could provide a better assessment of the long-term effects of this surgery. It can be used to inform the, usually young-adult, patients about their expected walking ability after the operation (van Hellemondt et al. 2005). It also allows comparing the functional outcome of TIO surgery to that of other treatment options such as Ganz's osteotomy (Ganz et al. 1988), for which gait analysis studies have been performed (Karam et al. 2011; Pedersen et al. 2006; Sucato et al. 2010). Several decrements (e.g., in walking speed and hip flexion pull-off power) after Ganz's osteotomy have been found (Karam et al. 2011; Sucato et al. 2010). Since the surgical approach is slightly different between TIO (usually a modified Smith-Peterson approach) and Ganz's osteotomy (usually either a classic Smith-Peterson or an abductor-sparing direct anterior approach), abnormalities in gait parameters after these respective operations may be related to the approach. Furthermore, the identification of specific gait and strength deficits might be useful for improving surgical techniques or postoperative rehabilitation protocols that may further enhance the functional outcome.

This study aimed to investigate the long-term outcome of TIO in terms of biomechanics of gait and muscle strength. Specifically, our objectives were to determine deviations in (1) spatiotemporal parameters, hip joint angles and joint moments during gait, and (2) hip and knee muscle strength in patients who had undergone TIO between two and ten years ago. We compared the results between the operated and non-operated limb and between patients and healthy controls.

Methods

Participants

Twelve women who had undergone TIO and eight healthy women in the same age range participated in this study. The indication for TIO was symptomatic hip dysplasia with a spherical femoral head, and without major damage to the cartilage (van Hellemondt et al. 2005). All patients were operated in the Sint Maartenskliniek, Nijmegen, The Netherlands by the same experienced surgeon. The surgical procedure (modified Tönnis osteotomy) has been described in detail (Kooijman et al. 1990). Patients between 18 and 70 years who had undergone a unilateral TIO between January 2003 and June 2010 were eligible for inclusion. This time window ensured that rehabilitation had been completed. Rehabilitation consisted of regular mobilization of the hip joint and strengthening exercises for the muscles of the hip region, and lasted for 3-12 months, depending on the patient's individual speed of recovery. In total, 54 patients were screened, of whom 34 were eligible for inclusion. Of those, 18 patients were willing to participate, and 12 were included after screening for exclusion criteria. We excluded patients that had any disease or other condition that could affect their gait, including severe hip pain, as well as patients with a Body Mass Index (BMI)>30 kg/m^2 because of difficulties in marker placement for gait analysis. Selection was unspecific regarding gender, but all 12 included patients were women.

The study procedure was approved by the local ethical committee of the region Arnhem-Nijmegen, the Netherlands (study code 2012/065). A written informed consent was obtained from each subject.

Clinical assessment

The participants were invited to the gait laboratory of the Radboud university medical center, Nijmegen, The Netherlands for a combined gait and muscle strength assessment session. We also obtained the Oxford (Dawson et al. 1996; Murray et al. 2007) (range 0-48) and Harris Hip Score (Harris 1969) (range 0-100) from the patients during a break in the session.

Gait analysis

The participants walked barefoot on an 8 m long walkway at self-selected comfortable walking speed. An integrated data collection was performed including three-dimensional motion capture with synchronized force plate recordings. A six-camera digital optical motion capture system (Vicon MX, Oxford, UK) was used to record the position of 35 retro-reflective markers placed on the lower limb and torso (100 Hz). The standard Vicon Plug-in-Gait marker set was used, with additional markers placed on the anterior side of the thigh and lower leg at 1/3 and 2/3 segment length, and on the fifth metatarsal head of the foot. Two custom-made force plates (AMTI, Watertown, MA, USA), embedded level in the laboratory floor measured ground reaction forces (1000 Hz) during the stance phase of the gait cycle.

No specific instructions were given other than 'walk naturally' to prevent participants from targeting the force plates. Trials were repeated until six successful trials had been recorded,

where 'successful' was defined as a trial in which each foot cleanly struck one of the two force plates. The gait analysis data of one patient and one control subject had to be discarded due to technical problems, leaving a group of 11 patients and 7 controls available for the gait analysis part of the study.

Data analysis

Heel strike and toe off events were identified using thresholding of ground reaction force data (heel contact when F>20 N, toe off when F<20 N). Spatiotemporal parameters were subsequently calculated based on a combination of these events and the heel and toe marker position data.

A 21 degrees of freedom kinematic model ('GaitLowerExtremityModel', as available in the AnyBody Managed Model Repository 1.5.1) consisting of trunk, pelvis, thigh, shank, talus and foot segments was scaled to each subject based on the marker trajectories using the AnyBody Modeling System (version 5.3.1, AnyBody Technology A/S, Aalborg, Denmark). The marker trajectories were initially filtered with a 5 Hz 2nd order Butterworth low-pass filter. Force plate data were low-pass filtered at 12 Hz with a 2nd order Butterworth filter. The model was based on the kinematic part of the Twente Lower Extremity Model dataset (Klein Horsman et al. 2007). After this procedure, lower limb joint angles were obtained by solving the inverse kinematics using the optimized parameters. At each joint, ideal torque generators were added. The segment masses were scaled using common scaling laws (Winter 1991), available in AnyBody. The model marker positions, segment lengths and knee joint axes were then optimized using a parameter optimization algorithm (Andersen et al. 2010). Finally, the kinematics and ground reaction forces were used as input for an inverse dynamic analysis (Damsgaard et al. 2006), in which joint moments were calculated in the local (ISB (Wu et al. 2002)) reference frames.

Our outcome variables of interest were spatiotemporal parameters, hip joint angles and moments in the sagittal and frontal planes. Each of these variables was averaged across trials to obtain subject 'ensemble' averages both for the operated and the non-operated limbs. The moments were normalized to the body weight (BW) and height (Ht) of the subject (%BW*Ht). In the sagittal plane, we determined the peak flexion and extension angles and moments. In the frontal plane, we used the adduction angle at 20% of the gait cycle in the analysis, since there was a peak in the angle at that particular phase of the gait cycle. Owing to the M-shaped curve of hip abduction moments during gait, we extracted two peak values, one in the first and one in the second half of the stance phase. For the healthy controls, we used the mean of the left and right limbs in the analyses.

Muscle strength

Isometric maximum voluntary contractions were recorded for hip abduction, and knee flexion and extension. Hip abduction strength was tested in side-lying position, with the tested hip at 0° flexion and 0° adduction, and the knee extended (Figure 3.1A). The non-tested hip was flexed at 45°, and the knee was flexed at 90° in order to prevent the contralateral limb from contributing to the maximum strength effort. The end piece (soft Velcro strap) of

a force transducer was applied just proximal to the femoral epicondyles perpendicular to the limb, and the other end of the transducer was rigidly attached to the testing bench.

For maximum knee flexion strength testing, subjects sat on the edge of a testing bench positioned close to a wall (Figure 3.1B). The knee and hip were flexed at 90°, and the end piece of the force transducer was applied just proximal to the malleoli. The other end was rigidly fixed to the wall, level with the end piece. During the contractions, manual pressure was applied by an assistant proximal to the top of the tested knee to prevent it from rising. Knee extension was tested in a custom-built chair with vertical backrest, with the knee and hip flexed at 90°, and with the end piece of the force transducer applied just proximal to the malleoli (Figure 3.1C). The subject was strapped to the chair to prevent the waist from rising.

Participants performed three maximum isometric contractions for four seconds each, separated by 30 seconds of rest. All subjects received the same verbal encouragements during the contractions to achieve maximum effort. The highest recorded maximal force was multiplied by the moment arm to the joint centre of the tested joint to obtain peak torque values. Raw data was low-pass filtered at 6 Hz with a 2nd order Butterworth filter and the peak torque was normalized by body weight.

Statistical analysis

Student's t-tests were used for comparing group characteristics, spatiotemporal parameters, kinematics and muscle strength tests between the patient and control groups. Paired samples t-tests were used for comparisons between operated and non-operated limbs. Hip joint moments during gait were tested with repeated-measures ANOVAs; one with phase of gait cycle (early and late stance) and limb (operated and non-operated) as within-subjects factors, and another with phase of gait cycle (early and late stance) as within-subjects factor and group (operated limb of patients and controls) as between-subjects factor. Post-hoc paired samples t-tests were used if the ANOVA indicated significant differences between the operated and the non-operated limb. The significance level was set at $p \leq 0.05$. For the muscle strength data, significance was set at $p \leq 0.01$ because of the number of t-tests performed (12). IBM SPSS Statistics 20.0.0.1 was used for all statistical analyses.

Results

Group characteristics

Descriptive characteristics of the patients who had undergone TIO and of the controls are shown in Table 3.1. No significant group differences were found for age, weight, height, or BMI. The participating patients were between 59 and 111 months post surgery. Their average Harris hip score was 'good' (84 points), and their average Oxford hip score was 'excellent' (42 points).

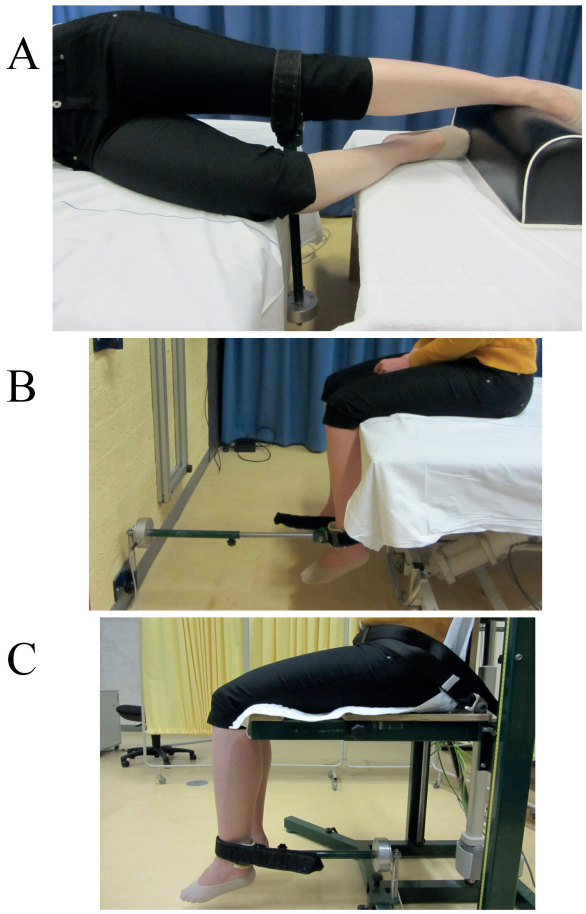

Figure 3.1. Experimental setup for muscle strength measurements. These were performed for (A) hip abduction, (B) knee flexion, and (C) knee extension. In all cases, the end piece (soft Velcro strap) of the force transducer was applied perpendicular to the limb, and the other end was rigidly attached to either a clinical testing bench, a wall, or a custom-built chair.

Spatiotemporal parameters

Spatiotemporal parameters are shown in Table 3.2. None of the parameters differed significantly between the groups. Within the patient group, the step length of the operated leg was 0.03 m smaller than that of the non-operated leg ($p = 0.019$), whereas the stance time was 1.2% longer ($p = 0.039$).

Kinematic gait parameters

The kinematics of the operated and non-operated limb did not differ significantly from controls (Figure 3.2A and 3.2C). There were also no differences between the operated and non-operated limbs.

Kinetic gait parameters

Hip abduction moments during stance are shown in Figure 3.2D. The operated limb had a different abduction moment pattern than the non-operated limb during the stance phase, as demonstrated by a significant phase x limb interaction effect ($F_{1,10} = 5.78$, $p = 0.037$); in early stance, the abduction moment in the operated limb was non-significantly lower than in the non-operated limb ($p = 0.129$), whereas in late stance it was non-significantly higher ($p = 0.192$). The main effect of limb was not significant ($F_{1,10} = 0.12$, $p = 0.742$). The operated limb was not significantly different from controls (group: $F_{1,16} = 0.00$, $p = 0.949$; phase x group: $F_{1,16} = 2.63$, $p = 0.125$).

Sagittal plane hip moments during stance are shown in Figure 3.2B. The hip flexion and extension moments generated by the operated limb of the patients were not different from the unaffected limb (limb: $F_{1,10} = 0.03$, $p = 0.861$, phase x limb: $F_{1,10} = 1.51$, $p = 0.247$). The operated limb did not differ from controls (group: $F_{1,16} = 2.62$, $p = 0.125$, phase x group: $F_{1,16} = 0.28$, $p = 0.601$).

Muscle strength

Abduction strength was significantly lower than healthy controls in both the operated and the non-operated limb (Figure 3.3), whereas differences in knee flexion and extension strength between patients and controls did not reach significance. The operated and non-operated limbs did not differ in any of the strength measurements.

Discussion

In this study, we found that patients who had undergone TIO (on average 80 months ago) did not have major abnormalities in their gait pattern compared to controls, but did exhibit subtle asymmetries between the operated and non-operated limbs. The operated limb had a smaller step length and longer stance time compared to the non-operated limb. In addition, the abduction moment pattern during the stance phase was significantly different between the operated and non-operated limbs. In terms of muscle strength, a bilateral abduction strength deficit was found. Muscle strength did not differ between the operated and the non-operated limb for any of the tested joints.

Interestingly, we found subtle asymmetries in hip abduction moments between the operated and non-operated limbs. This may represent a more cautious walking pattern, by enabling a more gradual transfer of the body's centre of mass over the operated limb, thereby reducing the peak hip abduction moment in early stance. This does not seem to be related to a lack of hip abductor strength, as there was no difference in strength between the operated and non-operated leg. The reduced step length and prolonged stance duration that we found in the operated limb, albeit rather small, may also point to an integral strategy in the frontal plane reflecting a more cautious walking pattern.

Table 3.1 Characteristics of patients after triple innominate osteotomy and controls

	TIO patients n = 12	**Controls** n = 8	**p***
Age (years)	34 (12)	33 (10)	0.910
Weight (kg)	66.8 (5.2)	66.2 (11.6)	0.894
Height (m)	1.67 (0.07)	1.72 (0.07)	0.343
BMI (kg/m²)	23.9 (2.4)	22.3 (3.0)	0.232
Time since surgery (months)	80 (18)		
Operated limb	L: 3, R: 9		
Harris Hip Score	84 (15)		
Oxford Hip Score	42 (5)		

Data are presented as mean (SD). * Student's t-test for weight and BMI, Mann-Whitney U test for age and height.

Table 3.2 Spatiotemporal parameters of patients after triple innominate osteotomy and controls

	TIO patients	**Controls**	**p***
Walking speed (m/s)	1.32 (0.14)	1.34 (0.22)	0.752
Cadence (steps/min)	116.7 (5.5)	115.2 (13.1)	0.733
Step length operated limb (m)	0.66‡ (0.08)	0.69† (0.06)	0.386
Step length non-operated limb (m)	0.69‡ (0.05)	0.69† (0.06)	0.924
Stride length (m)	1.35 (0.12)	1.40 (0.11)	0.477
Stance duration operated limb (% of gait cycle)	61.2§ (2.1)	60.0† (1.5)	0.202
Stance duration non-operated limb (% of gait cycle)	60.0§ (2.0)	60.0† (1.5)	0.961

Data are presented as mean (SD).
* Student's t-test.
† Mean of both legs.
‡ Significantly different between operated and non-operated limb (paired t-test: p = 0.019).
§ Significantly different between operated and non-operated limb (paired t-test: p = 0.039).

Compared to healthy controls, we found significantly reduced hip abduction strength in patients who had undergone TIO. Hip abductor weakness is a common finding in patients with hip dysplasia, frequently resulting in Trendelenburg's sign during gait (Romano et al. 1996; Steel 1973). Hence, the persisting weakness that we found may be reflective of severe muscle atrophy that had developed over many years prior to surgery and that did not fully recover despite postoperative rehabilitation. Alternatively, our patient group may have been less physically active than the controls, resulting in poorer muscle strength. We indeed observed a general trend of muscle strength reduction in all the tests performed, but

the pronounced weakness in hip abduction argues against an overall reduction in physical activity being the only responsible factor.

Our finding that hip abduction strength was substantially lower in patients compared to controls, whilst no main effect of group could be demonstrated for hip abduction moments during gait implies that the patients walked at a higher percentage of their maximum capacity. This may eventually result in gait pattern changes when patients become fatigued, as it has been shown that human gait is relatively sensitive to weakness in the hip abductor muscle group (van der Krogt et al. 2012). A gait pattern typical of abductor weakness (Trendelenburg's sign) may then emerge, involving pelvic drop at the contralateral side. This increases hip joint stress in the operated hip due to a decrease in joint contact area (Westhoff et al. 2006), which may speed up the development of osteoarthritis in the operated hip.

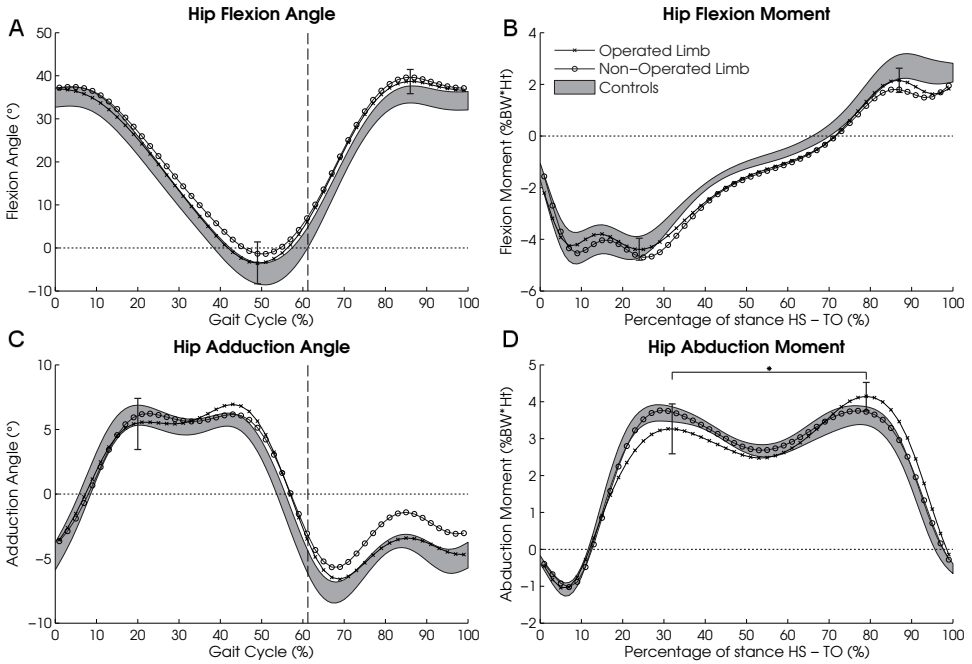

Figure 3.2. Hip kinematics and kinetics of patients after triple innominate osteotomy and healthy controls. Shown are (A) sagittal plane kinematics, (B) sagittal plane kinetics, (C) frontal plane kinematics, and (D) frontal plane kinetics. The kinematic data are normalized to full gait cycle (heel strike to ipsilateral heel strike); the kinetic data are normalized to the stance phase of the gait cycle (heel strike to ipsilateral toe off). Standard deviations of the mean of the operated limb are shown at the time points that were tested statistically (maximum extension angle, maximum flexion angle, hip adduction angle at 20% of the gait cycle, maximum extension moment, maximum flexion moment, and maximum hip abduction moment in early and late stance). The shaded areas represent equal boundaries of ±1SE for controls. The horizontal bracket and star in (D) indicate the significant interaction effect between the operated and the non-operated limb during the stance phase.

The clinical results of TIO at comparable follow-up times are generally 'good', 'excellent', or 'improved compared with before the operation' (de Kleuver et al. 1997; Hsin et al. 1996; Janssen et al. 2009), which is congruent with the results of our study. Hence, the functional status of our study population appears to be representative of the TIO group at large. To our knowledge, up to this point no studies have been published that employed gait analysis or maximum strength measurements to describe the functional outcome after TIO surgery. In contrast, results from gait analyses have been reported for patients after Ganz's periacetabular osteotomy (Ganz et al. 1988), which conceptually is a rather similar procedure to the modified Tönnis osteotomy used here (Kooijman et al. 1990). Our findings that patients after TIO did not demonstrate major gait deviations compares well to previous

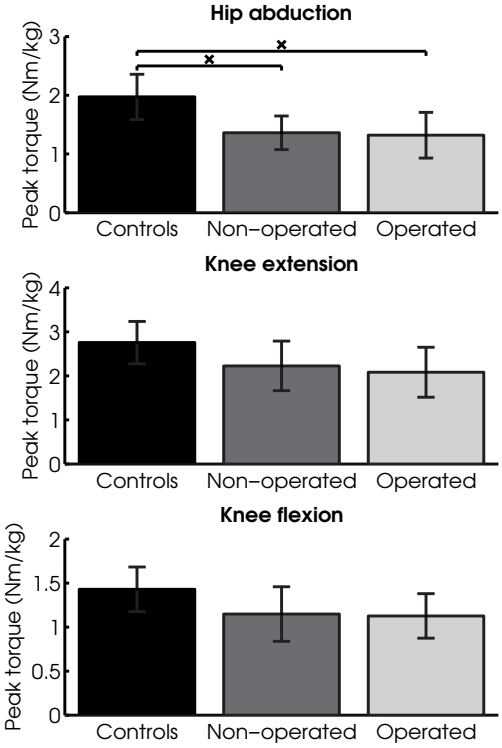

Figure 3.3. Maximum generated torque of patients who had undergone triple innominate osteotomy and controls. Peak torque values are given in Newton-meters, normalized to body weight. The error bars represent equal boundaries of ±1SD. [x] Indicates a statistically significant difference ($p \leq 0.01$).

results from patients after Ganz's osteotomy. After that surgery, no statistically significant differences from controls could be demonstrated in sagittal hip joint kinematics and kinetics (Pedersen et al. 2004; Pedersen et al. 2006) or frontal plane kinetics (Sucato et al. 2010). Similarly, Karam et al. investigated spatiotemporal gait parameters before and one year after Ganz's osteotomy (Karam et al. 2011) and found post-operative walking velocities, stride lengths and cadences very similar to our results. Thus, the relatively small differences in the

surgical approach between TIO and Ganz's osteotomy (even if it was abductor-sparing, as in the case of Sucato et al. (2010) do not appear to play a major role in long-term functional outcome.

Our study has certain limitations. First, we invited 34 patients to participate in the study, but only 18 responded, out of which 12 patients could be included. The non-responders and excluded patients might have had more pain or functional limitations than those included. Moreover, since there were only women in our study population, the results might not apply to men who underwent TIO. Second, although the study groups were similar with regard to age, gender, height, weight and BMI, we did not take confounding factors into account such as general activity level or participation in sports. As such, it is possible that the patients were less active than the controls and that, therefore, they had less muscle strength around the hip and knee joints. Third, we did not perform gait and strength measurements before the surgery. Such analyses could reveal whether the deviations in gait observed post-operatively in this study stem from pre-operatively adopted gait patterns. Fourth, we did not adjust the geometry of the operated hip joint in the AnyBody model. The joint's centre of rotation in our patients might have been slightly altered by the TIO, thereby influencing the joint moment calculations.

Conclusions

This study showed that patients who underwent TIO generally recovered well from their operation with regard to gait, but did exhibit subtle asymmetries between the operated and non-operated limbs several years after surgery. Muscle strength deficits were found bilaterally in hip abduction. Although the differences observed in gait were subtle, they may become clinically important in young or active patients who engage in high-level activities over many years. Thus, in further research in this patient group it is recommended to focus on gait adaptations after prolonged walking.

Acknowledgements

We gratefully acknowledge financial support by the European Commission FP7 Programme for the TLEMsafe project (http://www.tlemsafe.eu). The funding agency played no role in design, collection, analysis, interpretation of data, writing process, or in the decision to submit the paper for publication. We thank drs. Arno M. ten Ham for useful comments on the manuscript draft.

References

Andersen, M.S. , M. Damsgaard, B. MacWilliams, and J. Rasmussen. 2010. A computationally efficient optimisation-based method for parameter identification of kinematically determinate and over-determinate biomechanical systems, Comp. Meth. Biomech. Biomed. Eng., 13: 171-183.

Damsgaard, M., J. Rasmussen, S. T. Christensen, E. Surma, and M. de Zee. 2006. Analysis of musculoskeletal systems in the AnyBody Modeling System, Simul. Mod. Pract. Theory, 14: 1100-1111.

Dawson, J., R. Fitzpatrick, A. Carr, and D. Murray. 1996. Questionnaire on the perceptions of patients about total hip replacement, J. Bone Joint Surg. Br., 78: 185-190.

de Kleuver, M., M. A. Kooijman, P. W. Pavlov, and R. P. Veth. 1997. Triple osteotomy of the pelvis for acetabular dysplasia: results at 8 to 15 years, J. Bone Joint Surg. Br., 79: 225-229.

Faciszewski, T., S. S. Coleman, and G. Biddulph. 1993. Triple innominate osteotomy for acetabular dysplasia, J. Pediatr. Orthop., 13: 426-430.

Ganz, R., K. Klaue, T. S. Vinh, and J. W. Mast. 1988. A new periacetabular osteotomy for the treatment of hip dysplasias. Technique and preliminary results, Clin. Orthop. Relat. Res.: 26-36.

Guille, J. T., E. Forlin, S. J. Kumar, and G. D. MacEwen. 1992. Triple osteotomy of the innominate bone in treatment of developmental dysplasia of the hip, J. Pediatr. Orthop., 12: 718-721.

Harris, W. H. 1969. Traumatic arthritis of the hip after dislocation and acetabular fractures: treatment by mold arthroplasty. An end-result study using a new method of result evaluation, J. Bone Joint Surg. Am., 51: 737-755.

Hsin, J., R. Saluja, R. E. Eilert, and J. D. Wiedel. 1996. Evaluation of the biomechanics of the hip following a triple osteotomy of the innominate bone, J. Bone Joint Surg. Am., 78: 855-862.

Janssen, D., K. Kalchschmidt, and B. D. Katthagen. 2009. Triple pelvic osteotomy as treatment for osteoarthritis secondary to developmental dysplasia of the hip, Int. Orthop., 33: 1555-1559.

Karam, M.D., G. Yubo, and T. McKinley. 2011. Assessment of walking pattern pre and post peri-acetabular osteotomy, Iowa Orthop. J., 31: 83-89.

Klein Horsman, M. D., H. F. Koopman, F. C. van der Helm, L. P. Prose, and H. E. Veeger. 2007. Morphological muscle and joint parameters for musculoskeletal modelling of the lower extremity, Clin Biomech (Bristol, Avon), 22: 239-247.

Kolk, S., M. J. Minten, G. E. van Bon, W. H. Rijnen, A. C. Geurts, N. Verdonschot, and V. Weerdesteyn. 2014. Gait and gait-related activities of daily living after total hip arthroplasty: a systematic review, Clin Biomech (Bristol, Avon), 29: 705-718.

Kooijman, M. A., and P. W. Pavlov. 1990. Triple osteotomy of the pelvis. A review of 51 cases, Clin. Orthop. Relat. Res.: 133-137.

Learmonth, I. D., C. Young, and C. Rorabeck. 2007. The operation of the century: total hip replacement, Lancet, 370: 1508-1519.

Lin, D. H., M. H. Jan, T. K. Liu, Y. F. Lin, and S. M. Hou. 2007. Effects of anterolateral minimally invasive surgery in total hip arthroplasty on hip muscle strength, walking speed, and functional score, J. Arthrop., 22: 1187-1192.

Lindemann, U., C. Becker, I. Unnewehr, R. Muche, K. Aminin, H. Dejnabadi, T. Nikolaus, W. Puhl, K. Huch, and K. E. Dreinhofer. 2006. Gait analysis and WOMAC are complementary in assessing functional outcome in total hip replacement, Clin. Rehabil., 20: 413-420.

Murray, D. W., R. Fitzpatrick, K. Rogers, H. Pandit, D. J. Beard, A. J. Carr, and J. Dawson. 2007. The use of the Oxford hip and knee scores, J Bone Joint Surg Br, 89: 1010-1014.

Nakamura, S., S. Ninomiya, Y. Takatori, S. Morimoto, and T. Umeyama. 1998. Long-term outcome of rotational acetabular osteotomy: 145 hips followed for 10-23 years, Acta Orthop. Scand., 69: 259-265.

Nantel, J., N. Termoz, P. A. Vendittoli, M. Lavigne, and F. Prince. 2009. Gait patterns after total hip arthroplasty and surface replacement arthroplasty, Arch. Phys. Med. Rehabil., 90: 463-469.

Pedersen, E. N. G., T. Alkjaer, K. Soballe, and E. B. Simonsen. 2006. Walking pattern in 9 women with

hip dysplasia 18 months after periacetabular osteotomy, Acta Orthop., 77: 203-208.
Pedersen, E. N., E. B. Simonsen, T. Alkjaer, and K. Soballe. 2004. Walking pattern in adults with congenital hip dysplasia: 14 women examined by inverse dynamics, Acta Orthop. Scand., 75: 2-9.
Romano, C. L., C. Frigo, G. Randelli, and A. Pedotti. 1996. Analysis of the gait of adults who had residua of congenital dysplasia of the hip, J. Bone Joint Surg. Am., 78: 1468-1479.
Rosler, J., and C. Perka. 2000. The effect of anatomical positional relationships on kinetic parameters after total hip replacement, Int. Orthop., 24: 23-27.
Steel, H. H. 1973. Triple osteotomy of the innominate bone, J. Bone Joint Surg. Am., 55: 343-350.
Sucato, D. J., K. Tulchin, M. W. Shrader, A. DeLaRocha, T. Gist, and G. Sheu. 2010. Gait, Hip Strength and Functional Outcomes After a Ganz Periacetabular Osteotomy for Adolescent Hip Dysplasia, J. Pediatr. Orthop., 30: 344-350.
Tonnis, D., K. Behrens, and F. Tscharani. 1981. [A new technique of triple osteotomy for turning dysplastic acetabula in adolescents and adults (author's transl)], Z. Orthop. Ihre Grenzgeb., 119: 253-265.
van der Krogt, M. M., S. L. Delp, and M. H. Schwartz. 2012. How robust is human gait to muscle weakness?, Gait Posture, 36: 113-119.
van Hellemondt, G. G., H. Sonneveld, M. H. Schreuder, M. A. Kooijman, and M. de Kleuver. 2005. Triple osteotomy of the pelvis for acetabular dysplasia: results at a mean follow-up of 15 years, J. Bone Joint Surg. Br., 87: 911-915.
Wamper, K. E., I. N. Sierevelt, R. W. Poolman, M. Bhandari, and D. Haverkamp. 2010. The Harris hip score: Do ceiling effects limit its usefulness in orthopedics?, Acta Orthop., 81: 703-707.
Westhoff, B., A. Petermann, M. A. Hirsch, R. Willers, and R. Krauspe. 2006. Computerized gait analysis in Legg Calve Perthes disease--analysis of the frontal plane, Gait Posture, 24: 196-202.
Winter, D.A. 1991. The biomechanics and motor control of human movement: Normal, elderly and pathological (University of Waterloo Press).
Wu, G., S. Siegler, P. Allard, C. Kirtley, A. Leardini, D. Rosenbaum, M. Whittle, D. D. D'Lima, L. Cristofolini, H. Witte, O. Schmid, I. Stokes, Standardization, and Biomechanics Terminology Committee of the International Society of. 2002. ISB recommendation on definitions of joint coordinate system of various joints for the reporting of human joint motion--part I: ankle, hip, and spine. International Society of Biomechanics, J Biomech, 35: 543-548.

Chapter 3b

Gait and lower limb muscle strength in women with congenital hip dysplasia after total hip arthroplasty with femoral shortening

(abstract only)

Kolk, S., Rijnen, W.H., Verdonschot, N., Weerdesteyn, V.

Abstract

Background: Congenital hip dysplasia may, in severe cases, lead to cranial migration of the femoral head. To alleviate the associated pain and walking problems, total hip arthroplasty with acetabular reconstruction and femoral shortening can be performed. The purpose of this study was to quantify the functional outcome of this procedure.

Methods: We performed gait analyses and isometric hip (abduction and extension) and knee (flexion and extension) muscle strength tests in seven women who had undergone a unilateral total hip arthroplasty with femoral shortening (39±13y, time post-surgery: 45±52m). They walked at self-selected walking speed and wore their own shoes, which corrected the residual leg-length discrepancy. Kinematic and kinetic data were captured with a three-dimensional motion capture system (Vicon MX) and force plates embedded level in the laboratory floor. The data were analyzed using AnyBody 5.3.1 (AnyBody Technology A/S). We compared the results to reference values obtained from seven healthy peers (31±10y).

Results: Walking speed, cadence and step length were similar between patients and controls, but patients had a shorter single support phase on the operated side. The adduction angle in the operated limb was significantly larger than in the non-operated limb (Figure 3.4A). Kinetic deviations in the operated limb included lower hip abduction moments (Figure 3.4B; compared to controls), and a lower hip extension moment (compared to the non-operated limb). The operated limb had lower hip and knee muscle strength compared with controls in all directions, which was also true for hip strength on the non-operated side. The operated limb was weaker than the non-operated limb except for knee flexion.

Conclusions: Our results demonstrate that the patients had persisting gait deviations in the frontal plane with asymmetries between the operated and non-operated side. The observed gait deviations point to the occurrence of Trendelenburg's sign to compensate for abductor weakness. This is supported by the reduced abductor muscle strength obtained in the isometric measurements. It is unknown if there is potential to improve in this area, because of plausible structural changes in the muscle tissue stemming from many years of functioning at non-optimal lengths. Our results may help in informing patients about their expected walking ability.

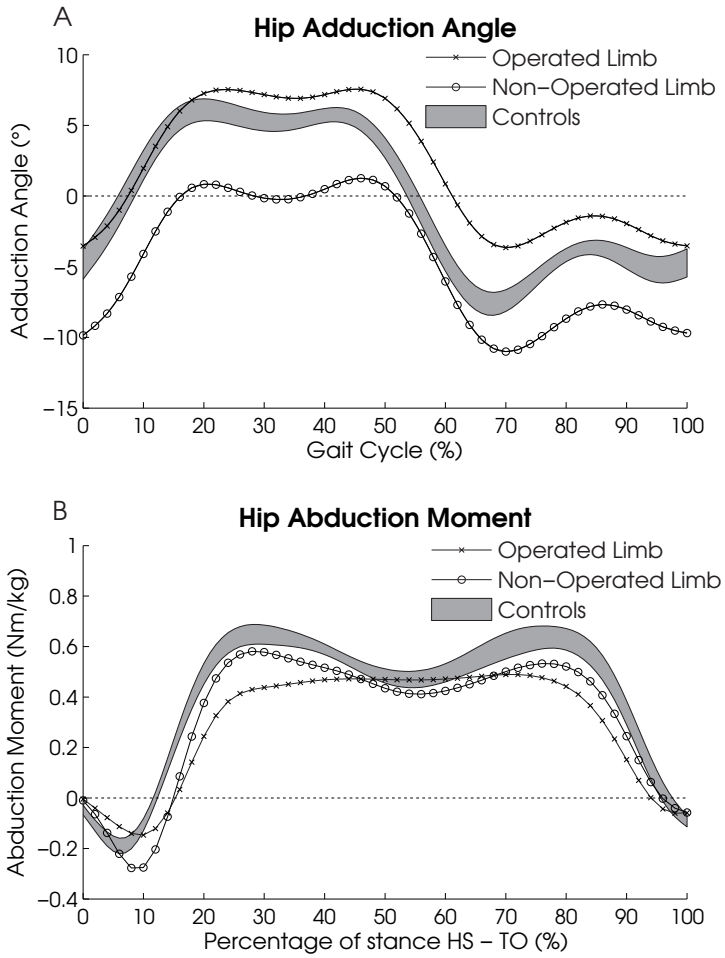

Figure 3.4. Frontal plane hip kinematics (A) and kinetics (B) of patients after total hip arthroplasty and healthy controls. The kinematic data are normalized to full gait cycle (heel strike to ipsilateral heel strike); the kinetic data are normalized to the stance phase of the gait cycle (heel strike to ipsilateral toe off). The shaded areas represent equal boundaries of ±1SE for controls.

Chapter 4

Can orthopedic oncologists predict functional outcome in patients with sarcoma after limb salvage surgery in the lower limb? A nationwide study.

Published as:

Kolk, S., Cox, K., Weerdesteyn, V., Hannink, G., Bramer, J., Dijkstra, S., Jutte, P., Ploegmakers, J., van de Sande, M., Schreuder, H., Verdonschot, N., and van der Geest, I. 2014. Can orthopedic oncologists predict functional outcome in patients with sarcoma after limb salvage surgery in the lower limb? A nationwide study, Sarcoma: 436598.

Abstract

Background: Accurate predictions of functional outcome after limb salvage surgery (LSS) in the lower limb are important for several reasons, including informing the patient preoperatively and, in some cases, deciding between amputation and LSS. This study aimed to elucidate the correlation between surgeon-predicted and patient-reported functional outcome of LSS in the Netherlands.

Methods: Twenty-three patients (between six months and ten years after surgery) and five independent orthopedic oncologists completed the Toronto Extremity Salvage Score (TESS) and the RAND-36 physical functioning subscale (RAND-36 PFS). The orthopedic oncologists made their predictions based on case descriptions (including MRI scans) that reflected the preoperative status.

Results: The correlation between patient-reported and surgeon-predicted functional outcome was "very poor" to "poor" on both scores (r^2 values ranged from 0.014 to 0.354). Patient-reported functional outcome was generally underestimated, by 8.7% on the TESS and 8.3% on the RAND-36 PFS. The most difficult and least difficult tasks on the RAND-36 PFS were also the most difficult and least difficult to predict, respectively. Most questions had a "poor" intersurgeon agreement.

Conclusions: It was difficult to accurately predict the patient-reported functional outcome of LSS. Surgeons' ability to predict functional scores can be improved the most by focusing on accurately predicting more demanding tasks.

Introduction

Limb salvage surgery (LSS) rather than amputation is the operation of choice in 70-85% of all malignant bone and soft tissue lower limb sarcomas (Gebhardt 2002; Veth et al. 2003). Since the oncological results for amputation and LSS in the surgical treatment of sarcomas are comparable (Ghert et al. 2005; Niimi et al. 2008), the decision to perform an amputation or LSS is based on the tumor size, the tumor location, patient preferences, the expected risk of complications and multiple reoperations, and the expected functional outcome (Ghert et al. 2005). If it is surgically possible, LSS is generally the preferred treatment, unless a poor functional outcome is expected. It has been shown that the functional outcome of LSS is superior to amputation, with the exception of below-knee amputation, which yields a similar function as limb salvage (Aksnes et al. 2008). The expected functional outcome of patients after LSS is thus an important part of the preoperative decision making process for the surgical treatment.

Several known predictors of functional outcome include tumor size, location, grade, bone resection, muscle involvement, use of radiotherapy and motor nerve sacrifice (Davis et al. 2000). The functional outcome is predicted by the surgeon based on these parameters combined with his/her clinical experience. However, to the best of our knowledge, there are no reports about how well surgeons are able to actually predict functional outcome after LSS. Insight into the level of accuracy of these predictions is important for several reasons. First, accurate predictions of functional outcome are highly relevant in informing the patient preoperatively about the expected final functional outcome. Second, in some cases, the predictions are helpful in deciding between amputation or LSS. Third, information about the correlation between predicted functional outcome and patient-reported functional outcome provides valuable information for surgeons in training.

In this study, we (1) aimed to establish whether orthopedic oncologists can accurately predict patient-reported functional outcome of LSS in the treatment of sarcoma in the lower limb in a selected group of patients. We also (2) examined whether there was a tendency to over- or underestimate patient-reported functional outcome. Additionally, (3) we sought to identify which items on the functional outcome scores were least difficult and which were most difficult to predict, and whether the surgeons agreed amongst themselves (interrater reliability) in their predictions.

Materials and Methods

Patients

We selected patients who had undergone a LSS for a sarcoma in the lower limb from a database of orthopedic oncologic patients at the department of orthopedic surgery of the Radboud University Medical Center (RUMC), Nijmegen, The Netherlands. The database contained 216 patients who had undergone LSS or amputation for any type of tumor in the hip or knee region. We selected patients using the following inclusion criteria: follow-up at least six months after the surgery (before July 1, 2012) for patients without

adjuvant treatment and at least twelve months for patients with adjuvant treatment, a maximum follow-up of ten years (after February 1, 2003), and age between 18-70 years, and preoperative MRI-scans had to be available. The follow-up of at least six months was chosen because functional scores tend to plateau within that time frame (Davis et al. 2000; Davis et al. 1996). We excluded patients who had a bone tumor with an intact cortical bone, as almost no functional deficits were expected to occur in those patients. Patients who had suffered local recurrence or complications that required reoperation in the last six months before the study were excluded. A flow chart of the patient selection is shown in Figure 4.1. Twenty-four patients were eligible for inclusion in the study, of whom 23 were successfully contacted. All 23 patients were included in the study. The study procedures were approved by the local ethical committee of the RUMC. Written informed consent was obtained from all participants.

Materials

To evaluate the functional outcome we used the Toronto Extremity Salvage Score (TESS) for the lower extremity and the RAND-36 physical functioning subscale (RAND-36 PFS). The TESS is a patient-reported questionnaire that has been specifically designed to measure the physical functional status of patients after limb-salvage surgery (Davis et al. 1996). It contains 30 questions, and the final score ranges from 0% to 100%, 100% being the highest achievable score. The RAND-36 PFS is intended to measure physical functioning in any patient cohort (van der Zee et al. 2012; van der Zee et al. 1996), which makes it more general than the TESS. Like the TESS, the RAND-36 PFS also is a patient-reported questionnaire. The RAND-36 PFS consists of ten questions, and the final score ranges from 0% to 100%, 100% being the highest achievable score. The RAND-36 PFS is identical to the SF-36 PFS. In addition to the TESS and RAND-36 PFS, we also used the RAND-36 pain subscale to examine postoperative pain levels. The RAND-36 pain subscale contains two questions; one regarding the amount of pain and one regarding the hindrance experienced due to pain when performing everyday activities in the previous four weeks (van der Zee et al. 2012; van der Zee et al. 1996). The final score ranges from 0% to 100%, where 100% represents no pain. We did not employ the Musculoskeletal Tumor Society score (Enneking et al. 1993), as that score is not patient-reported, and includes the domains of pain and emotional acceptance, which would have been impossible to predict solely on the basis of case descriptions.

A case description of each patient was made, which reflected the preoperative status of the patient. It contained the patient's age, sex, body mass index (BMI), tumor diagnosis, diagnostic MRI-scans, a description of the performed surgical procedure for tumor resection and reconstruction, whether the patient had received adjuvant pre- or postoperative chemo- or radiotherapy, and whether there were any complications from the surgery (a case example is shown in Figure 4.2). The information did not include follow-up time. If a reresection had been performed, the preoperative MRI scans from before the primary resection surgery were provided, rather than those made after the local recurrence. The case descriptions were distributed through a central electronic platform. Whenever bone was removed it was replaced by a tumor prosthesis and/or an allograft.

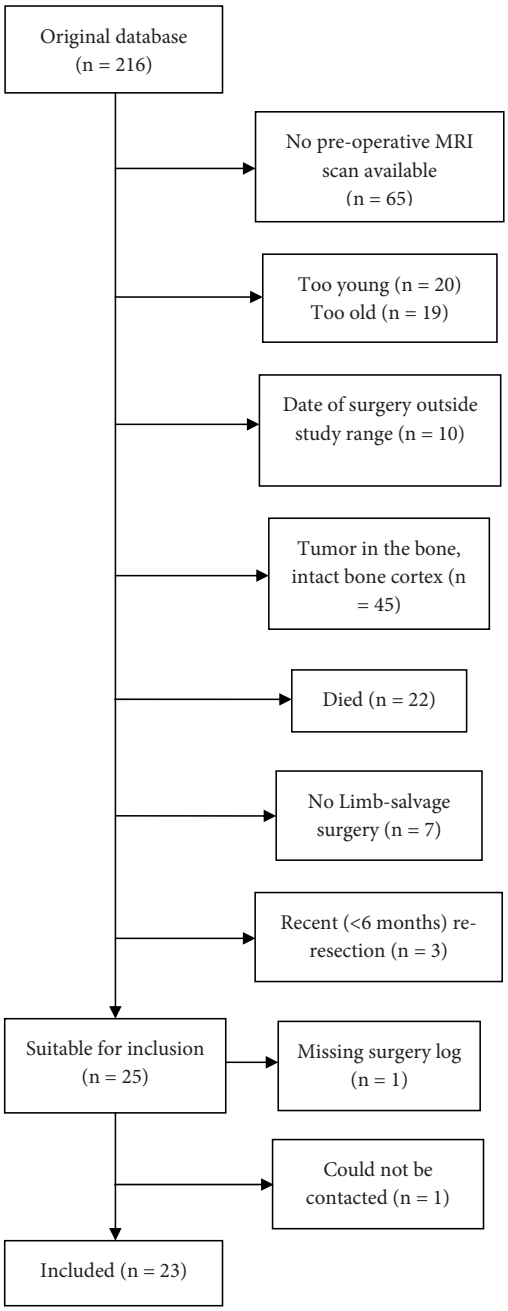

Figure 4.1. Flow chart of patient selection. Some patients fitted into multiple exclusion criteria (e.g., 'no pre-operative MRI scan available' and 'too old'); in such cases, the patient was counted as belonging to the first of those exclusion criteria.

Case 7: ♂ 37 years

BMI: 23,74 (83kg / 1m87^2)

Indication: Malignant fibrous hystiocytoma left distal femur, pre-treated with chemotherapy. An incision biopsy has been done on the left anterolateral side.

Surgical treatment: Extra-articular distal femur resection and reconstruction with tumour prosthesis.

Preoperative MRI:
Top row: Transversal (T1 – FS)
Middle row: Transversal (T1)
Bottom row: Sagittal (T1)

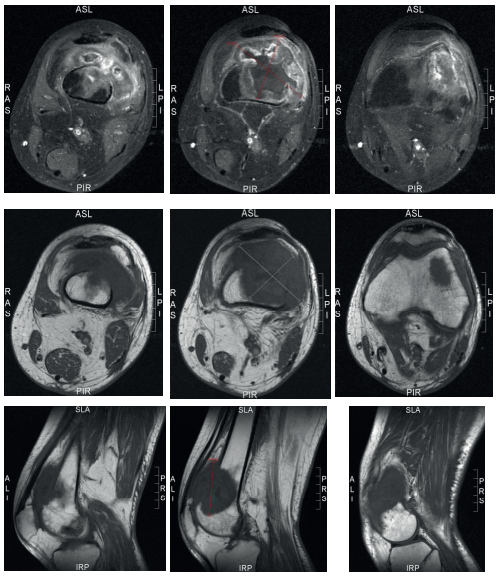

Figure 4.2. Example case as given to the orthopedic oncologists. This is patient 7 in Table 4.1.

Study procedures

The patients were interviewed about their current functional status in a structured telephone call (done by KC, an independent researcher who was not a medical doctor), consisting of the TESS, the RAND-36 PFS, and the RAND-36 pain subscale. Five independent orthopedic oncologists (JB, PD, PJ, JP, and MvdS), working in one of the other three Dutch orthopedic oncologic referral centers (other than the RUMC) participated in the study. They were asked to give a prediction of the total TESS score (one percentage for the total functional status of the patient without addressing all separate items), and a prediction of the ten individual items of the RAND-36 PFS, based on the case descriptions. They had never been involved in the treatment of the patients and were unaware of their patient-reported functional outcome. All orthopedic oncologists were experienced and specialized in orthopedic oncology. They were familiar with the employed functional scales, and were provided with a copy of the TESS questionnaire for reference.

Outcome measures and statistical analyses

Descriptive statistics were calculated and stated as mean ± standard deviation. We compared the patient-reported and surgeon-predicted TESS and RAND-36 PFS scores in three ways.

First, Pearson correlations were calculated between the patients' reported scores and individual surgeon predicted scores, as well as for the average scores of all the surgeons combined. The squared correlation coefficient, r^2- (coefficient of determination), represents the variation in the values of the patient-reported outcome that can be explained by variations in the value of the surgeon-predicted outcome (Taylor 1990). An r^2-value of 0.75-1.00 was

interpreted as a "very good" prediction, 0.50-0.74 as "good", 0.25-0.49 as "poor" and 0-0.24 as "very poor". The r^2-values were considered the primary outcome measure.

Second, the mean differences and 95% confidence intervals (95% CI) between the patient-reported scores on the TESS and RAND-36 PFS and the surgeon-predicted scores were calculated to reveal whether the predictions had a bias towards being too optimistic or pessimistic.

Third, the agreement between patient-reported and the median surgeon-predicted answers to the separate questions of the RAND-36 PFS were examined using percent agreement and Gwet's agreement coefficient (AC1). Compared with Cohen's Kappa (Cohen 1960, 1968), Gwet's AC1 has a more stable inter-rater reliability, and is less affected by prevalence and marginal probability (Wongpakaran et al. 2013). This allowed us to identify which questions were the least difficult and most difficult to predict. The intersurgeon agreement on each separate question was also calculated, using percent agreement and Gwet's AC1. To calculate the intersurgeon agreement on the TESS, we used the intraclass correlation coefficient (ICC; absolute single measure/absolute agreement). Agreement coefficients below 0.40 were considered to represent a "poor" agreement; between 0.40 and 0.59 'fair'; between 0.60 and 0.74 "good" and between 0.75 and 1.00 'excellent', analogous to commonly used guidelines for interexaminer agreement (Cicchetti 1994).

The associations between each separate variable (age, sex, BMI, pain, and time since surgery) and patient-reported TESS and RAND-36 were examined using univariate regression analyses to examine whether they were associated with the functional outcome scores.

Matlab R2011a (The Mathworks, Natick, MA, USA) and R version 3.0.2. (R Core Team 2014) were used for the statistical analyses.

Results

Patients

The characteristics of all 23 patients are listed in Table 4.1. The age at the time of surgery was 39.9 ± 18.8 years, and the time after surgery was 47 ± 27 months. All patients were ambulatory and able to at least walk short distances without a walking aid. Two patients (cases 10 and 21) had undergone a reresection; this was mentioned in the case file. All other patients had not suffered from local recurrence or complications that required follow-up surgery. The mean patient-reported scores were: TESS 87.0 ± 12.1, RAND-36 PFS 73.3 ± 18.7, and RAND-36 pain subscale 85.5 ± 24.7.

Surgeon predictions – TESS

The surgeon-predicted scores and their correlations with the patient-reported scores of all five surgeons and the average predictions of all surgeons on the TESS are shown in Figure 4.3 and in Table 4.2. The correlations with the patient-reported scores were "very poor" for all

Table 4.1 Patient Characteristics, Indication, Tumor Location, Surgical Treatment, Adjuvant Therapy, and Functional Scores

Pat. No	Gender, age (y)	BMI (kg/m2)	Indication	Tumor location	Side	Surgical treatment	Adjuvant therapy	Time post-OR (months)	TESS score	RAND-36 phys. func.	RAND-36 pain
1	M, 50	26.0	Paget's osteosarcoma	Distal femur	Left	Extra-articular distal femur resection including part of the quadriceps muscle. Reconstruction with tumor prosthesis, and biceps femoris tendon transposition for quadriceps reconstruction.	Pre- and postoperative chemotherapy.	67	79.6	65.0	89.8
2	M, 36	21.4	Clear cell chondrosarcoma	Proximal femur	Right	Proximal femur resection, including the greater trochanter. Reconstruction with tumor prosthesis.		28	89.2	70.0	67.3
3	V, 44	28.3	Mixoid liposarcoma next to the medial femoral epicondyle	Distal femur	Left	Soft tissue tumor resection, including the ligamentum collaterale mediale. Reconstruction of the pes anserinus.		75	98.3	100.0	100.0
4	V, 63	25.2	Sarcoma not otherwise specified tuberositas tibae	Proximal tibia	Left	Proximal tibia resection. Reconstruction with allograft and tumorprosthesis. Soft tissue closure with gastrocnemius transfer and splitskin graft.		62	95	75.0	100.0

5	V, 60	25.4	Liposarcoma	Medial thigh	Left	Resection soft-tissue tumor.		21	88.8	80.0	100.0
6	V, 66	25.2	Parosteal osteosarcoma	Distal femur	Right	Distal femur resection. Reconstruction with tumor prosthesis.		12	98.3	70.0	100.0
7	M, 37	23.7	Sarcoma not otherwise specified	Distal femur	Left	Extra-articular distal femur resection and reconstruction with tumor prosthesis.	Pre- and postoperative chemotherapy.	65	92.9	90.0	100.0
8	V, 60	24.1	Soft tissue sarcoma adductor muscles compartment	Medial thigh	Right	En block resection.	Preoperative chemotherapy.	14	93.1	90.0	100.0
9	V, 41	34.3	Chondrosarcoma grade 2	Proximal tibia	Left	Proximal tibia resection. Reconstruction with tumor prosthesis.		10	83.3	75.0	100.0
10	M, 47	28.7	Soft tissue sarcoma; previous incomplete resection	Thigh	Right	Re-resection.		105	96.7	85.0	79.6
11	M, 15	19.2	Osseous lipoma like liposarcoma	Proximal femur	Right	Proximal femur resection (osteotomy at 250mm) and reconstruction with tumor prosthesis.	Preoperative chemo- and radiotherapy.	46	82.8	60.0	79.6

12	V, 16	24.5	Osteosarcoma	Tibia shaft	Right	Segment resection tibia shaft, saving tibia epiphysis. Reconstruction with allograft, intramedullary pen, cement and plate osteosynthesis.	Pre- and postoperative chemotherapy.	30	92.5	75.0	100.0
13	V, 15	26.9	Osteosarcoma	Distal femur	Right	Distal femur resection (235 mm), reconstruction with tumor prosthesis.	Pre- and postoperative chemotherapy.	79	72.4	25.0	100.0
14	V, 65	25.9	Osteosarcoma	Distal femur	Left	Distal femur resection, reconstruction with tumor prosthesis.		55	79.8	60.0	0.0
15	V, 39	24.9	Synovial sarcoma between proximal fibula and tibia	Proximal fibula	Left	Proximal fibula resection, including lateral cortex of tibia. Reconstruction with plate and cement.		40	93.1	80.0	100.0
16	M, 59	25.8	Chondrosarcoma grade 2.	Distal femur	Left	Distal femur resection, reconstruction with tumor prosthesis.		7	52.9	50.0	79.6
17	V, 59	23.8	Soft tissue sarcoma not otherwise specified	Dorsal thigh	Right	Resection soft tissue tumor.	Postoperative radiotherapy.	51	60.8	45.0	100.0

18	M, 15	26.6	Teleangiectatic osteosarcoma	Distal femur	Left	Distal femur resection, reconstruction with tumor prosthesis.	Pre- and posto-perative chemo-therapy.	84	83.6	65.0	57.1
19	M, 21	24.2	Osteosarcoma	Distal femur	Left	Distal femur resection, reconstruction with tumor prosthesis.	Pre- and posto-perative chemo-therapy.	12	83.9	55.0	44.9
20	V, 30	21.7	Mixoïd liposarcoma	Rectus femoris	Left	Resection soft tissue sarcoma.		45	100.0	100.0	100.0
21	V, 49	26.8	Liposarcoma, previous incomplete resection	Antero-lateral thigh	Right	Re-resection (last part vastus lateralis anteromedial and distal).	Posto-perative radiothe-rapy.	50	95.8	90.0	69.4
22	M, 17	22.6	Osteosarcoma	Lateral femoral epicon-dyles	Right	Distal femur resection, reconstruction with tumor prosthesis.	Pre- and posto-perative chemo-therapy.	50	87.5	85.0	100.0
23	M, 14	21.5	Ewing's sarcoma	Dyafysis femur	right	Segment resection right femur. Reconstruction with allograft, intramedullary nail and plate osteosynthesis.	Pre- and posto-perative chemo-therapy.	77	100.0	100.0	100.0

surgeons, with the best correlation for surgeon 2 (r^2 = 0.185). The TESS was underestimated for most patient cases (Figure 4.3); the mean underestimation ranged from 1.5 to 22.6 percentage points (Table 4.2). The correlations with the patient-reported TESS formed by averaging all five surgeons' predictions were "very poor" (r^2 = 0.159) and underestimated patient-reported functional outcome by 8.7 (95% CI: 3.62-13.7) percentage points. The intersurgeon agreement on the TESS was "poor" with an ICC of 0.29 (95% CI: 0.10-0.53).

Table 4.2 Patient-Reported and Surgeon-Predicted Mean TESS and RAND-36 PFS Scores and Coefficients of Determination for TESS and RAND-36 PFS Scores

	TESS		**RAND-36 PFS**	
	Mean score[a]	r^2	Mean score[a]	r^2
Patient-reported	87.0 (12.1)		73.3 (18.7)	
Surgeon 1	75.6 (13.6)	0.167	50.9 (20.3)	0.142
Surgeon 2	83.6 (8.6)	0.185	78.7 (15.5)	0.336
Surgeon 3	82.5 (7.1)	0.096	70.2 (17.9)	0.354
Surgeon 4	85.5 (11.9)	0.014	72.2 (18.7)	0.081
Surgeon 5	64.3 (14.7)	0.088	52.8 (26.8)	0.118
Average of surgeons	78.3 (8.7)	0.159	65.0 (16.6)	0.255

[a] Scores are reported as mean (SD).

Surgeon predictions – RAND-36 PFS

The surgeon-predicted RAND-36 PFS scores and their correlations with the patient-reported scores are shown in Figure 4.4 and in Table 4.2. The correlations to the patient-reported scores were either "very poor" (surgeons 1, 4 and 5) or "poor" (surgeons 2 and 3). Surgeon 3's predictions had the highest correlation with the patient-reported scores (r^2 = 0.354). The patient-reported RAND-36 PFS score was underestimated by all surgeons, except for surgeon 2 (5.4 percentage points overestimation) (Table 4.2). The average correlations with the patient-reported scores were "poor" (r^2 = 0.255) and underestimated patient-reported functional outcome by 8.3 (95% CI: 0.64-16.0) percentage points.

In the analysis of the individual questions that make up the RAND-36 PFS, 'Climbing several flights of stairs' and 'Walking more than a mile' were the most difficult items to predict, with "poor" agreement coefficients (AC1) of 0.15 and 0.19, respectively, between surgeon-predicted and patient-reported scores (Table 4.3). 'Walking one block' and 'Bathing or dressing yourself' were the least difficult items to predict, with 'excellent' agreement coefficients of 0.81 and 0.76, respectively, between surgeon-predicted and patient-reported scores. Similar to the overall RAND-36 PFS scores, most of its separate questions were underestimated; only two questions were overestimated ('Bending, kneeling, or stooping' and 'Lifting or carrying groceries').

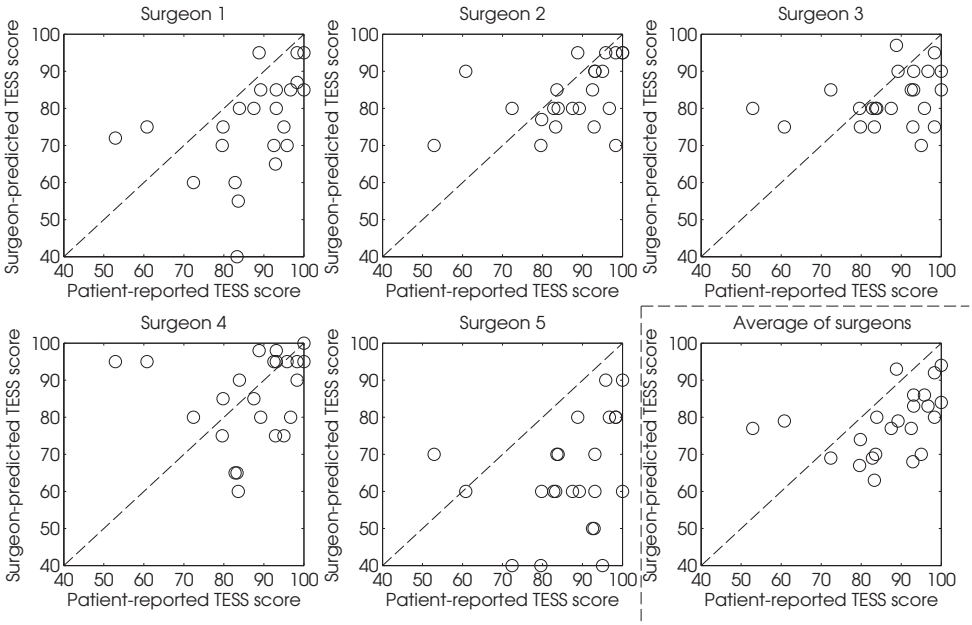

Figure 4.3. Scatter plots of patient-reported outcome and orthopedic tumor surgeon predictions on the Toronto Extremity Salvage Scale (TESS). The dashed lines indicate a hypothetical perfect correlation; if a patient case lies above or below this line, the functional outcome was overestimated or underestimated, respectively.

On most questions of the RAND-36 PFS, the inter-surgeon agreement coefficient was "poor", but there was a 'fair' agreement on 'Bathing or dressing yourself' and 'Moderate activities', and a "good" agreement on 'Vigorous activities' and 'Walking one block' (Table 4.3).

Other potential predictors

No correlations were found between the TESS or RAND-36 PFS and any of the potential predicting factors (Table 4.4).

Discussion

This national survey aimed to investigate how well orthopedic oncologists are able to predict the patient-reported functional outcome of patients that had undergone LSS in the lower limb. We found "very poor" to "poor" correlations between patient-reported outcomes and surgeon-predicted outcomes on both the TESS and the RAND-36 PFS. The orthopedic oncologists tended to underestimate patient-reported functional outcome on both scales. The most difficult tasks on the RAND-36 PFS were also the most difficult to predict, whereas for the least difficult tasks it was easy to predict that these could be performed without substantial limitations by nearly all patients. The intersurgeon agreement on the RAND-36 PFS questions was mostly "poor", but was "good" for some of the most and least demanding tasks. None of the potentially predicting factors were related to the primary outcome measures.

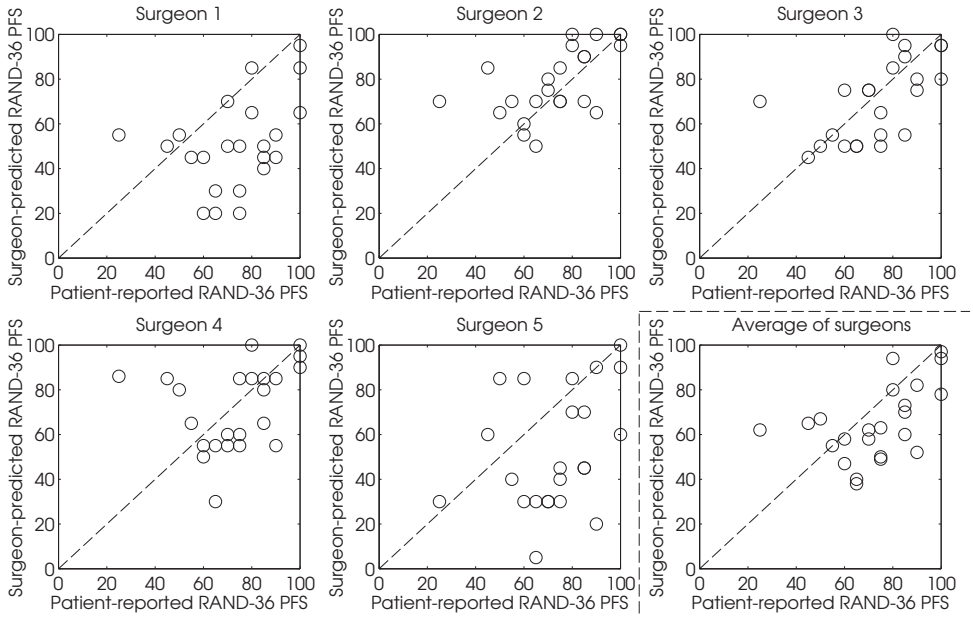

Figure 4.4. Scatter plots of patient-reported outcome and orthopedic tumor surgeon predictions on the RAND-36 physical functioning subscale (RAND-36 PFS). The dashed lines indicate a hypothetical perfect correlation; if a patient case lies above or below this line, the functional outcome was overestimated or underestimated, respectively.

Table 4.4 Coefficients of Determination Between Patient Characteristics and Functional Outcomes (TESS and RAND-36 Physical Functioning Subscale)

	TESS	**RAND-36 PFS**
	r^2	r^2
Age	0.011	0.001
Sex	0.024	0.001
Body mass index	0.008	0.003
Pain (RAND-36 pain subscale)	0.042	0.079
Time since surgery	0.036	0.015

Our results indicate that it was difficult for the participating orthopedic oncologists to accurately predict the patient-reported functional outcome of limb salvage surgery. On the TESS for instance, the coefficients of determination (r^2) between patient-reported and surgeon-predicted outcomes were lower than 0.20, indicating that less than 20% of the variance in TESS could be explained by the predictions made by the orthopedic oncologists. We did not expect such a poor predictive ability, considering the experience level of the orthopedic oncologists with limb salvage surgery. Several aspects may underlie this seemingly rather poor predictive ability.

First, each limb salvage patient presents a unique case in terms of anatomical involvement. Even in patients with the same type of tumor at a similar location, for instance the distal femur, final functional results can differ to a large extent. In part, this depends on the amount and precise location of soft tissue involvement, which may have been difficult to see from the limited set of MRI images in the case files. Moreover, patients are unique in terms of adaptive capacity. The adaptation of the patient to the new anatomical and sensorimotor situation plays a large role in the recovery of function (De Visser et al. 2000). The amount of adaptive capacity may have been hard or impossible to estimate by the orthopedic oncologists from the case files. Second, we measured functional outcome with questionnaires, which are inherently subjective. Thus, the patients' own perception of functioning may have played a large role in the functional outcome score. It might be that functional outcome measured by objective means, such as for example gait analysis, more closely reflects the orthopedic oncologists' predictions. Third, in the case files, we mimicked as well as possible the information typically available preoperatively to the surgeon in a clinical setting, but the study design did not permit the independent surgeons to review the medical history of the patients, nor to perform a physical examination before the surgery. As such, predictions of patient-reported functional outcome in a 'real' clinical setting (e.g., including a physical examination) might be more accurate than those made in this study. Fourth, patients who had a bone tumor with an intact cortical bone were not included; the patient-reported functional outcome in those patients would potentially have been less difficult to predict than that in the patients with larger tumors.

The poor predictive ability raises the question which other factors determine functional outcome in limb saving surgery, and to what degree. Davis et al. showed that large tumor size, deep lesions, high grade tumor, use of radiotherapy, bone resection, and motor nerve sacrifice are significantly related to increased disability on the TESS (Davis et al. 2000). In their study, those combined parameters were able to predict 20% of the variance in TESS score. This is in the same order of magnitude as the presently reported results, indicating that the surgeons were unable to 'add' predictive value on top of the given parameters in the case files. The rehabilitation protocol may also have an effect on functional outcome; Shehadeh et al. showed that adherence to a strict rehabilitation protocol after limb salvage surgery led to a relatively high level of functional outcome compared with other studies (Shehadeh et al. 2013). If we interpret our findings concurrent with those of Davis et al. and Shehadeh et al., it appears that still a large percentage of functional outcome cannot be predicted by the surgeon, nor by anatomical and surgery or adjuvant therapy-related factors, nor by rehabilitation protocols. Other factors that may play a significant role in the patient-reported functional outcome include the preoperative physical and mental state of the patient. For example, a patient who is highly motivated and athletic may recover to a far higher level of functioning than one who is less motivated and leads a sedentary lifestyle. From this perspective, one may intuitively expect a correlation between patient-reported functional outcome and age or BMI, but we did not find this (Table 4.4). Further studies are required to clarify the role each factor plays in patient-reported functional outcome after limb salvage surgery.

The orthopedic oncologists tended to underestimate patient-reported functional outcome on both the TESS and the RAND-36 PFS. Thus, it appears that the patients adapted to the

new anatomical and functional situation better than the surgeons predicted. It is possible that this is due to some surgeons being used to picturing a somewhat more pessimistic scenario to their patients so that the actual achieved functional result exceeds the patients' expectations. However, we specifically instructed the surgeons to provide their most accurate predictions of patient-reported functional outcome, rather than to provide predictions that they would share with patients. As for clinical relevance, we did not set a specific threshold, but the underestimation of patient-reported functional outcome on both the TESS and the RAND-36 PFS was rather consistent, as demonstrated by the 95% confidence intervals that did not pass through zero.

Interestingly, we found that the 'Walking one block' question was the least difficult to predict, whereas the 'Walking more than a mile' question was one of the most difficult to predict (only 'Climbing several flights of stairs' was more difficult to predict). It appears that the ultimate level of function that is reached in patients is hard to predict, whereas it is easier to predict lower levels of function. Thus, surgeons' ability to predict functional scores can be improved the most by focusing on accurately predicting more demanding tasks. Additional improvement might be gained by analyzing the prediction for the 'Bending, kneeling, or stooping' question. If the prediction for this question did not match with the patient-reported outcome, it was mostly overestimated (43.5% of cases). This overestimation breaks with the general trend to underestimate patient-reported functional outcome, and indicates that bending the knees is more difficult to do for patients than the median surgeon predicted.

The intersurgeon agreement on most RAND-36 PFS questions was "poor", indicating that there was a high inter-surgeon variability in the predictions to the questions. Notable exceptions were 'Walking one block' and 'Vigorous activities', with "good" intersurgeon agreement. The prior arguably is the least difficult activity on the scale, whereas the latter represents the most demanding activities on the scale (including running, heavy lifting and strenuous sports). However, this does not imply that there was also a high agreement with the patient-reported outcome; 'Vigorous activities' had only a 'fair' agreement with the patient-reported score. 'Walking one block', on the other hand, was the only question that had both an 'excellent' agreement with the patient-reported score, as well as a "good" intersurgeon agreement. This might be due to the surgeons' familiarity with predicting this basic level of functional outcome, or because being able to walk at least short distances is considered one of the criteria for attempting limb salvage surgery, and most patients indeed achieved that goal.

This study has some limitations. First, the surgeons only predicted the total TESS score, instead of predicting each of the 30 questions that comprise the score. This was done because some questions were already present in the much shorter RAND-36 PFS, and to reduce the time it would take the surgeons to predict the 23 cases. Second, we used a translated version of the TESS which has not been validated in Dutch. However, as the TESS is the gold standard assessment tool after limb salvage surgery we decided to use it (Clayer et al. 2012). The RAND-36 PFS has been validated in Dutch (van der Zee et al. 2012; van der Zee et al. 1996), and its results showed the same trend in the comparisons as the translated TESS. Third, we found a wide range of patient-reported functional outcome scores,

including in patients that had undergone similar surgery. Of course, each case is unique, but the perception of effort required to perform the activities in the questionnaires and the interpretation of the questions can vary between patients. Measuring actual functional outcome (e.g., in a movement laboratory or by observing patients in their home setting) could yield more knowledge of actual functioning, eliminate the subjectivity inherent in questionnaires, and establish the construct validity of the employed functional scoring systems. Fourth, the surgeons predicted the functional outcome based on a case description without being allowed to review the medical history of the patients or perform a physical examination. The time since surgery was also not provided, which might have negatively affected the predictions. This, however, does not explain the large differences found between predicted and patient-reported functional outcome nor does it explain the differences in predictions between surgeons. Furthermore, there was no correlation between the patient-reported functional scores and the time since surgery (Table 4.4).

Conclusions

It was difficult for the participating orthopedic oncologists to accurately predict the patient-reported functional outcome of limb salvage surgery. Patient-reported functional outcome tended to recover to a higher level than the surgeons predicted. The ultimate level of function that the patients reached was hard to predict, whereas it was easier to predict lower levels of function. Thus, surgeons' ability to predict functional scores can be improved the most by focusing on accurately predicting more demanding tasks. Intersurgeon agreement to most questions was "poor", indicating the high variability in the surgeons' predictions, and possibly, treatment decisions. The poor predicting ability warrants research into objective tools to assist orthopedic oncologists in the decision making process. Such tools could include, for instance, computational musculoskeletal models that prospectively calculate whether enough muscle strength remains to perform activities of daily living.

Acknowledgements

We gratefully acknowledge financial support by the European Commission (grant FP7-ICT-247860) for the TLEMsafe project (http://www.tlemsafe.eu).

References

Aksnes, L. H., H. C. Bauer, N. L. Jebsen, G. Folleras, C. Allert, G. S. Haugen, and K. S. Hall. 2008. Limb-sparing surgery preserves more function than amputation: a Scandinavian sarcoma group study of 118 patients, J Bone Joint Surg Br, 90: 786-794.

Cicchetti, Domenic V. 1994. Guidelines, criteria, and rules of thumb for evaluating normed and standardized assessment instruments in psychology, Psych Assess, 6: 284-290.

Clayer, M., S. Doyle, N. Sangha, and R. Grimer. 2012. The toronto extremity salvage score in unoperated controls: an age, gender, and country comparison, Sarcoma, 2012.

Cohen, J. 1960. A Coefficient of Agreement for Nominal Scales, Edu Psych Meas, 20: 37-46.

Cohen, J. 1968. Weighted Kappa - Nominal Scale Agreement with Provision for Scaled Disagreement or Partial Credit, Psych Bull, 70: 213-220.

Davis, A. M., J. G. Wright, J. I. Williams, C. Bombardier, A. Griffin, and R. S. Bell. 1996. Development of a measure of physical function for patients with bone and soft tissue sarcoma, Qual Life Res, 5: 508-516.

Davis, A.M., S. Sennik, A.M. Griffin, J.S. Wunder, B. O'Sullivan, C.N. Catton, and R.S. Bell. 2000. Predictors of functional outcomes following limb salvage surgery for lower-extremity soft tissue sarcoma, J Surg Oncol, 73: 206-211.

De Visser, E., T. Mulder, H. W. Schreuder, R. P. Veth, and J. Duysens. 2000. Gait and electromyographic analysis of patients recovering after limb-saving surgery, Clin Biomech (Bristol, Avon), 15: 592-599.

Enneking, W. F., W. Dunham, M. C. Gebhardt, M. Malawar, and D. J. Pritchard. 1993. A system for the functional evaluation of reconstructive procedures after surgical treatment of tumors of the musculoskeletal system, Clin Orthop Relat Res: 241-246.

Gebhardt, M. C. 2002. What's new in musculoskeletal oncology, J Bone Joint Surg Am, 84-A: 694-701.

Ghert, M.A., A. Abudu, N. Driver, A.M. Davis, A.M. Griffin, D. Pearce, L. White, B. O'Sullivan, C.N. Catton, R.S. Bell, and J.S. Wunder. 2005. The indications for and the prognostic significance of amputation as the primary surgical procedure for localized soft tissue sarcoma of the extremity, Ann Surg Oncol, 12: 10-17.

Niimi, R., A. Matsumine, K. Kusuzaki, S. Kuratsu, N. Araki, Y. Aoki, T. Ueda, I. Kudawara, A. Myoui, M. Ieguchi, N. Hashimoto, H. Yoshikawa, and A. Uchida. 2008. Usefulness of limb salvage surgery for bone and soft tissue sarcomas of the distal lower leg, J Cancer Res Clin Oncol, 134: 1087-1095.

R Core Team. 2014. R: A language and environment for statistical computing. http://www.R-project.org/. R Foundation for Statistical Computing.

Shehadeh, A., M. E. Dahleh, A. Salem, Y. Sarhan, I. Sultan, R. M. Henshaw, and A. J. Aboulafia. 2013. Standardization of rehabilitation after limb salvage surgery for sarcomas improves patients' outcome, Hematol Oncol Stem Cell Ther.

Taylor, R. 1990. Interpretation of the Correlation Coefficient: A Basic Review, J Diag Med Sonography: 35-39.

van der Zee, K. I., and R. Sanderman. 2012. Het meten van de algemene gezondheidstoestand met de RAND-36, een handleiding. Tweede herziene druk, UMCG / Rijksuniversiteit Groningen, Research Institute SHARE.

van der Zee, K. I., R. Sanderman, J. W. Heyink, and H. de Haes. 1996. Psychometric qualities of the RAND 36-Item Health Survey 1.0: a multidimensional measure of general health status, Int J Behav Med, 3: 104-122.

Veth, R., Hoesel R. van, M. Pruszczynski, J. Hoogenhout, B. Schreuder, and T. Wobbes. 2003. Limb salvage in musculoskeletal oncology, Lancet Oncol, 4: 343-350.

Wongpakaran, N., T. Wongpakaran, D. Wedding, and K. L. Gwet. 2013. A comparison of Cohen's Kappa and Gwet's AC1 when calculating inter-rater reliability coefficients: a study conducted with personality disorder samples, BMC Med Res Methodol, 13: 61.

Part II

New Perspectives on Functional Assessment
in Musculoskeletal Research

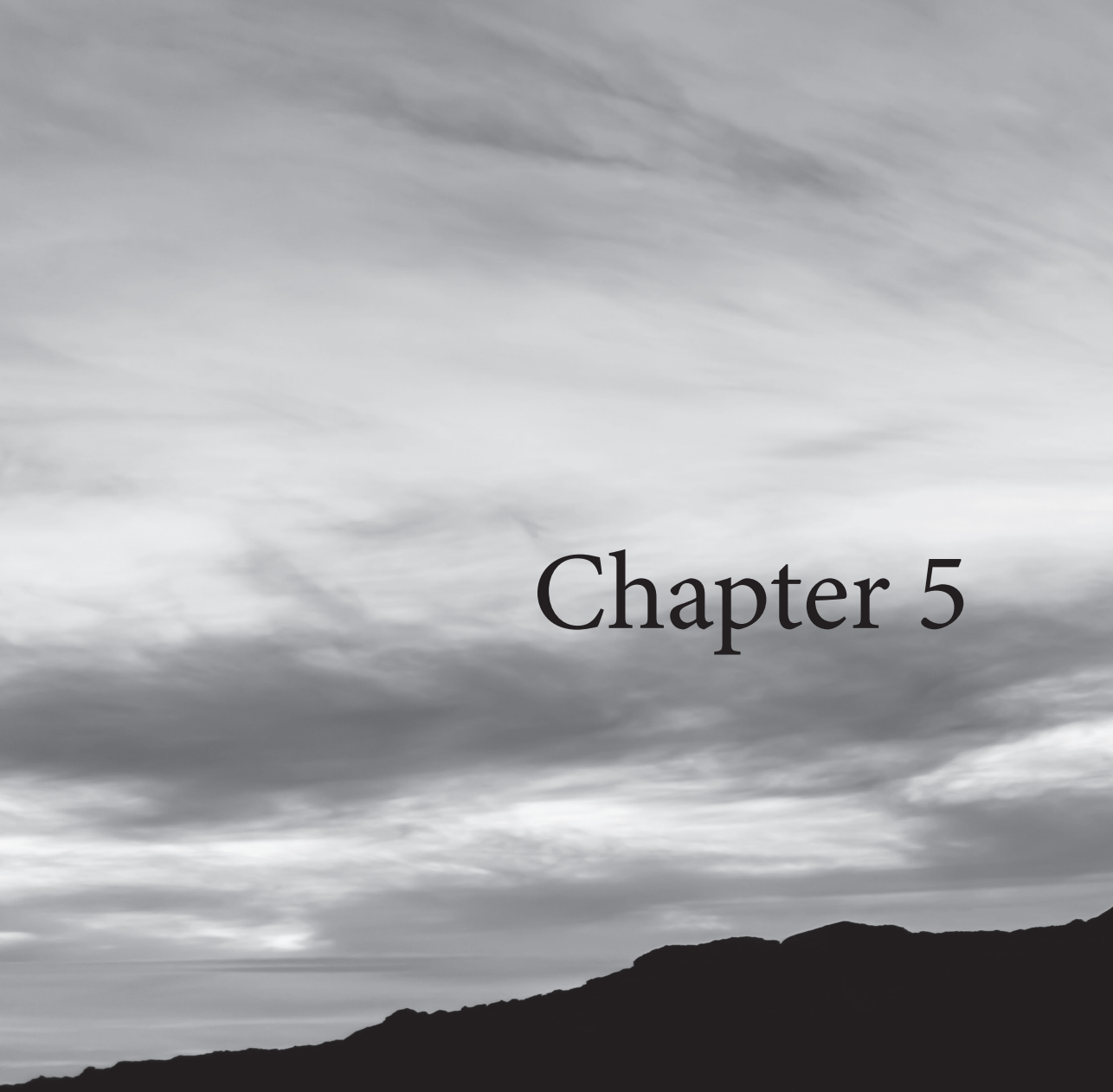

Chapter 5

Muscle activity during walking measured using 3D MRI segmentations and FDG-PET

Published as:

Kolk, S., Klawer, E.M.E., Schepers, J., Weerdesteyn, V., Visser, E.P., and Verdonschot, N. 2015. Muscle Activity during Walking Measured Using 3D MRI Segmentations and [18F]-fluorodeoxyglucose in Combination with Positron Emission Tomography, Medicine and Science in Sports and Exercise, 47: 1896-1905.

Abstract

Background: This study aimed to determine the contribution of each muscle of the lower limb to walking using positron emission tomography (PET) with [^{18}F]-fluorodeoxyglucose (FDG). Furthermore, we compared our results obtained using volumetric analysis of entire muscles with those obtained using a more traditional approach considering the uptake in only one slice in each segment.

Methods: Ten healthy subjects walked on a treadmill at self-selected comfortable walking speed for 90 min, 60 min before and 30 min after intravenous injection of 50 MBq FDG. A PET/computerized tomography scan of the lower limb was made subsequently. The three-dimensional contours of 39 muscles in the left lower limb were semiautomatically determined from magnetic resonance imaging scans. After nonrigidly registering the magnetic resonance imaging to the computerized tomography scans we superimposed the muscle contours on the PET scans.

Results: The muscles with the highest median FDG uptake among all subjects were the soleus, gluteus maximus, vastus lateralis, gastrocnemius medialis, and adductor magnus. We found a wide range of FDG uptake values among subjects, including in some of the most important muscles involved in walking (e.g., soleus, gluteus medius, gastrocnemius medialis). Compared with the volumetric analysis, the single slice analysis did not yield an accurate estimate of the FDG uptake in many of the most active muscles, including the gluteus medius and minimus (overestimated) as well as all the thigh muscles (underestimated).

Conclusions: The distribution of FDG among the muscles varied between subjects, suggesting that each subject had a unique activation pattern. The FDG uptake as estimated from single slices did not correspond well to the uptake obtained from volumetric analysis, which illustrates the added value of our novel three-dimensional image analysis techniques.

Introduction

Walking is one of the most important activities of daily living. It is a complex orchestration of muscular contractions with the goal of moving the body forward while maintaining stance stability (Perry et al. 2010). Understanding the individual contributions of the muscles involved in walking is important for a variety of purposes (including rehabilitation, medical education and the validation of musculoskeletal models), but until a few decades ago, it was not possible to measure the contributions of all muscles of the lower limb to walking because of limitations of existing measurement techniques.

Muscle activity during walking has been studied extensively using electromyography (EMG) (e.g., Burden 2010; Ericson et al. 1986; Inman et al. 1981). Although this method is convenient and noninvasive, it has several important limitations, as follows: deep-lying muscles cannot be measured unless needle electrodes are inserted invasively, only a limited number of muscles can be measured at the same time, a reference contraction is required if muscles are to be compared with each other, and adipose tissue and crosstalk from other muscles are confounding factors (De Luca 1997; Staudenmann et al. 2010). [^{18}F]-fluorodeoxyglucose in combination with positron emission tomography (FDG-PET) does not suffer from these drawbacks. It can be used to estimate muscle activity in all muscles of the lower limb (including the deep-lying muscles) in one session. The working principle of FDG-PET is that exercising muscles take up glucose (and FDG) from the blood to replenish their expended energy. Using a concurrently made magnetic resonance imaging (MRI) or computerized tomography (CT) scan for anatomical reference, the muscles can be identified and their individual FDG uptake can be quantified.

FDG-PET has been used for studying several exercises (e.g., cycling (Fujimoto et al. 2003; Gondoh et al. 2009), walking with a stride assistance system (Shimada et al. 2009a; Shimada et al. 2007), and simple flexion/extension exercises (Masood et al. 2014; Pappas et al. 2001; Rudroff et al. 2014)) since Fujimoto et al. first used it to analyze muscle activity during running (Fujimoto et al. 1996). Thus far, only a few studies have used FDG-PET for analyzing walking (Oi et al. 2003; Shimada et al. 2009b; Shimada et al. 2007). Oi et al. performed important work by comparing FDG uptake results with EMG and kinematic and kinetic studies, and demonstrating the concurrent validity of measuring the muscular activity of the lower limb with FDG-PET (Oi et al. 2003). Shimada et al. evaluated FDG uptake during walking with and without a stride assistance system (Shimada et al. 2007), and in older subjects compared with younger subjects (Shimada et al. 2009b). These studies, however, performed the quantification of the FDG uptake on one or only a few slices of the PET image. Thus, only a small portion of each muscle at a fixed cross-sectional level was analyzed. This raises the question whether analyzing such a small part provides an accurate representation of glucose uptake in the entire muscle. There are indications in the literature that muscle metabolism exhibits spatial heterogeneity. For instance, Pappas et al. found an inhomogeneous distribution of glucose uptake in the transverse direction and along the longitudinal axis of the biceps brachii after an elbow flexion exercise (Pappas et al. 2001). In the lower limb, Kalliokoski et al. demonstrated heterogeneous glucose uptake between the four quadriceps femoris muscles during a knee extension exercise (Kalliokoski et al. 2011). Besides the spatial heterogeneity, certain muscles may not even be included at the cross-sectional level at which the slice is taken.

With the advent of new MR image analysis techniques, it is now feasible to semiautomatically segment not just one or a few slices of muscles but entire muscles. To our knowledge, volumetric glucose uptake in entire muscles during walking has not yet been investigated. The purpose of this study was to quantify the activity of the muscles in the lower limb during walking, using FDG-PET scans and three-dimensional (3D) MRI segmentations. Furthermore, we aimed to determine whether the volumetric analysis would yield an appreciable benefit compared with analyzing only a single slice.

Methods

Subjects

Ten healthy subjects participated in this study (Table 5.1). They had no history of major injury, had not undergone orthopedic surgery on the lower limb, and had no history of ailment related to carbohydrate metabolism or to cardiac or muscular disease. One of the inclusion criteria was being able to walk for at least 90 min without any difficulty. The subjects were recruited from the research staff and a database of volunteers available at our department. We specifically chose to include a wide variety of subjects in this study in terms of age (23-60 yr), sex (five men and five women) and anthropometry (1.60 - 1.95 m, 55.5 - 91.7 kg). This was done because it was part of a larger research project that aimed to validate personalized musculoskeletal models of the subjects at a later stage (see e.g., Carbone et al. 2012). The study procedures were approved by the ethical committee of the region Arnhem-Nijmegen, the Netherlands. A written informed consent was obtained from each participant.

Table 5.1 Participant characteristics

Number of participants	10
Sex (M:F)	5 : 5
Age (years)	40 (16)
Weight (kg)	74.8 (11.9)
Height (m)	1.75 (0.11)
BMI (kg/m^2)	24.4 (2.3)
Walking speed (m/s)	1.26 (0.11)

Data are presented as mean (SD).

Protocol

The subjects walked on a treadmill at their own comfortable pace for 90 min, 60 min before and 30 min after injection with 53.6±1.8 MBq FDG (Figure 5.1). The walking speed was 1.26±0.11 m/s. The PET/CT scan was started 30 min after finishing the last walking phase, which allowed the subject to be transported from the treadmill to the nuclear medicine department in a wheelchair, to void any excess radioactivity, and to position the subject in the PET/CT scanner. In addition to the PET/CT scan, an MRI scan had been taken a few

weeks earlier for anatomical reference. Before the PET/CT scan commenced, the subject's legs were positioned on the table to reproduce as closely as possible their position as it was during the MRI scan using a ruler and a vacuum pillow that could be molded into the desired shape. Before the testing procedure, the subjects had to refrain from eating and drinking anything except water for at least six hours, and from participation in strenuous physical activity for two days.

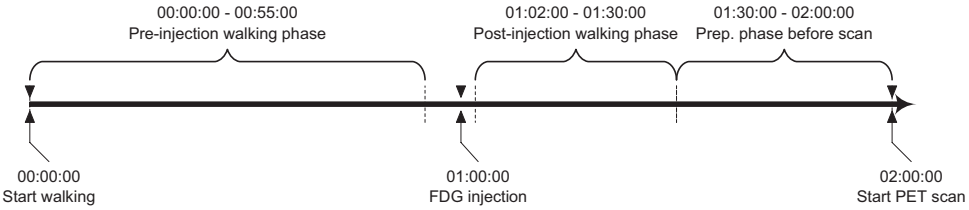

Figure 5.1. Timeline of the study protocol. The treadmill was stopped after 55 min of walking, to allow time for the subject to sit down and to insert the catheter for injection of FDG in a vein of the left forearm. The preparation phase before the scan consisted of transportation of the subject to the department of nuclear medicine in a wheelchair, and careful positioning of the subject on the scan table.

Tracer

FDG is a glucose analog, and as such, after entering the cell, FDG is phosphorylated into FDG-6-phosphate. However, FDG-6-phosphate is not a significant substrate for further metabolism. It is not converted into glycogen to any significant extent, and is not further metabolized in the glycolytic pathway. It thus becomes trapped within the cells, which is convenient from an imaging viewpoint (Cherry et al. 2012). It has a half-life time of 110 min.

Positron-emission tomography and CT scans

The PET/CT scans were made with a Biograph 40 mCT (Siemens AG, Erlangen, Germany) (Jakoby et al. 2011), in 3D mode, using an extended axial field of view of 216 mm. The PET scans lasted for four min per bed position. Eight to ten bed positions were acquired depending on the subject's height. Thus, the scan time was 32-40 min. The scan region ranged from the feet to at least the iliac crest, with 50 mm overlap in the bed positions. The slice thickness was 2.0 mm. The PET images were reconstructed with the TrueX algorithm (with a spatially varying point spread function) and the incorporation of time-of-flight measurements (Ultra-HD PET). Image reconstruction was performed using three iterations, 21 subsets, a matrix size of 512×512 and voxel spacing of 1.6 mm. After reconstruction, filtering was performed with a 3D Gaussian filter kernel with a full width at half maximum of 3.0 mm. The CT images used for attenuation correction were reconstructed with the B19f convolution kernel and a slice thickness of 5.0 mm, whereas the CT images used for anatomical reference were reconstructed with the B31f convolution kernel and slice thickness of 2.0 mm to correspond with the slice thickness of the PET images.

Magnetic resonance imaging scans

MRI scans were made with a Magnetom Skyra (Siemens AG, Erlangen, Germany) at 3 Tesla and with a 400 mm transaxial field of view. The feet and ankles were placed in a head/neck coil containing 20 elements; the other areas of the lower limb were scanned with body phased array coils containing 18 elements combined with a spine array coil containing 32 elements that was embedded in the table. The scan protocol was specifically designed to yield optimal distinction between muscle boundaries (based on Scheys et al. 2009). The settings were as follows: T1 weighted image (repetition time/echo time, 450-545/9 ms) with turbo spin echo; number of excitations, 3; two echoes per excitation; 92-195 echo trains per slice; matrix size, 512×512; no gap between slices; and in-plane resolution, 1.0×1.0 mm. Parallel imaging was not used, and there was no inversion pulse at the front end of the sequence. The hip, knee, and ankle regions were scanned with a 3.0 mm slice thickness, and the long bone regions in between were scanned with 8.0 mm slice thickness. This was done to obtain a higher level of detail in the areas where most muscles originate or insert. Six imaging stacks that covered the ankles (1), lower legs (1), knees (1) , thighs (2), and hip region (1) were used. An overlap of at least two 3.0 mm slices was used to allow proper "stitching" of the image stacks into a single integrated scan.

Image analysis

To obtain FDG uptake values of each individual muscle, several sequential steps were performed using Mimics (Materialise N.V., Leuven, Belgium), Matlab 2012b (The Mathworks, Natick, MA, USA) and Insight Segmentation and Registration Toolkit 4.5.2 (ITK) (Kitware Inc., Clifton Park, NY, USA).

1) Three-dimensional regions-of-interest (ROI) were drawn manually around the muscles of the left lower limb of one of the subjects from the axial images. The boundaries of the ROI thus reflected the muscle boundaries. In total, 39 muscles were segmented in this way (Table 5.2 and Figure 5.2). The resulting segmentation of the muscles in the lower limb will henceforth be called "atlas".

2) The atlas was used to semiautomatically segment the muscles in the left lower limb of the other nine subjects in Mimics. The workflow was as follows: (1) create an initial crude mask containing all the muscles using a threshold on the voxel intensities, (2) remove strong gradients from the mask, (3) remove remaining undesired structures (fat and bones) using pen strikes on approximately every fifth slice as user input, (4) register the atlas to the subject automatically using an algorithm based on nonrigid registration, and (5) in an automatic postprocessing step, the transformed segmentation was combined with the voxel intensity information from the MRI scan to obtain the muscle ROI of the subject. The muscle ROI were thoroughly checked and manually corrected by a researcher where necessary. Hence, this step produced a segmentation of all muscles of the left lower limb for each subject.

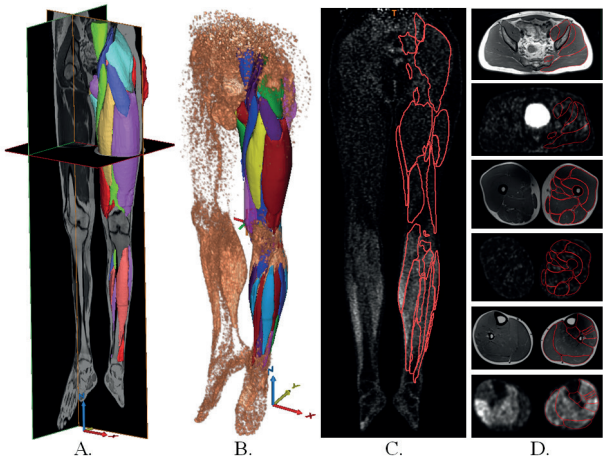

Figure 5.2. A: MRI scan with three-dimensional muscle ROI. B: PET scan with three-dimensional muscle ROI. C: Frontal view of a PET scan with muscle ROI. D: MRI and PET scan slices of the hip, thigh, and lower leg regions with muscle ROI as used in the slice-based analysis.

3) The MRI scan and its corresponding ROI were subsequently registered onto the CT scan using ITK. The registration results were again thoroughly checked and manually corrected by a researcher where necessary.

4) The ROI were exported per muscle as Digital Imaging and Communications in Medicine (DICOM) mask files. The DICOM file format is a standard method for transferring images and associated information between devices and software manufactured by various vendors, including those used in this study.

5) The ROI DICOM files and the subject's PET scan (obtained directly from the PET scanner in DICOM format) were opened in Matlab 2012b and multiplied using a custom algorithm. In the algorithm, the ones (reflecting the muscle's position) and zeros (surrounding area) in the ROI DICOM files were multiplied with the PET scan (gray values reflecting the FDG uptake in Bq/mL). The algorithm also extracted the rescale slope and intercept values from the PET DICOM headers, which were used to correct the FDG uptake values of the PET scan (in Bq/mL) for decay time since the start of the scan.

We emphasize that the PET DICOM files from which we extracted the FDG uptake values were obtained directly from the Biograph 40 mCT, and that they were thus not "morphed" or modified in any other way. Furthermore, we only analyzed the left lower limb in this study.

Analysis of volumetric uptake

The FDG uptake values per muscle were evaluated primarily with the volumetric %FDG uptake value. To obtain this value, we first calculated the volumetric mean standardized uptake value (SUV) of each muscle. The mean SUV reflects the average FDG uptake in a muscle, normalized by body mass and injected activity.

$$SUV = \frac{Measured\ activity\ (Bq)\ /\ Volume\ (mL)}{Injected\ activity\ (Bq)\ /\ Body\ mass\ (g)}$$

In this equation, the numerator is the mean radioactivity count from all the voxels in the muscle divided by the muscle volume. The denominator reflects the total injected activity divided by the total body mass. The SUV was corrected for decay between the injection and the start of the scan. Because the SUV is normalized by the muscle volume, small muscles can exhibit similar or higher SUV values than large muscles, even though the large muscles plausibly exert much more force and/or perform much more work during gait. Therefore, we multiplied each muscle's SUV by its volume. The resulting value was expressed as a percentage of the sum of the product of each muscle's SUV times its volume, yielding %FDG uptake as our primary outcome measure:

$$\%FDG_i = \frac{SUV_i \cdot Volume_i\ (mL)}{\sum_{j=1}^{39} SUV_j \cdot Volume_j\ (mL)}$$

where *i* is the index of the muscle and *j* is a summation index that includes all 39 muscles. The %FDG uptake values thus reflect the amount of FDG in each muscle relative to the total amount of FDG in the muscles of the limb.

Analysis of volumetric versus slice-based uptake

To allow comparison of our volumetric analysis with the commonly used method in the literature of analyzing single slices, the %FDG uptake values were calculated both for entire muscles, and at three discrete slice heights, as follows: 3 cm above the femoral head, 50% of the distance between the joint space of the knee and the top of the femoral head, and at 30% of the distance between the joint space of the knee and the tip of the lateral malleolus. These slice heights were based on commonly used slice heights in the literature for this type of study (Oi et al. 2003; Shimada et al. 2009a; Shimada et al. 2009b; Shimada et al. 2007; Tashiro et al. 1999). The percentage difference between the methods was calculated using the following formula:

$$\Delta\%FDG_i = \frac{\%FDG_{i,slice} - \%FDG_{i,whole}}{\frac{1}{2}(\%FDG_{i,slice} + \%FDG_{i,whole})}$$

where *i* is the index of the muscle. We did not want to choose either the volumetric or the slice-based data to be the "reference value", therefore, this unbiased version of the percentage difference was used. The comparison between methods was made only among the five most active muscles in each segment (based on the %FDG uptake values observed in the volumetric analysis) because differences in these muscles were considered the most relevant.

Sensitivity study

To examine the sensitivity of our results with regard to the effects of errors in identification of muscle boundaries, we took an offset of the muscles on the PET images by 1 mm (both dilated and eroded). We chose 1 mm because this is the pixel size on the MRI on which the original muscle ROI were drawn. To perform the sensitivity study, we created 3D models of the muscles as triangulated surfaces (Sterolithography (STL) file format). Then, we computed new muscle masks from these STL. The dilated and eroded STL were then multiplied by the PET data (step 5 as described earlier) to yield a new set of results. The results in terms of %FDG uptake were virtually insensitive to this manipulation; the differences between the original, dilated, and eroded results were in the order of mere tenths of percents (0.0%-0.7%). This was true for all muscles, including the very smallest, where the offset of 1 mm had a relatively large effect in terms of volume (in the order of 30%-50%). This lends confidence that our method of volumetrically extracting %FDG uptake values from semiautomatically processed scans was sufficiently accurate.

Results

Example PET and MRI scans with muscle ROI are shown in Figure 5.2.

Volumetric %FDG uptake

The muscles with the highest median %FDG uptake over all subjects were the soleus (17.1%), gluteus maximus (7.1%), vastus lateralis (5.8%), gastrocnemius medialis (5.6%) and adductor magnus (5.4%) (Figure 5.3). In general, the larger muscles had higher %FDG uptake, whereas the smaller muscles had lower uptake (Table 5.2).

In the hip region, besides the gluteus maximus, the gluteus medius and minimus also had high %FDG uptake (4.4% and 2.2%, respectively). The uptake in the gluteus medius, in particular, varied widely between subjects (2.5%-19.5%). The iliacus and psoas had lower %FDG uptake than the gluteal muscles (2.0% and 1.4%, respectively), and the uptake also varied less between subjects (1.2%-3.0% and 0.8%-1.7%, respectively).

In the thigh, the vastus lateralis (5.8%), adductor magnus (5.4%), vastus intermedius (4.3%) and vastus medialis (4.2%) had the highest median uptake. The FDG uptake in these muscles was relatively similar between subjects compared with that in the gluteal muscles.

In the lower leg, the soleus was by far the most active muscle (17.1%). The uptake in this muscle varied widely between subjects (8.8%-40.5%). The gastrocnemius medialis (5.6%) and tibialis anterior (4.8%) also exhibited a high median uptake. The uptake in the gastrocnemius medialis varied widely between subjects (1.9%-13.7%). The gastrocnemius lateralis had a much lower median uptake (1.9%) than the gastrocnemius medialis, and it also varied less (1.0%-4.6%).

The %FDG uptake data of all muscles in all subjects are available in Appendix 5.1.

Table 5.2 %FDG uptake values obtained with the volumetric and the single slice method

Muscle	Volume (mL)	%FDG (volumetric)	%FDG (single slice)	SUV (g/mL) (volumetric)	SUV (g/mL) (single slice)
Gluteus maximus	892	7,1%	8,1%	0,58	0,67
Gluteus medius	330	4,4%	8,8%	0,86	1,09
Gluteus minimus	86	2,2%	5,4%	1,56	1,92
Iliacus	184	2,0%	2,1%	0,78	0,69
Psoas	161	1,4%	1,0%	0,68	0,73
Pectineus	55	0,5%		0,80	
Piriformis	30	0,5%	2,9%	1,07	1,43
Obturator internus	47	0,5%		0,86	
Tensor fasciae latae	62	0,5%	0,2%	0,58	0,91
Obturator externus	26	0,3%		0,84	
Quadratus femoris	33	0,3%		0,80	
Gemellus inferior	5	0,1%		0,94	
Gemellus superior	3	0,0%		0,94	
Vastus lateralis	700	5,8%	4,6%	0,64	0,63
Adductor magnus	509	5,4%	3,3%	0,75	0,62
Vastus intermedius	457	4,3%	3,3%	0,75	0,71
Vastus medialis	480	4,2%	2,3%	0,68	0,74
Rectus femoris	260	1,9%	1,0%	0,58	0,57
Adductor longus	164	1,8%	0,6%	0,66	0,80
Semimembranosus	250	1,7%	1,2%	0,64	0,66
Biceps femoris caput longum	218	1,6%	1,8%	0,57	0,56
Adductor brevis	92	1,5%		1,16	
Sartorius	135	1,4%	0,6%	0,64	0,69
Semitendinosus	187	1,2%	1,0%	0,54	0,55
Biceps femoris caput breve	99	0,8%	0,2%	0,65	0,74
Gracilis	85	0,6%	0,5%	0,59	0,57
Soleus	594	17,1%	18,8%	2,34	2,29
Gastrocnemius medialis	256	5,6%	5,7%	2,31	2,57
Tibialis anterior	141	4,8%	5,7%	3,20	3,54
Gastrocnemius lateralis	108	1,9%	2,1%	1,14	1,43
Tibialis posterior	106	1,5%	1,2%	1,24	1,27
Extensor digitorum longus	48	1,5%	1,7%	2,57	2,72
Flexor hallucis longus	72	1,2%		1,20	
Extensor hallucis longus	41	1,2%		2,39	
Peroneus longus	57	1,0%	1,5%	1,22	1,34
Flexor digitorum longus	44	0,8%	0,7%	1,37	1,56
Peroneus brevis	53	0,7%		1,04	
Popliteus	20	0,4%		1,37	
Plantaris	7	0,1%		1,55	

Table is sorted by %FDG (volumetric). All volumes, SUV and %FDG values are presented as median values. Some muscles were not present in the slices at the discrete slice heights (based on the literature) that we analyzed, therefore there are no %FDG and SUV values for those muscles.

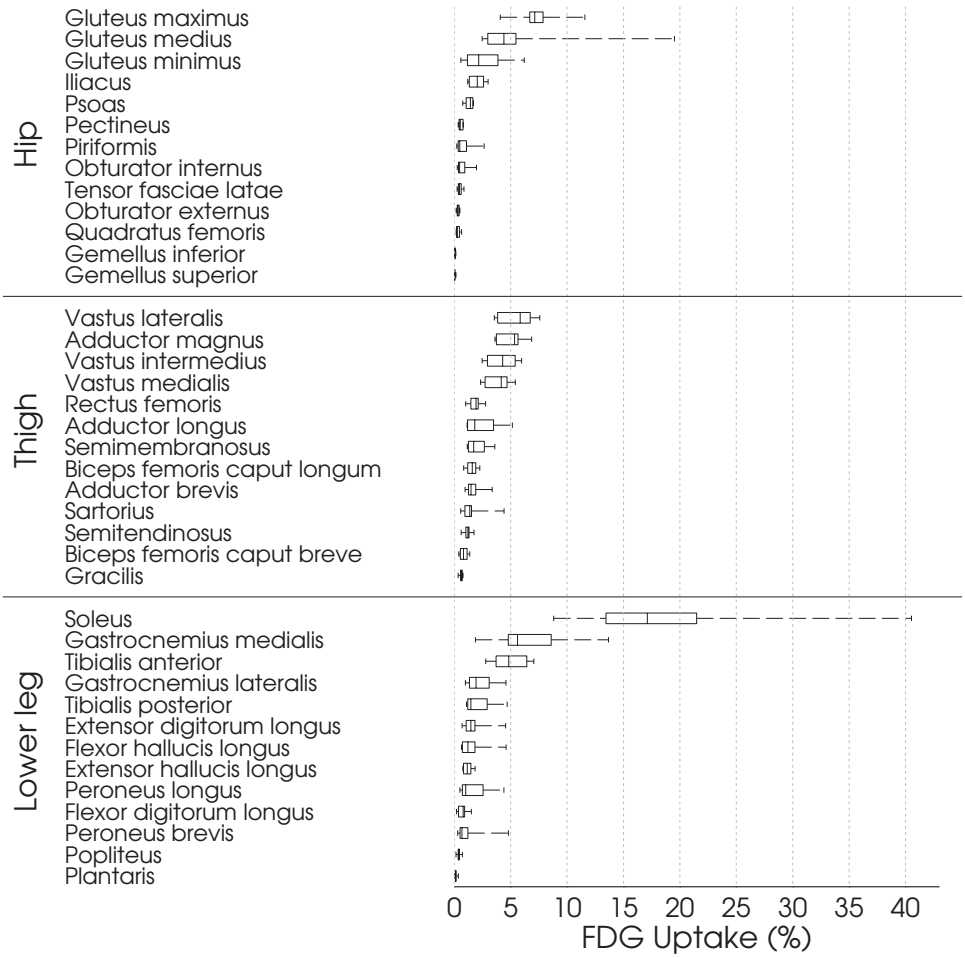

Figure 5.3. FDG uptake in the muscles in the left lower limb of all ten subjects. The boxplot shows the median, 25th and 75th percentiles, and the full range of uptake values (i.e. no values were considered outliers). The psoas was only partly segmented, because its uppermost cranial aspect was outside the scan area. Therefore, the muscle's uptake in this figure is lower than it is in reality.

Volumetric SUV

The muscles in the lower leg tended to exhibit greater SUV than those in the hip or thigh regions (Appendix 5.2); the mean SUV of all the muscles in the lower leg over all subjects was 2.04 g/mL, whereas it was 1.12 g/mL in the hip and 0.76 g/mL in the thigh. The tibialis anterior (3.20 g/mL), extensor digitorum longus (2.57 g/mL), extensor hallucis longus (2.39 g/mL), soleus (2.34 g/mL) and gastrocnemius medialis (2.31 g/mL) had the highest SUV overall. Several muscles that had high %FDG uptake, such as the gluteus maximus and the vastus lateralis, had comparatively low median SUV of 0.58 g/mL and 0.64 g/mL, respectively.

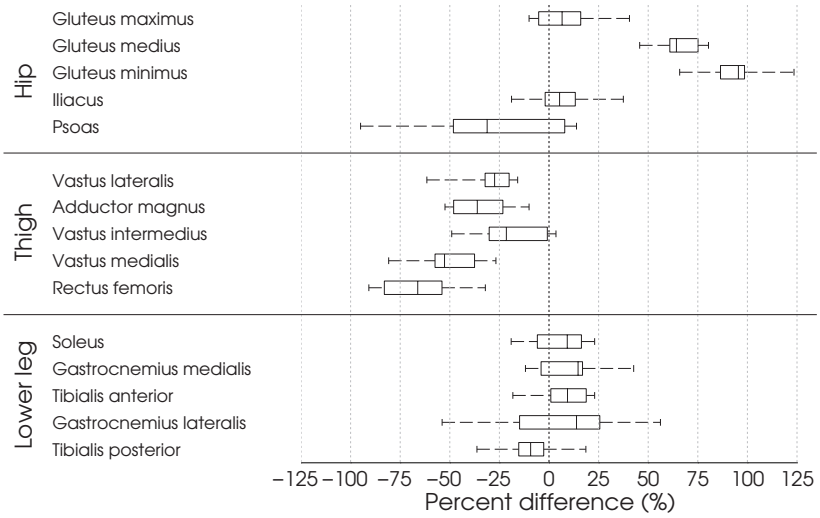

Figure 5.4. Differences in %FDG uptake between volumetric and slice-based analyses in the five most active muscles in each segment. In the plot, a positive/negative percentage indicates that the %FDG uptake was overestimated/underestimated by analyzing only a single slice. The psoas was only partly segmented in the volumetric analysis, because its uppermost cranial aspect was outside the scan area. Thus, the muscle's uptake was lower in the volumetric analysis than it was in reality, and the tendency of the slice-based method to underestimate that muscle's uptake would be even larger than it is presently.

The SUV data of all muscles in all subjects are available in Appendix 5.2.

Differences between volumetric and single slice analyses

There were large differences between the %FDG uptake as measured volumetrically compared with the %FDG uptake measured using the single slice technique. The differences of the five muscles in each segment that had the largest %FDG uptake are shown in Figure 5.4.

In the hip region, the %FDG uptake in the gluteus medius and minimus was severely overestimated when only a single slice was analyzed (between 45.7% and 80.4% and between 65.9% and 123.5%, respectively), whereas the uptake in the psoas tended to be underestimated (between -95.0% and 13.8%).

In the thigh, the %FDG uptake was underestimated when analyzing only a single slice in all muscles shown in Figure 5.4. The underestimation was most severe in the rectus femoris (between -90.8% and -32.1%).

In the lower leg, we did not find consistent under- or overestimation in %FDG uptake, but the ranges of differences between methods were roughly similar to those observed in the hip and thigh. The gastrocnemius lateralis had a particularly wide range of between -53.9% (underestimation) and 56.2% (overestimation).

Discussion

This study aimed to determine muscular activity during walking using a volumetric analysis of glucose uptake in entire muscles. The muscles with the highest median %FDG uptake were the soleus, gluteus maximus, vastus lateralis, gastrocnemius medialis and adductor magnus. We found a wide range of %FDG uptake values between subjects, including in some of the most important muscles involved in walking (e.g., soleus, gluteus medius, gastrocnemius medialis). Compared with the volumetric analysis, the single slice analysis did not yield an accurate estimate of the %FDG uptake in many of the most active muscles, including the gluteus medius and minimus (overestimated) and all the thigh muscles (underestimated).

The soleus and the gastrocnemius medialis were among the muscles that had the highest median uptake of FDG of the muscles in the lower limb, both in terms of %FDG uptake and SUV. As these muscles are both plantarflexors, this is consistent with literature stating that the generation of plantarflexion torque is key to forward propulsion and to prevent the body from falling forward while walking (Liu et al. 2006; Perry 1974; Winter 1983). The gluteus maximus and vastus lateralis also had high %FDG uptake values. These muscles are two of the primary hip and knee extensors, respectively. As such, they play a crucial role in providing support in the first half of stance (Pandy 2001; Winter 1980). The vastus lateralis took up more FDG than the vastus intermedius and medialis because of its larger volume. Combined, the median uptake of all three vasti was 14.3%, which demonstrates their importance in the walking motion.

The adductor magnus, much to our surprise, was one of the most active muscles during walking (median 5.4% FDG uptake). The adductor magnus also had the second highest SUV (0.75 g/ml) of the thigh muscles, indicating that its high %FDG uptake was not merely due to its large volume (509 mL). Although the temporal activation pattern of the adductor magnus during walking has been reported (using EMG) (Green et al. 1970), the quantitative activity of this muscle has remained understudied (Anderson et al. 2003). The consistently high %FDG uptake we observed in this muscle across subjects suggests that this muscle performs more work or exerts more force than commonly presumed. Previous work most often designated the hip abductors as the primary muscles controlling the hip in the frontal plane (e.g., Anderson et al. 2003; Liu et al. 2006; Perry 1974), with the adductors only tending to participate during the transfer phases between stance and swing (Perry et al. 2010). Therefore, we had expected that the largest hip abductor (gluteus medius, 4.4% FDG uptake) would be more active than any of the adductor muscles. Indeed, the gluteus medius had a higher median SUV (0.86 g/mL) than the adductor magnus (SUV=0.75 g/mL), but the adductor magnus had a larger volume, resulting in higher %FDG uptake. This result demonstrates the added value of the FDG-PET technique in revealing the activity of an entire muscle during gait, which would have been difficult to do with traditional measurement techniques (e.g., surface EMG) that measure only a small part of the muscle. Although other studies that used FDG-PET did analyze the FDG uptake in the hip adductors (Oi et al. 2003; Shimada et al. 2009b; Shimada et al. 2007), they examined the hip adductors only as a muscle group rather than differentiate between the muscles that comprise the group.

Like the adductor magnus, the gluteus minimus was surprisingly active. In spite of its small size (86 mL) compared with the functionally similar gluteus medius (330 mL), our results suggest that it made a large contribution to hip abduction and stabilization, as it took up roughly 50% of the FDG relative to the gluteus medius (Table 5.2). The gluteus minimus also had the highest SUV amongst all the muscles in the hip region (1.56 g/mL). This is in line with Oi et al., who found the SUV of the gluteus minimus during walking was the highest amongst the three gluteal muscles (Oi et al. 2003).

The iliacus and psoas are two muscles that flex the hip but have been difficult to examine with traditional methods (e.g., surface EMG) because of their anatomical position deep in the body. Although some authors have used intramuscular EMG to record the activity of these muscles, quantitative data about their contribution to walking have remained scarce (e.g. Andersson et al. 1997; Perry et al. 2010). In this study, we found that the %FDG uptake values of the iliacus and psoas were 2.0% and 1.4%, respectively. Even when added together, our data suggest that the activity of these muscles is rather low in normal walking compared to the ankle plantarflexors and dorsalflexors, hip extensors and abductors, and knee extensors and flexors. This is in agreement with Perry, who stated that the iliacus plays a small role in normal walking, although walking faster or slower increases its importance (Perry et al. 2010).

The large differences between subjects in %FDG uptake values in some muscles could indicate that each subject activated his/her muscles in a unique fashion. This notion is supported by previous studies that used surface EMG; Arsenault et al. found large and highly significant intersubject differences in the normalized (to maximum voluntary contraction) signal amplitude among healthy subjects, for instance in the soleus, rectus femoris, vastus medialis and tibialis anterior (Arsenault et al. 1986). Yang and Winter (Yang et al. 1984) and Winter and Yack (Winter et al. 1987) found intersubject coefficients of variation that are in the same order of magnitude as ours (Appendix 5.1). Given that we specifically chose to include subjects with a wide range of body types in this study, several factors could explain the variance in %FDG uptake, for instance, age. Subject 8 provides an illustration of the effect that a relatively high age (60 yr) might have had. The soleus had the highest uptake of all muscles and in all subjects except subject 8 (Appendix 5.1). That subject concurrently had the highest %FDG uptake in the gluteus maximus amongst all subjects. Thus, this subject might have shifted from exerting ankle plantarflexion torque to exerting more hip extension torque to achieve forward progression. In addition, this subject had the lowest psoas and iliacus activity of all subjects as well as the second lowest summed activity in the quadriceps of all subjects. These combined findings suggest an "elderly walking pattern"; they match exactly a redistribution pattern of joint torques observed by DeVita and Hortobagyi in elderly subjects when compared with that in younger subjects (DeVita et al. 2000). However, we did not observe the same pattern in any of the other three relatively old subjects (age 55-60 yr), so other factors (e.g., general physical fitness level) may also influence the degree to which each muscle is active during walking.

The volumetric and single slice analyses yielded systematically discrepant results in some of the muscles that were most active during walking (e.g., gluteus medius, vastus lateralis). Moreover, the muscles in which no systematic discrepancy was found (e.g., gastrocnemius

lateralis, iliacus), still exhibited a rather large range (from -53.9% to 56.2% and from -18.9% to 37.5%, respectively) around the "ideal" 0% difference. These findings illustrate the added value of analyzing entire muscles rather than only single slices on the quantification of %FDG uptake values. For this comparison, we took slices taken at discrete heights on the basis of the literature (Oi et al. 2003; Shimada et al. 2009a; Shimada et al. 2009b; Shimada et al. 2007; Tashiro et al. 1999). It may be argued that other slice heights might resemble the results more closely as obtained in the volumetric analysis. Therefore, in an additional sequence of assessments, we also examined the effects of taking slices at different heights but we were unable to find a single slice height in each segment that accurately represented the volumetric FDG uptake in all subjects.

Limitations

Our study has some limitations. First, the muscle segmentation might have some errors despite extensive examination of the intermediate and end results. Despite the fact that the MRI scan protocol was specifically designed for imaging muscle boundaries, the boundaries of some muscles were difficult to distinguish. However, the sensitivity analysis indicated that the effects of these possible errors on the volumetric %FDG uptake were small. Second, we had no control condition such as similar measurements of FDG uptake after a resting period. This could have revealed whether the baseline FDG uptake was similar between muscles and subjects. Unfortunately, it remains difficult to extend this type of experiment with control measurements because of ethical issues regarding the radiation dose. Third, the comfortable walking speed was unique for each subject and this might have influenced the %FDG uptake values. The intensity level of the protocol might also have been experienced differently by different subjects, although none of the subjects indicated that it was too intense or asked to have the speed of the treadmill reduced. We deliberately chose comfortable walking rather than a fixed walking speed to prevent subjects from being "forced" to walk at an unnatural pace; consequently, this might lead to unnatural muscle FDG uptake.

Another limitation inherent to studies that use FDG-PET to determine muscle activity, is the unknown relation between FDG uptake and the actual work performed or force exerted by a muscle. Muscle cells can use various substrates, including internal glycogen and triglyceride stores and plasma free fatty acids and glucose. The relative importance of these substrates depends on factors such as the intensity of the exercise (Romijn et al. 1993), the remaining muscle glycogen stores (Wahren et al. 1971), and the fiber type composition of the muscle (Henriksen et al. 1990). In our study, the exercise intensity was constant and rather low and the muscle glycogen stores were likely not depleted as a result. Thus, plasma glucose uptake likely remained constant (Romijn et al. 1993) in our study. The fiber type composition might have an influence on FDG uptake; muscles that have a high proportion of Type I fibers tend to be more metabolically active during exercise (Heinonen et al. 2012). The concurrent validity, however, of studying walking by FDG-PET compared with EMG and kinematic and kinetic studies has previously been shown by Oi et al. (Oi et al. 2003). The present results corroborate these findings, as the %FDG uptake in several known prime movers of gait (e.g., soleus, gluteus maximus, vasti, gastrocnemius medialis) was high, which also corresponds well with the literature on contributors to joint torques and powers (Anderson et al. 2003; Liu et al. 2006; Winter 1983).

Conclusions

The volumetric analysis of FDG uptake in the muscles of the lower limb yielded an extensive overview of the most active muscles during walking. The most active muscles in terms of %FDG uptake generally corresponded well with literature that used other methods such as inverse dynamics and EMG. Several muscles (adductor magnus, gluteus minimus) that were difficult to measure with traditional methods (e.g., surface EMG), because of their large size or their deep-lying position in the body, were found by FDG-PET to be very active during gait. The FDG uptake as measured in single slices did not correspond well to the FDG uptake obtained by volumetric analysis, which strongly illustrates the added value of our novel image analysis techniques. We intend to use these data to validate musculoskeletal models of these healthy subjects. In the future, it might be possible to analyze the gait of patients with orthopedic or neurological deficits, or to enable the construction of patient-specific rehabilitation protocols. To enable such next steps in patient populations, the protocol may need to be shortened. The innovative FDG-PET method as described in this chapter will assist in future steps toward a better understanding of musculoskeletal behavior of healthy subjects and patients.

Acknowledgements

We thank dr. Toshihiko Fujimoto for useful comments regarding the design of the study. We gratefully acknowledge financial support by the Seventh Framework Programme (FP7) of the European Union for the TLEMsafe project (http://www.tlemsafe.eu).

References

Anderson, F.C., and Pandy, M.G. 2003. Individual muscle contributions to support in normal walking, Gait Posture, 17: 159-169.

Andersson, E.A., Nilsson, J., and Thorstensson, A. 1997. Intramuscular EMG from the hip flexor muscles during human locomotion, Acta Physiol Scand, 161: 361-370.

Arsenault, A.B., Winter, D.A., and Marteniuk, R.G. 1986. Is there a 'normal' profile of EMG activity in gait?, Med Biol Eng Comput, 24: 337-343.

Burden, A. 2010. How should we normalize electromyograms obtained from healthy participants? What we have learned from over 25 years of research, J Electromyogr Kinesiol, 20: 1023-1035.

Carbone, V., van der Krogt, M.M., Koopman, H.F., and Verdonschot, N. 2012. Sensitivity of subject-specific models to errors in musculo-skeletal geometry, J Biomech, 45: 2476-2480.

Cherry, S.R., Sorenson, J.A., and Phelps, M.E. 2012. Physics in Nuclear Medicine (Saunders: Philadelphia, PA).

De Luca, C.J. 1997. The use of surface electromyography in biomechanics, J Appl Biomech, 13: 135-163.

DeVita, P., and Hortobagyi, T. 2000. Age causes a redistribution of joint torques and powers during gait, J Appl Physiol, 88: 1804-1811.

Ericson, M.O., Nisell, R., and Ekholm, J. 1986. Quantified electromyography of lower-limb muscles during level walking, Scand J Rehabil Med, 18: 159-163.

Fujimoto, T., Itoh, M., Kumano, H., Tashiro, M., and Ido, T. 1996. Whole-body metabolic map with positron emission tomography of a man after running, Lancet, 348: 266.

Fujimoto, T., Kemppainen, J., Kalliokoski, K.K., Nuutila, P., Ito, M., and Knuuti, J. 2003. Skeletal muscle glucose uptake response to exercise in trained and untrained men, Med Sci Sports Exerc, 35: 777-783.

Gondoh, Y., Tashiro, M., Itoh, M., Masud, M.M., Sensui, H., Watanuki, S., Ishii, K., Takekura, H., Nagatomi, R., and Fujimoto, T. 2009. Evaluation of individual skeletal muscle activity by glucose uptake during pedaling exercise at different workloads using positron emission tomography, J Appl Physiol, 107: 599-604.

Green, D.L., and Morris, J.M. 1970. Role of adductor longus and adductor magnus in postural movements and in ambulation, Am J Phys Med, 49: 223-240.

Heinonen, I., Nesterov, S.V., Kemppainen, J., Fujimoto, T., Knuuti, J., and Kalliokoski, K.K. 2012. Increasing exercise intensity reduces heterogeneity of glucose uptake in human skeletal muscles, PLoS One, 7: e52191.

Henriksen, E.J., Bourey, R.E., Rodnick, K.J., Koranyi, L., Permutt, M.A., and Holloszy, J.O. 1990. Glucose transporter protein content and glucose transport capacity in rat skeletal muscles, Am J Physiol, 259: E593-598.

Inman, V.T., Ralston, H.J., and Todd, F. 1981. Human Walking (Williams & Wilkins: Baltimore).

Jakoby, B.W., Bercier, Y., Conti, M., Casey, M.E., Bendriem, B., and Townsend, D.W. 2011. Physical and clinical performance of the mCT time-of-flight PET/CT scanner, Phys Med Biol, 56: 2375-2389.

Kalliokoski, K.K., Boushel, R., Langberg, H., Scheede-Bergdahl, C., Ryberg, A.K., Dossing, S., Kjaer, A., and Kjaer, M. 2011. Differential glucose uptake in quadriceps and other leg muscles during one-legged dynamic submaximal knee-extension exercise, Front Physiol, 2: 75.

Liu, M.Q., Anderson, F.C., Pandy, M.G., and Delp, S.L. 2006. Muscles that support the body also modulate forward progression during walking, J Biomech, 39: 2623-2630.

Masood, T., Bojsen-Moller, J., Kalliokoski, K.K., Kirjavainen, A., Aarimaa, V., Peter Magnusson, S., and Finni, T. 2014. Differential contributions of ankle plantarflexors during submaximal isometric muscle action: a PET and EMG study, J Electromyogr Kinesiol, 24: 367-374.

Oi, N., Iwaya, T., Itoh, M., Yamaguchi, K., Tobimatsu, Y., and Fujimoto, T. 2003. FDG-PET imaging of

lower extremity muscular activity during level walking, J Orthop Sci, 8: 55-61.
Pandy, M.G. 2001. Computer modeling and simulation of human movement, Annu Rev Biomed Eng, 3: 245-273.
Pappas, G.P., Olcott, E.W., and Drace, J.E. 2001. Imaging of skeletal muscle function using (18)FDG PET: force production, activation, and metabolism, J Appl Physiol (1985), 90: 329-337.
Perry, J. 1974. Kinesiology of lower extremity bracing, Clin Orthop Relat Res: 18-31.
Perry, J., and Burnfield, J.M. 2010. Gait analysis : normal and pathological function (SLACK: Thorofare, NJ).
Romijn, J.A., Coyle, E.F., Sidossis, L.S., Gastaldelli, A., Horowitz, J.F., Endert, E., and Wolfe, R.R. 1993. Regulation of endogenous fat and carbohydrate metabolism in relation to exercise intensity and duration, Am J Physiol, 265: E380-391.
Rudroff, T., Kindred, J.H., Benson, J.M., Tracy, B.L., and Kalliokoski, K.K. 2014. Greater glucose uptake heterogeneity in knee muscles of old compared to young men during isometric contractions detected by [(18)F]-FDG PET/CT, Front Physiol, 5: 198.
Scheys, L. 2009. Personalized musculoskeletal modeling based on magnetic resonance images: use for biomechanical analysis of gait, K.U. Leuven.
Shimada, H., Hirata, T., Kimura, Y., Naka, T., Kikuchi, K., Oda, K., Ishii, K., Ishiwata, K., and Suzuki, T. 2009a. Effects of a robotic walking exercise on walking performance in community-dwelling elderly adults, Geriatr Gerontol Int, 9: 372-381.
Shimada, H., Kimura, Y., Lord, S.R., Oda, K., Ishii, K., Suzuki, T., and Ishiwata, K. 2009b. Comparison of regional lower limb glucose metabolism in older adults during walking, Scand J Med Sci Sports, 19: 389-397.
Shimada, H., Kimura, Y., Suzuki, T., Hirata, T., Sugiura, M., Endo, Y., Yasuhara, K., Shimada, K., Kikuchi, K., Hashimoto, M., Ishikawa, M., Oda, K., Ishii, K., and Ishiwata, K. 2007. The use of positron emission tomography and [18F]fluorodeoxyglucose for functional imaging of muscular activity during exercise with a stride assistance system, IEEE Trans Neural Syst Rehabil Eng, 15: 442-448.
Staudenmann, D., Roeleveld, K., Stegeman, D.F., and van Dieen, J.H. 2010. Methodological aspects of SEMG recordings for force estimation--a tutorial and review, J Electromyogr Kinesiol, 20: 375-387.
Tashiro, M., Fujimoto, T., Itoh, M., Kubota, K., Fujiwara, T., Miyake, M., Watanuki, S., Horikawa, E., Sasaki, H., and Ido, T. 1999. 18F-FDG PET imaging of muscle activity in runners, J Nucl Med, 40: 70-76.
Wahren, J., Felig, P., Ahlborg, G., and Jorfeldt, L. 1971. Glucose metabolism during leg exercise in man, J Clin Invest, 50: 2715-2725.
Winter, D.A. 1980. Overall principle of lower limb support during stance phase of gait, J Biomech, 13: 923-927.
Winter, D.A. 1983. Energy generation and absorption at the ankle and knee during fast, natural, and slow cadences, Clin Orthop Relat Res: 147-154.
Winter, D.A., and Yack, H.J. 1987. EMG profiles during normal human walking: stride-to-stride and inter-subject variability, Electroencephalogr Clin Neurophysiol, 67: 402-411.
Yang, J.F., and Winter, D.A. 1984. Electromyographic amplitude normalization methods: improving their sensitivity as diagnostic tools in gait analysis, Arch Phys Med Rehabil, 65: 517-521.

Appendix 5.1: %FDG

		Subject													
		1	**2**	**3**	**4**	**5**	**6**	**7**	**8**	**9**	**10**	**median**	**min**	**max**	**CV**
Hip region	Gluteus maximus	4,1%	4,6%	7,2%	6,7%	7,0%	11,5%	7,9%	11,6%	7,4%	6,7%	7,1%	4,1%	11,6%	0,33
	Gluteus medius	2,5%	2,5%	4,0%	3,0%	5,5%	4,8%	4,3%	19,5%	6,1%	4,5%	4,4%	2,5%	19,5%	0,88
	Gluteus minimus	1,1%	0,6%	1,5%	1,2%	3,9%	3,0%	2,8%	4,8%	6,2%	1,2%	2,2%	0,6%	6,2%	0,71
	Iliacus	1,3%	1,5%	2,0%	2,1%	2,3%	3,0%	2,6%	1,2%	2,7%	1,3%	2,0%	1,2%	3,0%	0,32
	Psoas	1,1%	1,0%	1,4%	1,3%	1,6%	1,7%	1,7%	0,8%	1,7%	1,5%	1,4%	0,8%	1,7%	0,24
	Pectineus	0,5%	0,5%	0,8%	0,8%	0,4%	0,5%	0,8%	0,4%	0,7%	0,4%	0,5%	0,4%	0,8%	0,30
	Piriformis	2,7%	0,4%	1,1%	0,5%	0,2%	0,3%	0,5%	1,4%	0,6%	0,3%	0,5%	0,2%	2,7%	0,94
	Obturator internus	2,0%	0,3%	0,9%	1,4%	0,5%	0,7%	0,4%	0,3%	0,5%	0,4%	0,5%	0,3%	2,0%	0,76
	Tensor fasciae latae	0,3%	0,4%	0,4%	0,4%	0,5%	0,6%	0,6%	0,9%	0,5%	0,3%	0,5%	0,3%	0,9%	0,36
	Obturator externus	0,5%	0,4%	0,3%	0,3%	0,3%	0,4%	0,4%	0,2%	0,2%	0,3%	0,3%	0,2%	0,5%	0,34
	Quadratus femoris	0,2%	0,2%	0,4%	0,2%	0,3%	0,5%	0,5%	0,2%	0,7%	0,3%	0,3%	0,2%	0,7%	0,49
	Gemellus inferior	0,1%	0,0%	0,0%	0,1%	0,1%	0,1%	0,1%	0,1%	0,1%	0,1%	0,1%	0,0%	0,1%	0,49
	Gemellus superior	0,2%	0,0%	0,0%	0,0%	0,0%	0,1%	0,1%	0,0%	0,1%	0,1%	0,0%	0,0%	0,2%	0,81
	Sum hip region	**16,5%**	**12,4%**	**20,1%**	**18,0%**	**22,5%**	**27,3%**	**22,7%**	**41,3%**	**27,3%**	**17,3%**				
Thigh region	Vastus lateralis	3,6%	3,8%	6,7%	6,4%	6,4%	7,6%	7,4%	3,8%	4,7%	5,3%	5,8%	3,6%	7,6%	0,28
	Adductor magnus	4,0%	3,6%	5,7%	5,3%	5,4%	6,9%	5,7%	3,7%	5,5%	3,6%	5,4%	3,6%	6,9%	0,23
	Vastus intermedius	2,5%	3,0%	5,9%	4,6%	4,9%	6,0%	5,4%	2,8%	4,0%	3,2%	4,3%	2,5%	6,0%	0,31
	Vastus medialis	2,4%	2,3%	5,4%	4,7%	4,2%	5,3%	4,2%	2,7%	4,2%	3,2%	4,2%	2,3%	5,4%	0,29
	Rectus femoris	1,5%	1,3%	2,1%	1,8%	1,9%	2,0%	2,8%	1,0%	2,4%	2,0%	1,9%	1,0%	2,8%	0,27
	Adductor longus	1,2%	1,2%	1,5%	5,1%	1,2%	2,2%	2,1%	3,9%	3,5%	1,1%	1,8%	1,1%	5,1%	0,61
	Semimembranosus	2,6%	1,2%	1,7%	1,7%	1,3%	3,6%	1,8%	1,2%	2,7%	2,8%	1,7%	1,2%	3,6%	0,40
	Biceps femoris caput longum	1,2%	0,9%	1,4%	1,9%	1,4%	1,9%	1,8%	0,8%	2,1%	2,3%	1,6%	0,8%	2,3%	0,32
	Adductor brevis	2,0%	1,4%	1,2%	1,6%	1,0%	1,3%	1,3%	3,4%	1,9%	1,7%	1,5%	1,0%	3,4%	0,40
	Sartorius	0,6%	1,0%	1,5%	1,4%	1,1%	1,5%	1,6%	4,4%	1,4%	0,8%	1,4%	0,6%	4,4%	0,71
	Semitendinosus	1,2%	1,0%	1,2%	1,3%	1,3%	1,1%	0,9%	0,6%	1,6%	1,8%	1,2%	0,6%	1,8%	0,27
	Biceps femoris caput breve	0,4%	0,7%	0,9%	0,8%	1,2%	1,0%	1,2%	0,5%	1,4%	0,5%	0,8%	0,4%	1,4%	0,39
	Gracilis	0,3%	0,6%	0,7%	0,8%	0,6%	0,6%	0,7%	0,6%	0,6%	0,6%	0,6%	0,3%	0,8%	0,19
	Sum thigh	**23,5%**	**22,0%**	**36,0%**	**37,2%**	**31,8%**	**40,9%**	**36,8%**	**29,5%**	**35,9%**	**29,0%**				
Lower leg	Soleus	39,5%	40,5%	17,3%	17,0%	15,2%	13,5%	21,2%	8,8%	11,5%	21,5%	17,1%	8,8%	40,5%	0,53
	Gastrocnemius medialis	5,1%	1,9%	8,6%	6,6%	13,7%	4,8%	4,0%	4,9%	6,1%	9,9%	5,6%	1,9%	13,7%	0,51
	Tibialis anterior	7,0%	5,0%	4,6%	6,4%	7,1%	2,9%	2,8%	3,7%	5,2%	4,4%	4,8%	2,8%	7,1%	0,32
	Gastrocnemius lateralis	2,3%	1,0%	4,0%	1,3%	1,4%	1,8%	1,7%	4,6%	2,0%	3,1%	1,9%	1,0%	4,6%	0,52
	Tibialis posterior	1,1%	1,7%	3,4%	1,2%	1,1%	2,9%	2,0%	1,2%	4,7%	1,3%	1,5%	1,1%	4,7%	0,59
	Extensor digitorum longus	0,7%	4,6%	1,2%	3,4%	1,1%	0,9%	1,6%	1,7%	1,8%	1,3%	1,5%	0,7%	4,6%	0,66
	Flexor hallucis longus	0,6%	4,6%	0,7%	0,7%	1,2%	1,4%	2,3%	1,2%	0,8%	1,8%	1,2%	0,6%	4,6%	0,78
	Extensor hallucis longus	1,5%	1,9%	0,8%	1,7%	1,0%	0,8%	0,8%	1,0%	1,3%	1,4%	1,2%	0,8%	1,9%	0,32
	Peroneus longus	0,5%	2,6%	1,2%	4,4%	0,7%	0,8%	1,1%	0,6%	1,0%	3,2%	1,0%	0,5%	4,4%	0,82
	Flexor digitorum longus	0,2%	0,9%	0,7%	0,4%	1,5%	0,9%	1,5%	0,6%	0,9%	0,4%	0,8%	0,2%	1,5%	0,55
	Peroneus brevis	0,8%	0,6%	0,8%	1,4%	1,2%	0,5%	0,6%	0,3%	0,5%	4,8%	0,7%	0,3%	4,8%	1,15
	Popliteus	0,5%	0,3%	0,4%	0,2%	0,5%	0,4%	0,5%	0,4%	0,7%	0,4%	0,4%	0,2%	0,7%	0,35
	Plantaris	0,2%	0,1%	0,1%	0,1%	0,1%	0,1%	0,4%	0,2%	0,1%	0,1%	0,1%	0,1%	0,4%	0,62
	Sum lower leg	**59,9%**	**65,6%**	**43,8%**	**44,8%**	**45,8%**	**31,8%**	**40,5%**	**29,2%**	**36,7%**	**53,6%**				

Appendix 5.2: SUV (g/mL)

		Subject													
		1	2	3	4	5	6	7	8	9	10	median	min	max	CV
Hip region	Gluteus maximus	0,44	0,48	0,63	0,58	0,58	0,70	0,53	1,40	0,65	0,56	0,58	0,44	1,40	0,41
	Gluteus medius	0,76	0,63	0,84	0,79	1,23	0,87	0,72	5,74	1,43	1,05	0,86	0,63	5,74	1,10
	Gluteus minimus	1,72	0,74	1,07	0,82	3,42	1,55	1,56	6,67	4,41	1,21	1,56	0,74	6,67	0,85
	Iliacus	0,60	0,71	0,69	0,87	0,85	0,96	0,69	0,94	1,07	0,58	0,78	0,58	1,07	0,20
	Psoas	0,54	0,60	0,80	0,93	0,76	0,60	0,71	0,65	0,87	0,55	0,68	0,54	0,93	0,18
	Pectineus	0,67	0,81	0,79	0,97	0,70	0,91	0,62	1,23	0,90	0,66	0,80	0,62	1,23	0,22
	Piriformis	8,18	1,13	1,30	1,34	0,83	1,02	0,73	4,43	0,93	0,86	1,07	0,73	8,18	0,83
	Obturator internus	4,18	0,74	1,17	2,80	0,74	1,10	0,77	0,90	0,82	0,67	0,86	0,67	4,18	0,62
	Tensor fasciae latae	0,38	0,46	0,61	0,59	0,57	0,62	0,50	1,12	0,68	0,46	0,58	0,38	1,12	0,32
	Obturator externus	1,73	0,82	0,80	1,08	0,79	1,10	0,69	0,80	0,86	0,91	0,84	0,69	1,73	0,16
	Quadratus femoris	0,61	0,66	0,87	0,86	0,78	1,13	0,69	0,97	0,83	0,62	0,80	0,61	1,13	0,20
	Gemellus inferior	1,02	0,78	0,82	1,09	0,85	1,29	0,79	1,24	1,09	0,69	0,94	0,69	1,29	0,23
	Gemellus superior	2,05	0,57	0,73	0,86	0,96	1,28	0,93	1,15	1,06	0,76	0,94	0,57	2,05	0,24
	Sum hip region	**1,76**	**0,70**	**0,86**	**1,04**	**1,01**	**1,01**	**0,76**	**2,09**	**1,20**	**0,74**				
Thigh region	Vastus lateralis	0,46	0,47	0,66	0,71	0,62	0,70	0,60	0,73	0,66	0,48	0,64	0,46	0,73	0,15
	Adductor magnus	0,81	0,55	0,70	0,87	0,69	0,82	0,62	0,87	0,94	0,60	0,75	0,55	0,94	0,19
	Vastus intermedius	0,52	0,55	0,74	0,78	0,75	0,79	0,66	0,89	0,75	0,55	0,75	0,52	0,89	0,16
	Vastus medialis	0,45	0,52	0,72	0,76	0,61	0,76	0,65	0,99	0,71	0,52	0,68	0,45	0,99	0,21
	Rectus femoris	0,41	0,46	0,61	0,59	0,58	0,71	0,56	0,63	0,77	0,47	0,58	0,41	0,77	0,17
	Adductor longus	0,65	0,60	0,64	2,51	0,68	0,91	0,61	3,76	1,49	0,52	0,66	0,52	3,76	0,86
	Semimembranosus	0,93	0,51	0,61	0,59	0,53	0,72	0,52	0,66	0,95	0,68	0,64	0,51	0,95	0,21
	Biceps femoris caput longum	0,52	0,42	0,55	0,59	0,56	0,61	0,52	0,59	0,66	0,61	0,57	0,42	0,66	0,12
	Adductor brevis	1,58	1,32	0,80	1,53	0,89	0,95	0,66	3,95	1,87	1,00	1,16	0,66	3,95	0,71
	Sartorius	0,38	0,52	0,72	0,70	0,58	0,77	0,57	3,05	0,80	0,52	0,64	0,38	3,05	0,88
	Semitendinosus	0,65	0,43	0,59	0,56	0,52	0,74	0,50	0,52	0,65	0,51	0,54	0,43	0,74	0,16
	Biceps femoris caput breve	0,45	0,46	0,66	0,64	0,76	0,78	0,61	0,74	1,01	0,50	0,65	0,45	1,01	0,24
	Gracilis	0,38	0,47	0,60	0,62	0,54	0,64	0,58	0,87	0,64	0,49	0,59	0,38	0,87	0,19
	Sum thigh	**0,63**	**0,56**	**0,66**	**0,88**	**0,64**	**0,76**	**0,59**	**1,40**	**0,92**	**0,57**				
Lower leg	Soleus	6,88	7,03	2,36	2,42	1,93	1,10	2,31	2,32	1,77	2,66	2,34	1,10	7,03	0,64
	Gastrocnemius medialis	2,27	0,76	2,47	1,59	3,54	1,05	0,90	3,33	2,60	2,34	2,31	0,76	3,54	0,50
	Tibialis anterior	5,07	4,34	2,75	4,14	3,55	1,10	1,07	3,43	2,96	2,37	3,20	1,07	5,07	0,41
	Gastrocnemius lateralis	1,42	0,82	1,58	0,73	0,87	0,84	0,81	4,23	1,81	1,55	1,14	0,73	4,23	0,76
	Tibialis posterior	1,05	1,55	1,93	1,22	1,12	1,26	1,09	1,51	3,23	0,97	1,24	0,97	3,23	0,45
	Extensor digitorum longus	2,55	6,62	1,92	4,87	2,76	1,11	1,16	2,95	1,73	2,60	2,57	1,11	6,62	0,64
	Flexor hallucis longus	1,19	6,98	1,01	1,11	1,22	0,87	1,93	1,50	1,08	2,55	1,20	0,87	6,98	0,95
	Extensor hallucis longus	4,18	4,67	1,38	3,28	2,43	1,07	1,05	3,28	2,16	2,34	2,39	1,05	4,67	0,50
	Peroneus longus	1,11	3,18	1,69	5,20	1,24	0,85	0,86	1,15	1,20	4,01	1,22	0,85	5,20	0,74
	Flexor digitorum longus	0,98	1,67	1,57	0,94	1,41	1,24	1,46	1,32	1,57	1,18	1,37	0,94	1,67	0,17
	Peroneus brevis	0,99	1,26	1,27	2,30	0,97	0,95	0,83	1,01	1,07	3,63	1,04	0,83	3,63	0,62
	Popliteus	2,24	1,09	1,13	0,88	1,77	1,30	1,35	2,66	2,56	1,38	1,37	0,88	2,66	0,41
	Plantaris	1,65	0,58	0,98	0,67	1,97	0,97	2,05	3,05	1,77	1,44	1,55	0,58	3,05	0,53
	Sum lower leg	**2,43**	**3,12**	**1,69**	**2,26**	**1,91**	**1,05**	**1,30**	**2,44**	**1,96**	**2,23**				
	Mean all muscles	**1,61**	**1,46**	**1,07**	**1,39**	**1,18**	**0,94**	**0,88**	**1,98**	**1,36**	**1,18**				

Chapter 6

Symmetry and spatial distribution of muscle glucose uptake in the lower limbs during walking measured using FDG-PET

(Submitted)

Kolk, S., Klawer, E.M.E., Visser, E.P., Lobeek, D., Schepers, J., Verdonschot, N., Weerdesteyn, V.

Abstract

Background: This study aimed to elucidate whether muscle activity (in terms of glucose uptake) between the legs can be considered symmetrical during walking. Furthermore, we aimed to determine whether the [^{18}F]-fluorodeoxyglucose (FDG) was distributed heterogeneously throughout each muscle, and if so, whether areas of high uptake would be clustered.

Methods: Ten healthy participants walked on a treadmill at self-selected comfortable walking speed for a total of 90 minutes, 60 minutes before and 30 minutes after intravenous injection of 50 MBq FDG. Thereafter, a PET/CT scan of the lower limb was acquired. Three-dimensional muscle contours of 78 (=39x2) muscles of the left and right lower limb were semi-automatically determined from MRI scans. After non-rigid registration, those muscle contours were used to extract FDG uptake from the PET scans.

Results: Large asymmetries were observed in the lower leg muscles (e.g., median absolute asymmetry index of 42% in the gastrocnemius medialis) and in the gluteus minimus (30% asymmetry) and gluteus medius (15% asymmetry), whereas the uptake in the thighs was relatively symmetrical between the limbs (<6% asymmetry). These were not related to limb-dominance nor to inter-limb differences in muscle volume. The FDG distribution was not distributed normally; most voxels had a relatively low SUV, and a minority of voxels had a relatively high SUV. The voxels with higher FDG uptake were distributed heterogeneously; they were clustered in virtually all muscles.

Conclusions: The findings in this study challenge the common assumption of symmetry in muscle activity between the limbs in healthy subjects. The clustering of voxels with high uptake suggests that even in this prolonged repetitive task, different spatial regions of muscles contribute differently to walking than others.

Introduction

Walking involves a complex integration of muscular contractions with the goal of maintaining stance stability and forward progression. Walking in healthy persons has traditionally been assumed to be a symmetrical motion, either from assumption or for convenience of data collection and analysis (Sadeghi et al. 2000). This assumption may be considered reasonable, as most healthy persons walk without a limp or other visible evidence of asymmetry. However, several studies have found that the legs and individual muscles do not necessarily behave symmetrically during gait. For instance, asymmetries in kinematics (Gundersen et al. 1989; Maupas et al. 1999) and muscle activation (Arsenault et al. 1986a; Ounpuu et al. 1989) have been reported. A better understanding of these asymmetries is important, for instance in determining ranges of normal (healthy) asymmetry, beyond which a patient with a certain pathology is considered to be truly asymmetrical. Also, asymmetry is an important consideration in validating musculo-skeletal models, which generally assume that healthy persons walk with equal activity levels in muscles in both legs (Ackermann et al. 2010; Anderson et al. 2001).

To assess muscle activation patterns, researchers typically utilize surface electromyography (EMG). This method is convenient and noninvasive, but has disadvantages such as a limited number of muscles that can be measured simultaneously, the need for a reference contraction if muscles are to be compared with each other, inability to measure deep-lying muscles and deep-lying aspects of superficial muscles, and confounding factors such as crosstalk and adipose tissue (De Luca 1997; Staudenmann et al. 2010). In most surface EMG applications, the electrodes are placed in discrete locations on the skin superficial to the muscle. The resulting EMG data are generally considered to reflect the activity of the muscle as a whole. However, it is known (e.g., from multi-channel EMG studies) that the spatial activity of muscle regions can be heterogeneous (Hodson-Tole et al. 2013; Kalliokoski et al. 2007; Kinugasa et al. 2011; Laaksonen et al. 2013; Pappas et al. 2001; Staudenmann et al. 2009). For example, during standing, the gastrocnemius medialis was found to be more active in the distal region than in the proximal region (Hodson-Tole et al. 2013). Moreover, the activity level of muscle regions can shift depending on exercise intensity, as was found in the gastrocnemius medialis in an isometric plantar flexion exercise at varying contraction levels (Kinugasa et al. 2011). Finally, it is known from positron emission tomography (PET) studies, that the overall heterogeneity of glucose uptake in muscles varies depending on the exercise intensity; the heterogeneity decreasing with increasing exercise intensity (Heinonen et al. 2012). Region-specific activation may influence the magnitude and direction of forces that are applied to tendons (Rahemi et al. 2014), which may, for instance, have relevance in the study of injury mechanisms or muscle diseases. Insight into region-specific activation could also be useful for validating musculo-skeletal models, which often contain multiple musculo-tendon actuators per muscle, each of which with its own specific calculated activation level during a given activity (e.g., walking, stair negotiation or other activities of daily living).

Positron emission tomography with [^{18}F]-fluorodeoxyglucose (FDG) is a technique that can be used to assess glucose uptake in entire muscles during activity in both limbs, as well as region-specific differences in glucose uptake within muscles. This technique is based

on the principle that contracting muscles take up glucose (and FDG) from the blood to replenish their expended energy. Although muscle cells can use various substrates (e.g., internal glycogen and triglyceride stores, plasma free fatty acids), the plasma glucose uptake is likely constant in a low intensity exercise such as walking (Romijn et al. 1993). Several authors have already used FDG-PET to investigate muscle activity during walking (Kindred et al. 2015; Kolk et al. 2015; Oi et al. 2003; Shimada et al. 2009; Shimada et al. 2007), but asymmetries between muscles in the left and right legs, and region-specific activation within muscles have not yet been studied. In part, this may have been due to the analyses of the FDG uptake data being limited to single slices of the PET scan, instead of taking the uptake in the entire muscle into account. Using three-dimensional MRI segmentation techniques, the added value of analyzing the uptake in the entire muscles was shown in previous work from our group (Kolk et al. 2015).

This study's aims were threefold. First, we aimed to elucidate whether muscle activity (in terms of glucose uptake) between the legs can be considered symmetrical during walking. Second, we aimed to determine whether the FDG uptake was heterogeneous throughout each muscle. Third, in case the uptake would be heterogeneous, we aimed to investigate whether muscle regions that exhibited high uptake would be clustered.

Methods

The subjects, protocol and scans have been described in detail previously (Kolk et al. 2015), and will therefore be described only briefly.

Subjects

Ten healthy subjects with no history of major injury, orthopedic surgery on the lower limb, ailment related to carbohydrate metabolism, or cardiac or muscular disease participated in this study. There were five men and five women, age 23-60 years, height 1.60 m to 1.95 m, weight 55.5 kg to 91.7 kg. The dominant limb was determined to be the limb used to kick a ball (Chapman et al. 1987; Seeley et al. 2008). All procedures were approved by the local ethical committee and written informed consent was obtained from all participants.

Protocol

The protocol consisted of 90 minutes of walking on a treadmill at self-selected comfortable pace; 60 minutes before and 30 minutes after injection with 53.6±1.8 MBq FDG. The injected activity was low since the scans were made in 3D mode and through the use of time-of-flight technology on a latest generation PET scanner (Jakoby et al. 2011). When walking ceased, subjects rested for 30 minutes, and then a PET/CT scan of the lower limb was acquired. The subjects had refrained from eating and drinking anything except water for at least six hours, and from participating in strenuous physical activities for two days before the session.

Positron-emission tomography and CT scans

The PET and CT scans were made with a Biograph 40 mCT (Siemens AG, Erlangen, Germany), from the feet to at least the iliac crest. The slice thickness of the PET scan was 2.0 mm, and image reconstruction was performed with a matrix size of 512x512 and voxel size of 1.6 x 1.6 mm. The images were filtered using a 3D Gaussian filter with a kernel width of 3 mm full width at half maximum. The CT images were used both for attenuation correction (reconstruction with 5.0 mm slice thickness, B19f convolution kernel), and anatomical reference (reconstruction with 2.0 mm slice thickness, B31f convolution kernel).

Magnetic resonance imaging scans

The MRI scans were acquired with a Magnetom Skyra (Siemens AG, Erlangen, Germany) at 3 Tesla. The slice thickness was 3.0 mm in the hip, knee and ankle regions, and 8.0 mm in the long bone regions in between, such that a higher level of detail was available in the areas where most muscles originate or insert. The scan parameters (TR/TE: 450-545/9 ms) were set to achieve optimal visibility of muscle boundaries (Kolk et al. 2015; Scheys 2009).

Image analysis

The end goal of the image analysis phase was to extract FDG uptake values from each of 78 muscles (39 muscles in both limbs, see Kolk et al. 2015) from the PET scans. To achieve this, three-dimensional regions-of-interest (ROIs) that reflected the muscle boundaries were needed. Several sequential steps were taken using Mimics (Materialise N.V., Leuven, Belgium), Matlab 2012b (the Mathworks, Natick, MA, USA) and the Image Segmentation and Registration Toolkit 4.5.2 (ITK) (Kitware Inc., Clifton Park, NY, USA).

1) Using the MRI scan of the left lower limb of the first of the healthy subjects, 39 muscles were segmented manually on the axial slices in Mimics. These 'stacked' two-dimensional boundaries of each muscle formed three-dimensional ROIs. This complete segmentation will henceforth be referred to as 'atlas'.

2) The muscles in the left lower limb of the other nine subjects were semi-automatically segmented in Mimics, using the atlas of muscle ROIs and an algorithm based on non-rigid registration of the MRI scans. More detail can be found in (Kolk et al. 2015). The resulting muscle segmentations were thoroughly checked and manually corrected where necessary.

3) The MRI scans and muscle ROIs of the left lower limb of all ten subjects were mirrored to their respective right lower limb, again with an algorithm based on non-rigid registration. Since the orientation of both limbs was not always perpendicular to the axial direction of the scan, and the fact that left-to-right anatomical differences might exist, the left and right limbs were treated as separate entities. Therefore, segmentation of the muscles of the right limb was checked and corrected again where necessary.

4) The MRI scan and the muscle ROIs were registered onto the CT scan, using ITK. The muscle ROIs were manually checked and corrected where necessary, this time using the CT scan as the anatomical reference. Since the CT and PET scans were taken with the subject lying on the table in the same position, no further adjustment of muscle ROIs was necessary once the muscle ROIs properly reflected the muscle contours on the CT scan.

5) The muscle ROIs were exported as DICOM (Digital Imaging and Communications in Medicine) mask files.

6) The DICOM mask files and the PET DICOM files (which were obtained directly from the PET scanner) were loaded into Matlab. Then, the ones (reflecting the muscle's location) and zeros (all surrounding areas) in the DICOM mask files were multiplied with the PET scan (containing grey values reflecting the FDG uptake in Bq/mL). The FDG uptake values were corrected for decay time since the start of the scan using the rescale slope and intercept values extracted from the DICOM headers.

An important note is that the PET DICOM files from which we extracted the FDG uptake values were obtained directly from the Biograph 40 mCT; they were not 'morphed' or altered in any way.

Analysis of asymmetry

To analyze the amount of asymmetry between the dominant and non-dominant lower limbs, we used the absolute symmetry index (ASI) and the symmetry index (SI) (Becker et al. 1995; Furlong et al. 2015; Herzog et al. 1989; Schoeman et al. 2013). The equations for the SI and ASI of muscle *i* are:

$$SI_i = \frac{SUV_{i,dominant} - SUV_{i,non-dominant}}{\frac{1}{2}(SUV_{i,dominant} + SUV_{i,non-dominant})} \times 100\%, and\ ASI_i = |SI_i|$$

Where SUV is the mean Standardized Uptake Value of that muscle (Kubota et al. 1985; Lucignani et al. 2004). The SUV reflects the normalized, mean FDG uptake in a muscle, and is given by the following formula for muscle *i*:

$$SUV_i = \frac{Measured\ total\ activity\ in\ muscle\ (Bq)\ /\ Muscle\ volume\ (mL)}{Injected\ activity\ (Bq)\ /\ Body\ mass\ (g)}$$

We corrected the SUV for radioactive decay between the injection and the start of the scan. Since the SUV is normalized by the muscle volume, and volume differences might exist between muscles in the dominant and the non-dominant lower limb, these could have influenced the SUVs. Therefore, we also multiplied the SUV by the muscle volume, and refer to this value as the absolute uptake value (AUV).

The SI provided a measure for analyzing whether systematic differences existed in uptake between the dominant and the non-dominant limb, whereas absolute values of SI indicated the degree of non-directional asymmetries. Only the five largest muscles (in terms of

volume) in each segment (pelvis, thigh, lower leg) were analyzed, since in previous work, those muscles were found to provide the largest contributions to walking (Kolk et al. 2015). Hence, in total we considered 30 muscles (15 on each side) for the analyses.

Heterogeneous uptake

Heterogeneity in uptake within muscles was examined using the skewness of the FDG uptake. The skewness provides a measure for the symmetry of the probability distribution, which for this study was an advantage over the coefficient of variation, which only provides a measure for the spread of the distribution (the coefficients of variation have been reported previously (Kolk et al. 2015)). If the distribution has equally long and thick tails to the left and to the right, the skew is zero. If the most frequently occurring FDG uptake values clustered at the lower end of the distribution and the tail pointed towards the higher scores, the skewness was positive, and vice versa for negative skew (Field 2013).

Clustering

To examine the degree to which voxels with high SUVs were clustered in a given muscle, we first classified the voxels that were amongst those with the highest five percent uptake as being 'hot' voxels, and the other voxels (i.e. 95 percent of the voxels) as 'cold' voxels. We then calculated for each hot voxel with how many hot voxels it shared a border (number of hot neighbors – NHN). This calculation was also done for determining the number of hot voxels that bordered each cold voxel. The calculation in both cases was performed using a custom algorithm written in Matlab that detected the 6-point connectivity of the voxel. The average number of hot neighbors per hot voxel was then divided by the average number of hot neighbors per cold voxel. Since there were 19 times (=95/5) less hot voxels than cold voxels, the denominator was multiplied by 19. This yielded a dimensionless index we will call the 'cluster index'. The cluster index of muscle *i* is given by:

$$cluster\ index_i = \frac{\frac{1}{m}\sum_{h=1}^{h=m} NHN_h}{\frac{1}{n}\sum_{c=1}^{c=n} NHN_c \times 19}$$

The numerator reflects the average number of hot voxels *m* per hot voxel *h*. The denominator reflects the average corrected number of hot voxels *n* per cold voxel *c*. A cluster index of 0 would correspond to a situation where there is a homogeneous spread of the hot voxels throughout the muscle, whereas a higher cluster index value would indicate a tendency for hot voxels to cluster.

Statistical analysis

The distributions of the SUV and AUV values of each of the 30 muscles were tested for normality with Kolmogorov-Smirnov tests. Since about half of these tests indicated that data were not normally distributed, we used non-parametric tests (Wilcoxon matched-pair signed-rank) for all comparisons between muscles of the dominant and the non-dominant limb. The significance level was set at $p \leq 0.05$.

Results

Inter-limb asymmetries

There were large asymmetries in uptake between all muscles in both limbs, as indicated by the absolute symmetry indices (ASI) (Table 6.1). These differences were most pronounced in the lower leg, where median ASI values between 12% (soleus, tibialis posterior) and 42% (gastrocnemius medialis) were found. For individual subjects, differences up to 98% were found (tibialis anterior). In the hip region, the gluteus minimus and medius exhibited the largest asymmetry (median ASI of 30% and 15%, respectively). The uptake in the thighs was relatively symmetrical between the limbs; median ASI were 10% or lower in all muscles. All but one subjects had at least one asymmetry that was larger than 25% (Table 6.1, last column).

Table 6.1 Absolute Symmetry Indices of SUV for muscles of the lower limb during walking

Muscle	ASI	Number of subjects >25% ASI	Subject numbers >25% ASI
Gluteus maximus	5% (0% - 49%)	1	8
Gluteus medius	15% (1% - 86%)	2	5, 8
Gluteus minimus	30% (1% - 64%)	6	2, 5, 7, 8, 9, 10
Iliacus	8% (2% - 18%)	0	-
Psoas	8% (2% - 25%)	1	5
Adductor magnus	6% (1% - 13%)	0	-
Vastus lateralis	8% (0% - 9%)	0	-
Vastus intermedius	3% (0% - 15%)	0	-
Vastus medialis	3% (0% - 19%)	0	-
Rectus femoris	3% (1% - 72%)	1	9
Soleus	12% (0% - 65%)	3	2, 4, 9
Gastrocnemius medialis	42% (3% - 93%)	7	1, 3, 4, 5, 7, 9, 10
Gastrocnemius lateralis	28% (3% - 73%)	6	1, 2, 4, 8, 9, 10
Tibialis posterior	12% (3% - 82%)	4	1, 2, 3, 5
Tibialis anterior	39% (3% - 98%)	6	2, 3, 4, 8, 9, 10

ASI: Absolute Symmetry Index. Values are given as median (range).

With regard to the direction of these asymmetries, SUVs were not significantly different between the dominant and the non-dominant limb in 14 out of 15 muscles (Table 6.2). The median symmetry indices were smaller than 25% in all muscles, and smaller than 10% in 12 out of 15 muscles (Figure 6.1). Similar to the SUV-based comparisons, when inter-limb muscle volume differences were taken into account (AUV), none of the 15 muscles exhibited significant systematic differences in AUV between the dominant and the non-dominant limb (Table 6.2).

Table 6.2 Standardized and Absolute Uptake Values for muscles of the lower limb during walking

Muscle	SUV dom. limb (g/mL)	SUV non-dom. limb (g/mL)	AUV dom. limb (g)	p-values SUV dom. vs. non-dom. limb*	p-values AUV dom. vs. non-dom. limb*
Gluteus maximus	0.62 (0.46 – 0.85)	0.58 (0.44 – 1.40)	565 (335 – 752)	0.20	0.65
Gluteus medius	0.85 (0.63 – 2.30)	0.86 (0.66 – 5.74)	321 (164 – 764)	0.88	0.33
Gluteus minimus	1.26 (0.70 – 5.68)	1.56 (0.82 – 6.67)	142 (52 – 798)	0.51	0.58
Iliacus	0.72 (0.57 – 1.00)	0.77 (0.58 – 1.07)	138 (95 – 209)	0.51	0.29
Psoas	0.76 (0.50 – 1.01)	0.68 (0.54 – 0.93)	128 (56 – 171)	0.09	0.09
Adductor magnus	0.72 (0.54 – 1.02)	0.75 (0.53 – 0.94)	359 (240 – 636)	0.80	0.96
Vastus lateralis	0.64 (0.44 – 0.68)	0.64 (0.46 – 0.73)	420 (268 – 592)	0.06	0.06
Vastus intermedius	0.71 (0.49 – 0.79)	0.75 (0.52 – 0.89)	311 (237 – 623)	0.05	0.24
Vastus medialis	0.66 (0.45 – 0.82)	0.68 (0.45 – 0.99)	270 (207 – 486)	0.06	0.14
Rectus femoris	0.56 (0.39 – 1.64)	0.58 (0.41 – 0.77)	146 (90 – 459)	0.17	0.51
Soleus	2.40 (1.00 – 7.03)	2.34 (1.10 – 6.88)	1215 (536 – 4960)	0.80	0.88
Gastrocnemius medialis	1.50 (0.76 – 3.25)	2.31 (0.82 – 3.54)	393 (229 – 611)	0.14	0.14
Gastrocnemius lateralis	0.97 (0.72 – 3.04)	1.14 (0.63 – 4.23)	124 (55 – 377)	0.45	0.51
Tibialis posterior	1.42 (1.06 – 3.41)	1.18 (0.97 – 3.23)	140 (77 – 442)	0.07	0.29
Tibialis anterior	1.66 (1.02 – 4.40)	2.86 (1.07 – 5.07)	230 (117 – 879)	0.07	0.07

SUV: Standardized Uptake Value. AUV: Absolute Uptake Value. SUV and AUV values are given as median (range). *Wilcoxon matched-pair signed-rank test (2 samples). Bold face indicates a significant difference.

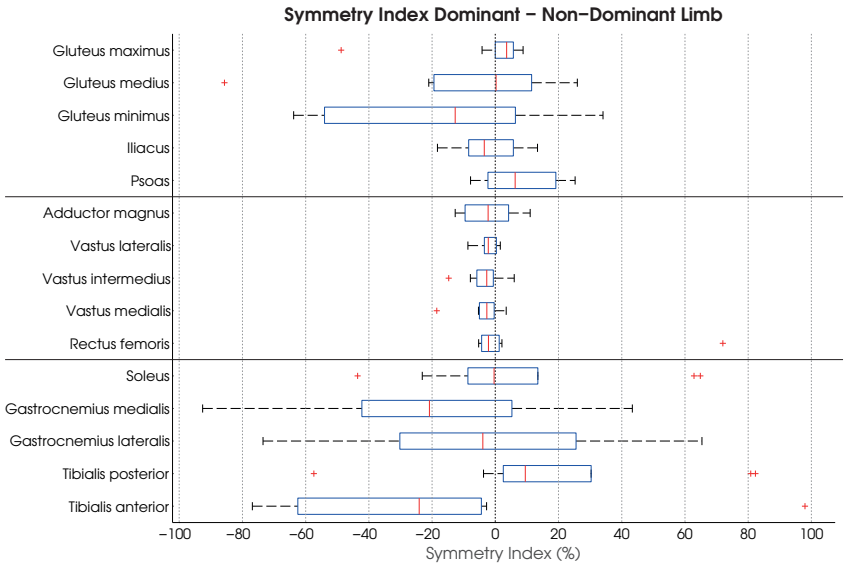

Figure 6.1. Box plot of the symmetry index, which shows the differences in uptake between the muscles in the dominant and the non-dominant lower limb. On each box, the central mark is the median, the edges of the box are the 25th (q1) and 75th (q3) percentiles, the whiskers extend to the most extreme data points not considered outliers, and outliers are plotted individually. Points are drawn as outliers if they are larger than q3 + 1.5*(q3 – q1) or smaller than q1 – 1.5*(q3 – q1).

Heterogeneity of FDG uptake

The SUVs of the individual voxels within muscles tended to be concentrated at the lower end of the histograms, with a tail towards the higher SUVs, as indicated by the median skewness values that were higher than zero in all muscles, and higher than one in 10 out of 15 muscles (Figure 6.2). Example histograms of muscles with low (0.5), typical (1.4) and high (2.1) skewness are shown in Figure 6.3G, H, and I, respectively. The adductor magnus had the highest median skewness (2.8 and 2.5 for the dominant and non-dominant limbs, respectively), as well as the widest range of skewness values between subjects (ranging from 1.2 to 10.6 in the dominant limb). In addition, the gluteal muscles also exhibited relatively large skewness values. The tibialis anterior was the only muscle that was hardly skewed at all (median skewness 0.3 in the dominant limb and 0.2 in the non-dominant limb). From Figure 6.2 it is also evident that there were large inter-subject differences in the skewness values in the vast majority of muscles, with the exception of the quadriceps muscles and the tibialis anterior.

Clustering of FDG uptake

In all muscles, voxels with high FDG uptake tended to cluster together rather than being distributed heterogeneously. This is indicated by the cluster index, which was higher than one for all muscles (Figure 6.4). The clustering was most pronounced in the adductor magnus, soleus, tibialis posterior and non-dominant gluteus minimus, with median cluster

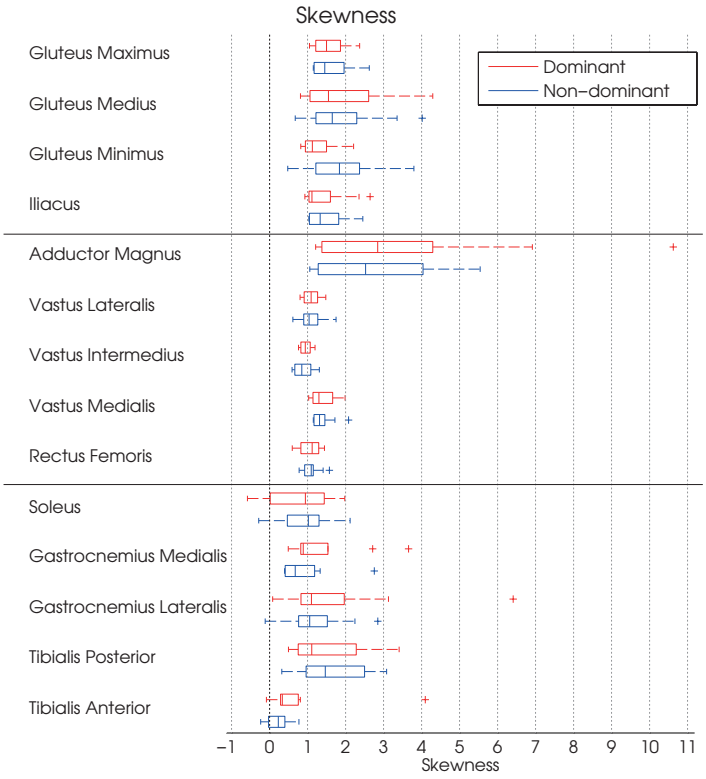

Figure 6.2. Skewness of the FDG uptake distribution in the muscles in the dominant and the non-dominant lower limb. A skewness of zero would indicate a normal, Gaussian distribution, whereas higher skewness values such as observed in the figure indicate that the most frequently occurring FDG uptake values clustered at the lower end of the distribution and the tail pointed towards the higher scores. On each box, the central mark is the median, the edges of the box are the 25th (q1) and 75th (q3) percentiles, the whiskers extend to the most extreme data points not considered outliers, and outliers are plotted individually. Points are drawn as outliers if they are larger than q3 + 1.5*(q3 – q1) or smaller than q1 – 1.5*(q3 – q1).

indices of two or more. Clustering was relatively low in the quadriceps muscles, as indicated by the median cluster indices of 1.3-1.8, and this observation was consistent across subjects. In contrast, the degree of clustering varied widely between subjects in most of the other muscles.

The locations of clustered areas also varied greatly between subjects for any given muscle. For example, the stretch of clustering that is visible in Figure 6.3B and C in the cranial, medial aspect of the soleus was present in four subjects, whereas the other six subjects had clustered areas elsewhere, or the clustered areas were smaller and more scattered throughout the muscle. Hence, we found clustering of high FDG uptake, but could not identify any consistent intra-muscular pattern of FDG uptake in any of the 15 muscles amongst the 10 healthy subjects included in this study.

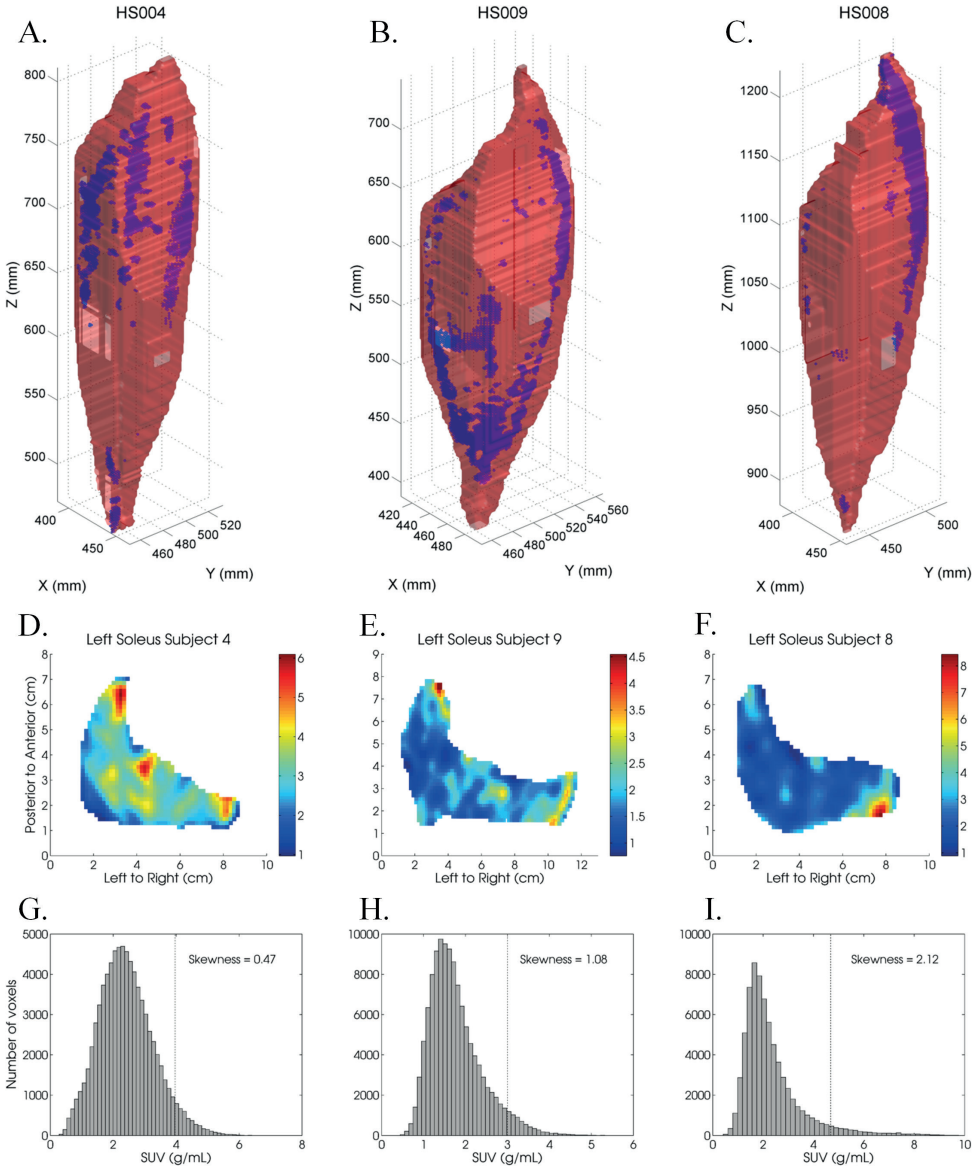

Figure 6.3. A-C: Three-dimensional rendering of the soleus muscle for three subjects, including marked 'hot' voxels in blue. The X, Y and Z-coordinates reflect the anterior-posterior, left-right and distal-proximal directions, respectively. They are shown in the DICOM patient coordinate system. D-F: Slice of the soleus muscle taken at 2/3 of its height, with colors indicating the uptake value (SUV, i.e. g/mL). The soleus in the middle was the largest; this subject was male, whereas subjects 4 and 8 were females. G-I: Histograms of the distribution of the entire muscle's FDG uptake across the spectrum of uptake values. The histogram that corresponds with the lowest skewness value (on the left) is rather bell-shaped, whilst the other two clearly are not.

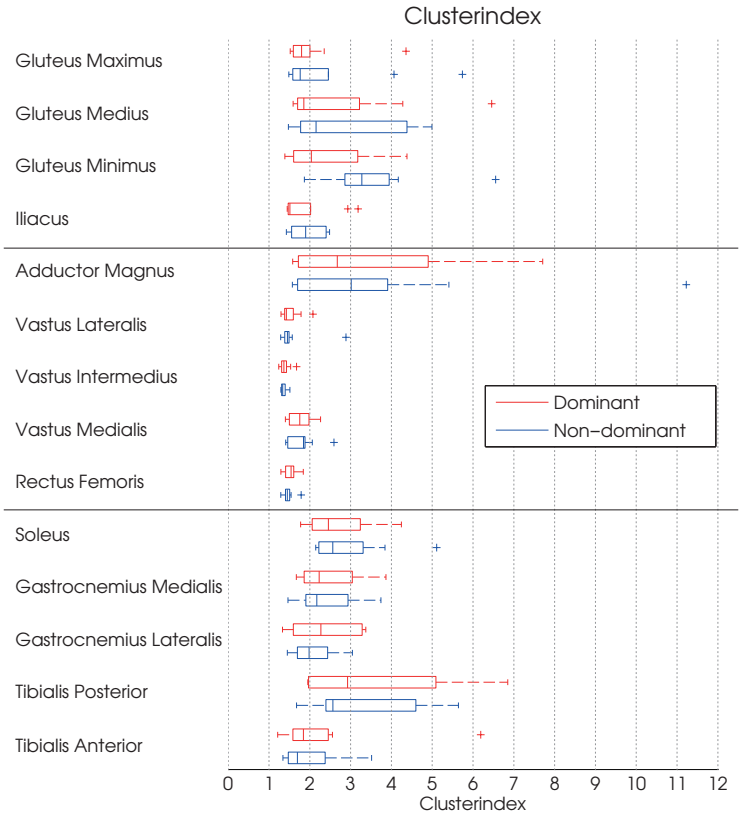

Figure 6.4. Clusterindices per muscle. A clusterindex of zero would indicate a homogeneous distribution of the 'hot' voxels of FDG across the muscle, whereas higher values are indicative of a clustering effect. On each box, the central mark is the median, the edges of the box are the 25th (q1) and 75th (q3) percentiles, the whiskers extend to the most extreme data points not considered outliers, and outliers are plotted individually. Points are drawn as outliers if they are larger than q3 + 1.5*(q3 – q1) or smaller than q1 – 1.5*(q3 – q1).

Discussion

This study aimed to determine asymmetries in FDG uptake between muscles in the dominant and the non-dominant lower limb, as well as to determine heterogeneities in FDG uptake within muscles during walking, using three-dimensional MRI-based whole-muscle segmentations. Large inter-limb differences in uptake were found in the lower leg muscles and in the gluteus medius and gluteus minimus (differences up to 98% were found), whereas the uptake in the thighs was relatively symmetrical between the limbs. FDG uptake was not systematically higher in the dominant or the non-dominant limb in any muscle, including when inter-limb muscle volume differences were taken into account. The skew of the SUVs was to the right almost exclusively, indicating that most voxels had a relatively low SUV, and that a minority of voxels had a relatively high SUV. Rather than being homogeneously distributed in the muscle, the voxels with high SUV tended to cluster in virtually all muscles,

the clustering being strongest in the adductor magnus, the ankle plantar flexors, and the gluteus medius and minimus.

Considering that the subjects were healthy, our finding that there were large asymmetries in muscle FDG uptake between the limbs in several muscles was unexpected. According to traditional assumptions and a substantial body of literature (for overview, see Sadeghi et al. 2000), gait in the absence of disease has been supposed and found to be symmetrical. However, this notion is still under debate (Sadeghi et al. 2000), and the body of evidence supporting some asymmetry is also substantial. For example, in a large retrospective study (182 subjects), peak hip and knee flexion and adduction moments during walking exceeded 10% asymmetry in more than half of the participants (Lathrop-Lambach et al. 2014). Similar studies that looked at spatiotemporal parameters, kinematics, and ground reaction forces also found significant asymmetries in these parameters (Gundersen et al. 1989; Herzog et al. 1989; Maupas et al. 1999). There are also studies that found asymmetries in muscle activity using EMG (Arsenault et al. 1986a; Ounpuu et al. 1989). Nevertheless, in the present study, the asymmetries in terms of glucose uptake of more than 25% and even 50% that we found in many muscles, particularly in the lower leg, were larger than in any literature.

A first possible explanation for the large asymmetries could be limb dominance, but the direction of the asymmetries in uptake varied widely between subjects and was not consistently pointing towards the dominant or the non-dominant limb in any muscle. A second explanation for a muscle being more active in one limb than in the contralateral limb, would be that it is compensating for similarly asymmetric co-activation in an antagonist muscle. Yet, we did not observe such a trend in the uptake data, and there were several subjects who actually showed an opposite effect. A third possible explanation for the large inter-limb asymmetries is that the muscles in either the dominant or the non-dominant limb would have different degrees of work efficiency. However, if this were the case, it would have been likely that a given muscle would consistently show a higher degree of efficiency (and thus, lower uptake) in either the dominant or in the non-dominant lower limb across subjects, which was not observed. Finally, a fourth explanation is that a very active muscle could be compensating for reduced activity in another muscle that has a similar functional role. For example, high activity in one of the plantar flexors (e.g., soleus) could be accompanied by a lower activity in the other plantar flexors (mainly medial and lateral gastrocnemius). Such a trend was not observed; subjects who had a high AUV in the soleus generally also had a high uptake in the medial and lateral gastrocnemius, and vice versa. Hence, it remains difficult to explain the large asymmetries, and this warrants further research using other methods (e.g., EMG and kinematic and kinetic gait analysis) in conjunction with the FDG-PET technique.

Interestingly, the distribution of the SUVs across the voxels comprising each muscle did not follow a Gaussian curve, but was instead skewed to the right in almost all muscles. This indicates that there was a relatively large number of voxels which exhibited an SUV that was substantially lower than the mean SUV of the entire muscle. This high degree of skew is in line with Heinonen et al., who used FDG-PET to examine the heterogeneity of glucose uptake in the quadriceps during exercise at different intensity levels (Heinonen et al. 2012). Albeit in a different task (cycling), it was found that the heterogeneity of glucose uptake in the quadriceps was relatively high at low exercise intensity levels, and that it decreased

with increasing exercise intensity levels (30%, 55% and 75% of maximum VO2). Since level walking at comfortable speed is generally considered a low intensity exercise, the high degree of skew that we observed is in line with this literature (Heinonen et al. 2012). The fact that skewness might be related to the intensity level of the activity opens the question whether it may be related to the fiber type composition of the muscle. This does not appear to be the case; the soleus has a very high type I fiber percentage of 87.7% (Johnson et al. 1973) and exhibited an average degree of skew. Similarly, the rectus femoris, which has a very low type I fiber percentage of 38.1% (and, consequently, a high type II fiber percentage of 61.9%) (Johnson et al. 1973), also exhibited only an average degree of skew. The adductor magnus and tibialis anterior, however, have lower percentages of type I fibers than the soleus (58.4% and 73.1%, respectively (Johnson et al. 1973)), yet these exhibited the most (adductor magnus) and least (tibialis anterior) skewed distributions.

The voxels with high uptake of FDG were clustered instead of being distributed homogeneously throughout the muscle, especially in the adductor magnus, the ankle plantar flexors, and the gluteus medius and minimus. This suggests that most of the work during walking is performed by limited regions within muscles. Since comfortable level walking is an aerobic activity, and since it is known that the different types of muscle fibers are organized in regions of different composition rather than being homogeneously distributed (Chanaud et al. 1991), the observed regional uptake differences could be due to regional differences in muscle fiber types. In conjunction, due to the size principle, the recruitment of motor units (MUs) in theory causes region-specific muscle activation when a certain specific demand is placed on the muscle (Hodson-Tole et al. 2013; Holtermann et al. 2005). In simple tasks (e.g., isometric exercises), this phenomenon of region-specific activation has been confirmed using modern techniques such as multi-channel electromyography (Holtermann et al. 2005; Staudenmann et al. 2009), MRI (Kinugasa et al. 2011) as well as FDG-PET (Kalliokoski et al. 2007; Pappas et al. 2001). Our results are in line with these findings and suggest that, also in a more complex task (walking), region-specific differences in muscle activation exist in almost all muscles.

Rather than forming consistent patterns across subjects, the spatial distribution of FDG uptake in the muscles was very variable. Typically, three or four subjects could be grouped into one category of regional uptake (e.g., cranial, medial aspect in the soleus such as in Figure 6.3B and C), but no consistent patterns were observed across all subjects in any muscle. It is known that activation of anatomical regions within a muscle can be related to a specific functional task that needs to be performed (Brown et al. 2007; Hodson-Tole et al. 2013), or to mechanical demands (Higham et al. 2008) or force direction demands (Staudenmann et al. 2009). It also seems to be the case here that different spatial regions of muscles contribute differently to walking than others. Again, this warrants further research as to how and why these specific patterns differ between individuals and how they affect the walking pattern.

Limitations

This study has some limitations. First, the inter-subject variation in SUVs was high in some muscles, and the current sample size was too small to attribute this to any particular characteristic of these healthy subjects such as age, body mass index or general fitness level. However, high inter-subject variability in muscle activation during walking has been shown to exist with techniques such as EMG as well (Arsenault et al. 1986b; Winter et al. 1987; Yang et al. 1984). Second, our experimental protocol did not include a control condition such as resting. Therefore, it was not possible to assess whether the observed intra-muscular heterogeneities in FDG uptake were attributable to the walking task or (partly) due to varying levels of resting metabolism within muscles. Extending the protocol was not allowed by the medical ethical board at our hospital due to ethical constraints regarding the radiation dose to these healthy subjects. The board initially denied the study and we had to reduce the dose of the CT scan to be allowed to perform the study. Furthermore, our measurement protocol did not include gait analysis. This would have allowed us to test our visual observation that the healthy subjects walked symmetrically. Third, our walking time was long (90 minutes), which has two disadvantages. One is in transitioning from research on healthy subjects to clinical applications, as patients may change their gait during the prolonged walking task due to pain or fatigue in certain muscles. The other disadvantage is that FDG-PET is a cumulative measurement that provides no temporal information. Therefore, activation of different regions within each muscle may have shifted during the task, which makes interpretation of the region-specific uptake results difficult. Future work could focus on examining region-specific FDG uptake in a simpler, more controlled task, or it could focus on combining FDG-PET with multi-channel electromyography, such that changes in MU recruitment can be tracked over time and coupled with the FDG-PET results.

Conclusions

The volumetric analysis of FDG uptake in both lower limbs after walking showed that muscle activity (in terms of glucose uptake) was symmetrical in the thigh muscles, whereas it was highly asymmetric in the lower leg and gluteal muscles in many subjects. These findings challenge the common assumption of symmetry between the limbs in healthy subjects. Practically all of the inter-subject differences disappeared when the results were averaged across subjects, which underlines that averaging individual subject data stemming from both limbs may preclude asymmetries from being noticed or reported. Studies that have the goal of validating muscle activation levels using subject-specific musculoskeletal models, will need to be cautious that muscle activity for the most active muscles during the activity (e.g., lower leg and gluteal muscles for walking) needs to be validated for each subject and each limb individually. As for the FDG distribution within muscles, there was a majority of voxels that had an SUV that was lower than the mean SUV, and there was a minority of voxels with a relatively high SUV in almost all muscles. Those 'hot' voxels tended to cluster rather than being spread homogeneously throughout the muscle, but those clusters were not located in consistent locations in a given muscle across subjects. The inconsistent locations of 'hot' clusters highlights the added value of performing a three-dimensional analysis of uptake rather than examining uptake in only a single slice for each muscle. Future research could

focus on revealing the relation of active versus resting FDG uptake levels, on measuring kinematics and kinetics while the exercise is performed, and on combining the cumulative FDG-PET measurement with a temporal-sensitive method such as multi-channel EMG. Using FDG-PET to measure muscle activity remains an exciting new technique, which has the potential to further improve our understanding of muscle contributions during exercise in many ways, including in detecting differences in muscle activity levels between subjects, between limbs, and between regions within muscles.

Acknowledgements

We thank dr. Toshihiko Fujimoto for useful comments regarding the design of the study. We gratefully acknowledge financial support by the Seventh Framework Programme (FP7) of the European Union (Grant agreement no: 247860) for the TLEMsafe project: http://www.tlemsafe.eu/.

References

Ackermann, M., and van den Bogert, A.J. 2010. Optimality principles for model-based prediction of human gait, J Biomech, 43: 1055-1060.

Anderson, F.C., and Pandy, M.G. 2001. Static and dynamic optimization solutions for gait are practically equivalent, J Biomech, 34: 153-161.

Arsenault, A.B., Winter, D.A., and Marteniuk, R.G. 1986a. Bilateralism of EMG profiles in human locomotion, Am J Phys Med, 65: 1-16.

Arsenault, A.B., Winter, D.A., and Marteniuk, R.G. 1986b. Is there a 'normal' profile of EMG activity in gait?, Med Biol Eng Comput, 24: 337-343.

Becker, H.P., Rosenbaum, D., Kriese, T., Gerngross, H., and Claes, L. 1995. Gait asymmetry following successful surgical treatment of ankle fractures in young adults, Clin Orthop Relat Res: 262-269.

Brown, J.M., Wickham, J.B., McAndrew, D.J., and Huang, X.F. 2007. Muscles within muscles: Coordination of 19 muscle segments within three shoulder muscles during isometric motor tasks, J Electromyogr Kinesiol, 17: 57-73.

Chanaud, C.M., Pratt, C.A., and Loeb, G.E. 1991. Functionally complex muscles of the cat hindlimb. V. The roles of histochemical fiber-type regionalization and mechanical heterogeneity in differential muscle activation, Exp Brain Res, 85: 300-313.

Chapman, J.P., Chapman, L.J., and Allen, J.J. 1987. The measurement of foot preference, Neuropsychologia, 25: 579-584.

De Luca, C.J. 1997. The use of surface electromyography in biomechanics, J Appl Biomech, 13: 135-163.

Field, A.P. 2013. Discovering statistics using IBM SPSS statistics: and sex and drugs and rock 'n' roll (SAGE: London).

Furlong, L.-A.M., and Harrison, A.J. 2015. Differences in plantarflexor function during a stretch-shortening cycle task due to limb preference, Laterality, 20: 128-140.

Gundersen, L.A., Valle, D.R., Barr, A.E., Danoff, J.V., Stanhope, S.J., and Snyder-Mackler, L. 1989. Bilateral analysis of the knee and ankle during gait: an examination of the relationship between lateral dominance and symmetry, Phys Ther, 69: 640-650.

Heinonen, I., Nesterov, S.V., Kemppainen, J., Fujimoto, T., Knuuti, J., and Kalliokoski, K.K. 2012. Increasing exercise intensity reduces heterogeneity of glucose uptake in human skeletal muscles, PLoS One, 7: e52191.

Herzog, W., Nigg, B.M., Read, L.J., and Olsson, E. 1989. Asymmetries in ground reaction force patterns in normal human gait, Med Sci Sports Exerc, 21: 110-114.

Higham, T.E., Biewener, A.A., and Wakeling, J.M. 2008. Functional diversification within and between muscle synergists during locomotion, Biol Lett, 4: 41-44.

Hodson-Tole, E.F., Loram, I.D., and Vieira, T.M. 2013. Myoelectric activity along human gastrocnemius medialis: different spatial distributions of postural and electrically elicited surface potentials, J Electromyogr Kinesiol, 23: 43-50.

Holtermann, A., Roeleveld, K., and Karlsson, J.S. 2005. Inhomogeneities in muscle activation reveal motor unit recruitment, J Electromyogr Kinesiol, 15: 131-137.

Jakoby, B.W., Bercier, Y., Conti, M., Casey, M.E., Bendriem, B., and Townsend, D.W. 2011. Physical and clinical performance of the mCT time-of-flight PET/CT scanner, Phys Med Biol, 56: 2375-2389.

Johnson, M.A., Polgar, J., Weightman, D., and Appleton, D. 1973. Data on the distribution of fibre types in thirty-six human muscles. An autopsy study, J Neurol Sci, 18: 111-129.

Kalliokoski, K.K., Bojsen-Moller, J., Seppanen, M., Johansson, J., Kjaer, M., Teras, M., and Magnusson, S.P. 2007. Contraction-induced [18F]-fluoro-deoxy-glucose uptake can be measured in human calf muscle using high-resolution PET, Clin Physiol Funct Imaging, 27: 239-241.

Kindred, J.H., Ketelhut, N.B., and Rudroff, T. 2015. Glucose uptake heterogeneity of the leg muscles

is similar between patients with multiple sclerosis and healthy controls during walking, Clin Biomech (Bristol, Avon), 30: 159-165.

Kinugasa, R., Kawakami, Y., Sinha, S., and Fukunaga, T. 2011. Unique spatial distribution of in vivo human muscle activation, Exp Physiol, 96: 938-948.

Kolk, S., Klawer, E.M.E., Schepers, J., Weerdesteyn, V., Visser, E.P., and Verdonschot, N. 2015. Muscle Activity during Walking Measured Using 3D MRI Segmentations and [18F]-Fluorodeoxyglucose in Combination with Positron Emission Tomography, Med Sci Sports Exerc, 47: 1896-1905.

Kubota, K., Matsuzawa, T., Ito, M., Ito, K., Fujiwara, T., Abe, Y., Yoshioka, S., Fukuda, H., Hatazawa, J., Iwata, R., and et al. 1985. Lung tumor imaging by positron emission tomography using C-11 L-methionine, J Nucl Med, 26: 37-42.

Laaksonen, M.S., Kemppainen, J., Kyrolainen, H., Knuuti, J., Nuutila, P., and Kalliokoski, K.K. 2013. Regional differences in blood flow, glucose uptake and fatty acid uptake within quadriceps femoris muscle during dynamic knee-extension exercise, Eur J Appl Physiol, 113: 1775-1782.

Lathrop-Lambach, R.L., Asay, J.L., Jamison, S.T., Pan, X., Schmitt, L.C., Blazek, K., Siston, R.A., Andriacchi, T.P., and Chaudhari, A.M. 2014. Evidence for joint moment asymmetry in healthy populations during gait, Gait Posture, 40: 526-531.

Lucignani, G., Paganelli, G., and Bombardieri, E. 2004. The use of standardized uptake values for assessing FDG uptake with PET in oncology: a clinical perspective, Nucl Med Commun, 25: 651-656.

Maupas, E., Paysant, J., Martinet, N., and Andre, J. 1999. Asymmetric leg activity in healthy subjects during walking, detected by electrogoniometry, Clin Biomech (Bristol, Avon), 14: 403-411.

Oi, N., Iwaya, T., Itoh, M., Yamaguchi, K., Tobimatsu, Y., and Fujimoto, T. 2003. FDG-PET imaging of lower extremity muscular activity during level walking, J Orthop Sci, 8: 55-61.

Ounpuu, S., and Winter, D.A. 1989. Bilateral electromyographical analysis of the lower limbs during walking in normal adults, Electroencephalogr Clin Neurophysiol, 72: 429-438.

Pappas, G.P., Olcott, E.W., and Drace, J.E. 2001. Imaging of skeletal muscle function using (18)FDG PET: force production, activation, and metabolism, J Appl Physiol (1985), 90: 329-337.

Rahemi, H., Nigam, N., and Wakeling, J.M. 2014. Regionalizing muscle activity causes changes to the magnitude and direction of the force from whole muscles-a modeling study, Front Physiol, 5: 298.

Romijn, J.A., Coyle, E.F., Sidossis, L.S., Gastaldelli, A., Horowitz, J.F., Endert, E., and Wolfe, R.R. 1993. Regulation of endogenous fat and carbohydrate metabolism in relation to exercise intensity and duration, Am J Physiol, 265: E380-391.

Sadeghi, H., Allard, P., Prince, F., and Labelle, H. 2000. Symmetry and limb dominance in able-bodied gait: a review, Gait Posture, 12: 34-45.

Scheys, L. 2009. Personalized musculoskeletal modeling based on magnetic resonance images: use for biomechanical analysis of gait, K.U. Leuven.

Schoeman, M., Diss, C.E., and Strike, S.C. 2013. Asymmetrical loading demands associated with vertical jump landings in people with unilateral transtibial amputation, J Rehabil Res Dev, 50: 1435-1447.

Seeley, M.K., Umberger, B.R., and Shapiro, R. 2008. A test of the functional asymmetry hypothesis in walking, Gait Posture, 28: 24-28.

Shimada, H., Kimura, Y., Lord, S.R., Oda, K., Ishii, K., Suzuki, T., and Ishiwata, K. 2009. Comparison of regional lower limb glucose metabolism in older adults during walking, Scand J Med Sci Sports, 19: 389-397.

Shimada, H., Kimura, Y., Suzuki, T., Hirata, T., Sugiura, M., Endo, Y., Yasuhara, K., Shimada, K., Kikuchi, K., Hashimoto, M., Ishikawa, M., Oda, K., Ishii, K., and Ishiwata, K. 2007. The use of positron emission tomography and [18F]fluorodeoxyglucose for functional imaging of muscular activity during exercise with a stride assistance system, IEEE Trans Neural Syst

Rehabil Eng, 15: 442-448.
Staudenmann, D., Kingma, I., Daffertshofer, A., Stegeman, D.F., and van Dieen, J.H. 2009. Heterogeneity of muscle activation in relation to force direction: a multi-channel surface electromyography study on the triceps surae muscle, J Electromyogr Kinesiol, 19: 882-895.
Staudenmann, D., Roeleveld, K., Stegeman, D.F., and van Dieen, J.H. 2010. Methodological aspects of SEMG recordings for force estimation--a tutorial and review, J Electromyogr Kinesiol, 20: 375-387.
Winter, D.A., and Yack, H.J. 1987. EMG profiles during normal human walking: stride-to-stride and inter-subject variability, Electroencephalogr Clin Neurophysiol, 67: 402-411.
Yang, J.F., and Winter, D.A. 1984. Electromyographic amplitude normalization methods: improving their sensitivity as diagnostic tools in gait analysis, Arch Phys Med Rehabil, 65: 517-521.

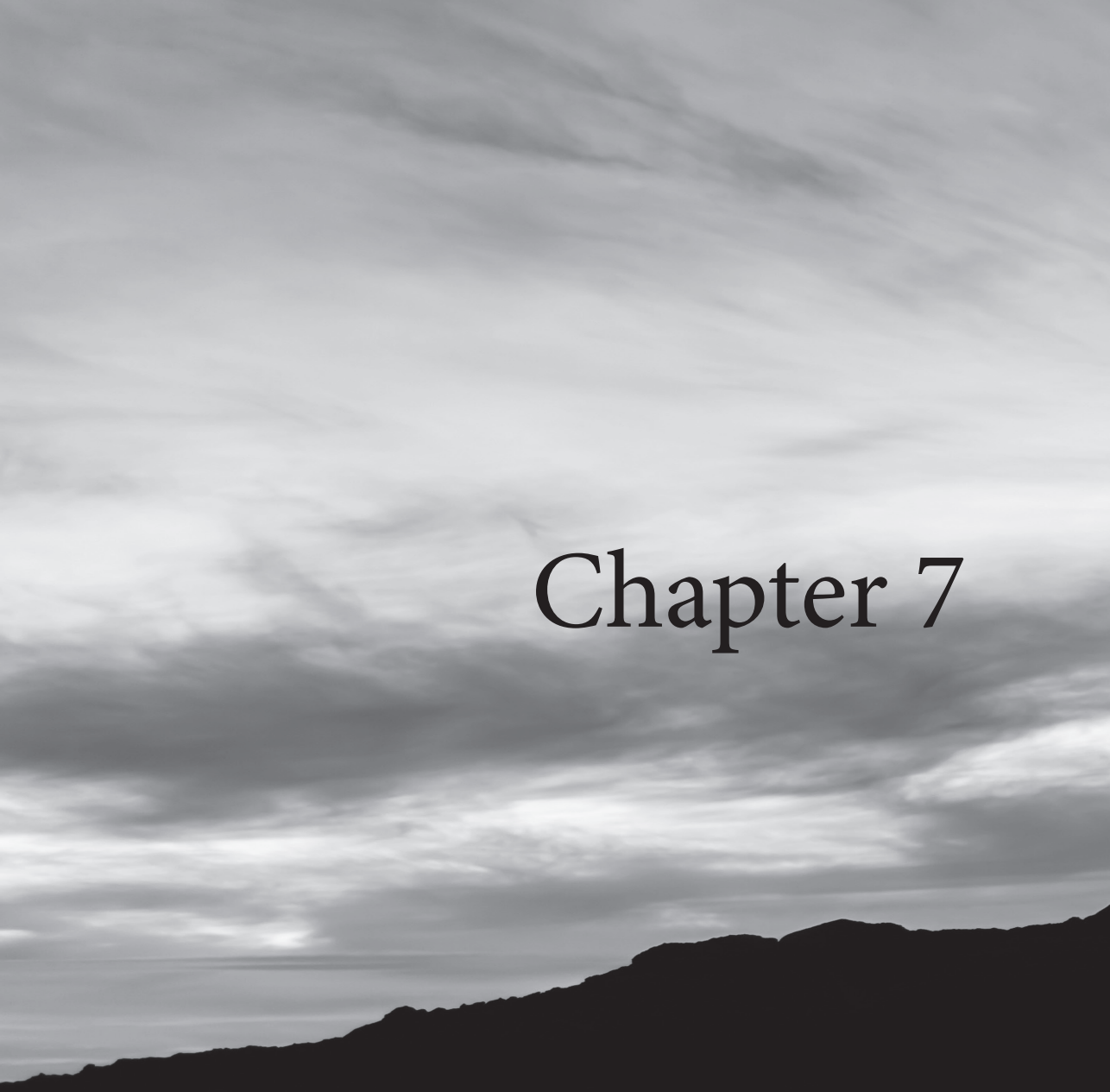

Chapter 7

Quantitative validation of subject-specific musculoskeletal models of the lower extremity using FDG-PET

(Submitted)

Carbone, V., Kolk, S., van der Krogt, M.M., Schepers, J.,
Weerdesteyn, V., Koopman, H.F.J.M., Verdonschot, N.

Abstract

Background: Validation of musculoskeletal models represents a crucial challenge to gain the necessary confidence for clinical applications, such as surgical planning and decision making in orthopedics. Electromyography and, recently, near infrared spectroscopy have been used as convenient and non-invasive techniques for indirect validation of models. However, they can be applied only to a small number of superficial muscles. Positron emission tomography (PET) combined with the radioactive tracer [^{18}F]-fluorodeoxyglucose (FDG) is a novel approach that allows measuring the muscular activity of all muscles of the lower extremity, including the deep muscles, in a single session.

Methods: In this study, we used FDG-PET for validation of subject-specific musculoskeletal models, comparing the measured glucose uptake %FDG with the predicted metabolic energy consumption $\%E_m$ for all the muscles of the lower extremity.

Results: When analyzing each individual subject, good to very good correlations were found between %FDG and $\%E_m$ (Spearman's ρ = 0.87±0.04, Pearson's r = 0.77±0.10). Higher correlations were found when analyzing results averaged over ten healthy subjects (Spearman's ρ = 0.96, Pearson's r = 0.91). Correlations were slightly higher for subject-specific models compared to generic models, but this was not significant (p = 0.17).

Conclusions: We conclude that FDG-PET should be considered as a complimentary validation tool to electromyography.

Introduction

Recent improvements in medical imaging techniques and increase of computational power have allowed estimating subject-specific parameters of musculoskeletal (MS) geometry (Carbone 2016; Hausselle et al. 2014; Scheys et al. 2009) and muscle-tendon (MT) architecture (Carbone 2016; Hainisch et al. 2012; van Campen et al. 2014) in a semi-automatic way. Since the use of MS models in clinical applications such as surgical planning and decision making in orthopedics (Cohen et al. 2003; Reinbolt et al. 2009; Taddei et al. 2012) is increasing, extensive validation of model predictions is crucial (Lund et al. 2012; Prilutsky et al. 2002).

In-vivo measurement of muscle and joint reaction forces requires special tools, such as use of optic-fiber technique (Finni et al. 2000), in situ buckle-type force transducers (Gregor et al. 1991), or instrumented joint replacements (Bergmann et al. 2001; Fregly et al. 2012). For these reasons, direct validation of MS models is inherently difficult, costly and ethically problematic to perform.

Comparison of electromyography (EMG) measurements with predicted muscle forces represent a more common example of indirect validation of MS models (Asadi Nikooyan et al. 2011; Giroux et al. 2013). Next to EMG, measurement of local oxygen consumption of muscle tissue, reflecting the energy consumption process, through near infrared spectroscopy (NIRS) has been proposed as a validation tool for musculoskeletal models (Praagman et al. 2006; Praagman et al. 2003). Although both EMG and NIRS are convenient and non-invasive techniques for indirect validation of MS models, they share important limitations such as the limited number of muscles that can be measured at the same time, the lack of information on deep-lying muscles, and the fact that adipose tissue and crosstalk from other muscles are important confounding factors.

Positron emission tomography (PET) combined with the radioactive tracer [^{18}F]-fluorodeoxyglucose (FDG) is a novel technique that can be used to measure the intensity of carbohydrate metabolism in muscle tissue (Kemppainen et al. 2002). Unlike EMG and NIRS, FDG-PET can be used to estimate activity in all muscles of the lower extremity, including the deep muscles, in a single session (Kolk et al. 2015). Recently, FDG-PET has been successfully used to measure the intensity of muscular activity of the lower extremity during aerobic exercises such as walking (Oi et al. 2003; Shimada et al. 2007), running (Fujimoto et al. 1996; Fujimoto et al. 2000; Tashiro et al. 1999), and cycling (Gondoh et al. 2009). It has been shown that FDG-PET is able to distinguish the relative contributions of individual muscles to joint moments (Masood et al. 2014; Pappas et al. 2001), and to show differences between subjects with different age or physical conditions (Fujimoto et al. 2003; Kolk et al. 2015; Rudroff et al. 2013; Shimada et al. 2009). Hence, it can be used to indirectly measure the functional differences in the muscle recruitment process. Oi et al. (2003) compared FDG uptake results with EMG and kinematic and kinetic studies and demonstrated the validity of measuring the muscular activity of the lower extremity with FDG-PET. Therefore, FDG-PET seems to be a promising tool for validation of MS models.

In this study, we used FDG-PET for validation of comprehensive musculoskeletal models. We compared the activity of all muscles of the lower extremity during walking,

previously measured on ten healthy subjects using FDG-PET (Kolk et al. 2015), with the metabolic energy consumption predicted by ten subject-specific models, based on MRI and dynamometry data (Carbone 2016). Moreover, we aimed to determine whether subject-specific models provided better predictions than generic models when compared to FDG-PET measurements.

Methods

TLEMsafe healthy subjects dataset

A dataset of ten healthy subjects (five males, age 40.1±15.7 years, height 174.9±11.1 cm, weight 74.8±11.9 kg, BMI 24.4±2.3 kg/m^2, fat percentage 27.8±5.8%) was obtained at the Radboud University Medical Center in Nijmegen, the Netherlands. For each subject, an MRI scan of the lower extremity was obtained (3T, T1-weighted axial spin echo (SE), voxel size of 1.0*1.0*3.0 mm for pelvis, knee and ankle region, and 1.0*1.0*8.0 mm for the remaining upper and lower leg) (Figure 7.1A) using a Siemens 3T MAGNETOM® Skyra (Siemens AG, Munich, Germany). Then, 3D motion data (Vicon®) with synchronized custom built force plate data (AMTI, Watertown, MA, USA) were recorded during walking trials at a level walkway (Figure 7.1B). Thirty-five optical markers were placed according to the Vicon® Plug-in-Gait model (Vicon®, 2002), with ten additional markers placed on the right and left thigh, shank, medial femoral epicondyle, medial malleolus and fifth metatarsal head of the foot. For each subject, three gait trials at comfortable walking speed (CWS) were selected. Subsequently, for each subject, an extensive set of isometric and isokinetic torques during maximal voluntary contractions were measured using a Biodex Dynamometer (Biodex Medical Systems) (Figure 7.1C) for ankle plantar/dorsiflexion, knee flexion/extension, hip flexion/extension and hip abduction/adduction.

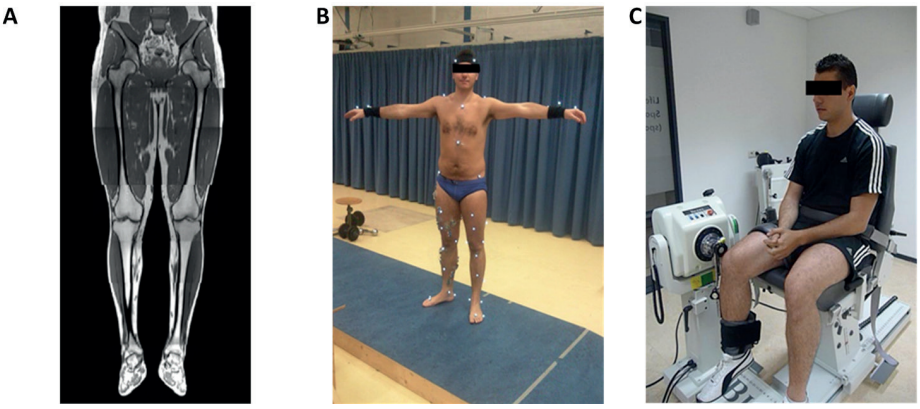

Figure 7.1. TLEMsafe healthy subjects' dataset. A. MRI scan of the lower extremities. B. Healthy subject wearing reflective markers and wireless EMG sensors during a recording session of 3D motion analysis and force plate data. C. Measurement of isometric and isokinetic torques during maximal voluntary contraction using a Biodex Dynamometer (Biodex Medical Systems).

FDG-PET volumetric analysis

Each subject walked on a treadmill at the same CWS measured in the gait lab for 90 minutes, 60 minutes before and 30 minutes after injection with FDG. Then, thirty minutes after finishing the last walking phase, a PET/CT scan was obtained using a Biograph 40 mCT (Siemens AG, Erlangen, Germany) in 3D mode, using an extended axial field of view of 216 mm and slice thickness of 2.0 mm, with the subject's legs positioned on the table to reproduce as closely as possible their position as during the MRI scan.

Muscle volumes of the left lower extremity were semi automatically segmented from MRI scans and subsequently registered onto the corresponding PET/CT scan, in order to obtain FDG uptake values for each individual muscle (Figure 7.2). Finally, %FDG uptake values were calculated to reflect the amount of FDG accumulated in each muscle relative to the total amount of FDG in all muscles of the lower extremity. More details about the FDG-PET protocol and medical imaging analysis, and complete results of the study are presented in (Kolk et al. 2015). Study procedures were approved by the ethical committee of the region Arnhem-Nijmegen, The Netherlands, and written informed consent was obtained from each subject.

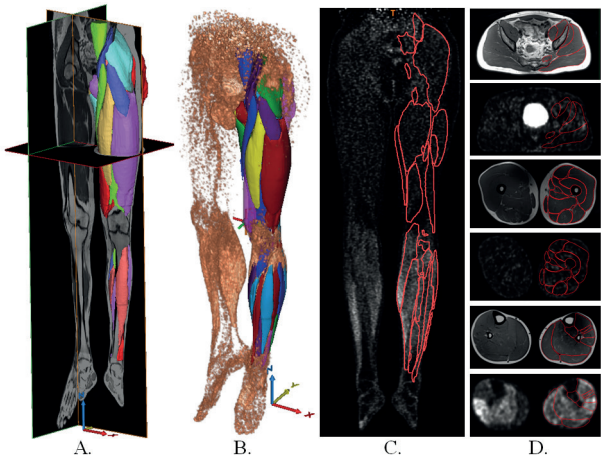

Figure 7.2. FDG-PET volumetric analysis: A. MRI scan with segmented muscle volumes. B. Segmented muscle volumes registered onto the PET scan. C. Frontal view of a PET scan with registered muscle volumes. D. MRI and PET scan slices of the hip, femur and tibia regions, with the registered muscle volumes.

Musculoskeletal models

Modeling was performed using the Twente Lower Extremity Model 2.0 (Carbone et al. 2015) implemented in the AnyBody Modeling System™ ver. 6.0.3 (AnyBody Technology A/S, Aalborg, Denmark) (Figure 7.3). TLEM 2.0 represents a comprehensive MS geometry dataset including medical images (CT and MRI) and segmented bone and muscle volumes (Figure 7.3A and 3B). The model consisted of 12 body segments, 11 joints and 21 degrees-

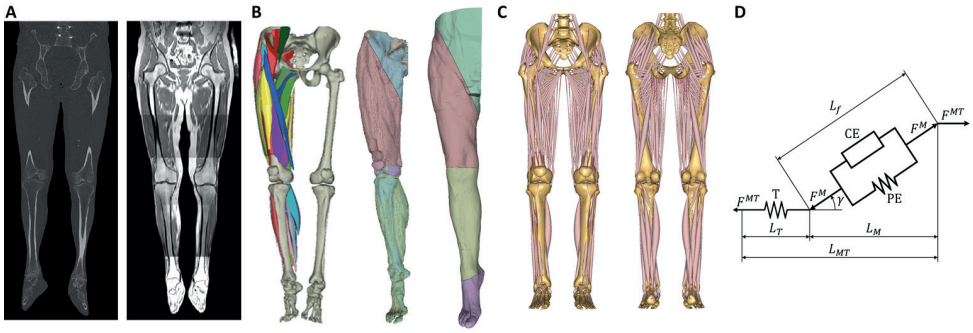

Figure 7.3. TLEM 2.0 dataset. From left to right: A. CT and MRI scans. B. Bone surfaces, muscle volumes, and subcutaneous fat and skin volumes segmented from MRI and CT scans. C. TLEM 2.0 model implemented in the AnyBody Modeling System™ ver. 6.0.3 (AnyBody Technology A/S, Aalborg, Denmark), anterior and posterior view. It consisted of 12 body segments: HAT (Head, Arm and Trunk), pelvis, and right and left femur, patella, tibia, talus and foot. The fibula was considered as one unit in combination with the tibia. The model comprised 11 joints: L5S1 and left and right hip, knee, patella/femur, talocrural and subtalar. The L5S1 and hip joints were modeled as a ball-and-socket, defined by a rotation center and three orthogonal axes. The knee, talocrural and subtalar joints were defined as a hinge, with a fixed rotation center and axis. The patella could rotate with respect to the femur around a rotation axis with a fixed rotation center. The patellar tendon was defined as a non-deformable element that connected the patella to the tibia. Thus, without introducing an extra Degree of Freedom (DOF), the orientation and position of the patella depended solely on the knee flexion angle. The orientation and position of the center of mass of the pelvis with respect to a 3D global frame, together with the joint rotations of the L5S1, hip, knee, talocrural and subtalar joints, resulted in a model with 21 DOFs. D. Schematic representation of three-elements Hill-type muscle-tendon element (Zajac 1989). The MT element consists of an active muscle, represented by a contractile element CE in parallel with a passive element PE, in series with an elastic tendon T, modelled as a nonlinear spring. L_f is the muscle fiber length, L_t is the tendon length, γ is the pennation angle between the muscle fiber and the tendon. L_{MT} is the total length of the MT element, which is equal to the sum of tendon length L_t and muscle-fiber length L_f adjusted by pennation angle γ (i.e. $L_{MT} = L_t + L_f \cos \gamma$). Force in the tendon F^{MT} is equal to the summed force in the muscle fibers F^M adjusted by pennation angle gamma (i.e. $F^{MT} = F^M \cos \gamma$).

of-freedom (Figure 7.3C). To accurately describe the functionality of the MS system, each leg contained in total 55 MT parts whose mechanical effect was described by 166 three-elements Hill-type MT elements (Zajac 1989) (Figure 7.3D).

For each subject, a generic and a subject-specific model was created:

Generic model

The TLEM 2.0 model was scaled using linear scaling laws, based on the relative position of the measured optical markers using a parameter optimization algorithm (Andersen et al. 2010).

Subject-specific model

Personalized MS geometry of the 10 healthy subjects were obtained from the MRI scan of each subject, using the TLEM 2.0 dataset as a starting template (Carbone 2016). Then, muscle volumes were semi-automatically segmented from MRI using Mimics (Materialise N.V., Leuven, Belgium), and functional scaling was applied to MT parameters, in order to find the best possible match between the strength profile measured during dynamometry measurements and the maximal torque predicted by the model (Carbone 2016) (Figure 7.4).

Simulations

For each subject and each gait trial, inverse dynamic analysis and static optimization problems were solved to calculate the MT forces necessary to reproduce the measured gait trials, based on the recorded 3D motion analysis and force plate data. The muscle recruitment problem was solved minimizing the sum of the cubes of muscle activations at each time step (Crowninshield et al. 1981), using a normalization factor based on the muscle volume according to (Happee et al. 1995). In total, 10 healthy subjects * 3 gait trials * 2 models = 60 simulations were performed and analyzed in this study.

For each MT element, the mechanical power was calculated as:

$$P_{mech} = F^{MT} v_{MT} = F^{MT} \dot{L_{MT}}$$

where F^{MT} represents the predicted MT force, and v_{MT} represents the lengthening velocity of the MT element, calculated as the first derivative of the total length of the MT element. Then, the metabolic power of each MT element was calculated based on the efficiency on the contractile element as:

$$P_m = \frac{P_{mech}}{\mu}, \begin{cases} \mu = 0.25 & \text{for shortening} \quad \dot{L_{MT}} < 0 \\ \mu = -1.20 & \text{for lengthening} \quad \dot{L_{MT}} > 0 \end{cases}$$

assuming an efficiency μ = 25% for concentric muscle work (De Haan et al. 1989) and μ = -120% for eccentric work (Asmussen 1953), as previously used by Voigt et al. (1995), in order to reflect the thermodynamic fact that muscle work is irreversible, and that even negative muscle work requires positive combustion. Metabolic power was then integrated over a complete gait cycle in order to calculate metabolic energy consumption. Metabolic energy consumption E_m of each muscle was calculated as the sum of each corresponding MT element. For each subject, the average metabolic energy consumption over 3 gait trials at CWS was calculated. $\%E_m$ values were calculated to reflect the amount of E_m in each muscle relative to the total amount of E_m in all muscles of the left lower extremity. For each subject, the average metabolic energy consumption over 3 gait trials at CWS was calculated. One-tailed Wilcoxon rank sum tests (α = 0.05) were performed to test if subject-specific models predicted a significantly lower energy consumption compared to generic models.

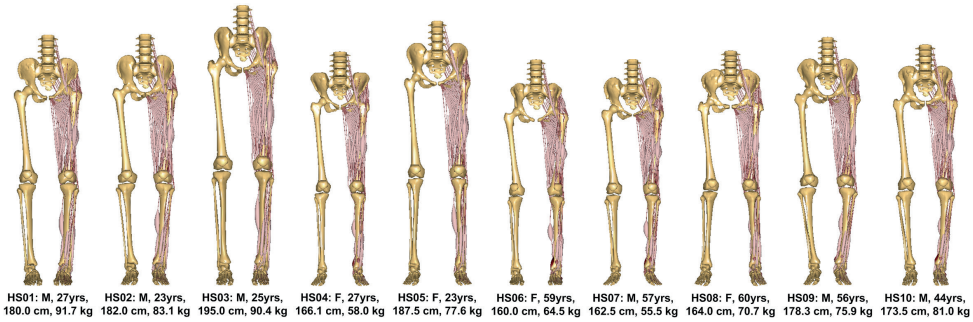

Figure 7.4. Ten subject-specific musculoskeletal models of the lower extremity, based on MRI and dynamometry measurements.

Analysis

For each muscle, the %FDG uptake values measured through the PET/CT scans were compared with the metabolic energy consumption $\%E_m$ predicted by the generic and subject-specific models, with respect to the complete lower extremity and for the pelvis, upper leg and lower leg regions. Correlations between %FDG and $\%E_m$ were assessed using two metrics: the Spearman's rank correlation coefficient ρ, to assess how well their relationship could be described using a monotonic function, and the Pearson product-moment correlation coefficient r, as a measure of their linear correlation. Spearman's ρ and Pearson's r were calculated for each individual subject and for the average %FDG and $\%E_m$ per muscle calculated over all ten healthy subjects, with respect to the complete lower extremity, and for the pelvis, upper leg and lower leg regions separately. One-tailed Wilcoxon rank sum tests ($\alpha = 0.05$) were performed to test if subject-specific models showed a significantly higher correlation with %FDG compared to generic models.

Results

The average metabolic power P_m during the gait cycle was equal to 3.82±0.44 W/kg for generic models and 3.73±0.48 W/kg for subject-specific models, which were not significantly different ($p = 0.13$).

Qualitatively, the predicted $\%E_m$ metabolic energy consumption, and the measured %FDG uptakes corresponded well (Figure 7.5). Quantitatively, the muscles in the lower leg consumed most of the metabolic energy ($\%E_m$ equal to 48.1±3.4% and 46.2±4.4% for generic and subject-specific models, respectively), which was similar to the FDG-PET data (%FDG equal to 45.2±11.1%) (Table 7.1). The subject-specific models showed higher $\%E_m$ in the pelvis region than in the upper leg (30.8±4.9% and 23.1±3.8%, respectively), whereas this was the other way around in the FDG-PET data (%FDG equal to 22.6±7.7% and 32.3±5.9% in the pelvis and upper leg region, respectively) and in the generic models ($\%E_m$ equal to 24.5±3.4% and 27.4±3.4% in the pelvis and upper leg region, respectively).

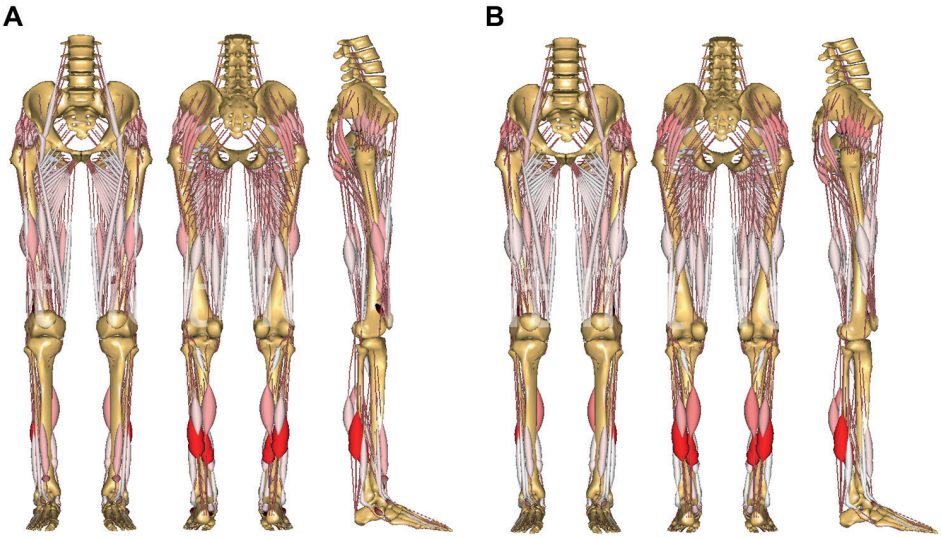

Figure 7.5. Qualitative comparison of distribution between muscles of: A. %FDG uptake, based on PET volumetric analysis, and B. $\%E_m$ metabolic energy consumption, predicted using subject-specific musculoskeletal models (anterior, posterior and lateral view). Color of muscles is proportional to the %FDG and $\%E_m$ values. Results are averaged over ten healthy subjects.

Many similarities were found between the muscles with the highest %FDG uptake and the muscles with the highest $\%E_m$ metabolic energy consumption (Table 7.2); The Soleus was consistently the most consuming muscle (%FDG equal to 20.6%, $\%E_m$ equal to 20.1% and 21.7% for generic and subject-specific models, respectively), followed by the Gastrocnemius Medialis, the Gluteal muscles and the Adductor Magnus. The $\%E_m$ of the Gastrocnemius Medialis was consistently overestimated by the models (17.0% and 10.0% for generic and subject-specific models, respectively) compared to %FDG (6.6%). Between the Gluteal muscles, the Gluteus Maximus and Gluteus Minimus showed consistent results, while the Gluteus Medius had a relatively large $\%E_m$ (7.5% and 9.1% for generic and subject-specific models, respectively) compared to %FDG (5.7%). The Tibialis Anterior and the Vasti muscles exhibited a much smaller $\%E_m$ compared to %FDG, while the Iliopsoas and the Rectus Femoris showed a larger $\%E_m$ compared to %FDG. The detailed results of %FDG uptake and $\%E_m$ metabolic energy consumption of all muscles for all ten healthy subjects are available in Appendix 7.1-7.5.

Table 7.1 Distribution of %FDG uptake and $\%E_m$ metabolic energy consumption between pelvis, upper and lower leg

	%FDG				$\%E_m$ - Generic Model				$\%E_m$ - Subject-specific Model			
	mean	**std**	**min**	**max**	**mean**	**std**	**min**	**max**	**mean**	**std**	**min**	**max**
Pelvis	22,6%	7,7%	12,4%	41,3%	24,5%	3,4%	16,1%	27,6%	30,8%	4,9%	20,7%	37,2%
Upper leg	32,3%	5,9%	22,0%	40,9%	27,4%	3,4%	24,3%	34,4%	23,1%	3,8%	15,6%	29,3%
Lower leg	45,2%	11,1%	29,2%	65,6%	48,1%	3,4%	40,8%	55,1%	46,2%	4,4%	38,3%	54,6%

%FDG uptake based on PET volumetric analysis, $\%E_m$ metabolic energy consumption predicted using generic and subject-specific musculoskeletal models. Results are averaged over ten healthy subjects.

Table 7.2 Comparison between the %FDG uptake and $\%E_m$ metabolic energy consumption of the ten muscles showing the highest %FDG uptake values

	%FDG				$\%E_m$ - Generic Model				$\%E_m$ - Subject-specific Model			
	mean	**std**	**min**	**max**	**mean**	**std**	**min**	**max**	**mean**	**std**	**min**	**max**
Soleus	20.6%	11.0%	8.8%	40.5%	20.1%	3.1%	14.5%	25.0%	21.7%	5.3%	11.0%	27.9%
Gluteus Maximus	7.5%	2.5%	4.1%	11.6%	4.1%	1.5%	1.3%	5.6%	6.9%	2.5%	3.3%	10.9%
Gastrocnemius Medialis	6.6%	3.4%	1.9%	13.7%	17.0%	1.3%	15.2%	19.9%	10.0%	5.9%	2.4%	19.1%
Gluteus Medius	5.7%	5.0%	2.5%	19.5%	7.5%	1.6%	5.1%	9.3%	9.1%	1.6%	5.8%	10.8%
Vastus Lateralis	5.6%	1.5%	3.6%	7.6%	5.4%	2.5%	1.2%	9.8%	1.4%	1.5%	0.3%	4.2%
Adductor Magnus	4.9%	1.1%	3.6%	6.9%	2.4%	0.8%	1.1%	3.6%	3.7%	1.9%	0.9%	7.8%
Tibialis Anterior	4.9%	1.6%	2.8%	7.1%	2.3%	1.0%	1.3%	4.9%	2.1%	1.0%	1.1%	4.2%
Vastus Intermedius	4.2%	1.3%	2.5%	6.0%	0.4%	0.2%	0.1%	0.7%	1.5%	1.9%	0.0%	4.9%
Vastus Medialis	3.9%	1.1%	2.3%	5.4%	1.7%	0.7%	0.5%	3.0%	2.0%	1.6%	0.3%	5.7%
Gluteus Minimus	2.6%	1.9%	0.6%	6.2%	3.7%	0.5%	2.8%	4.4%	3.6%	1.5%	1.3%	6.0%

%FDG uptake based on PET volumetric analysis, $\%E_m$ metabolic energy consumption predicted using generic and subject-specific musculoskeletal models. Results are averaged over ten healthy subjects.

Good correlation was found between the %FDG uptake values and $\%E_m$ metabolic energy consumption (Table 7.3). When analyzing each individual healthy subject, good to very good correlations were found for generic models (mean $\rho = 0.88\pm0.04$, mean $r = 0.74\pm0.09$) and for subject-specific models (mean $\rho = 0.87\pm0.04$, mean $r = 0.77\pm0.10$) and for the complete lower extremity, but the difference was not significant ($p = 0.17$). Very good correlations were found for the pelvis region (mean $\rho = 0.85\pm0.10$ and mean $r = 0.71\pm0.15$ for generic models, mean $\rho = 0.84\pm0.05$ and mean $r = 0.78\pm0.13$ for subject-specific models) and lower leg (mean $\rho = 0.71\pm0.12$ and mean $r = 0.85\pm0.07$ for generic models, mean $\rho = 0.71\pm0.12$ and mean $r = 0.88\pm0.08$ for subject-specific models), while poor correlation was found for the upper leg (mean $\rho = 0.24\pm0.22$ and mean $r = 0.24\pm0.26$ for generic models, mean $\rho = 0.20\pm0.31$ and mean $r = 0.18\pm0.27$ for subject-specific models). Correlation values were higher when analyzing %FDG and $\%E_m$ results averaged over the ten healthy subjects ($\rho = 0.91$ and $r = 0.84$ for generic models, $\rho = 0.96$ and $r = 0.91$ for subject-specific models) (Figure 7.6, Table 7.3). On the level of segments, very good correlations were found for the

Table 7.3 Spearman's rank correlation ρ and Pearson product-moment correlation r between %FDG uptake and $\%E_m$ metabolic energy consumption

	Mean values of the correlations between %FDG and $\%E_m$ calculated for each of the ten healthy subjects								Correlations between the %FDG and $\%E_m$ values averaged over ten healthy subjects			
	Generic				Subject-specific				Generic		Subject-specific	
	ρ		r		ρ		r		ρ	r	ρ	r
	mean	**std**	**mean**	**std**	**mean**	**std**	**mean**	**std**				
Pelvis	0.85	0.10	0.71	0.15	0.84	0.05	0.78	0.13	0.91	0.83	0.95	0.92
Upper leg	0.24	0.22	0.24	0.26	0.20	0.31	0.18	0.27	0.26	0.35	0.15	0.27
Lower leg	0.71	0.12	0.85	0.07	0.71	0.12	0.88	0.08	0.89	0.87	0.89	0.95
Lower extremity	0.88	0.04	0.74	0.09	0.87	0.04	0.77	0.10	0.91	0.84	0.96	0.91

%FDG uptake based on PET volumetric analysis, $\%E_m$ metabolic energy consumption predicted using generic and subject-specific musculoskeletal models.

pelvis region (ρ = 0.91 and r = 0.83 for generic models, ρ = 0.95 and r = 0.92 for subject-specific models) and lower leg (ρ = 0.89 and r = 0.87 for generic models, ρ = 0.89 and r = 0.95 for subject-specific models), but poor correlation was found for the upper leg (ρ = 0.26 and r = 0.35 for generic models, ρ = 0.15 and r = 0.27 for subject-specific models).

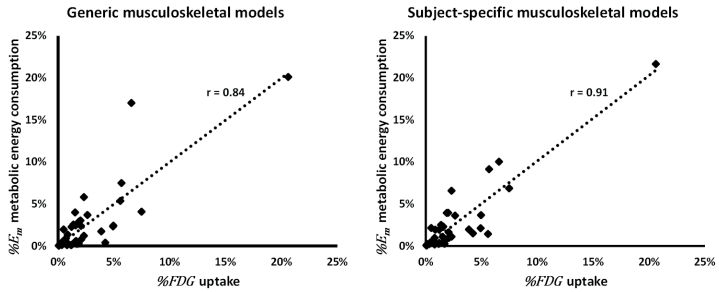

Figure 7.6. Linear correlation between %FDG uptake, based on PET volumetric analysis, and $\%E_m$ metabolic energy consumption, predicted using generic and subject-specific musculoskeletal models. and values were averaged over ten healthy subjects. Linear trend lines are based on Pearson product-moment correlation coefficient *r*.

Discussion

In this study, we used FDG-PET to indirectly validate muscle energy consumption predictions during walking made by generic and subject-specific MS models. The validity of FDG-PET to measure muscular activity during walking has been previously demonstrated by (Oi et al. 2003), however to our knowledge this is the first time that MS model predictions have been compared with FDG-PET data. In general, high correlations were found between the measured %FDG uptake and the predicted $\%E_m$ metabolic energy consumption, giving more confidence on the validity of the model outcomes when it comes to relative contributions of muscles to walking.

Almost 50% of the predicted $\%E_m$ metabolic energy was consumed by muscles in the lower leg, in particular the Soleus and the Gastrocnemius, in accordance with the %FDG uptake values, confirming the key role of the ankle plantarflexors during walking (Liu et al. 2006; Winter 1983). Moreover, the fact that a deep and relatively small muscle like the Gluteus Minimus appeared among the most consuming muscles during gait, according to both %FDG and $\%E_m$ and as previously indicated by Oi et al. (2003), shows the advantages of FDG-PET compared to EMG, which allows to measure only the superficial muscles.

High correlations were found between %FDG uptake and $\%E_m$ metabolic energy consumption in the pelvis region and the lower leg, while poor correlation was found in the upper leg. This result may be dependent on the task analyzed, since %FDG uptake values during gait showed small variability between muscles within the upper leg (Kolk et al. 2015). Results are likely to be different for more demanding task such as running or stair climbing.

Unlike the FDG-PET results, the models predicted larger $\%E_m$ metabolic energy consumption in the pelvis region, in particular the Gluteal and Iliopsoas muscles that provide stability to the hip joint during gait. They also predicted a smaller consumption in the upper leg, in particular in the Vasti muscles compared to the Rectus Femoris, probably due to the fact that the model includes a 1 degree-of-freedom knee joint that requires less muscle-induced stability. A thorough understanding of these kinds of features of the models remains very important to be able to explain their outcomes, and in order to further improve their predictions.

Subject-specific models used in this study predicted more realistic MT forces and muscle activity during gait compared to generic models (Carbone 2016). These differences resulted in slight improvements in the predicted metabolic power consumption and in the correlation between %FDG uptakes and $\%E_m$ metabolic energy consumption. However, it was not possible to statistically prove the significance of these improvements, probably due to the fact that FDG-PET is not accurate enough to detect the improvements of personalized models for healthy subjects and for relatively simple tasks such as walking. Differences between generic and subject-specific models are likely to be magnified for more strenuous activities such as running, climbing stairs or getting up from a chair, and when analyzing patients affected by musculoskeletal pathologies, where larger differences in MS geometry and MT parameters are expected.

On average, predicted metabolic power P_m (3.82 W/kg for generic models and 3.73 W/kg for subject-specific models) was lower than the measured values found in literature (4.67 W/kg) (Inman et al. 1981). However, P_m depended exclusively on the predicted mechanical power of the muscles of the lower leg, while the measured metabolic power consumption based on the oxygen uptake, included the contribution of the muscles of the upper body and the resting metabolism. Moreover, the precise relation between metabolic energy consumption and predicted muscle forces is unknown. We assumed the same efficiency for all the muscles, whereas uptake of the glucose into a muscle depends on many factors, including the fiber types (Henriksen et al. 1990). Hence, it is possible that the different fiber composition in the muscles of the lower extremity (Johnson et al. 1973) affects the efficiency and energy consumption of muscles. FDG-PET results provides precious information to better understand the functional differences in the muscle energy consumption and recruitment process, and should be used to improve the static optimization criteria used in MS models, for example introducing energy-based cost functions as suggested by Praagman et al. (Praagman et al. 2006).

The main limitation of the FDG-PET results is that they depend on the quality of the medical images used and on the segmentation accuracy. Errors in muscle segmentation would directly affect the glucose uptake measurement, however Kolk et al. (Kolk et al. 2015) showed that the method used in this study had a small sensitivity to this kind of errors. Compared to EMG, FDG-PET results have a cumulative nature, therefore the measured glucose uptake represents an accumulation of all the muscle metabolic activity during the task and cannot be used to measure temporal variations of muscle force or energy consumption. Also, validity of this method to measure muscular activity has been proven only for aerobic tasks. Most importantly, FDG-PET requires specialized equipment and

involves a low dose of radiation, hence it is difficult to perform repeated measurements on the same subject because of ethical issues.

Conclusions

In conclusion, the high to very high correlation between the measured %FDG and the predicted $\%E_m$ that was found when analyzing each individual subject and when analyzing averaged results gives great confidence on the validity of the model outcomes when analyzing muscle function during gait. However, significant improvements in the subject-specific models compared to generic models were not proven. Given its advantages and limitations, FDG-PET should be considered as a complimentary tool to EMG when validating MS models.

Acknowledgements

We gratefully acknowledge financial support by the Seventh Framework Programme (FP7) of the European Union (Grant agreement no: 247860) for the TLEMsafe project: http://www.tlemsafe.eu/. Heartfelt thanks to the Radiology Department of the Radboud University Medical Center for their hospitality and helpfulness during the medical imaging sessions.

References

Andersen, M.S., Damsgaard, M., MacWilliams, B., and Rasmussen, J. 2010. A computationally efficient optimisation-based method for parameter identification of kinematically determinate and over-determinate biomechanical systems, Comp. Meth. Biomech. Biomed. Eng., 13: 171-183.

Asadi Nikooyan, A., Veeger, H.E.J., Chadwick, E.K.J., Praagman, M., and van der Helm, F.C.T. 2011. Development of a comprehensive musculoskeletal model of the shoulder and elbow, Medical & Biological Engineering & Computing, 49: 1425-1435.

Asmussen, E. 1953. Positive and Negative Muscular Worknegative muscular work, Acta Physiologica Scandinavica, 28: 364-382.

Bergmann, G., Deuretzbacher, G., Heller, M., Graichen, F., Rohlmann, A., Strauss, J., and Duda, G.N. 2001. Hip contact forces and gait patterns from routine activities, Journal of Biomechanics, 34: 859-871.

Carbone, V. 2016. Subject-specific lower extremity modeling, PhD Thesis, University of Twente.

Carbone, V., Fluit, R., Pellikaan, P., van der Krogt, M.M., Janssen, D., Damsgaard, M., Vigneron, L., Feilkas, T., Koopman, H.F., and Verdonschot, N. 2015. TLEM 2.0 - a comprehensive musculoskeletal geometry dataset for subject-specific modeling of lower extremity, J Biomech, 48: 734-741.

Cohen, Z.A., Henry, J.H., McCarthy, D.M., Mow, V.C., and Ateshian, G.A. 2003. Computer simulations of patellofemoral joint surgery: Patient-specific models for tuberosity transfer, American Journal of Sports Medicine, 31: 87-98.

Crowninshield, R.D., and Brand, R.A. 1981. A physiologically based criterion of muscle force prediction in locomotion, J. Biomech., 14: 793-801.

De Haan, A., Vanvan Ingen Schenau, G.J., Ettema, G.J., Huijing, P.A., and Lodder, M.A. 1989. Efficiency of rat medial gastrocnemius muscle in contractions with and without an active prestretch, Journal of Experimental Biology, 141: 327-341.

Finni, T., Komi, P.V., and Lepola, V. 2000. In vivo human triceps surae and quadriceps femoris muscle function in a squat jump and counter movement jump, European Journal of Applied Physiology, 83: 416-426.

Fregly, B.J., Besier, T.F., Lloyd, D.G., Delp, S.L., Banks, S.A., Pandy, M.G., and D'Lima, D.D. 2012. Grand challenge competition to predict in vivo knee loads, Journal of Orthopaedic Research, 30: 503-513.

Fujimoto, T., Itoh, M., Kumano, H., Tashiro, M., and Ido, T. 1996. Whole-body metabolic map with positron emission tomography of a man after running, Lancet, 348: 266.

Fujimoto, T., Itoh, M., Tashiro, M., Yamaguchi, K., Kubota, K., and Ohmori, H. 2000. Glucose uptake by individual skeletal muscles during running using whole-body positron emission tomography, Eur J Appl Physiol, 83: 297-302.

Fujimoto, T., Kemppainen, J., Kalliokoski, K.K., Nuutila, P., Ito, M., and Knuuti, J. 2003. Skeletal muscle glucose uptake response to exercise in trained and untrained men, Med Sci Sports Exerc, 35: 777-783.

Giroux, M., Moissenet, F., and Dumas, R. 2013. EMG-based validation of musculo-skeletal models for gait analysis, Computer Methods in Biomechanics and Biomedical Engineering, 16: 152-154.

Gondoh, Y., Tashiro, M., Itoh, M., Masud, M.M., Sensui, H., Watanuki, S., Ishii, K., Takekura, H., Nagatomi, R., and Fujimoto, T. 2009. Evaluation of individual skeletal muscle activity by glucose uptake during pedaling exercise at different workloads using positron emission tomography, J Appl Physiol, 107: 599-604.

Gregor, R.J., Komi, P.V., Browning, R.C., and Järvinen, M. 1991. A comparison of the triceps surae and residual muscle moments at the ankle during cycling, Journal of Biomechanics, 24: 287-297.

Hainisch, R., Gfoehler, M., Zubayer-Ul-Karim, M., and Pandy, M.G. 2012. Method for determining musculotendon parameters in subject-specific musculoskeletal models of children developed

from MRI data, Multibody System Dynamics, 28: 143-156.
Happee, R., and Van der Helm, F.C. 1995. The control of shoulder muscles during goal directed movements, an inverse dynamic analysis, J. Biomech., 28: 1179-1191.
Hausselle, J., Assi, A., El Helou, A., Jolivet, E., Pillet, H., Dion, E., Bonneau, D., and Skalli, W. 2014. Subject-specific musculoskeletal model of the lower limb in a lying and standing position, Computer Methods in Biomechanics and Biomedical Engineering, 17: 480-487.
Henriksen, E.J., Bourey, R.E., Rodnick, K.J., Koranyi, L., Permutt, M.A., and Holloszy, J.O. 1990. Glucose transporter protein content and glucose transport capacity in rat skeletal muscles, American Journal of Physiology, 259: E593-598.
Inman, V.T., Ralston, H.J., and Todd, F. 1981. Human Walking (Williams & Wilkins: Baltimore).
Johnson, M.A., Polgar, J., Weightman, D., and Appleton, D. 1973. Data on the distribution of fibre types in thirty-six human muscles: An autopsy study, Journal of the Neurological Sciences, 18: 111-129.
Kemppainen, J., Fujimoto, T., Kalliokoski, K.K., Viljanen, T., Nuutila, P., and Knuuti, J. 2002. Myocardial and skeletal muscle glucose uptake during exercise in humans, J Physiol, 542: 403-412.
Kolk, S., Klawer, E.M.E., Schepers, J., Weerdesteyn, V., Visser, E.P., and Verdonschot, N. 2015. Muscle Activity during Walking Measured Using 3D MRI Segmentations and [18F]-Fluorodeoxyglucose in Combination with Positron Emission Tomography, Med Sci Sports Exerc, 47: 1896-1905.
Liu, M.Q., Anderson, F.C., Pandy, M.G., and Delp, S.L. 2006. Muscles that support the body also modulate forward progression during walking, Journal of Biomechanics, 39: 2623-2630.
Lund, M.E., de Zee, M., Andersen, M.S., and Rasmussen, J. 2012. On validation of multibody musculoskeletal models, Proceedings of the Institution of Mechanical Engineers. Part H: Journal of Engineering in Medicine, 226: 82-94.
Masood, T., Bojsen-Moller, J., Kalliokoski, K.K., Kirjavainen, A., Aarimaa, V., Peter Magnusson, S., and Finni, T. 2014. Differential contributions of ankle plantarflexors during submaximal isometric muscle action: a PET and EMG study, J Electromyogr Kinesiol, 24: 367-374.
Oi, N., Iwaya, T., Itoh, M., Yamaguchi, K., Tobimatsu, Y., and Fujimoto, T. 2003. FDG-PET imaging of lower extremity muscular activity during level walking, J Orthop Sci, 8: 55-61.
Pappas, G.P., Olcott, E.W., and Drace, J.E. 2001. Imaging of skeletal muscle function using (18)FDG PET: force production, activation, and metabolism, J Appl Physiol (1985), 90: 329-337.
Praagman, M., Chadwick, E.K.J., van der Helm, F.C.T., and Veeger, H.E.J. 2006. The relationship between two different mechanical cost functions and muscle oxygen consumption, J. Biomech., 39: 758-765.
Praagman, M., Veeger, H.E.J., Chadwick, E.K.J., Colier, W.N.J.M., and van der Helm, F.C.T. 2003. Muscle oxygen consumption, determined by NIRS, in relation to external force and EMG, Journal of Biomechanics, 36: 905-912.
Prilutsky, B.I., and Zatsiorsky, V.M. 2002. Optimization-based models of muscle coordination, Exercise and sport sciences reviews, 30: 32.
Reinbolt, J.A., Fox, M.D., Schwartz, M.H., and Delp, S.L. 2009. Predicting outcomes of rectus femoris transfer surgery, Gait & Posture, 30: 100-105.
Rudroff, T., Kalliokoski, K.K., Block, D.E., Gould, J.R., Klingensmith, W.C., and Enoka, R.M. 2013. PET/CT imaging of age- and task-associated differences in muscle activity during fatiguing contractions, Journal of Applied Physiology, 114: 1211-1219.
Scheys, L., Loeckx, D., Spaepen, A., Suetens, P., and Jonkers, I. 2009. Atlas-based non-rigid image registration to automatically define line-of-action muscle models: A validation study, Journal of Biomechanics, 42: 565-572.
Shimada, H., Kimura, Y., Lord, S.R., Oda, K., Ishii, K., Suzuki, T., and Ishiwata, K. 2009. Comparison of regional lower limb glucose metabolism in older adults during walking, Scand J Med Sci Sports, 19: 389-397.
Shimada, H., Kimura, Y., Suzuki, T., Hirata, T., Sugiura, M., Endo, Y., Yasuhara, K., Shimada, K.,

Kikuchi, K., Hashimoto, M., Ishikawa, M., Oda, K., Ishii, K., and Ishiwata, K. 2007. The use of positron emission tomography and [18F]fluorodeoxyglucose for functional imaging of muscular activity during exercise with a stride assistance system, IEEE Trans Neural Syst Rehabil Eng, 15: 442-448.

Taddei, F., Martelli, S., Valente, G., Leardini, A., Benedetti, M.G., Manfrini, M., and Viceconti, M. 2012. Femoral loads during gait in a patient with massive skeletal reconstruction, Clinical Biomechanics, 27: 273-280.

Tashiro, M., Fujimoto, T., Itoh, M., Kubota, K., Fujiwara, T., Miyake, M., Watanuki, S., Horikawa, E., Sasaki, H., and Ido, T. 1999. 18F-FDG PET imaging of muscle activity in runners, J Nucl Med, 40: 70-76.

van Campen, A., Pipeleers, G., De Groote, F., Jonkers, I., and De Schutter, J. 2014. A new method for estimating subject-specific muscle-tendon parameters of the knee joint actuators: A simulation study, International Journal for Numerical Methods in Biomedical Engineering, 30: 969-987.

Voigt, M., Bojsen-Moller, F., Simonsen, E.B., and Dyhre-Poulsen, P. 1995. The influence of tendon Youngs modulus, dimensions and instantaneous moment arms on the efficiency of human movement, Journal of Biomechanics, 28: 281-291.

Winter, D.A. 1983. Energy generation and absorption at the ankle and knee during fast, natural, and slow cadences, Clinical Orthopaedics and Related Research: 147-154.

Zajac, F.E. 1989. Muscle and tendon: properties, models, scaling, and application to biomechanics and motor control, Critical reviews in biomedical engineering, 17: 359-411.

Appendix 7.1: %FDG uptake - Ten healthy subjects

		Subject														
		1	**2**	**3**	**4**	**5**	**6**	**7**	**8**	**9**	**10**	**mean**	**std**	**median**	**min**	**max**
Hip region	Gemellus Inferior	0,1%	0,0%	0,0%	0,1%	0,1%	0,1%	0,1%	0,1%	0,1%	0,1%	0,1%	0,0%	0,1%	0,0%	0,1%
	Gemellus Superior	0,2%	0,0%	0,0%	0,0%	0,0%	0,1%	0,1%	0,0%	0,1%	0,1%	0,1%	0,0%	0,0%	0,0%	0,2%
	Gluteus Maximus	4,1%	4,6%	7,2%	6,7%	7,0%	11,5%	7,9%	11,6%	7,4%	6,7%	7,5%	2,3%	7,1%	4,1%	11,6%
	Gluteus Medius	2,5%	2,5%	4,0%	3,0%	5,5%	4,8%	4,3%	19,5%	6,1%	4,5%	5,7%	4,8%	4,4%	2,5%	19,5%
	Gluteus Minimus	1,1%	0,6%	1,5%	1,2%	3,9%	3,0%	2,8%	4,8%	6,2%	1,2%	2,6%	1,8%	2,2%	0,6%	6,2%
	Iliacus	1,3%	1,5%	2,0%	2,1%	2,3%	3,0%	2,6%	1,2%	2,7%	1,3%	2,0%	0,6%	2,0%	1,2%	3,0%
	Obturator Externus	0,5%	0,4%	0,3%	0,3%	0,3%	0,4%	0,4%	0,2%	0,2%	0,3%	0,3%	0,1%	0,3%	0,2%	0,5%
	Obturator Internus	2,0%	0,3%	0,9%	1,4%	0,5%	0,7%	0,4%	0,3%	0,5%	0,4%	0,7%	0,5%	0,5%	0,3%	2,0%
	Pectineus	0,5%	0,5%	0,8%	0,8%	0,4%	0,5%	0,8%	0,4%	0,7%	0,4%	0,6%	0,2%	0,5%	0,4%	0,8%
	Piriformis	2,7%	0,4%	1,1%	0,5%	0,2%	0,3%	0,5%	1,4%	0,6%	0,3%	0,8%	0,7%	0,5%	0,2%	2,7%
	Psoas Major	1,1%	1,0%	1,4%	1,3%	1,6%	1,7%	1,7%	0,8%	1,7%	1,5%	1,4%	0,3%	1,4%	0,8%	1,7%
	Quadratus Femoris	0,2%	0,2%	0,4%	0,2%	0,3%	0,5%	0,5%	0,2%	0,7%	0,3%	0,3%	0,2%	0,3%	0,2%	0,7%
	Tensor Fasciae Latae	0,3%	0,4%	0,4%	0,4%	0,5%	0,6%	0,6%	0,9%	0,5%	0,3%	0,5%	0,2%	0,5%	0,3%	0,9%
	SUM	**16,5%**	**12,4%**	**20,1%**	**18,0%**	**22,5%**	**27,3%**	**22,7%**	**41,3%**	**27,3%**	**17,3%**	**22,6%**	**7,7%**	**21,3%**	**12,4%**	**41,3%**
Thigh region	Adductor Brevis	2,0%	1,4%	1,2%	1,6%	1,0%	1,3%	1,3%	3,4%	1,9%	1,7%	1,7%	0,6%	1,5%	1,0%	3,4%
	Adductor Longus	1,2%	1,2%	1,5%	5,1%	1,2%	2,2%	2,1%	3,9%	3,5%	1,1%	2,3%	1,3%	1,8%	1,1%	5,1%
	Adductor Magnus	4,0%	3,6%	5,7%	5,3%	5,4%	6,9%	5,7%	3,7%	5,5%	3,6%	4,9%	1,1%	5,4%	3,6%	6,9%
	Biceps Femoris Caput Breve	0,4%	0,7%	0,9%	0,8%	1,2%	1,0%	1,2%	0,5%	1,4%	0,5%	0,9%	0,3%	0,8%	0,4%	1,4%
	Biceps Femoris Caput Longum	1,2%	0,9%	1,4%	1,9%	1,4%	1,9%	1,8%	0,8%	2,1%	2,3%	1,6%	0,5%	1,6%	0,8%	2,3%
	Gracilis	0,3%	0,6%	0,7%	0,8%	0,6%	0,6%	0,7%	0,6%	0,6%	0,6%	0,6%	0,1%	0,6%	0,3%	0,8%
	Rectus Femoris	1,5%	1,3%	2,1%	1,8%	1,9%	2,0%	2,8%	1,0%	2,4%	2,0%	1,9%	0,5%	1,9%	1,0%	2,8%
	Sartorius	0,6%	1,0%	1,5%	1,4%	1,1%	1,5%	1,6%	4,4%	1,4%	0,8%	1,5%	1,0%	1,4%	0,6%	4,4%
	Semimembranosus	2,6%	1,2%	1,7%	1,7%	1,3%	3,6%	1,8%	1,2%	2,7%	2,8%	2,0%	0,8%	1,7%	1,2%	3,6%
	Semitendinosus	1,2%	1,0%	1,2%	1,3%	1,3%	1,1%	0,9%	0,6%	1,6%	1,8%	1,2%	0,3%	1,2%	0,6%	1,8%
	Vastus Intermedius	2,5%	3,0%	5,9%	4,6%	4,9%	6,0%	5,4%	2,8%	4,0%	3,2%	4,2%	1,3%	4,3%	2,5%	6,0%
	Vastus Lateralis	3,6%	3,8%	6,7%	6,4%	6,4%	7,6%	7,4%	3,8%	4,7%	5,3%	5,6%	1,5%	5,8%	3,6%	7,6%
	Vastus Medialis	2,4%	2,3%	5,4%	4,7%	4,2%	5,3%	4,2%	2,7%	4,2%	3,2%	3,9%	1,1%	4,2%	2,3%	5,4%
	SUM	**23,5%**	**22,0%**	**36,0%**	**37,2%**	**31,8%**	**40,9%**	**36,8%**	**29,5%**	**35,9%**	**29,0%**	**32,3%**	**5,9%**	**33,8%**	**22,0%**	**40,9%**
Lower leg	Extensor Digitorum Longus	0,7%	4,6%	1,2%	3,4%	1,1%	0,9%	1,6%	1,7%	1,8%	1,3%	1,8%	1,2%	1,5%	0,7%	4,6%
	Extensor Hallucis Longus	1,5%	1,9%	0,8%	1,7%	1,0%	0,8%	0,8%	1,0%	1,3%	1,4%	1,2%	0,4%	1,2%	0,8%	1,9%
	Flexor Digitorum Longus	0,2%	0,9%	0,7%	0,4%	1,5%	0,9%	1,5%	0,6%	0,9%	0,4%	0,8%	0,4%	0,8%	0,2%	1,5%
	Flexor Hallucis Longus	0,6%	4,6%	0,7%	0,7%	1,2%	1,4%	2,3%	1,2%	0,8%	1,8%	1,5%	1,1%	1,2%	0,6%	4,6%
	Gastrocnemius Lateralis	2,3%	1,0%	4,0%	1,3%	1,4%	1,8%	1,7%	4,6%	2,0%	3,1%	2,3%	1,1%	1,9%	1,0%	4,6%
	Gastrocnemius Medialis	5,1%	1,9%	8,6%	6,6%	13,7%	4,8%	4,0%	4,9%	6,1%	9,9%	6,6%	3,2%	5,6%	1,9%	13,7%
	Peroneus Brevis	0,8%	0,6%	0,8%	1,4%	1,2%	0,5%	0,6%	0,3%	0,5%	4,8%	1,2%	1,3%	0,7%	0,3%	4,8%
	Peroneus Longus	0,5%	2,6%	1,2%	4,4%	0,7%	0,8%	1,1%	0,6%	1,0%	3,2%	1,6%	1,3%	1,0%	0,5%	4,4%
	Plantaris	0,2%	0,1%	0,1%	0,1%	0,1%	0,1%	0,4%	0,2%	0,1%	0,1%	0,1%	0,1%	0,1%	0,1%	0,4%
	Popliteus	0,5%	0,3%	0,4%	0,2%	0,5%	0,4%	0,5%	0,4%	0,7%	0,4%	0,4%	0,1%	0,4%	0,2%	0,7%
	Soleus	39,5%	40,5%	17,3%	17,0%	15,2%	13,5%	21,2%	8,8%	11,5%	21,5%	20,6%	10,4%	17,1%	8,8%	40,5%
	Tibialis Anterior	7,0%	5,0%	4,6%	6,4%	7,1%	2,9%	2,8%	3,7%	5,2%	4,4%	4,9%	1,5%	4,8%	2,8%	7,1%
	Tibialis Posterior	1,1%	1,7%	3,4%	1,2%	1,1%	2,9%	2,0%	1,2%	4,7%	1,3%	2,1%	1,2%	1,5%	1,1%	4,7%
	SUM	**59,9%**	**65,6%**	**43,8%**	**44,8%**	**45,8%**	**31,8%**	**40,5%**	**29,2%**	**36,7%**	**53,6%**	**45,2%**	**11,1%**	**44,3%**	**29,2%**	**65,6%**

Appendix 7.2: $\%E_m$ metabolic energy consumption - Ten healthy subjects - Generic musculoskeletal models

		Subject														
		1	**2**	**3**	**4**	**5**	**6**	**7**	**8**	**9**	**10**	**mean**	**std**	**median**	**min**	**max**
Hip region	Gemellus Inferior	0,0%	0,0%	0,1%	0,0%	0,0%	0,0%	0,0%	0,0%	0,0%	0,0%	0,0%	0,0%	0,0%	0,0%	0,1%
	Gemellus Superior	0,0%	0,0%	0,0%	0,0%	0,0%	0,0%	0,0%	0,1%	0,0%	0,0%	0,0%	0,0%	0,0%	0,0%	0,1%
	Gluteus Maximus	3,3%	5,2%	4,8%	2,6%	1,3%	5,6%	2,7%	5,6%	4,7%	5,0%	4,1%	1,4%	4,7%	1,3%	5,6%
	Gluteus Medius	9,3%	7,7%	5,1%	8,8%	5,4%	8,3%	7,8%	5,5%	9,0%	7,9%	7,5%	1,5%	7,8%	5,1%	9,3%
	Gluteus Minimus	4,3%	3,4%	3,1%	4,1%	2,8%	3,8%	3,9%	3,4%	3,7%	4,4%	3,7%	0,5%	3,8%	2,8%	4,4%
	Iliacus	3,7%	2,5%	2,4%	3,5%	2,1%	3,1%	3,8%	3,1%	2,7%	3,3%	3,0%	0,6%	3,1%	2,1%	3,8%
	Obturator Externus	0,4%	0,4%	0,3%	0,6%	0,3%	0,3%	0,4%	0,7%	0,4%	0,5%	0,4%	0,1%	0,4%	0,3%	0,7%
	Obturator Internus	0,1%	0,2%	0,3%	0,2%	0,1%	0,3%	0,2%	0,4%	0,2%	0,2%	0,2%	0,1%	0,2%	0,1%	0,4%
	Pectineus	0,5%	0,3%	0,3%	0,6%	0,4%	0,5%	0,8%	0,7%	0,4%	0,5%	0,5%	0,2%	0,5%	0,3%	0,8%
	Piriformis	0,4%	0,2%	0,4%	0,2%	0,2%	0,5%	0,3%	0,7%	0,5%	0,6%	0,4%	0,2%	0,4%	0,2%	0,7%
	Psoas Major	3,0%	2,0%	1,9%	2,9%	1,6%	2,7%	3,2%	3,0%	2,2%	2,9%	2,5%	0,5%	2,8%	1,6%	3,2%
	Quadratus Femoris	0,1%	0,1%	0,2%	0,1%	0,0%	0,1%	0,1%	0,1%	0,1%	0,1%	0,1%	0,1%	0,1%	0,0%	0,2%
	Tensor Fasciae Latae	2,1%	1,9%	1,7%	2,5%	1,8%	1,8%	2,0%	1,7%	2,0%	2,1%	2,0%	0,2%	1,9%	1,7%	2,5%
	SUM	**27,2%**	**24,0%**	**20,6%**	**26,1%**	**16,1%**	**27,0%**	**25,2%**	**25,0%**	**25,9%**	**27,6%**	**24,5%**	**3,4%**	**25,6%**	**16,1%**	**27,6%**
Thigh region	Adductor Brevis	0,2%	0,1%	0,1%	0,3%	0,1%	0,1%	0,5%	0,5%	0,1%	0,3%	0,2%	0,2%	0,2%	0,1%	0,5%
	Adductor Longus	1,4%	0,7%	0,5%	1,5%	0,6%	1,2%	2,2%	1,7%	0,8%	1,4%	1,2%	0,5%	1,3%	0,5%	2,2%
	Adductor Magnus	2,5%	1,8%	1,7%	2,8%	5,6%	0,6%	2,1%	2,8%	2,2%	1,9%	2,4%	1,2%	2,1%	0,6%	5,6%
	Biceps Femoris Caput Breve	1,5%	1,2%	0,9%	1,6%	1,0%	1,2%	1,3%	1,3%	1,6%	1,8%	1,3%	0,3%	1,3%	0,9%	1,8%
	Biceps Femoris Caput Longum	2,5%	3,1%	2,3%	2,4%	1,1%	2,1%	2,4%	1,5%	3,5%	3,6%	2,4%	0,7%	2,4%	1,1%	3,6%
	Gracilis	0,8%	0,5%	0,5%	1,0%	0,5%	0,7%	1,1%	1,3%	0,8%	0,7%	0,8%	0,3%	0,7%	0,5%	1,3%
	Rectus Femoris	2,5%	3,8%	2,9%	3,6%	0,4%	2,6%	3,5%	2,9%	3,0%	3,9%	2,9%	1,0%	3,0%	0,4%	3,9%
	Sartorius	5,2%	3,4%	3,1%	4,4%	2,0%	4,2%	4,9%	3,9%	3,8%	4,9%	4,0%	0,9%	4,0%	2,0%	5,2%
	Semimembranosus	2,3%	2,2%	1,6%	2,4%	4,7%	2,0%	2,1%	2,1%	2,3%	2,3%	2,4%	0,8%	2,2%	1,6%	4,7%
	Semitendinosus	2,6%	2,1%	1,3%	2,3%	4,9%	1,3%	2,1%	2,0%	2,0%	2,2%	2,3%	1,0%	2,1%	1,3%	4,9%
	Vastus Intermedius	0,2%	0,4%	0,5%	0,6%	0,7%	0,4%	0,3%	0,4%	0,2%	0,1%	0,4%	0,2%	0,4%	0,1%	0,7%
	Vastus Lateralis	3,0%	5,4%	6,8%	7,7%	9,8%	6,0%	4,9%	5,4%	3,3%	1,2%	5,4%	2,3%	5,4%	1,2%	9,8%
	Vastus Medialis	1,0%	1,7%	2,1%	2,5%	3,0%	1,8%	1,7%	1,7%	1,3%	0,5%	1,7%	0,7%	1,7%	0,5%	3,0%
	SUM	**25,8%**	**26,5%**	**24,4%**	**33,1%**	**34,4%**	**24,3%**	**28,9%**	**27,5%**	**25,0%**	**24,7%**	**27,4%**	**3,4%**	**26,1%**	**24,3%**	**34,4%**
Lower leg	Extensor Digitorum Longus	0,3%	0,2%	0,2%	0,3%	0,3%	0,2%	0,3%	0,4%	0,3%	0,3%	0,3%	0,0%	0,3%	0,2%	0,4%
	Extensor Hallucis Longus	0,1%	0,1%	0,1%	0,2%	0,1%	0,1%	0,1%	0,2%	0,2%	0,2%	0,1%	0,0%	0,1%	0,1%	0,2%
	Flexor Digitorum Longus	0,2%	0,0%	0,1%	0,1%	0,1%	0,1%	0,2%	0,0%	0,1%	0,1%	0,1%	0,0%	0,1%	0,0%	0,2%
	Flexor Hallucis Longus	1,0%	0,2%	0,2%	0,6%	0,3%	0,7%	0,9%	0,4%	0,4%	0,5%	0,5%	0,3%	0,5%	0,2%	1,0%
	Gastrocnemius Lateralis	5,6%	5,7%	7,2%	5,0%	6,0%	6,4%	5,4%	5,8%	5,8%	5,3%	5,8%	0,6%	5,7%	5,0%	7,2%
	Gastrocnemius Medialis	16,8%	17,5%	19,9%	15,2%	16,2%	17,6%	15,6%	16,2%	17,9%	17,2%	17,0%	1,3%	17,0%	15,2%	19,9%
	Peroneus Brevis	0,2%	0,0%	0,2%	0,1%	0,1%	0,1%	0,1%	0,1%	0,0%	0,0%	0,1%	0,0%	0,1%	0,0%	0,2%
	Peroneus Longus	0,8%	0,4%	0,3%	0,6%	0,5%	0,8%	0,7%	0,5%	0,6%	0,5%	0,6%	0,2%	0,6%	0,3%	0,8%
	Plantaris	0,2%	0,2%	0,2%	0,1%	0,2%	0,2%	0,1%	0,2%	0,2%	0,2%	0,2%	0,0%	0,2%	0,1%	0,2%
	Popliteus	0,2%	0,2%	0,2%	0,3%	0,3%	0,2%	0,3%	0,2%	0,3%	0,2%	0,2%	0,0%	0,2%	0,2%	0,3%
	Soleus	17,8%	23,2%	25,0%	14,5%	23,8%	19,4%	18,6%	20,2%	19,4%	19,3%	20,1%	3,0%	19,4%	14,5%	25,0%
	Tibialis Anterior	2,0%	1,8%	1,3%	3,2%	1,4%	2,0%	1,9%	3,1%	3,5%	3,0%	2,3%	0,8%	2,0%	1,3%	3,5%
	Tibialis Posterior	2,0%	0,1%	0,1%	0,7%	0,2%	1,0%	1,7%	0,4%	0,4%	1,0%	0,8%	0,6%	0,6%	0,1%	2,0%
	SUM	**47,1%**	**49,6%**	**55,1%**	**40,8%**	**49,6%**	**48,8%**	**45,9%**	**47,6%**	**49,1%**	**47,7%**	**48,1%**	**3,4%**	**48,2%**	**40,8%**	**55,1%**

Appendix 7.3: $\%E_m$ metabolic energy consumption - Ten healthy subjects - Subject-specific musculoskeletal models

		Subject														
		1	**2**	**3**	**4**	**5**	**6**	**7**	**8**	**9**	**10**	**mean**	**std**	**median**	**min**	**max**
Hip region	Gemellus Inferior	0,0%	0,2%	0,0%	0,0%	0,0%	0,0%	0,0%	0,0%	0,0%	0,2%	0,1%	0,1%	0,0%	0,0%	0,2%
	Gemellus Superior	0,1%	0,1%	0,0%	0,0%	0,0%	0,0%	0,1%	0,1%	0,0%	0,1%	0,1%	0,0%	0,1%	0,0%	0,1%
	Gluteus Maximus	6,1%	8,8%	4,5%	6,7%	7,8%	3,3%	3,6%	10,9%	9,3%	7,6%	6,9%	2,4%	7,2%	3,3%	10,9%
	Gluteus Medius	10,8%	9,5%	5,8%	8,8%	8,3%	10,3%	8,7%	8,0%	10,6%	10,5%	9,1%	1,5%	9,1%	5,8%	10,8%
	Gluteus Minimus	4,8%	2,4%	2,4%	5,8%	3,0%	6,0%	3,9%	1,3%	3,3%	3,2%	3,6%	1,4%	3,3%	1,3%	6,0%
	Iliacus	5,3%	3,2%	3,9%	5,5%	2,1%	3,8%	5,2%	3,7%	2,8%	3,9%	3,9%	1,0%	3,8%	2,1%	5,5%
	Obturator Externus	0,1%	0,2%	0,0%	0,3%	0,1%	0,2%	0,4%	0,5%	0,2%	0,2%	0,2%	0,1%	0,2%	0,0%	0,5%
	Obturator Internus	0,7%	1,6%	0,5%	0,2%	0,0%	0,7%	0,0%	0,5%	0,7%	0,2%	0,5%	0,4%	0,5%	0,0%	1,6%
	Pectineus	0,5%	0,4%	0,8%	1,1%	0,3%	0,3%	0,1%	0,3%	0,5%	0,4%	0,5%	0,3%	0,4%	0,1%	1,1%
	Piriformis	1,2%	0,6%	0,9%	0,3%	0,0%	0,7%	1,0%	1,2%	2,5%	1,2%	1,0%	0,7%	0,9%	0,0%	2,5%
	Psoas Major	2,2%	2,2%	0,2%	2,9%	1,5%	2,3%	2,7%	5,0%	1,9%	4,1%	2,5%	1,3%	2,3%	0,2%	5,0%
	Quadratus Femoris	0,0%	0,1%	0,0%	0,0%	0,0%	0,0%	0,0%	1,1%	0,9%	0,7%	0,3%	0,4%	0,0%	0,0%	1,1%
	Tensor Fasciae Latae	1,9%	2,2%	1,6%	0,9%	1,3%	1,6%	2,7%	4,6%	2,8%	1,7%	2,1%	1,0%	1,8%	0,9%	4,6%
	SUM	**33,7%**	**31,5%**	**20,7%**	**32,4%**	**24,3%**	**29,2%**	**28,5%**	**37,2%**	**35,7%**	**34,3%**	**30,8%**	**4,9%**	**32,0%**	**20,7%**	**37,2%**
Thigh region	Adductor Brevis	0,0%	0,2%	0,1%	0,6%	0,3%	0,1%	0,4%	0,5%	0,2%	0,1%	0,3%	0,2%	0,2%	0,0%	0,6%
	Adductor Longus	0,4%	0,6%	0,7%	2,0%	1,1%	0,5%	3,5%	0,5%	1,0%	0,5%	1,1%	0,9%	0,7%	0,4%	3,5%
	Adductor Magnus	2,3%	3,0%	7,8%	3,9%	5,6%	3,5%	2,2%	3,3%	4,0%	0,9%	3,7%	1,8%	3,4%	0,9%	7,8%
	Biceps Femoris Caput Breve	2,6%	2,6%	0,4%	2,3%	1,5%	2,2%	3,1%	0,3%	2,3%	1,9%	1,9%	0,9%	2,2%	0,3%	3,1%
	Biceps Femoris Caput Longum	1,5%	2,0%	2,5%	1,4%	2,2%	4,8%	3,9%	1,8%	1,1%	1,8%	2,3%	1,1%	1,9%	1,1%	4,8%
	Gracilis	0,4%	0,4%	0,1%	0,7%	0,2%	0,2%	0,6%	0,3%	0,7%	0,2%	0,4%	0,2%	0,4%	0,1%	0,7%
	Rectus Femoris	4,1%	3,2%	2,9%	7,8%	2,2%	4,6%	3,2%	2,2%	4,0%	4,9%	3,9%	1,5%	3,6%	2,2%	7,8%
	Sartorius	2,3%	1,0%	0,2%	1,1%	0,3%	0,3%	1,1%	1,6%	1,9%	1,1%	1,1%	0,7%	1,1%	0,2%	2,3%
	Semimembranosus	1,7%	2,1%	1,5%	1,7%	0,6%	1,3%	0,3%	4,7%	0,3%	1,8%	1,6%	1,2%	1,6%	0,3%	4,7%
	Semitendinosus	2,3%	3,4%	1,9%	4,3%	1,8%	0,1%	2,4%	0,1%	1,1%	1,8%	1,9%	1,2%	1,9%	0,1%	4,3%
	Vastus Intermedius	0,4%	4,7%	0,4%	0,2%	4,9%	2,1%	0,0%	1,1%	1,1%	0,0%	1,5%	1,8%	0,7%	0,0%	4,9%
	Vastus Lateralis	1,3%	0,4%	0,3%	1,4%	1,9%	3,7%	4,2%	0,3%	0,4%	0,3%	1,4%	1,4%	0,9%	0,3%	4,2%
	Vastus Medialis	1,4%	0,4%	5,7%	2,1%	2,2%	1,0%	1,9%	3,4%	1,3%	0,3%	2,0%	1,5%	1,6%	0,3%	5,7%
	SUM	**20,9%**	**24,0%**	**24,7%**	**29,3%**	**25,0%**	**24,7%**	**26,9%**	**20,2%**	**19,3%**	**15,6%**	**23,1%**	**3,8%**	**24,3%**	**15,6%**	**29,3%**
Lower leg	Extensor Digitorum Longus	0,3%	1,2%	0,4%	1,0%	0,2%	0,7%	1,5%	1,0%	1,2%	0,4%	0,8%	0,4%	0,8%	0,2%	1,5%
	Extensor Hallucis Longus	0,1%	0,3%	0,3%	0,3%	0,2%	0,2%	1,4%	0,5%	0,1%	0,2%	0,3%	0,4%	0,2%	0,1%	1,4%
	Flexor Digitorum Longus	0,0%	0,1%	0,4%	0,0%	0,0%	0,1%	0,0%	0,9%	0,1%	0,0%	0,2%	0,3%	0,0%	0,0%	0,9%
	Flexor Hallucis Longus	1,3%	3,7%	3,7%	1,2%	2,7%	3,0%	1,3%	2,5%	1,3%	1,9%	2,3%	1,0%	2,2%	1,2%	3,7%
	Gastrocnemius Lateralis	11,8%	4,8%	7,1%	6,4%	5,6%	5,2%	0,7%	5,8%	11,6%	6,6%	6,6%	3,1%	6,1%	0,7%	11,8%
	Gastrocnemius Medialis	3,2%	4,0%	15,0%	13,3%	14,4%	6,0%	14,3%	8,5%	2,4%	19,1%	10,0%	5,6%	10,9%	2,4%	19,1%
	Peroneus Brevis	0,4%	0,0%	0,5%	0,7%	0,2%	0,1%	0,1%	0,3%	0,1%	0,1%	0,2%	0,2%	0,2%	0,0%	0,7%
	Peroneus Longus	0,2%	0,4%	0,3%	0,8%	0,1%	0,3%	0,9%	0,7%	0,5%	0,1%	0,4%	0,3%	0,4%	0,1%	0,9%
	Plantaris	0,1%	0,0%	0,1%	0,3%	0,3%	0,1%	0,4%	0,2%	0,4%	0,2%	0,2%	0,1%	0,2%	0,0%	0,4%
	Popliteus	1,0%	0,1%	0,3%	0,1%	0,1%	0,4%	0,8%	0,2%	0,5%	0,7%	0,4%	0,3%	0,4%	0,1%	1,0%
	Soleus	24,4%	27,0%	22,2%	11,0%	25,4%	27,9%	20,9%	19,5%	23,2%	15,1%	21,7%	5,0%	22,7%	11,0%	27,9%
	Tibialis Anterior	1,8%	1,8%	1,3%	3,0%	1,3%	1,6%	1,7%	1,1%	3,3%	4,2%	2,1%	1,0%	1,7%	1,1%	4,2%
	Tibialis Posterior	0,8%	1,0%	3,1%	0,3%	0,3%	0,4%	0,5%	1,3%	0,4%	1,5%	1,0%	0,8%	0,7%	0,3%	3,1%
	SUM	**45,4%**	**44,5%**	**54,6%**	**38,3%**	**50,7%**	**46,1%**	**44,6%**	**42,5%**	**45,1%**	**50,1%**	**46,2%**	**4,4%**	**45,2%**	**38,3%**	**54,6%**

Appendix 7.4: E_m metabolic energy consumption (J/kg)- Ten healthy subjects - Generic musculoskeletal models

		Subject														
		1	**2**	**3**	**4**	**5**	**6**	**7**	**8**	**9**	**10**	**mean**	**std**	**median**	**min**	**max**
Hip region	Gemellus Inferior	0,00	0,00	0,00	0,00	0,00	0,00	0,00	0,00	0,00	0,00	0,00	0,00	0,00	0,00	0,00
	Gemellus Superior	0,00	0,00	0,00	0,00	0,00	0,00	0,00	0,00	0,00	0,00	0,00	0,00	0,00	0,00	0,00
	Gluteus Maximus	0,15	0,20	0,21	0,09	0,05	0,24	0,12	0,23	0,17	0,18	0,16	0,06	0,17	0,05	0,24
	Gluteus Medius	0,44	0,29	0,22	0,32	0,23	0,35	0,34	0,23	0,32	0,28	0,30	0,06	0,30	0,22	0,44
	Gluteus Minimus	0,20	0,13	0,14	0,15	0,12	0,16	0,17	0,14	0,13	0,16	0,15	0,02	0,15	0,12	0,20
	Iliacus	0,18	0,09	0,10	0,13	0,09	0,13	0,17	0,13	0,09	0,12	0,12	0,03	0,12	0,09	0,18
	Obturator Externus	0,02	0,01	0,01	0,02	0,01	0,01	0,02	0,03	0,01	0,02	0,02	0,00	0,02	0,01	0,03
	Obturator Internus	0,00	0,01	0,01	0,01	0,01	0,01	0,01	0,02	0,01	0,01	0,01	0,00	0,01	0,00	0,02
	Pectineus	0,03	0,01	0,01	0,02	0,02	0,02	0,04	0,03	0,01	0,02	0,02	0,01	0,02	0,01	0,04
	Piriformis	0,02	0,01	0,02	0,01	0,01	0,02	0,01	0,03	0,02	0,02	0,02	0,01	0,02	0,01	0,03
	Psoas Major	0,14	0,08	0,08	0,11	0,07	0,11	0,14	0,13	0,08	0,11	0,10	0,02	0,11	0,07	0,14
	Quadratus Femoris	0,00	0,00	0,01	0,00	0,00	0,00	0,00	0,01	0,00	0,00	0,00	0,00	0,00	0,00	0,01
	Tensor Fasciae Latae	0,10	0,07	0,07	0,09	0,08	0,08	0,08	0,07	0,07	0,08	0,08	0,01	0,08	0,07	0,10
	SUM	**1,28**	**0,90**	**0,90**	**0,95**	**0,68**	**1,15**	**1,09**	**1,04**	**0,92**	**0,99**	**0,99**	**0,16**	**0,97**	**0,68**	**1,28**
Thigh region	Adductor Brevis	0,01	0,00	0,00	0,01	0,01	0,01	0,02	0,02	0,00	0,01	0,01	0,01	0,01	0,00	0,02
	Adductor Longus	0,07	0,03	0,02	0,06	0,03	0,05	0,10	0,07	0,03	0,05	0,05	0,02	0,05	0,02	0,10
	Adductor Magnus	0,12	0,07	0,08	0,10	0,23	0,03	0,09	0,12	0,08	0,07	0,10	0,05	0,08	0,03	0,23
	Biceps Femoris Caput Breve	0,07	0,05	0,04	0,06	0,04	0,05	0,06	0,06	0,06	0,06	0,05	0,01	0,06	0,04	0,07
	Biceps Femoris Caput Longum	0,12	0,12	0,10	0,09	0,05	0,09	0,10	0,06	0,12	0,13	0,10	0,03	0,10	0,05	0,13
	Gracilis	0,04	0,02	0,02	0,04	0,02	0,03	0,05	0,05	0,03	0,03	0,03	0,01	0,03	0,02	0,05
	Rectus Femoris	0,12	0,14	0,13	0,13	0,02	0,11	0,15	0,12	0,11	0,14	0,12	0,04	0,12	0,02	0,15
	Sartorius	0,25	0,13	0,13	0,16	0,08	0,18	0,21	0,16	0,14	0,18	0,16	0,04	0,16	0,08	0,25
	Semimembranosus	0,11	0,08	0,07	0,09	0,20	0,08	0,09	0,09	0,08	0,08	0,10	0,03	0,09	0,07	0,20
	Semitendinosus	0,12	0,08	0,06	0,08	0,21	0,06	0,09	0,08	0,07	0,08	0,09	0,04	0,08	0,06	0,21
	Vastus Intermedius	0,01	0,01	0,02	0,02	0,03	0,02	0,01	0,02	0,01	0,00	0,02	0,01	0,02	0,00	0,03
	Vastus Lateralis	0,14	0,20	0,30	0,28	0,41	0,25	0,21	0,22	0,12	0,04	0,22	0,10	0,22	0,04	0,41
	Vastus Medialis	0,05	0,06	0,09	0,09	0,13	0,08	0,07	0,07	0,05	0,02	0,07	0,03	0,07	0,02	0,13
	SUM	**1,22**	**0,99**	**1,07**	**1,21**	**1,45**	**1,03**	**1,25**	**1,15**	**0,89**	**0,89**	**1,11**	**0,17**	**1,11**	**0,89**	**1,45**
Lower leg	Extensor Digitorum Longus	0,01	0,01	0,01	0,01	0,01	0,01	0,01	0,01	0,01	0,01	0,01	0,00	0,01	0,01	0,01
	Extensor Hallucis Longus	0,01	0,00	0,00	0,01	0,01	0,00	0,01	0,01	0,01	0,01	0,01	0,00	0,01	0,00	0,01
	Flexor Digitorum Longus	0,01	0,00	0,00	0,00	0,00	0,00	0,01	0,00	0,00	0,00	0,00	0,00	0,00	0,00	0,01
	Flexor Hallucis Longus	0,05	0,01	0,01	0,02	0,01	0,03	0,04	0,02	0,01	0,02	0,02	0,01	0,02	0,01	0,05
	Gastrocnemius Lateralis	0,26	0,21	0,31	0,18	0,25	0,27	0,23	0,24	0,21	0,19	0,24	0,04	0,24	0,18	0,31
	Gastrocnemius Medialis	0,79	0,66	0,87	0,56	0,68	0,75	0,68	0,68	0,64	0,62	0,69	0,09	0,68	0,56	0,87
	Peroneus Brevis	0,01	0,00	0,01	0,00	0,01	0,00	0,01	0,00	0,00	0,00	0,00	0,00	0,00	0,00	0,01
	Peroneus Longus	0,04	0,01	0,01	0,02	0,02	0,03	0,03	0,02	0,02	0,02	0,02	0,01	0,02	0,01	0,04
	Plantaris	0,01	0,01	0,01	0,01	0,01	0,01	0,01	0,01	0,01	0,01	0,01	0,00	0,01	0,01	0,01
	Popliteus	0,01	0,01	0,01	0,01	0,01	0,01	0,01	0,01	0,01	0,01	0,01	0,00	0,01	0,01	0,01
	Soleus	0,84	0,87	1,10	0,53	1,00	0,82	0,80	0,84	0,69	0,69	0,82	0,15	0,83	0,53	1,10
	Tibialis Anterior	0,09	0,07	0,06	0,12	0,06	0,09	0,08	0,13	0,12	0,11	0,09	0,02	0,09	0,06	0,13
	Tibialis Posterior	0,09	0,00	0,01	0,03	0,01	0,04	0,07	0,02	0,01	0,04	0,03	0,03	0,02	0,00	0,09
	SUM	**2,22**	**1,86**	**2,41**	**1,49**	**2,09**	**2,08**	**1,98**	**1,98**	**1,74**	**1,72**	**1,96**	**0,25**	**1,98**	**1,49**	**2,41**

Appendix 7.5: E_m metabolic energy consumption (J/kg)- Ten healthy subjects - Subject-specific musculoskeletal models

		Subject														
		1	**2**	**3**	**4**	**5**	**6**	**7**	**8**	**9**	**10**	**mean**	**std**	**median**	**min**	**max**
Hip region	Gemellus Inferior	0,00	0,00	0,00	0,00	0,00	0,00	0,00	0,00	0,00	0,01	0,00	0,00	0,00	0,00	0,01
	Gemellus Superior	0,01	0,00	0,00	0,00	0,00	0,00	0,00	0,01	0,00	0,00	0,00	0,00	0,00	0,00	0,01
	Gluteus Maximus	0,29	0,28	0,20	0,24	0,32	0,13	0,15	0,47	0,31	0,28	0,27	0,09	0,28	0,13	0,47
	Gluteus Medius	0,51	0,30	0,25	0,32	0,34	0,43	0,36	0,34	0,35	0,39	0,36	0,07	0,35	0,25	0,51
	Gluteus Minimus	0,23	0,08	0,10	0,21	0,12	0,25	0,16	0,06	0,11	0,12	0,14	0,06	0,12	0,06	0,25
	Iliacus	0,25	0,10	0,17	0,20	0,09	0,16	0,21	0,16	0,09	0,15	0,16	0,05	0,16	0,09	0,25
	Obturator Externus	0,00	0,01	0,00	0,01	0,00	0,01	0,02	0,02	0,01	0,01	0,01	0,01	0,01	0,00	0,02
	Obturator Internus	0,04	0,05	0,02	0,01	0,00	0,03	0,00	0,02	0,02	0,01	0,02	0,02	0,02	0,00	0,05
	Pectineus	0,03	0,01	0,04	0,04	0,01	0,01	0,00	0,01	0,02	0,02	0,02	0,01	0,01	0,00	0,04
	Piriformis	0,06	0,02	0,04	0,01	0,00	0,03	0,04	0,05	0,08	0,05	0,04	0,02	0,04	0,00	0,08
	Psoas Major	0,10	0,07	0,01	0,11	0,06	0,10	0,11	0,22	0,06	0,15	0,10	0,05	0,10	0,01	0,22
	Quadratus Femoris	0,00	0,00	0,00	0,00	0,00	0,00	0,00	0,05	0,03	0,03	0,01	0,02	0,00	0,00	0,05
	Tensor Fasciae Latae	0,09	0,07	0,07	0,03	0,05	0,07	0,11	0,20	0,09	0,06	0,09	0,04	0,07	0,03	0,20
	SUM	**1,61**	**1,00**	**0,91**	**1,17**	**1,00**	**1,21**	**1,17**	**1,60**	**1,19**	**1,28**	**1,21**	**0,22**	**1,18**	**0,91**	**1,61**
Thigh region	Adductor Brevis	0,00	0,00	0,00	0,02	0,01	0,00	0,02	0,02	0,01	0,00	0,01	0,01	0,01	0,00	0,02
	Adductor Longus	0,02	0,02	0,03	0,07	0,05	0,02	0,15	0,02	0,03	0,02	0,04	0,04	0,03	0,02	0,15
	Adductor Magnus	0,11	0,10	0,34	0,14	0,23	0,15	0,09	0,14	0,13	0,03	0,15	0,08	0,14	0,03	0,34
	Biceps Femoris Caput Breve	0,13	0,08	0,02	0,08	0,06	0,09	0,13	0,01	0,08	0,07	0,08	0,04	0,08	0,01	0,13
	Biceps Femoris Caput Longum	0,07	0,06	0,11	0,05	0,09	0,20	0,16	0,08	0,04	0,07	0,09	0,05	0,07	0,04	0,20
	Gracilis	0,02	0,01	0,00	0,02	0,01	0,01	0,03	0,01	0,02	0,01	0,02	0,01	0,01	0,00	0,03
	Rectus Femoris	0,20	0,10	0,13	0,28	0,09	0,19	0,13	0,10	0,13	0,18	0,15	0,06	0,13	0,09	0,28
	Sartorius	0,11	0,03	0,01	0,04	0,01	0,01	0,04	0,07	0,06	0,04	0,04	0,03	0,04	0,01	0,11
	Semimembranosus	0,08	0,07	0,07	0,06	0,03	0,06	0,01	0,20	0,01	0,07	0,07	0,05	0,06	0,01	0,20
	Semitendinosus	0,11	0,11	0,08	0,15	0,07	0,01	0,10	0,01	0,04	0,07	0,07	0,05	0,08	0,01	0,15
	Vastus Intermedius	0,02	0,15	0,02	0,01	0,20	0,09	0,00	0,05	0,04	0,00	0,06	0,07	0,03	0,00	0,20
	Vastus Lateralis	0,06	0,01	0,01	0,05	0,08	0,15	0,17	0,01	0,01	0,01	0,06	0,06	0,03	0,01	0,17
	Vastus Medialis	0,07	0,01	0,25	0,08	0,09	0,04	0,08	0,15	0,04	0,01	0,08	0,07	0,07	0,01	0,25
	SUM	**1,00**	**0,76**	**1,09**	**1,06**	**1,03**	**1,02**	**1,11**	**0,87**	**0,64**	**0,59**	**0,92**	**0,18**	**1,01**	**0,59**	**1,11**
Lower leg	Extensor Digitorum Longus	0,01	0,04	0,02	0,04	0,01	0,03	0,06	0,04	0,04	0,02	0,03	0,02	0,03	0,01	0,06
	Extensor Hallucis Longus	0,01	0,01	0,01	0,01	0,01	0,01	0,06	0,02	0,00	0,01	0,01	0,01	0,01	0,00	0,06
	Flexor Digitorum Longus	0,00	0,00	0,02	0,00	0,00	0,00	0,00	0,04	0,00	0,00	0,01	0,01	0,00	0,00	0,04
	Flexor Hallucis Longus	0,06	0,12	0,16	0,04	0,11	0,13	0,05	0,11	0,04	0,07	0,09	0,04	0,09	0,04	0,16
	Gastrocnemius Lateralis	0,56	0,15	0,31	0,23	0,23	0,21	0,03	0,25	0,39	0,25	0,26	0,13	0,24	0,03	0,56
	Gastrocnemius Medialis	0,15	0,13	0,66	0,48	0,59	0,25	0,59	0,37	0,08	0,72	0,40	0,23	0,42	0,08	0,72
	Peroneus Brevis	0,02	0,00	0,02	0,02	0,01	0,01	0,00	0,01	0,00	0,00	0,01	0,01	0,01	0,00	0,02
	Peroneus Longus	0,01	0,01	0,02	0,03	0,00	0,01	0,04	0,03	0,02	0,00	0,02	0,01	0,01	0,00	0,04
	Plantaris	0,00	0,00	0,00	0,01	0,01	0,00	0,02	0,01	0,01	0,01	0,01	0,01	0,01	0,00	0,02
	Popliteus	0,05	0,00	0,01	0,00	0,00	0,02	0,03	0,01	0,02	0,03	0,02	0,01	0,01	0,00	0,05
	Soleus	1,16	0,86	0,98	0,40	1,04	1,15	0,86	0,84	0,77	0,57	0,86	0,23	0,86	0,40	1,16
	Tibialis Anterior	0,08	0,06	0,06	0,11	0,05	0,07	0,07	0,05	0,11	0,16	0,08	0,03	0,07	0,05	0,16
	Tibialis Posterior	0,04	0,03	0,13	0,01	0,01	0,02	0,02	0,06	0,01	0,05	0,04	0,04	0,03	0,01	0,13
	SUM	**2,16**	**1,42**	**2,41**	**1,38**	**2,08**	**1,90**	**1,84**	**1,83**	**1,50**	**1,88**	**1,84**	**0,31**	**1,86**	**1,38**	**2,41**

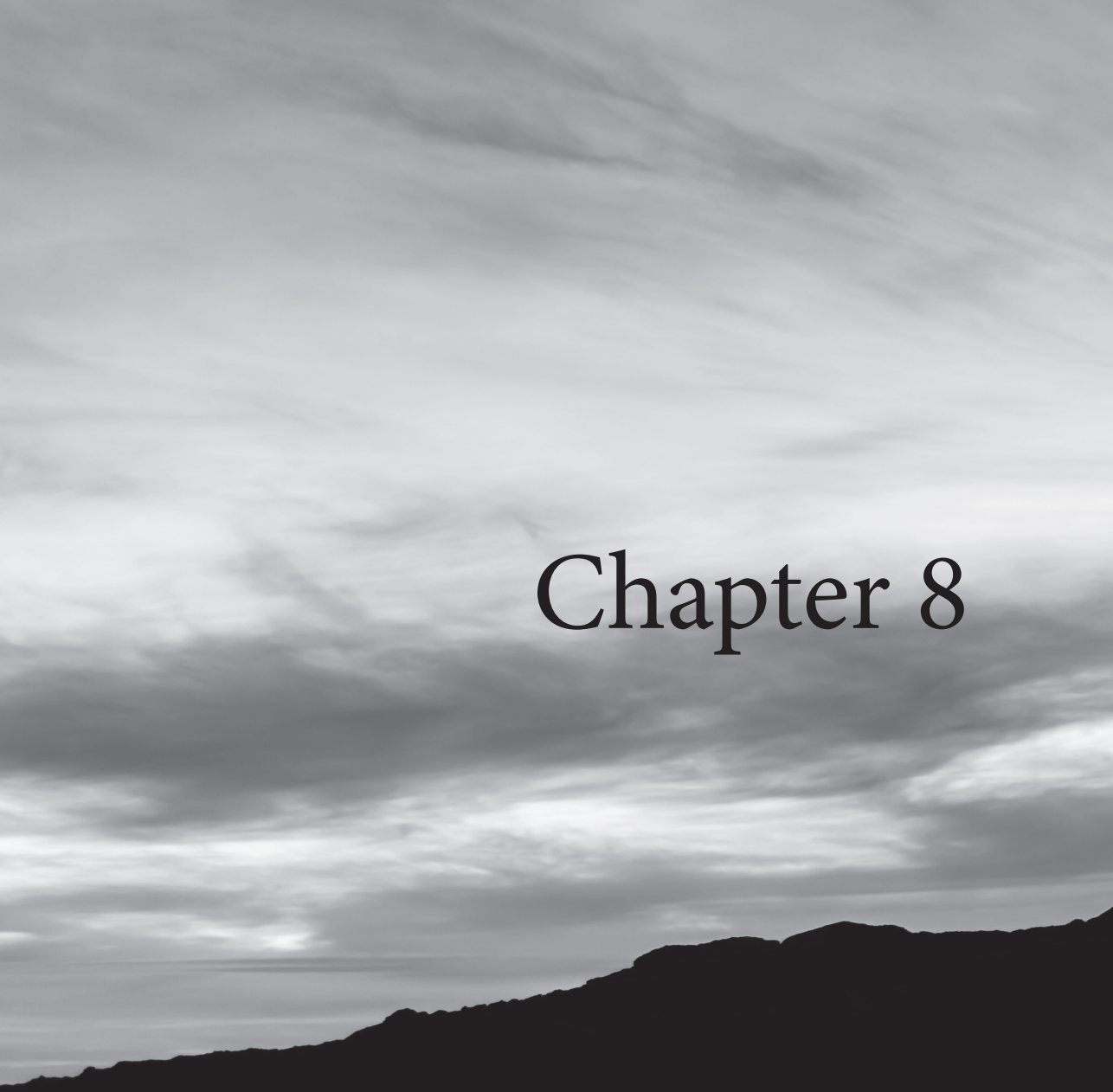

Chapter 8

Summary and General Discussion

Summary of key findings: Part I

The first goal of this thesis was to provide insight into the current status and challenges regarding functional outcome after three different orthopedic interventions: total hip arthroplasty, triple innominate osteotomy, and limb salvage surgery of the lower limb. In **chapter 2**, we aimed to answer the question 'What is the current level of functional outcome after total hip arthroplasty, assessed with objective measurement methods, during gait and gait-related activities of daily living?'. To this end, we performed a systematic review of the literature using broad search terms in the MEDLINE database. The inclusion criteria were as follows: primary osteoarthritis as indication, comparison with healthy controls or comparison between the operated and the non-operated limbs, and a follow-up period of at least six months after surgery. The search yielded 2177 citations, of which 35 articles were included. It was found that in the operated hip, patients had reduced sagittal range of motion, peak extension, sagittal power generation, abduction moment, and external rotation moment compared to healthy controls during gait. Most of these findings (sagittal hip range of motion, hip abduction moment, hip external rotation moment) could not be attributed to a difference in walking speed, as they were also present in studies that matched walking speed between the groups. Stair ascent and descent did not magnify the impairments found during level walking, although deficits in hip kinetics in all three planes were present during ascent. One of the most consistent findings during walking and stair ascent was a lower hip abduction moment, which also appeared to be independent of the surgical approach.

In **chapters 3a and 3b**, we sought to answer the question 'To what extent is the functional outcome in terms of gait and lower limb strength after triple innominate osteotomy and total hip arthroplasty with femoral shortening similar to healthy controls and comparable between the limbs?'. In **chapter 3a**, the long-term effects of triple innominate osteotomy on gait and muscle strength were investigated. Gait analyses and isometric strength tests were performed in twelve women (age 34±12 years) who had undergone unilateral triple innominate osteotomy (80±18 months before the study). Results were compared with an age- (33±10 years) and gender-matched control group of eight healthy women. In general, the gait of women who had undergone triple innominate osteotomy was similar to their healthy peers, but subtle differences were found between the operated and non-operated limbs. The abduction moment pattern during stance was significantly different between the operated and non-operated limbs. Furthermore, the muscle strength measurements revealed that the abduction strength in both limbs was significantly reduced compared to controls. We concluded that the patients generally recovered well from their operation in terms of gait, with only small asymmetries detected between the limbs. The bilateral abductor strength deficit implies that the patients walked at a higher percentage of their maximum capacity. This may eventually lead to alterations in gait when the patients become fatigued, which is relevant for these young patients who may still want to engage in sports or other strenuous activities for many years to come.

In **chapter 3b**, we aimed to quantify the functional outcome of total hip arthroplasty with acetabular reconstruction and femoral shortening in congenital hip dysplasia patients. Gait analyses and isometric strength tests were performed in seven women after surgery (age: 39±13 years, time post-surgery: 45±52 months) as well as in seven healthy peers (age: 31±10

years). It was found that the adduction angle in the operated limb was significantly larger than in the non-operated limb. Furthermore, the abduction moment was significantly lower compared to controls. In terms of strength, the operated limb was significantly weaker compared with controls in hip abduction, hip extension, knee flexion and knee extension. The operated limb was weaker than the non-operated limb in all measurements, except for knee flexion. We concluded that the observed gait deviations in the frontal plane point to Trendelenburg's sign to compensate for abductor weakness; this finding was supported by the abductor strength measurements. The potential for improving the abductor strength and gait is unclear, since structural changes in the muscle tissue may have taken place during the many years of functioning at non-optimal lengths before the surgery.

In **chapter 4**, the purpose was to answer the question 'Are orthopedic oncologists able to accurately predict the functional effects of limb salvage surgery in the lower limb?'. To this end, 23 patients (between six months and ten years after surgery) and five independent orthopedic oncologists completed the Toronto Extremity Salvage Score (TESS) and the RAND-36 physical functioning subscale (RAND-36 PFS). The surgeons made their predictions based on patient case descriptions (including MRI scans) that reflected the pre-operative status. We found "very poor" to "poor" correlations between patient-reported outcomes and surgeon-predicted outcomes on both scales, with a tendency for the surgeons to underestimate the patient-reported functional outcome. Furthermore, the inter-surgeon agreement on most RAND-36 PFS questions was "poor," indicating that there was a high variability in the predictions to the questions. Thus, it was difficult for the participating surgeons to accurately predict the patient-reported functional outcome of limb salvage surgery. This warrants research into objective tools that could help the orthopedic oncologists in the decision making process. These tools could include musculoskeletal models, which prospectively calculate whether the patient will have enough residual muscle strength after the operation to perform activities of daily living.

Summary of key findings: Part II

The second goal of this thesis was to explore the possibilities of FDG-PET in providing fundamental insight into the musculoskeletal system, and its potential as a supporting technique to help in solving some of the identified challenges surrounding functional outcome. In **chapter 5**, the aim was to answer the question 'Which muscles in the lower limb are of primary importance during walking?'. In that chapter, positron emission tomography (PET) with [^{18}F]-fluorodeoxyglucose (FDG) was used, which is a novel methodology based on the increased uptake of glucose and FDG in exercising muscles. Ten healthy subjects walked on a treadmill at self-selected comfortable walking speed for 85 min, 55 min before and 30 min after intravenous injection of 50 MBq FDG. Thereafter, a PET/CT scan of the lower limb was made. The three-dimensional contours of 39 muscles in the left lower limb were semi-automatically determined from magnetic resonance imaging scans, using newly developed advanced algorithms in the Mimics Innovation Suite (Materialise N.V., Leuven, Belgium). After non-rigidly registering the magnetic resonance imaging to the computerized tomography scans, the muscle contours were superimposed on the PET scans. We found that the most active muscles during walking were the soleus, gluteus maximus, vastus lateralis,

gastrocnemius medialis, and adductor magnus. The range of FDG uptake values was large between subjects, including in some of the most important muscles involved in walking (e.g., soleus, gluteus medius, gastrocnemius medialis). The most active muscles identified in the study generally corresponded well with literature that used other methods, such as inverse dynamics and electromyography. Several muscles (e.g., adductor magnus, gluteus minimus) that have previously remained difficult to measure with traditional methods (e.g., surface EMG) because of their large size, or their deep-lying position in the body, were found by FDG-PET to be very active during gait. Compared with traditional methods used in the field, which involve measuring the FDG uptake in only a single slice of the scan, the three-dimensional analysis that was performed yielded different results in many of the most active muscles. This illustrates the added value of our extensive three-dimensional analysis of muscle activity with FDG-PET.

In **chapter 6**, the questions we aimed to answer were 'Are the muscles in the lower limb active symmetrically during walking?' and 'Is muscle activity homogeneous or region-specific during walking?'. The methodology was largely the same as in chapter 5, with the exception that the right lower limb was also segmented in this study. The lower leg muscles exhibited particularly large asymmetries (e.g., median 42% asymmetry in the gastrocnemius medialis). Asymmetries were also identified in the gluteus medius (15% asymmetry) and gluteus minimus (30% asymmetry), whereas the uptake in the thighs was relatively symmetrical between the limbs (<6% asymmetry). The FDG distribution was not distributed normally; most voxels had a relatively low standardized uptake value (SUV), and a minority of voxels had a relatively high SUV. The areas of higher FDG uptake were not distributed randomly throughout the muscles, but were clustered together in virtually all muscles. The findings of the study challenge the common assumption that muscle activation between the limbs is symmetrical in healthy subjects. The clustering of voxels with high uptake indicates that even in this prolonged repetitive task, certain regions of muscles contribute more to walking than other regions.

In **chapter 7**, we sought to answer the question 'Can FDG-PET be used to validate healthy subject-specific musculoskeletal models?'. Validation of musculoskeletal models is an important but challenging step towards their application in a clinical setting, such as in surgical planning. The FDG-PET methodology presented in chapters 5 and 6 could be a solution to this problem. Subject-specific musculoskeletal models of the same ten healthy subjects were constructed, using advanced techniques such as muscle anatomy segmented from MRI scans and functional scaling based on joint strength measurements. The muscles that were most active during walking as identified in chapter 5 (soleus, gluteus maximus, vastus lateralis, gastrocnemius medialis, and adductor magnus) were also generally the most active muscles in the models in terms of the amount of energy used. The measured muscle glucose uptake from the PET scan in each individual subject exhibited 'good' to 'very good' correlations with the model estimate of metabolic energy consumption (Spearman's ρ = 0.87±0.04, Pearson's r = 0.77±0.10). When the uptake values of each muscle were averaged over the ten subjects, higher correlations were found (Spearman's ρ = 0.96, Pearson's r =0.91). We concluded that FDG-PET appears to be a valuable complimentary method in addition to electromyography for validating musculoskeletal models.

General Discussion

This general discussion reflects on the work described in this thesis. It will also be explored how the findings further enhance our understanding of how the musculoskeletal system behaves in healthy persons, and in patients treated with the selected orthopedic interventions. Furthermore, limitations that should be considered are discussed, and directions for future research will be highlighted. Finally, the current status and potential future role of musculoskeletal modeling in evaluating and predicting functional outcome after orthopedic surgery will be discussed.

Part I: New perspectives on functional assessment in orthopedic surgery

Gait and hip muscle strength after total hip arthroplasty and triple innominate osteotomy

After each of the hip surgeries discussed in chapters 2, 3a, and 3b, a common observation was that the hip kinetics in the frontal plane deviated from healthy controls, or from the non-operated hip. Lifting the foot on the non-operated side to perform swing removes the support for that side of the pelvis, as the body weight is medial to the supporting (operated) hip. This leads to an adduction moment that needs to be stabilized by the hip abductors (i.e. primarily the gluteus medius and minimus). We indeed identified the hip abductors as being weaker than controls after triple innominate osteotomy and total hip arthroplasty with femoral shortening. The consequences of a reduced hip abduction strength and abduction moment during gait may not be immediately apparent in the frontal plane hip kinematics. Based on the studies in this thesis, the severity of the abduction deficit appeared to scale with the severity of the disease, and the extent of the surgical intervention. In the patients who underwent triple innominate osteotomy, no deviations in frontal plane hip kinematics from controls were found. After total hip arthroplasty for primary osteoarthritis, out of a total of 35 studies, only four studies reported frontal plane hip kinematics (Beaulieu et al. 2010; Bennett et al. 2008; Madsen et al. 2004; Varin et al. 2013). Of those, only two reported hip adduction angles, and both found it reduced compared to controls (Beaulieu et al. 2010; Varin et al. 2013). Finally, the most severely affected patients, who underwent total hip arthroplasty with femoral shortening, exhibited increased adduction angles during gait compared to the contralateral side, indicative of pelvic drop. Recommendations that can be made for all three patient categories are that rehabilitation protocols, surgical approaches, and musculoskeletal modeling efforts should focus on the hip abductors. The abductors are already focused on in rehabilitation protocols for all three types of hip surgery, but this may need to be intensified if the patients are to reach normal hip kinetics.

When it comes to abductor muscle strength, even in the patients who underwent triple innominate osteotomy and were affected the least by abduction deficits during gait, the abductor muscles were weaker bilaterally by about 35% compared to controls. Studies that used musculoskeletal simulations have found that in some healthy subjects, gait deviations

emerged already at 60% loss of muscle strength of the gluteus medius (van der Krogt et al. 2012). Although the abductor weakness that we identified in our study affected gait only mildly, this does imply that patients walked at a higher percentage of their capacity. As a result, they may alter their gait in a potentially harmful way when walking long distances, or as they get older and their muscles get weaker. Anecdotally, almost all women who had undergone triple innominate osteotomy indicated during the measurement session that they felt tired sooner than their family and friends, when shopping or going for a walk. Given that the abductor weakness was bilateral in our patient cohort (which was operated unilaterally), it is unlikely that the weakness in that muscle group was due to soft tissue damage inflicted during the operation itself. Instead, it might be due to a general reduction in activity level in the patients compared to their healthy peers. To test this hypothesis, future work could focus on also measuring general activity level in both groups; for example, using wearable activity monitors (Jantunen et al. 2016; Sprint et al. 2016).

For patients suffering from congenital hip dysplasia, pain and limitations in activities of daily living are more severe than for patients with primary osteoarthritis or with earlier stages of hip dysplasia, especially in the case of high luxation of the femoral head. In that case, the pre-operative anatomical deformity is much larger, and the muscles around the hip, particularly the abductors, have been functioning at non-optimal lengths for years. Therefore, the expected functional outcome after total hip arthroplasty with acetabular reconstruction and femoral shortening can be expected to be less good than for the other patients. Our results for frontal plane hip kinetics are in line with the limited literature that exists on the subject (Lai et al. 2001). The other studies that have been published in this field have been limited to spatiotemporal parameters (Kyriazis et al. 2002), sagittal plane kinematics (Marangoz et al. 2010), or pre-operative gait analysis (Romano et al. 1996). Future work in this patient group could focus on prospectively including patients with hip dysplasia and tracing how their gait develops from before until after total hip arthroplasty with femoral shortening, in order to fully map causes for gait abnormalities and to develop targeted muscle strengthening exercises or gait retraining. We remark that nowadays, in the Netherlands and most other countries in the western world, there is extensive screening for congenital hip dysplasia in infants, and the disease can be effectively treated during infancy using a brace, which has greatly reduced the prevalence of this condition in adulthood. Still, the treatment with a brace is not always successful, and patients with an immigration background were frequently not screened as babies and left untreated. For the patients that suffer from the consequences of untreated congenital hip dysplasia, it is perhaps even more important than in primary osteoarthritis patients to restore functional outcome to the highest possible level, since they are, on average, much younger (usually 35-55 years) than patients who undergo surgery for primary osteoarthritis (usually above 60 years). Aiming to achieve the optimal functional outcome for every patient is not an easy task, as the goal of achieving normal walking mechanics may be unattainable for many patients. Factors including surgical approach (Madsen et al. 2004) and persisting pre-operative impairments (Bennett et al. 2008; Foucher et al. 2007; Lugade et al. 2010) may predispose patients to restricted possible outcomes.

Influence of surgical approach

Any orthopedic intervention on the hip inherently includes some form of temporary or permanent damage to muscles, tendons, or ligaments. Therefore, it is reasonable to anticipate that the surgical approach has some effect on the objectively measured gait parameters assessed in this thesis, and that this effect might be different for each surgical approach. Surprisingly, this could not be firmly established. For example, in total hip arthroplasty for primary osteoarthritis (chapter 2), studies that included patients operated with the potentially abductor-harming lateral or anterolateral approach did not find reduced abductor moments more consistently than studies that used the posterior approach (which spares the abductor musculature) (e.g., Beaulieu et al. 2010; Mont et al. 2007; Perron et al. 2000; Varin et al. 2013). Similarly, studies that included patients operated with the posterior approach (in which the external rotators are released) did not find reduced external rotation moments more consistently than the ones that used other approaches (e.g., Beaulieu et al. 2010; Foucher et al. 2011). Firm conclusions cannot be drawn on this basis, however, since the magnitude of differences between patients and controls was not taken into account in chapter 2. To firmly establish the effect of each surgical approach on post-operative kinematics and kinetics, several dedicated studies that included patients operated with different surgical approaches have been performed (Foucher et al. 2011; Kiss et al. 2012; Leuchte et al. 2007; Madsen et al. 2004). All of those studies and several clinical studies (e.g., Graves et al. 2016; Leunig et al. 2013) that used patient-reported outcomes found no or small differences between approaches. For triple innominate osteotomy and Ganz's osteotomy, which are functionally rather similar osteotomies but which employ different approaches to the hip, the surgical approach also did not appear to significantly influence the post-operative functional outcome as measured by gait analyses (Janssen et al. 2009; Karam et al. 2011; Pedersen et al. 2006; Sucato et al. 2010). Thus, the surgical approach to the hip appears to play only a modest role in the recovery of gait after surgery. In spite of this seemingly limited effect on functional outcome, new approaches to the hip are still being investigated for various reasons. For example, a new medial inguinal approach for total hip arthroplasty in the treatment of primary osteoarthritis was presented at the International Society for Technology in Arthroplasty 2016 (Lucente 2016). The new approach led to reduced surgery times, lower blood loss, lower complication rates, significantly faster recovery times, and a more aesthetically pleasing scar compared to conventional approaches. Moreover, the muscles of the hip were claimed to remain totally unharmed. However, long term follow-up and functional outcome data were not yet available. It will be interesting to see how this particular approach and other surgical approaches and assistive techniques develop in the coming years, and whether positive effects on objective functional outcome parameters can be demonstrated.

Persistence of pre-operative deviations

The gait deficits that we identified in chapters 2, 3a and 3b might be remnants of the gait pattern that developed pre-operatively as a result of pain-avoiding compensation strategies (Beaulieu et al. 2010; Foucher et al. 2007; Foucher et al. 2011). Specifically, several of the most important deficits identified in chapter 2, the sagittal range of hip motion, and the abduction and external rotation moments about the operated hip after total hip arthroplasty

have previously been found to be persisting from before the operation (Foucher et al. 2007). Patients may not be able to reverse the losses of muscle strength due to disuse to avoid pain preceding the surgery, a period which takes several years in most cases. It has indeed been shown that although hip muscle strength (abduction, extension, and flexion) increases significantly around the operated hip after one year compared to the pre-operative situation, it still does not reach the level of the contralateral side (Shih et al. 1994). Because of this persistence, increased muscle strengthening regimens, both before and after surgery, appear justified. In more severely affected patients, such as those with congenital hip dysplasia, one might expect gait to be worse pre-operatively than post-operatively; for example, in the form of an increased adduction angle and a reduced abduction moment. However, this is not necessarily the case: some studies found that some of their less severely affected patients actually had an *in*creased hip abduction moment compared to controls (Romano et al. 1996). We can only speculate about the notion that this might be explained by the progression of the disease over the years. Initially, patients may attempt to achieve as much joint surface area in the affected hip as possible, through an increased hip abduction moment leading to less pelvic drop. Then, as they develop luxation and it becomes more and more painful to produce a high abduction moment, they may gradually be forced to switch to a different strategy of lower abduction moments and resulting pelvic drop, and higher adduction angles.

Musculoskeletal modeling of hip patients

When looking at the current level of functional outcome achieved by hip patients, as shown in chapters 2, 3a, and 3b, it is important to remark that, in general, the patients were doing well. With total hip arthroplasty being a very successful surgery in general (Learmonth et al. 2007), even for severely affected patients with hip dysplasia (Colo et al. 2016), and triple innominate osteotomy being an intervention that leads to 'very good' or 'excellent' outcomes (de Kleuver et al. 1997; Janssen et al. 2009), one may wonder if there is room for added value through supportive analyses such as obtained through musculoskeletal modeling. What might such analyses yield that can improve the functional status of the patients post-operatively? Recommendations on the surgical approach to the hip could be one, but this has only a modest role in recovery, and this is something that depends on the preference of the surgeon (in primary osteoarthritis), or that is largely dictated by the surgical requirements of the intervention (in patients with hip dysplasia), such as exposure of the joint. Recommendations on the optimal location of the reconstructed center of rotation of the hip, the femoral offset and the degree of anteversion could be another aspect to analyze with musculoskeletal models. For example, more favorable abductor moment arms could be achieved by medialization of the reconstructed acetabulum and choosing an implant with a larger femoral offset. It is important to note that even such seemingly simple recommendations are difficult to make, as there are also downsides associated with medialization, including additional loss of medial acetabular bone stock, increased joint reaction forces, and proprioceptive changes (Lenaerts et al. 2008; Terrier et al. 2014). This trade-off that might not pay off in each patient (Terrier et al. 2014), coupled with the already very good outcomes observed in patients after total hip arthroplasty and triple innominate osteotomy, limit the added value that musculoskeletal models can bring. Furthermore, the group of patients who could potentially benefit most from improved functional outcome and from elaborate musculoskeletal analyses (the severely affected patients with hip dysplasia)

is, as mentioned previously, becoming smaller and smaller due to improved screening and treatment in infancy. Therefore, it is reasonable to conclude that musculoskeletal models probably have a modest added value in hip patients, and that their value might be larger in other patient categories.

Towards improving the functional outcome of limb salvage surgery

In spite of considerable progress in the treatment of patients suffering from sarcoma of the lower limb (Veth et al. 2003), patients who have undergone limb salvage surgery will generally have a reduced level of functioning of the affected limb as a result of resections of bone, muscle, nerve, or combinations of those. This was not different in the population examined in this thesis, as measured by the Toronto Extremity Salvage Score (TESS) and the RAND-36 physical functioning subscale (RAND-36 PFS) scales. The most important finding was that the post-operative level of functioning was difficult to predict, even for experienced orthopedic oncologists. The low level of inter-surgeon agreement on most questions of the RAND-36 PFS indicates the high variability in the surgeons' predictions, and suggests that also treatment decisions may vary between surgeons. Of course, this can be expected for treating almost any disease with a low prevalence, and even more so for limb salvage surgery, which is one of the most complicated orthopedic interventions. Nonetheless, the poor predictive capability and the variations identified between surgeons warrant future work, which could proceed along several avenues. The first would be to also take general activity level and expected adaptive capacity of the patient into account when predicting functional outcome. This is challenging to quantify, but it is known to play a large role in functional recovery (De Visser et al. 2000). Second, instead of measuring functional outcome with questionnaires, more comprehensive objective means (such as gait analysis) could be employed as an additional outcome measure to reduce the inherent subjectivity in questionnaires (Lindemann et al. 2006). Indeed, until now, it is still unknown if the questionnaires we used are related to objective gait parameters. Third, tools could be developed that aim to assist the orthopedic oncologists in the decision making process, such as musculoskeletal models (Fluit 2015). Musculoskeletal models could be a powerful tool to analyze the complex biomechanical problems associated with limb salvage surgery, and provide a pre-operative prediction of the functional effects of the surgery or identify target areas for rehabilitation. It can be expected that image-based, patient-specific musculoskeletal models are more suitable than generic models to study the functional outcome after limb salvage surgery, due to the wide variability in location and shape of the tumors. Fluit et al. (2015) performed explorative work in this area. They described a method to develop patient-specific musculoskeletal models for patients after limb salvage surgery, based on image data from MRI, combined with information from the surgical log (Figure 8.1).

The models were animated using traditional inverse dynamics and a novel predictive gait model (Fluit et al. 2014), and subsequently validated using marker trajectories (for the kinematics) and electromyography (for the muscle activity levels) obtained post-operatively. The patient-specific models indeed tended to be more accurate for predicting kinematics and muscle activity levels than generic models of the patients (Fluit 2015). However, there is still a lot of work to be done before these models can become more widely used. For instance, although work has been done to investigate which parameters of the

musculoskeletal models are most crucial to characterize (e.g., tendon slack length, optimal fiber length, origin and insertion points of prime movers, and maximal isometric muscle force (Carbone 2016; Carbone et al. 2012; Van Campen et al. 2014)), these parameters are still hard to truly personalize. They require detailed (i.e. lengthy) MRI scans with specific scan settings that allow the geometric parameters to be extracted, and extensive (thus burdensome) measurements of isometric maximum joint torques for the measurement of muscle parameters. Once those measurements are obtained, analyzing the data and the personalization process still takes a lot of time, even in the case of a healthy person. When creating a musculoskeletal model of a patient post-operatively and using that model to make predictions, assumptions about what will happen during the intervention may play an even larger role than the most crucial parameters for healthy persons. Therefore, future work is needed to disentangle the effects of step-by-step personalization of the musculoskeletal models on the predicted functional outcome, and the supporting role that these models might play in the treatment decision making process for limb salvage surgery. Such work would need to include extensive validation measurements before it can be applied to aid in clinical decision making. Part II of this thesis focused on one of the most promising new validation techniques.

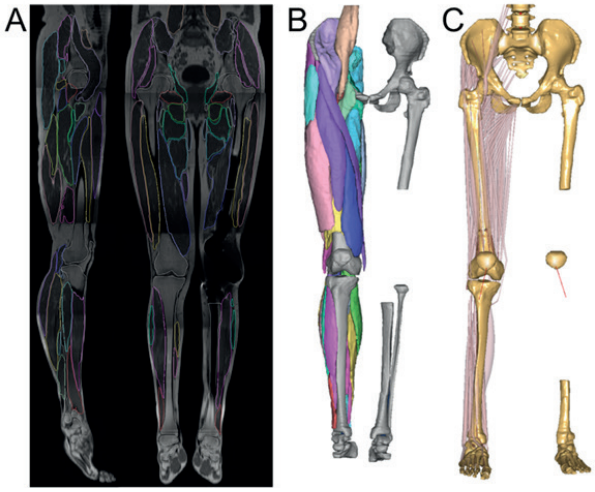

Figure 8.1. A: Example of the results of semi-automatic segmentation of muscles from MRI scans. B: Three-dimensional visualization of the segmented bones and muscles. C: Image-based post-operative subject-specific musculoskeletal model that has been based on the segmented bones and muscles from the MRI scan and the surgical log. Only the muscles of the right limb are shown.

Part II: New perspectives on functional assessment in musculoskeletal research

Muscle activity during walking measured using FDG-PET: Implications for research

Over the course of the last two decades, the use of FDG-PET in studying the musculoskeletal system during various activities has increased. This is not surprising given some major benefits of this technique, such as the ability to investigate a large number of muscles simultaneously (including the muscles that lie deep in the body that are almost inaccessible with electromyography), the ability to measure muscular activity in entire muscles rather than a limited (often superficial) region, and the freedom of movement for participants to perform a task unhindered by wires or by physical limitations of an experimental area. In spite of these benefits, up to now, studies that used FDG-PET have been limited to examining FDG uptake in discrete slices of the muscle (e.g., Fujimoto et al. 2003; Gondoh et al. 2009; Oi et al. 2003; Shimada et al. 2009a; Shimada et al. 2009b; Shimada et al. 2007). The reason for this is twofold: first, segmentation of the muscles to allow for quantification of FDG uptake in every individual muscle was labor-intensive. To illustrate this, assuming analysis of a single slice per muscle, if one wants to segment all ~40 muscles (excluding the feet) in both the left and right lower limbs in ten subjects, there are already 800 muscle boundaries that need to be drawn manually. If entire muscle volumes are to be examined, and assuming a slice thickness of 2 mm, there would be well over 100.000 regions of interest to manually delineate. Second, and more importantly, it was assumed in the past that the FDG uptake measured in a discrete slice containing part of the muscle would be representative for the uptake in the entire muscle. The work presented in this thesis contributed to this knowledge by showing that this is not the case. There were several muscles that are important for walking (e.g., the gluteus medius and minimus and the thigh muscles) in which the uptake was grossly under or overestimated when merely examining single slices. This highlights how novel image analysis techniques can be utilized to advance our understanding of the musculoskeletal system, and it also opens doors to a better understanding of patients with different pathologies.

Clinical applications

Although FDG-PET has mainly been applied in a research context in healthy persons, the prospect of using the technique in patients with different pathologies is appealing. The technique offers the perspective of being able to show which muscles are activated less than 'normal', and which are more active and might be compensating for other muscles or for underlying pathology. This would be useful information; for example, in patients who have undergone joint replacement, who have had an anterior cruciate ligament reconstruction, or who are suffering from neurological disease. The findings obtained through FDG-PET could provide clues for therapies targeted at reducing those differences from 'normal' that could be harmful. It could be used pre- and post-operatively to evaluate the adaptation of the musculature before and after certain surgical interventions with a level of inter- and intramuscular detail that is higher than possible with other methods. For example, the asymmetric activation of the individual muscles in the quadriceps could be measured

before and after anterior cruciate ligament reconstruction to determine the success of the surgery, since such asymmetries are known to exist in the quadriceps as a whole (Lepley 2015; Palmieri-Smith et al. 2015). Similarly, FDG-PET could also be used for examining the effects of different rehabilitation protocols. For the patients who have undergone limb salvage surgery as discussed in part I of this thesis, FDG-PET analysis could increase our fundamental understanding of muscle adaptation after such an extensive intervention. For example, it is clinically known that if the gastrocnemii are released from the femur in case of a tumor in the distal femur area, they partially re-attach themselves onto the muscle belly of the soleus. This fascinating adaptive capacity of the musculoskeletal system could be studied in more detail with FDG-PET. The mechanisms by which the adaptations occur and to what degree the gastrocnemii and other muscles around the knee are activated after surgery are largely unknown, and this knowledge could aid the pre-surgical planning process. It could also be used in the validation of predictions made by musculoskeletal models. The measurement protocol may need to be shortened if patients are to be studied. Note that other techniques, such as electromyography, could also be used to measure muscle adaptations after surgery; but in the case used as an example, it might prove difficult to distinguish the signal of the reattached gastrocnemii from that originating from the cranial part of the soleus due to crosstalk.

The role of FDG-PET in validating musculoskeletal models

In spite of significant progress in the capabilities of musculoskeletal models over the past decades, like any other type of model, they still rely on simplifications and assumptions. These include, amongst others, the behavior of musculotendon units (Zajac 1989), the cost function used to calculate muscle activity (Praagman et al. 2006) and, for healthy subjects, the symmetry between the left and right limbs with regard to both anatomy and function (Ackermann et al. 2010; Anderson et al. 2001). The work presented in chapters 6 and 7 of this thesis demonstrated that there was a wide variety of FDG uptake between subjects, between the left and right limb, and even within muscles. This has implications for musculoskeletal modeling in that the models will need to reflect those uptake differences between subjects, limbs, and within muscles as well as possible. It seems obvious that most of the variety will never be possible to predict using generic musculoskeletal models, and that subject-specific parameters such as muscle volumes, segment lengths, joint models, muscle compartments, fiber types, and perhaps even the way a person moves, will need to be taken into consideration when constructing the models. The work presented in chapter 8 aimed to determine if the simulated muscle activity of generic and subject-specific musculoskeletal models would correspond with the FDG uptake from PET on the level of the entire limb, segments (pelvis, thigh and lower leg), and muscles. In the entire limb, the predicted metabolic power (3.82 W/kg for generic models and 3.73 W/kg for subject-specific models) was similar to measured values from the literature (4.67 W/kg (Inman et al. 1981)), taking into account the fact that the measured value included the entire upper body and resting metabolism of the whole body. The W/kg-values could not be directly compared to the FDG-PET measurements, but indicate that the methodology of calculating power with the muscle model introduced in chapter 8 appears to be valid. On the level of lower limb segments, the measured percentage FDG values and simulated percentage Energy values of both generic and subject-specific models corresponded reasonably well, at 45-50% in the lower leg, and

20-30% in both pelvis and thigh. On the level of muscles, the most important observation was that the most active muscles, as identified in chapter 6 (soleus, gluteus maximus, vastus lateralis, gastrocnemius medialis, and adductor magnus), also tended to be the most active ones in the model predictions for most subjects. Furthermore, correlations calculated taking all muscles into account and averaged over all subjects were high (Spearman's ρ = 0.91, Pearson's r = 0.84 for generic models, ρ = 0.95, Pearson's r = 0.92 for subject-specific models). Whilst these correlations are certainly very high and show the potential of FDG-PET for the validation of musculoskeletal models, there are still a few important limitations to consider when interpreting the results.

The first is that correlations were low in the thigh (mean ρ = 0.24±0.22, r = 0.24±0.26 for generic models, mean ρ = 0.20±0.31, r = 0.18±0.27 for subject-specific models). The activity in the vasti was generally underestimated by the models, whereas that of the rectus femoris was overestimated. This might have been due to the type of knee joint in the model, which was a simple hinge joint that did not require any lateral stabilization from the vasti. A second limitation is that, whilst the models were 'subject-specific' in terms of anatomy and functional scaling based on dynamometry, they were not made subject-specific in terms of muscle physiology. One of the factors that plays a role in muscle glucose uptake and efficiency is the muscle's fiber type distribution (Henriksen et al. 1990; Johnson et al. 1973), whereas the cost function used in the static optimization process (in which the muscle activities are calculated), was always the same. The cost function used in our study was a simple minimization of the cubed muscle activities (Crowninshield et al. 1981), using a normalization factor based on the muscle volume according to Happee et al. (Happee et al. 1995). Other, energy-based cost-functions have been proposed (Praagman et al. 2006), which might be more suitable to reflect the complex interplay between muscles. A third 'limitation' is that subject-specific models had only slightly higher correlations with the FDG-PET measurements than generic models for most measures. This could be due to two problems: the subject-specific models were not that much more representative of real-life physiology than the generic ones, or the FDG-PET measurements did not reflect the true muscle energy consumption for the models to be compared to. In the prior case, this would be unfortunate, since a lot of time and effort was performed in creating subject-specific models (Carbone 2016), which seemingly did not yield a large benefit in the comparisons with FDG-PET. On the other hand, one might argue that most of the correlations between models and simulations were already very high for the generic models (order of 0.8-0.9), and that there was not much room for improvement. In the latter case, while it is known that the FDG-PET measurements certainly do not represent the whole truth in terms of energy consumption (e.g., the role of alternative energy sources is not included in the measurements), its concurrent validity for studying walking has been demonstrated (Oi et al. 2003 and chapter 5).

Limitations of FDG-PET

An aspect that makes it difficult to use PET images on a stand-alone basis is the absence of anatomic structures in the images. Therefore, a CT or MRI scan that provides information on the location of anatomical structures is necessary. Muscle boundaries, which were of particular interest in the work presented in this thesis, are hard to distinguish on CT scans, since their attenuation coefficient is similar to that of the surrounding muscle tissue. In

contrast, certain specific T1-weighted MRI imaging protocols provide excellent visibility of muscle boundaries (Kolk et al. 2014; Scheys 2009). Ideally, the MRI scan would be made concurrently with the PET scan (in the same machine at the same time) in order to maintain co-registration. In the work presented in this thesis, there were a few weeks between the PET-CT scan and the MRI scan. A crude PET-MRI co-registration was accomplished by placing the subject on the scan bed using rulers and angle measurements, but this needed to be refined in an additional step. The MRI scans (including the muscle regions-of-interest) had to be transposed and morphed to correspond with the PET and CT scans. The latter two scans were made while the patient was lying on the scan bed in an unchanged position between the scans, negating the need to transpose or morph those two scans onto each other.

A limitation specific to the use of FDG to measure muscle glucose uptake is that the relation between FDG uptake and the actual work performed or force exerted by a muscle is unknown. Various alternative energy sources are available to the muscle cells, including plasma free fatty acids, triglyceride stores, and internal glycogen. The combination of substrates that was used by each muscle in each subject might have varied in our study, even during the exercise. To limit the effects of varying substrates as much as possible, the exercise intensity was kept low, at a constant level, and maintained for a long time with the aim of maintaining a steady state in glucose uptake from the blood. Ideally, we would also have measured the FDG uptake in the subjects after a period of rest on a day separate from the walking exercise. Working this way, subjects could serve as their own controls to establish a baseline metabolism of FDG uptake in each subject. Unfortunately, this was not possible due to ethical constraints regarding the radiation dose imposed on these healthy subjects.

Recommendations and future perspectives for using FDG-PET

Recently (following FDA approval in 2011), the first PET-MRI scanners have been introduced into clinics. This type of scanner has, for example, been used in studying the heart (Ferda et al. 2016; Lau et al. 2016), the brain (Schutz et al. 2016), predicting radiotherapy treatment response (Wong et al. 2016), and in staging cancer (Paspulati et al. 2015). It has not yet been applied in the study of muscle activity. Future work should aim to assess the feasibility of hybrid PET-MRI scanners in studying muscle activity for three main reasons. First, the technique obliterates the need for transposing and morphing to obtain co-registration, thereby simplifying the image analysis process and potentially improving its accuracy. Second, the 'one-stop-shop' PET-MRI scanner saves time, since a separate MRI scanning session is no longer required. Third, it avoids the CT scan altogether, which reduces the level of radiation exposure to the subject. It is important to note that PET-MRI also has several important disadvantages with respect to PET-CT, which include difficulties in determining the attenuation correction for the PET data. To generate artifact-free, quantitatively accurate PET images, attenuation and scatter correction are crucial (Bailey 1998; Zaidi et al. 2003). In PET-CT scanners, these attenuation maps are obtained by the CT scan. If such a scan is not available, as in PET-MRI, the attenuation map needs to be estimated based on the MRI scan, which may introduce errors (Lee et al. 2016).

One of the most promising capabilities of FDG-PET in the context of measuring muscle activity, as demonstrated in this thesis, is the ability to detect spatial distribution of FDG

within a muscle. The reconstruction of an image from a modern PET scanner typically has a voxel size of about 1-2 mm. This is roughly similar to the size of a muscle biopsy, but in contrast to a biopsy sample, the PET scan offers information about the activity in the entire volume of the muscle. From multi-channel electromyography studies, it is known that the spatial activation of muscle fibers in a muscle is not uniform; it is influenced by at least the contraction intensity and fatigue (Farina et al. 2008; Kleine et al. 2000). An FDG-PET measurement offers an additional, and in many ways improved, measurement of the spatial distribution of activity within muscles (given the already stated disadvantages of electromyography) (Pappas et al. 2001). Measuring the intramuscular distribution of FDG, in theory, also allows musculoskeletal modelers to validate their models not just on the level of whole muscles, but to go much further and also validate muscle activity levels for each individual muscle-tendon element within muscles. For example, the recent TLEM 2.0 model as presented by Carbone and Fluit et al. (2015), based on cadaver measurements on a single specimen, contains no less than 166 of these elements per leg (e.g., the adductor magnus consists of 13 muscle-tendon elements in the model). Muscle activation in all of these elements might be individually compared to the FDG-PET measurements. Note that PET using FDG as the tracer is not suitable as the sole validation technique in musculoskeletal modeling, because it only measures cumulative muscle activity over periods of time, rather than the timing of each muscle's activation within the gait cycle or other exercise. It should, therefore, be considered as a complimentary technique to other, time-sensitive techniques such as electromyography, ultrasound, or near-infrared spectroscopy.

An alternative and interesting way of using PET is not by using FDG and static imaging (as was done in this thesis), but by using tracers that decay faster and dynamic imaging. This entails imaging a tracer's kinetics within the tissues as it is being taken up by those tissues. In a way, this technique is able to provide 'live' insight into the metabolism. The most frequently used isotope in this context is [^{15}O], either as oxygen or water molecules. These tracers can be used to form a measure of the amount of tissue perfusion. As such, it also measures aerobic metabolism like with FDG. Unlike [^{18}F], however, there is no trapping process, and the half-life time is also much shorter (122 seconds), allowing an almost instantaneous measurement of blood flow in a tissue. The feasibility of using [^{15}O]-H2O in combination with PET has already been demonstrated for a simple knee extension exercise (Kalliokoski et al. 2000). Two clear disadvantages of using this technique are that the exercises that can be performed are limited because of the participant's position in the scanner tunnel (as opposed to being able to move around freely such as in walking), and that if the limb under investigation is moving during the scan (or even if muscles are contracting and changing shape), this hampers the accurate capture of the image. These disadvantages have led to tracers with longer half-life times (such as [^{18}F]-FDG), becoming more popular in the study of muscle activity during exercise.

The cumulative nature of the FDG accumulation in cells, due to the trapping process as explained in the introduction of this thesis, has both advantages and disadvantages. The participants in our study walked for a long time (90 minutes) and, therefore, it is tempting to state that the metabolic uptake data can be considered to be reliable because of the steady state of walking (particularly, the FDG uptake into the cells) that surely would have occurred during such a long walk. However, since the PET images were captured after the exercise

and contain no temporal information at all, it was impossible to see if the distribution of FDG changed during the exercise. Subjects could have switched between several muscle recruitment strategies during the 90 minutes of exercise. Future work could elucidate this aspect in several ways. First, several PET scans could be made during the exercise bout. For example, a PET scan of only one bed position, focusing on either the lower leg muscles, the thigh muscles, or the hip muscles, could be repeated at certain intervals during an exercise. If 15 min of exercise, followed by 3-5 min of scanning would be repeated several times (e.g., four times), the FDG's distribution within muscles in the region of interest could be examined temporally. Second, a method that is sensitive to temporal changes in muscle activity, such as multi-channel electromyography (Holtermann et al. 2005; Staudenmann et al. 2009), could be used concurrently during the ongoing exercise, to image temporal shifts in regional muscle activity. Due to the inherent superficial nature of multi-channel electromyography, this would likely be feasible only for the lower leg muscles. If, from either of these proposed methods it is found that there are no temporal changes in the activity levels of muscle regions, this would provide a way to validate the use of the FDG-PET technique for measuring spatial distribution of muscle activity during prolonged exercise. It might also provide guidelines for future studies aiming to shorten the exercise time as much as possible, for example in the case of studying pathology.

Concluding remarks

This thesis offers several new insights in the functional outcome after different types of orthopedic surgery, as well as in musculoskeletal research and modeling. Through literature review, gait analyses, and strength measurements, we identified that the largest deficit in patients who had undergone any of the three investigated forms of hip surgery concerned the loss of hip abduction moment (not always limited to the operated side). This was the case during gait and stair ascent, as well as during strength measurements, with the magnitude of the deficit depending on the type of surgery performed. This highlights the need for rehabilitation protocols, surgical approaches, and musculoskeletal modeling efforts to focus on the hip abductors. Another insight was that the post-operative level of functional outcome after limb salvage surgery was difficult to predict, even for experienced orthopedic oncologists, warranting research into musculoskeletal models that might be able to help them in the pre-operative decision making process. The first promising steps have already been taken in that direction, during the TLEMsafe project (Fluit 2015; Verdonschot 2014).

In the second part of this thesis, we used a combination of FDG-PET and advanced three-dimensional MRI segmentation techniques to determine muscle activity in all muscles of the hip, thigh, and lower leg in healthy subjects. The benefits of our three-dimensional segmentation techniques became clear when we compared the volumetric muscle activity results to those obtained using single slice-based analysis techniques that had been used in the field up to that point. The findings also challenged the common notion of symmetry in muscle activity between both limbs in healthy subjects, which could have important implications in musculoskeletal modeling. The intramuscular uptake data offers the potential next step in validation of musculoskeletal models; namely, validation not only on the level of whole muscle, but also on the level of the musculotendon units that comprise the muscle.

Finally, we already performed the first comparison of energy consumption measured with FDG-PET with the energy consumption predicted by personalized musculoskeletal models and found 'good' to 'very good' correlations, although additional work to achieve further personalization remains to be done (Carbone 2016), in order to explain the many remaining differences between the measurements and the models. In spite of drawbacks, such as ethical constraints and the relative novelty and unknowns associated with FDG-PET in measuring muscle activity, it remains important to acknowledge its greatest strengths compared to techniques such as surface electromyography. It can be used to obtain information from deep-lying muscles, it can measure all muscles simultaneously, it does not require reference contractions, and it does not suffer from reduced signal quality due to adipose tissue and crosstalk from other muscles. Therefore, we pose that FDG-PET should be considered as a valuable addition to the validation techniques available in musculoskeletal modeling, and that it holds great promise in studying and quantifying pathological conditions in patients suffering from various types of musculoskeletal disease.

References

Ackermann, M., and van den Bogert, A.J. 2010. Optimality principles for model-based prediction of human gait, J Biomech, 43: 1055-1060.

Anderson, F.C., and Pandy, M.G. 2001. Static and dynamic optimization solutions for gait are practically equivalent, J Biomech, 34: 153-161.

Bailey, D.L. 1998. Transmission scanning in emission tomography, Eur J Nucl Med, 25: 774-787.

Beaulieu, M.L., Lamontagne, M., and Beaule, P.E. 2010. Lower limb biomechanics during gait do not return to normal following total hip arthroplasty, Gait Posture, 32: 269-273.

Bennett, D., Humphreys, L., O'Brien, S., Kelly, C., Orr, J.F., and Beverland, D.E. 2008. Gait kinematics of age-stratified hip replacement patients--a large scale, long-term follow-up study, Gait Posture, 28: 194-200.

Carbone, V. 2016. Subject-specific lower extremity modeling, PhD Thesis, University of Twente.

Carbone, V., Fluit, R., Pellikaan, P., van der Krogt, M.M., Janssen, D., Damsgaard, M., Vigneron, L., Feilkas, T., Koopman, H.F., and Verdonschot, N. 2015. TLEM 2.0 - a comprehensive musculoskeletal geometry dataset for subject-specific modeling of lower extremity, J Biomech, 48: 734-741.

Carbone, V., van der Krogt, M.M., Koopman, H.F., and Verdonschot, N. 2012. Sensitivity of subject-specific models to errors in musculo-skeletal geometry, J Biomech, 45: 2476-2480.

Colo, E., Rijnen, W.H.C., Gardeniers, J.W.M., van Kampen, A., and Schreurs, B.W. 2016. Satisfying Results of Primary Hip Arthroplasty in Patients With Hip Dysplasia at a Mean Followup of 20 Years, Clinical orthopaedics and related research, 474: 2462-2468.

Crowninshield, R.D., and Brand, R.A. 1981. A physiologically based criterion of muscle force prediction in locomotion, J. Biomech., 14: 793-801.

de Kleuver, M., Kooijman, M.A., Pavlov, P.W., and Veth, R.P. 1997. Triple osteotomy of the pelvis for acetabular dysplasia: results at 8 to 15 years, J. Bone Joint Surg. Br., 79: 225-229.

De Visser, E., Mulder, T., Schreuder, H.W., Veth, R.P., and Duysens, J. 2000. Gait and electromyographic analysis of patients recovering after limb-saving surgery, Clin Biomech (Bristol, Avon), 15: 592-599.

Farina, D., Leclerc, F., Arendt-Nielsen, L., Buttelli, O., and Madeleine, P. 2008. The change in spatial distribution of upper trapezius muscle activity is correlated to contraction duration, J Electromyogr Kinesiol, 18: 16-25.

Ferda, J., Hromadka, M., and Baxa, J. 2016. Imaging of the myocardium using 18F-FDG-PET/MRI, Eur J Radiol.

Fluit, R. 2015. Functional outcome prediction after surgery: a bridge too far?, University of Twente.

Fluit, R., Andersen, M.S., Kolk, S., Verdonschot, N., and Koopman, H.F.J.M. 2014. Prediction of ground reaction forces and moments during various activities of daily living, J. Biomech., 47: 2321-2329.

Foucher, K.C., Hurwitz, D.E., and Wimmer, M.A. 2007. Preoperative gait adaptations persist one year after surgery in clinically well-functioning total hip replacement patients, J. Biomech., 40: 3432-3437.

Foucher, K.C., Wimmer, M.A., Moisio, K.C., Hildebrand, M., Berli, M.C., Walker, M.R., Berger, R.A., and Galante, J.O. 2011. Time course and extent of functional recovery during the first postoperative year after minimally invasive total hip arthroplasty with two different surgical approaches–a randomized controlled trial, J Biomech, 44: 372-378.

Fujimoto, T., Kemppainen, J., Kalliokoski, K.K., Nuutila, P., Ito, M., and Knuuti, J. 2003. Skeletal muscle glucose uptake response to exercise in trained and untrained men, Med Sci Sports Exerc, 35: 777-783.

Gondoh, Y., Tashiro, M., Itoh, M., Masud, M.M., Sensui, H., Watanuki, S., Ishii, K., Takekura, H., Nagatomi, R., and Fujimoto, T. 2009. Evaluation of individual skeletal muscle activity by glucose uptake during pedaling exercise at different workloads using positron emission

tomography, J Appl Physiol, 107: 599-604.
Graves, S.C., Dropkin, B.M., Keeney, B.J., Lurie, J.D., and Tomek, I.M. 2016. Does Surgical Approach Affect Patient-reported Function After Primary THA?, Clinical orthopaedics and related research, 474: 971-981.
Happee, R., and Van der Helm, F.C. 1995. The control of shoulder muscles during goal directed movements, an inverse dynamic analysis, J. Biomech., 28: 1179-1191.
Henriksen, E.J., Bourey, R.E., Rodnick, K.J., Koranyi, L., Permutt, M.A., and Holloszy, J.O. 1990. Glucose transporter protein content and glucose transport capacity in rat skeletal muscles, Am J Physiol, 259: E593-598.
Holtermann, A., Roeleveld, K., and Karlsson, J.S. 2005. Inhomogeneities in muscle activation reveal motor unit recruitment, J Electromyogr Kinesiol, 15: 131-137.
Inman, V.T., Ralston, H.J., and Todd, F. 1981. Human Walking (Williams & Wilkins: Baltimore).
Janssen, D., Kalchschmidt, K., and Katthagen, B.D. 2009. Triple pelvic osteotomy as treatment for osteoarthritis secondary to developmental dysplasia of the hip, Int. Orthop., 33: 1555-1559.
Jantunen, H., Wasenius, N., Salonen, M.K., Perala, M.M., Osmond, C., Kautiainen, H., Simonen, M., Pohjolainen, P., Kajantie, E., Rantanen, T., von Bonsdorff, M.B., and Eriksson, J.G. 2016. Objectively measured physical activity and physical performance in old age, Age and ageing.
Johnson, M.A., Polgar, J., Weightman, D., and Appleton, D. 1973. Data on the distribution of fibre types in thirty-six human muscles. An autopsy study, J Neurol Sci, 18: 111-129.
Kalliokoski, K.K., Kemppainen, J., Larmola, K., Takala, T.O., Peltoniemi, P., Oksanen, A., Ruotsalainen, U., Cobelli, C., Knuuti, J., and Nuutila, P. 2000. Muscle blood flow and flow heterogeneity during exercise studied with positron emission tomography in humans, Eur J Appl Physiol, 83: 395-401.
Karam, M.D., Yubo, G., and McKinley, T. 2011. Assessment of walking pattern pre and post peri-acetabular osteotomy, Iowa Orthop. J., 31: 83-89.
Kiss, R.M., and Illyes, A. 2012. Comparison of gait parameters in patients following total hip arthroplasty with a direct-lateral or antero-lateral surgical approach, Hum Mov Sci, 31: 1302-1316.
Kleine, B.U., Schumann, N.P., Stegeman, D.F., and Scholle, H.C. 2000. Surface EMG mapping of the human trapezius muscle: the topography of monopolar and bipolar surface EMG amplitude and spectrum parameters at varied forces and in fatigue, Clinical neurophysiology : official journal of the International Federation of Clinical Neurophysiology, 111: 686-693.
Kolk, S., Klawer, E.M.E., Schepers, J., Weerdesteyn, V., Visser, E.P., and Verdonschot, N. 2014. Muscle activity during walking measured using 3D MRI segmentations and FDG-PET, Med Sci Sports Exerc, in press.
Kyriazis, V., and Rigas, C. 2002. Temporal gait analysis of hip osteoarthritic patients operated with cementless hip replacement, Clin Biomech (Bristol, Avon), 17: 318-321.
Lai, K.A., Lin, C.J., Jou, I.M., and Su, F.C. 2001. Gait analysis after total hip arthroplasty with leg-length equalization in women with unilateral congenital complete dislocation of the hip--comparison with untreated patients, J Orthop Res, 19: 1147-1152.
Lau, J.M., and Zheng, J. 2016. Disease-specific cardiovascular positron emission tomography/magnetic resonance imaging: a brief review of the current literature, Quant Imaging Med Surg, 6: 297-307.
Learmonth, I.D., Young, C., and Rorabeck, C. 2007. The operation of the century: total hip replacement, Lancet, 370: 1508-1519.
Lee, D.H., and Lee, J.M. 2016. Whole-body PET/MRI for colorectal cancer staging: Is it the way forward?, J Magn Reson Imaging.
Lenaerts, G., De Groote, F., Demeulenaere, B., Mulier, M., Van der Perre, G., Spaepen, A., and Jonkers, I. 2008. Subject-specific hip geometry affects predicted hip joint contact forces during gait, J Biomech, 41: 1243-1252.
Lepley, L.K. 2015. Deficits in Quadriceps Strength and Patient-Oriented Outcomes at Return to

Activity After ACL Reconstruction: A Review of the Current Literature, Sports Health, 7: 231-238.

Leuchte, S., Luchs, A., and Wohlrab, D. 2007. [Measurement of ground reaction forces after total hip arthroplasty using different surgical approaches], Zeitschrift fur Orthopadie und Ihre Grenzgebiete, 145: 74-80.

Leunig, M., Faas, M., von Knoch, F., and Naal, F.D. 2013. Skin crease 'bikini' incision for anterior approach total hip arthroplasty: surgical technique and preliminary results, Clin Orthop Relat Res, 471: 2245-2252.

Lindemann, U., Becker, C., Unnewehr, I., Muche, R., Aminin, K., Dejnabadi, H., Nikolaus, T., Puhl, W., Huch, K., and Dreinhofer, K.E. 2006. Gait analysis and WOMAC are complementary in assessing functional outcome in total hip replacement, Clin. Rehabil., 20: 413-420.

Lucente, L. 2016. A new surgical technique to the positioning of hip prosthetic implants: The medial-inguinal approach. In International Society for Technology in Arthroplasty. Boston, MA.

Lugade, V., Wu, A., Jewett, B., Collis, D., and Chou, L.S. 2010. Gait asymmetry following an anterior and anterolateral approach to total hip arthroplasty, Clin Biomech (Bristol, Avon), 25: 675-680.

Madsen, M.S., Ritter, M.A., Morris, H.H., Meding, J.B., Berend, M.E., Faris, P.M., and Vardaxis, V.G. 2004. The effect of total hip arthroplasty surgical approach on gait, J. Orthop. Res., 22: 44-50.

Marangoz, S., Atilla, B., Gok, H., Yavuzer, G., Ergin, S., Tokgozoglu, A.M., and Alpaslan, M. 2010. Gait analysis in adults with severe hip dysplasia before and after total hip arthroplasty, Hip Int, 20: 466-472.

Mont, M.A., Seyler, T.M., Ragland, P.S., Starr, R., Erhart, J., and Bhave, A. 2007. Gait analysis of patients with resurfacing hip arthroplasty compared with hip osteoarthritis and standard total hip arthroplasty, J Arthroplasty, 22: 100-108.

Verdonschot, N. 2014. TLEMsafe: Improving safety and predictability of complex musculoskeletal surgery using a patient-specific navigation system, Accessed 16-04-2017. https://www.youtube.com/watch?v=jD-6KQfGjgM.

Oi, N., Iwaya, T., Itoh, M., Yamaguchi, K., Tobimatsu, Y., and Fujimoto, T. 2003. FDG-PET imaging of lower extremity muscular activity during level walking, J Orthop Sci, 8: 55-61.

Palmieri-Smith, R.M., and Lepley, L.K. 2015. Quadriceps Strength Asymmetry After Anterior Cruciate Ligament Reconstruction Alters Knee Joint Biomechanics and Functional Performance at Time of Return to Activity, Am J Sports Med, 43: 1662-1669.

Pappas, G.P., Olcott, E.W., and Drace, J.E. 2001. Imaging of skeletal muscle function using (18)FDG PET: force production, activation, and metabolism, J Appl Physiol (1985), 90: 329-337.

Paspulati, R.M., Partovi, S., Herrmann, K.A., Krishnamurthi, S., Delaney, C.P., and Nguyen, N.C. 2015. Comparison of hybrid FDG PET/MRI compared with PET/CT in colorectal cancer staging and restaging: a pilot study, Abdom Imaging, 40: 1415-1425.

Pedersen, E.N.G., Alkjaer, T., Soballe, K., and Simonsen, E.B. 2006. Walking pattern in 9 women with hip dysplasia 18 months after periacetabular osteotomy, Acta Orthop., 77: 203-208.

Perron, M., Malouin, F., Moffet, H., and McFadyen, B.J. 2000. Three-dimensional gait analysis in women with a total hip arthroplasty, Clin Biomech, 15: 504-515.

Praagman, M., Chadwick, E.K.J., van der Helm, F.C.T., and Veeger, H.E.J. 2006. The relationship between two different mechanical cost functions and muscle oxygen consumption, J. Biomech., 39: 758-765.

Romano, C.L., Frigo, C., Randelli, G., and Pedotti, A. 1996. Analysis of the gait of adults who had residua of congenital dysplasia of the hip, J. Bone Joint Surg. Am., 78: 1468-1479.

Scheys, L. 2009. Personalized musculoskeletal modeling based on magnetic resonance images: use for biomechanical analysis of gait, K.U. Leuven.

Schutz, L., Lobsien, D., Fritzsch, D., Tiepolt, S., Werner, P., Schroeter, M.L., Berrouschot, J., Saur, D., Hesse, S., Jochimsen, T., Rullmann, M., Sattler, B., Patt, M., Gertz, H.J., Villringer, A., Classen, J., Hoffmann, K.T., Sabri, O., and Barthel, H. 2016. Feasibility and acceptance of simultaneous

amyloid PET/MRI, Eur J Nucl Med Mol Imaging.
Shih, C.H., Du, Y.K., Lin, Y.H., and Wu, C.C. 1994. Muscular recovery around the hip joint after total hip arthroplasty, Clinical orthopaedics and related research: 115-120.
Shimada, H., Hirata, T., Kimura, Y., Naka, T., Kikuchi, K., Oda, K., Ishii, K., Ishiwata, K., and Suzuki, T. 2009a. Effects of a robotic walking exercise on walking performance in community-dwelling elderly adults, Geriatr Gerontol Int, 9: 372-381.
Shimada, H., Kimura, Y., Lord, S.R., Oda, K., Ishii, K., Suzuki, T., and Ishiwata, K. 2009b. Comparison of regional lower limb glucose metabolism in older adults during walking, Scand J Med Sci Sports, 19: 389-397.
Shimada, H., Kimura, Y., Suzuki, T., Hirata, T., Sugiura, M., Endo, Y., Yasuhara, K., Shimada, K., Kikuchi, K., Hashimoto, M., Ishikawa, M., Oda, K., Ishii, K., and Ishiwata, K. 2007. The use of positron emission tomography and [18F]fluorodeoxyglucose for functional imaging of muscular activity during exercise with a stride assistance system, IEEE Trans Neural Syst Rehabil Eng, 15: 442-448.
Sprint, G., Cook, D.J., and Schmitter-Edgecombe, M. 2016. Unsupervised detection and analysis of changes in everyday physical activity data, J Biomed Inform, 63: 54-65.
Staudenmann, D., Kingma, I., Daffertshofer, A., Stegeman, D.F., and van Dieen, J.H. 2009. Heterogeneity of muscle activation in relation to force direction: a multi-channel surface electromyography study on the triceps surae muscle, J Electromyogr Kinesiol, 19: 882-895.
Sucato, D.J., Tulchin, K., Shrader, M.W., DeLaRocha, A., Gist, T., and Sheu, G. 2010. Gait, Hip Strength and Functional Outcomes After a Ganz Periacetabular Osteotomy for Adolescent Hip Dysplasia, J. Pediatr. Orthop., 30: 344-350.
Terrier, A., Levrero Florencio, F., and Rudiger, H.A. 2014. Benefit of cup medialization in total hip arthroplasty is associated with femoral anatomy, Clinical orthopaedics and related research, 472: 3159-3165.
Van Campen, A., Pipeleers, G., De Groote, F., Jonkers, I., and De Schutter, J. 2014. A new method for estimating subject-specific muscle-tendon parameters of the knee joint actuators: a simulation study, International journal for numerical methods in biomedical engineering, 30: 969-987.
van der Krogt, M.M., Delp, S.L., and Schwartz, M.H. 2012. How robust is human gait to muscle weakness?, Gait Posture, 36: 113-119.
Varin, D., Lamontagne, M., and Beaule, P.E. 2013. Does the anterior approach for THA provide closer-to-normal lower-limb motion?, Journal of Arthroplasty, 28: 1401-1407.
Veth, R., van, H.R., Pruszczynski, M., Hoogenhout, J., Schreuder, B., and Wobbes, T. 2003. Limb salvage in musculoskeletal oncology, Lancet Oncol, 4: 343-350.
Wong, K.H., Panek, R., Welsh, L.C., McQuaid, D., Dunlop, A., Riddell, A., Murray, I., Du, Y., Chua, S., Koh, D.M., Bhide, S., Nutting, C.M., Oyen, W.J., Harrington, K.J., and Newbold, K.L. 2016. The predictive value of early assessment after one cycle of induction chemotherapy with 18F-FDG-PET/CT and DW-MRI for response to radical chemoradiotherapy in head and neck squamous cell carcinoma, J Nucl Med.
Zaidi, H., and Hasegawa, B. 2003. Determination of the attenuation map in emission tomography, J Nucl Med, 44: 291-315.
Zajac, F.E. 1989. Muscle and tendon: properties, models, scaling, and application to biomechanics and motor control, Critical reviews in biomedical engineering, 17: 359-411.

Nederlandse Samenvatting: Deel I

Het eerste doel van dit proefschrift was om inzicht te verkrijgen in de huidige status en uitdagingen aangaande de functionele uitkomst na drie verschillende orthopedische operaties: totale heupvervanging, drievoudige heuposteotomie en een beensparende operatie. In **hoofdstuk 2** was ons doel om de vraag 'Wat is het huidige niveau van functionaliteit na totale heupvervanging tijdens lopen en loopgerelateerde activiteiten van het dagelijks leven, gemeten met objectieve meetmethoden?' te beantwoorden. We hebben de wetenschappelijke literatuur bestudeerd, gebruikmakend van veelomvattende zoektermen in de MEDLINE database. De inclusiecriteria waren als volgt: primaire osteoartritis als indicatie, waarbij een vergelijking werd gemaakt tussen patiënten en gezonde controles, of een vergelijking tussen de geopereerde en niet geopereerde zijde, en een opvolgingstijd van tenminste zes maanden na de operatie. De literatuurstudie leidde tot 2177 artikelen, waarvan er 35 werden geïncludeerd. In de geopereerde heup hadden de patiënten tijdens het lopen een verminderd saggitaal bewegingsbereik en maximale extensie, en genereerden ze een lager saggitaal vermogen, een lager abductiemoment en een lager extern rotatiemoment vergeleken met gezonde controles. De meeste van deze bevindingen (saggitaal bewegingsbereik, abductiemoment, extern rotatiemoment) waren niet te wijten aan een verlaagde loopsnelheid, aangezien deze bevindingen ook werden gevonden in studies die de loopsnelheid gelijk hielden tussen patiënten en controles. Bij traplopen (zowel omhoog als naar beneden) werden de verschillen tussen patiënten en controles niet uitvergroot ten opzichte van tijdens het lopen, hoewel de patiënten wel lagere heupmomenten genereerden tijdens het omhoog traplopen. Een van de meeste consistente bevindingen tijdens zowel lopen op vlakke ondergrond als tijdens het omhoog traplopen, was een verminderd abductiemoment dat bovendien onafhankelijk leek te zijn van de chirurgische benadering van het heupgewricht.

In de **hoofdstukken 3a en 3b** zochten we naar een antwoord op de vraag 'In welke mate is de functionele uitkomst met betrekking tot het lopen en de kracht in de benen na een drievoudige heuposteotomie en na totale heupvervanging met femorale inkorting gelijk aan gezonde controles en vergelijkbaar tussen de benen?'. In **hoofdstuk 3a** hebben we de langetermijn gevolgen van drievoudige heuposteotomie op het lopen en op de kracht in de benen onderzocht. Dit hebben we gedaan met behulp van gangbeeldanalyse en isometrische krachtmetingen bij twaalf vrouwen (leeftijd 34±12 jaar) die de operatie 80±18 maanden geleden hadden ondergaan. De resultaten vergeleken we met een controlegroep bestaande uit acht vrouwen die even oud waren als de studiegroep (33±10 jaar). Over het algemeen was het looppatroon van de vrouwen die een drievoudige heuposteotomie hadden ondergaan gelijk aan dat van de controlegroep, maar er werden wel kleine verschillen gevonden tussen de geopereerde en de niet geopereerde zijde. Het patroon van het abductiemoment in de standfase was significant verschillend tussen de geopereerde en de niet geopereerde zijde. Verder toonden de krachtmetingen aan dat de abductiekracht significant was verminderd in beide zijden ten opzichte van de gezonde controles. We concludeerden dat de patiënten over het algemeen goed waren hersteld van hun operatie op het gebied van het lopen, en dat er slechts kleine verschillen werden gevonden tussen de geopereerde en de niet geopereerde zijde. Het tweezijdige krachtsverschil in de abductoren impliceert dat de patiënten op een hoger percentage van hun maximale kracht liepen. Dit zou uiteindelijk kunnen leiden tot aanpassingen van het looppatroon als de patiënten moe worden, hetgeen relevant is voor

deze jonge patiënten die wellicht nog vele jaren willen kunnen sporten en andere zware activiteiten willen kunnen uitvoeren.

In **hoofdstuk 3b** hadden we als doel om de functionele uitkomst van totale heupvervanging met heupkomreconstructie en femorale inkorting te meten bij patiënten met erfelijke heupdysplasie. Dit hebben we gedaan met behulp van gangbeeldanalyses en isometrische krachtmetingen bij zeven vrouwen die deze operatie hadden ondergaan (leeftijd: 39±13 jaar, tijd na operatie: 45±52 maanden), en ook bij zeven gezonde vrouwen (leeftijd: 31±10 jaar). Een van de bevindingen was dat de adductiehoek in de geopereerde heup significant groter was tijdens het lopen dan die in de niet geopereerde heup. Verder was het abductiemoment significant lager dan dat van de gezonde controles. Bij de krachtmetingen bleek dat de geopeerde zijde significant zwakker was dan de controles tijdens heupabductie, heupextensie, knieflexie en knieextensie. De geopereerde zijde was bovendien zwakker dan de niet geopeerde zijde tijdens alle metingen behalve knieflexie. De afwijkingen in het looppatroon in het frontale vlak duidden op een zogenaamd teken van Trendelenburg, wat een compensatiemechanisme is voor zwakte in de abductoren. Deze bevinding werd ondersteund door de metingen van de abductiekracht. Het is nog de vraag of er verbeteringspotentieel is voor de abductiekracht en het looppatroon, aangezien er mogelijk structurele veranderingen hebben opgetreden in de spieren tijdens de vele jaren voorafgaand aan de operatie, waarin de spieren hebben moeten functioneren op een niet optimale lengte.

In **hoofdstuk 4** hadden we als doel om de vraag 'Zijn orthopedisch oncologen in staat om de functionele effecten van een beensparende operatie te voorspellen?' te beantwoorden. We hebben drieëntwintig patiënten (tussen zes en tien jaar na operatie) en vijf onafhankelijke orthopedisch oncologen gevraagd om twee vragenlijsten te beantwoorden. Dit waren de zogenaamde 'Toronto Extremity Salvage Score (TESS)' en de 'RAND-36 physical functioning subscale (RAND-36 PFS)'. De orthopedisch oncologen baseerden hun voorspellingen van de functionele uitkomst op een casus beschrijving van iedere patiënt die hun status (inclusief MRI scans) voor de operatie weergaf. We vonden "zeer lage" to "lage" correlaties tussen de uitkomsten zoals weergegeven door de patiënten en die van de orthopedisch oncologen op beide vragenlijsten, en de orthopedisch oncologen hadden de neiging om de uitkomsten die waren gerapporteerd door de patiënten te onderschatten. Verder waren de orthopedisch oncologen het vaak niet met elkaar eens: de overeenkomst op de meeste vragen in de RAND-36 PFS was "laag", hetgeen erop duidt dat er een hoge variabiliteit was tussen de antwoorden van de orthopedisch oncologen. Het bleek dus lastig voor de deelnemende orthopedisch oncologen om de functionele uitkomst van beensparende operaties te voorspellen. Dit toont aan dat er meer onderzoek gedaan zou moeten worden naar objectieve methoden die de orthopedisch oncologen kunnen helpen tijdens het kiezen van de beste behandeling. Een van die methoden zou het gebruikmaken van spierskeletmodellen kunnen zijn. Met zulke modellen zou op voorhand kunnen worden berekend of de patiënt nog genoeg spierkracht over zal hebben na de operatie om activiteiten van het dagelijks leven uit te voeren.

Nederlandse Samenvatting: Deel II

Het tweede doel van dit proefschrift was om te ontdekken wat de mogelijkheden van FDG-PET zijn om fundamenteel inzicht te verkrijgen in het spierskeletsysteem tijdens lopen, en ook om te weten te komen wat de potentie van de techniek is om de eerder geïdentificeerde uitdagingen met betrekking tot functionele uitkomst op te lossen. **Hoofdstuk 5** had als doel om de vraag 'Welke spieren in de onderste extremiteit zijn het meest belangrijk tijdens het lopen?'. In dat hoofdstuk werd positron emissie tomografie (PET) in combinatie met [^{18}F]-fluodeoxyglucose (FDG) gebruikt. Dit is een nieuwe methodologie die gebaseerd is op de toename van de opname van glucose en FDG in spieren die actief zijn. Hiertoe liepen tien gezonde proefpersonen op een loopband op zelfgekozen snelheid gedurende 85 minuten; 55 minuten voor en 30 minuten na een intraveneuze injectie met 50 MBq FDG. Daarna werd er een PET/CT scan gemaakt van de onderste extremiteit. De driedimensionale contouren van 39 spieren in de linker onderste extremiteit werden halfautomatisch bepaald met behulp van MRI scans en nieuwe geavanceerde algoritmes in de Mimics Innovation Suite (Materialise N.V., Leuven, Belgium). Nadat de MRI scans op een niet rigide manier waren geregistreerd op de CT scans, werden de spiercontouren op de PET scans gelegd. Het bleek dat de meest actieve spieren tijdens het lopen de soleus, gluteus maximus, vastus lateralis, gastrocnemius medialis en adductor magnus waren. Er waren wel grote verschillen tussen proefpersonen, ook in enkele van de meest belangrijke spieren tijdens het lopen (bijvoorbeeld de soleus, gluteus medius en gastrocnemius medialis). De spieren die we identificeerden als zijnde meest actief, waren over het algemeen dezelfde spieren die ook al in eerdere studies waren geïdentificeerd met behulp van andere methoden zoals inverse dynamica en elektromyografie. Een aantal spieren (bijvoorbeeld de adductor magnus en de gluteus minimus) die voorheen lastig te meten waren met bestaande technieken zoals oppervlakte elektromyografie vanwege hun grootte of hun diep liggende positie in het lichaam, werden door FDG-PET geïdentificeerd als zeer actief tijdens het lopen. Vergeleken met bestaande methoden voor het analyseren van de hoeveelheid FDG in spieren waarbij slechts in één plakje van de scan wordt gemeten, leidde onze driedimensionale analyse tot een ander resultaat in veel van de meest actieve spieren. Dit toont de toegevoegde waarde van onze uitgebreide driedimensionale analyse van spieractiviteit met behulp van FDG-PET.

In **hoofdstuk 6** zochten we antwoorden op de vragen 'Zijn de spieren van de linker en rechter onderste extremiteit symmetrisch actief tijdens het lopen?' en 'Zijn de spieren homogeen actief of zijn er specifieke regio's binnen spieren die actiever zijn dan andere tijdens lopen?'. De methodologie was grotendeels gelijk aan die van hoofdstuk 5, met de toevoeging dat ditmaal ook het rechterbeen werd geanalyseerd. De spieren van de onderbenen vertoonden forse asymmetrieën (bijvoorbeeld een mediane asymmetrie van 42% in de gastrocnemius medialis). Er werden ook asymmetrieën gevonden in de gluteus medius (15% asymmetrie) en gluteus minimus (30% asymmetrie), terwijl de FDG opname in de spieren van het dijbeen relatief symmetrisch was tussen beide benen (<6% asymmetrie). De FDG opname was niet normaal verdeeld binnen spieren; de meeste voxels hadden een relatief lage SUV (gestandaardiseerde opname waarde), terwijl een kleine hoeveelheid voxels juist een relatief hoge SUV vertoonde. De gebieden waar de FDG opname hoger was, waren niet willekeurig verdeeld binnen de spieren, maar vormden clusters in vrijwel alle spieren. De bevindingen van deze studie demonstreren dat het niet vanzelfsprekend is dat spieractiviteit

altijd symmetrisch is tussen de beide benen in gezonde proefpersonen. Het feit dat er clusters werden gevormd van voxels met hoge uptake toont aan dat zelfs in een langdurige, repetitieve handeling als lopen, bepaalde regio's van spieren een hogere bijdrage leveren aan de loopbeweging dan anderen.

In **hoofdstuk 7** zochten we naar een antwoord op de vraag 'Kan FDG-PET worden gebruikt voor het valideren van spierskeletmodellen van gezonde proefpersonen?'. De validatie van spierskeletmodellen is een belangrijke maar moeilijk te nemen horde richting het gebruik van dit soort modellen in de klinische praktijk, zoals bij het plannen van orthopedische operaties. Het gebruiken van FDG-PET zoals getoond in de hoofdstukken 5 en 6 zou een oplossing kunnen zijn voor dit probleem. We construeerden proefpersoonspecifieke spierskeletmodellen van dezelfde tien gezonde proefpersonen met geavanceerde technieken zoals spieranatomie gesegmenteerd op MRI scans en functionele schaling gebaseerd op krachtmetingen. De spieren die in hoofdstuk 5 reeds waren geïdentificeerd als zijnde meest actief tijdens het lopen (soleus, gluteus maximus, vastus lateralis, gastrocnemius medialis en adductor magnus), waren over het algemeen ook het meeste actief in de spierskeletmodellen. De met behulp van PET gemeten FDG opname in de spieren in elke proefpersoon had een 'goede' to 'zeer goede' correlatie met het energieverbruik in de spier, berekend met de spierskeletmodellen (Spearman's ρ = 0.87±0.04, Pearson's r = 0.77±0.10). Toen de gemiddelde FDG opname van elke spier over alle tien proefpersonen werd berekend, werden de correlaties hoger (Spearman's ρ = 0.96, Pearson's r =0.91). We concludeerden dat FDG-PET een waardevolle nieuwe techniek lijkt als aanvulling op elektromyografie voor het valideren van spierskeletmodellen.

PhD Portfolio

Institute for Health Sciences Radboudumc

Radboud Universiteit Radboudumc

Name PhD student: S. Kolk	PhD period: 01-07-2010 / 10-04-2018
Department: Rehabilitation	Promotor(s): Prof. dr. ir. N. Verdonschot, Prof. dr. A.C.H. Geurts
Graduate School: Radboud Institute for Health Sciences	Co-promotor(s): Dr. V. Weerdesteyn

	Year(s)	ECTS
TRAINING ACTIVITIES		
a) Courses and Workshops		
RIHS Introduction Course for PhD Students, Radboudumc	2010	1
Course Good Clinical Practice, Radboudumc	2011	1
Opensim Workshop ISB Technical Group on Computer Simulations in Biomechancs, Brussels, Belgium	2011	1
Proficiency in English – Cambridge ESOL Level 3, Radboudumc	2011	3
Cursus Begeleiden van Onderzoeksstages, Radboudumc	2011	0.5
Loopbaanmanagement, Radboudumc	2012	1
Solliciteren en Netwerken, Radboudumc	2013	1
c) Symposia and Congresses (PP = poster presentation, OP = oral presentation)		
Dutch Biomedical Engineering Society, Egmond aan Zee (OP)	2011	1
International Society for Posture and Gait Research, Trondheim, Norway	2012	1
Organized and Attended RIHS PhD Retreat, Wageningen (PP)	2012	1
Organized and Attended RIHS PhD Retreat, Wageningen (PP)	2013	1
American Society of Biomechanics, Omaha, NB, USA (PP)	2013	1
World Congress of Biomechanics, Boston, MA, USA (OP)	2014	2
d) Other		
Member of RIHS PhD Council	2012-2013	2
Chairman of RIHS PhD Council	2013-2014	2
TEACHING ACTIVITIES		
f) Supervision of internships		
MSc internship - O. Schenk	2012	1
MSc internship - M.J. Minten	2012	1
MSc internship - J. Luijten	2012	1
MSc internship - K. Cox	2013	1
MSc internship - E.M.E. Klawer	2013	3
MSc internship - D. Lobeek	2013	1
TOTAL		**27.5**

List of Publications

Janusz, L., Witkowski, M., Carbone, V., **Kolk, S.**, Adamczyk, M., Sitnik, R., van der Krogt, M.M., Verdonschot, N. 2013. Lower body kinematics evaluation based on a multidirectional four-dimensional structured light measurement, Journal of Biomedical Optics, 18(5): 056014.

Kolk, S., Minten, M.J., van Bon, G.E., Rijnen, W.H., Geurts, A.C., Verdonschot, N., Weerdesteyn, V. 2014. Gait and gait-related activities of daily living after total hip arthroplasty: a systematic review, Clinical Biomechanics, 29: 705-718.

Kolk, S., Cox, K., Weerdesteyn, V., Hannink, G., Bramer, J., Dijkstra, S., Jutte, P., Ploegmakers, J., van de Sande, M., Schreuder, H., Verdonschot, N., van der Geest, I. 2014. Can orthopedic oncologists predict functional outcome in patients with sarcoma after limb salvage surgery in the lower limb? A nationwide study, Sarcoma: 436598.

Fluit, R., Andersen, M.S., **Kolk, S.**, Verdonschot, N., Koopman, H.F.J.M., 2014. Prediction of ground reaction forces and moments during various activities of daily living, Journal of Biomechanics, 47: 2321–2329.

Kolk, S., Fluit, R., Luijten, J., Heesterbeek, P.J., Geurts, A.C., Verdonschot, N., Weerdesteyn, V. 2015. Gait and lower limb muscle strength in women after triple innominate osteotomy, BMC Musculoskeletal Disorders, 16: 68.

Kolk, S., Klawer, E.M.E., Schepers, J., Weerdesteyn, V., Visser, E.P., Verdonschot, N. 2015. Muscle Activity during Walking Measured Using 3D MRI Segmentations and [18F]-fluorodeoxyglucose in Combination with Positron Emission Tomography, Medicine and Science in Sports and Exercise, 47: 1896-1905.

Kolk, S., Klawer, E.M.E., Visser, E.P., Lobeek, D., Schepers, J., Verdonschot, N., Weerdesteyn, V. Symmetry and spatial distribution of muscle glucose uptake in the lower limbs during walking measured using FDG-PET, Submitted.

Carbone, V., **Kolk, S.**, van der Krogt, M.M., Schepers, J., Weerdesteyn, V., Koopman, H.F.J.M., Verdonschot, N. Quantitative validation of subject-specific musculoskeletal models of the lower extremity using FDG-PET, Submitted.

Carbone, V., van der Krogt, M.M., **Kolk, S.**, Schepers, J., Koopman, H.F.J.M., Verdonschot, N. Effect of image-based scaling of musculoskeletal geometry of the lower extremity on model predictions, Submitted.

Carbone, V., van der Krogt, M.M., **Kolk, S.**, Schepers, J., Koopman, H.F.J.M., Verdonschot, N. Effect of global optimization of muscle-tendon parameters of the lower extremity on model predictions, Submitted.

Dankwoord

Er hebben veel mensen geholpen bij de totstandkoming van dit proefschrift, die ik op deze plek wil bedanken. Ten eerste wil ik alle patiënten en gezonde proefpersonen danken voor hun bereidheid om mee te doen aan de verschillende studies. De data die ik daarbij verzameld heb is van grote waarde, getuige de niet één, maar drie proefschriften die mijn projectgenoten en ik erop hebben gebaseerd.

Dan wil ik graag mijn (co-)promotoren bedanken: Nico, Vivian en Sander. Wat waren jullie een sterk team, en wat was het een voorrecht om met jullie samen te werken! Nico, bedankt voor je frisse blik en waardevolle inzichten die mij vaak nog eens deden nadenken over de resultaten. Ondanks je overvolle agenda had je altijd tijd voor mij en dat waardeer ik zeer. Ik vind het erg leuk dat we nog altijd samenwerken en elkaar regelmatig tegenkomen op congressen. Vivian, ik zal nooit vergeten dat je me belde om me te vertellen dat ik was aangenomen. Dit is misschien wel het beste telefoontje dat ik ooit heb gehad! Onze samenwerking voelde meteen heel vertrouwd en we klikten erg goed met elkaar. Tijdens mijn promotie stond je deur als dagelijks begeleider altijd open en had je vaak goede ideeën om nuances aan te brengen, of om een studie net iets anders op te stellen en daardoor sterk te verbeteren, of zelfs hele studies te conceptualiseren. Ik heb ook veel geleerd van je inzichten over mijn conceptartikelen, bedankt daarvoor. Sander, hartelijk bedankt voor je waardevolle opmerkingen en feedback op mijn artikelen. Je wist altijd bruikbare aanwijzingen te geven, met niet alleen wát je zou veranderen, maar ook waarom. Vervolgens heb ik die kennis direct toegepast op alle volgende artikelen. Ik kan nog steeds niet geloven hoe zoveel talent voor wetenschap en klinisch werk in één persoon kan samenkomen.

Dear TLEMsafe partners, thank you for the privilege of working with you all. Starting from different perspectives, it was amazing to see the synergy between the partners develop over the years. We are still harvesting the fruits of this labor (e.g. TLEM 2.0 in AnyBody's model repository, and the Muscle Segmentation module in Materialise's Mimics Innovation Suite). Vincenzo and René, as fellow PhD students in the project we have been through thick and thin. Where it was up to me to collect all data in the project, it was up to you to extensively use that data to build and validate musculoskeletal models. I think that collaboration worked out very well, with three successful PhD theses as a result. Thank you for all the years of pleasant collaboration and that you are my paranimfs! I will also never forget our trips together with Pim, Hielke, and Steven to the various European consortium meetings, including stops in Hamburg (waking up like the movie 'The Hangover'), Kattegat (where penguins live), and Munich (Octoberfest exactly during our consortium meeting, what a coincidence!).

Graag wil ik ook alle stagiaires bedanken die hebben bijgedragen aan dit proefschrift. Olga, we hebben samen de gezonde proefpersonen gemeten met behulp van FDG-PET en jij hebt de eerste analyses uitgevoerd op de data. Dit heeft twee congrespresentaties opgeleverd, Bedankt! Michiel, bedankt voor je zoekwerk in de literatuur. Dit heeft de basis gelegd voor de studie over patiënten na een totale heupvervanging. Jim, dankzij jou verliep de studie met triple osteotomie patiënten heel vlot, bedankt! Kevin, je hebt grotendeels de vragenlijststudie uitgevoerd en de patiënten bevraagd naar hun functionele status. Bedankt hiervoor! Edzo, je

hebt bergen werk verzet om de FDG-PET data te koppelen aan de MRI beelden en dat heeft zich vertaald in meerdere fraaie artikelen. Bedankt voor al je inzet. Daphne, bedankt voor je inzichten bij het interpreteren van de FDG-PET data, en ook voor de gezelligheid en om af en toe te tennissen na werktijd.

Wim Schreurs, Wim Rijnen, Ingrid en Gerjon, bedankt voor jullie input vanuit Orthopedie en de prettige samenwerking. Petra, de samenwerking met jou en de Sint Maartenskliniek verliep erg goed, bedankt daarvoor. Eric en Martin, bedankt voor jullie adviezen over de PET studie. Bregina en Mark, met jullie was het altijd aangenaam om metingen te doen op de afdeling Anatomie en Fysiologie. Kristian, we hebben vele MRI scans gemaakt! Op een bepaald moment kwam ik meerdere keren per week langs met proefpersonen om scans te maken. Bedankt voor al jullie hulp!

Mijn dank gaat ook uit naar mijn collega onderzoekers van de afdeling: Digna, Jorik, Noortje, Mark, Roos, Lotte, Mariska, Arjen, Ellen, Merel, Joyce, Milou, Bas, Frank, Jolanda, Lotte, Mark, Hanneke, Anita, Chantal, Jos en Mariëlle. Roomies Noortje, Jorik en Digna, jullie in het bijzonder bedankt voor de gezelligheid en dat we altijd lief en leed konden delen. Jullie zorgden voor een goede sfeer, onder andere wanneer we vrijdagmiddag naar de Aesculaaf gingen om nog even een pintje te pakken, en natuurlijk bij de SYTYCC competities.

Roland, bedankt voor alle technische ondersteuning. Vaak gingen we op strooptocht door het hele Radboud, op zoek naar de juiste apparatuur bij verschillende afdelingen. Op een bepaald moment vonden we onder het stof een stoel uit begin jaren '90 om spierkrachten mee te meten. Die werkte nog op diskettes en stond al zeker tien jaar stil. Misschien hadden we het elektrisch circuit toch beter even na kunnen kijken vóórdat we hem op het stopcontact aansloten, want op een bepaald moment kwamen de vonken eruit en was er een kleine brand. Never a dull moment! Geert, jij ook enorm bedankt voor de ondersteuning in verschillende vormen in de loop der jaren. Naast technische ondersteuning heb je ook geholpen bij het doen van metingen en met het uitvoeren van de literatuur review.

Mede leden van de NCEBP PhD council, Tessel, Lotte, Nathalie, Jan, Jorik, Saskia en Sanaz, het was leuk en leerzaam om samen aan iets te werken naast onze promotietrajecten.

Jorik, Arjen, Geert en Roland, bedankt voor de gezellige klaverjasavonden. We hebben heel wat legendarische handjes gespeeld! Sommige daarvan zijn zelfs voor eeuwig op de gevoelige plaat vastgelegd en zullen we onze kleinkinderen nog over vertellen.

Gijs, Sander en Sten, bedankt voor de vele gezellige klaverjasavonden. We hadden onszelf als doel gesteld om elke keer in een andere kroeg af te spreken; ik denk dat dit goed is gelukt! Sten, onze Magic avonden waren ook altijd geslaagd en een mooie gelegenheid om nog eens lekker te nerden en onze studententijd in Sjeepee langzaam af te bouwen.

Pim, Lianne, Gijs, Sabine, Sten, Miriam, Hannes, Marjolein, Kitty, Arris, Gert-Jan, Alexandra, Karen, Emiel, Han, Ellen, Joost, ik geniet altijd van ons jaarlijkse kerstdinerweekend en hoop dat we dit nog vele jaren voortzetten! Maaike, bedankt voor je gezelschap, de stabiliteit tijdens vele jaren, en alle leuke dingen die we hebben meegemaakt.

Gert-Jan en Jurgen, we kennen elkaar al lang en maken vaak mooie trips. Van Terschelling to Transnistrië, het ene land nog exotischer dan het andere. Het wordt alweer hoog tijd om weer eens een mooie trip in te plannen.

Collega's en vrienden van Materialise, dankzij jullie voelde ik me direct thuis in België. Hartelijk bedankt om me steeds tijdens de lunchpauzes te vragen of ik al een datum voor de verdediging heb. Inmiddels ben ik fier dat ik het Vlaamse vocabulaire al aardig onder de knie heb, met woorden als kuisen (=schoonmaken), proper (=schoon), schoon (=mooi), lopen (=hardlopen) en natuurlijk de Bicky burger. Marnic, bedankt voor het samen bezoeken van vele festivals, game edities, fitness sessies, eten bij de frituur, en dat we een epic DJ-duo vormen bij de parties van Materialise. Onze doorbraak buiten het bedrijf zal vast niet lang meer op zich laten wachten!

Lieve pap en mam en zussie, bedankt voor jullie onvoorwaardelijke steun en liefde. Het is niet in woorden uit te drukken hoeveel ik om jullie geef en hoe dankbaar ik ben voor jullie. Ik lijk wel steeds verder van jullie weg te verhuizen (eerst Nijmegen, nu Leuven). Gelukkig spreken we elkaar vaak en komen jullie wel eens bij me langs in België.

Lieve Kati, bedankt voor je steun in de laatste fase van het afmaken van dit proefschrift. We hebben het erg fijn samen en ik denk dat we elkaar perfect aanvullen. Voor zover je het nog niet wist: ik hou van je en sa täidad mu südame rõõmuga!

Sjoerd Kolk, December 2017

Curriculum Vitae

Sjoerd Kolk was born in Enschede on October 23, 1985. From 1997 to 2003, he attended secondary school at the Bonhoeffer College in Enschede. In 2003, he began his studies in Biomedical Engineering at the University of Twente in Enschede. Sjoerd performed internships at the Hospital La Timone in Marseille, France in 2008, and at the Oregon Health and Sciences University in Portland, Oregon, United States of America in 2009. He obtained his Master of Science in Biomedical Engineering in 2010. After graduating, he began working on his PhD project, the results of which are described in this thesis. Sjoerd's PhD project was embedded in the European collaboration project TLEMsafe. The goal of this project was to improve the functional outcome of complex orthopedic surgery through personalized musculoskeletal modeling and surgical navigation. The consortium consisted of a number of companies and Universities: AnyBody Technology from Denmark, Brainlab from Germany, Materialise from Belgium, Radboud University Nijmegen and University of Twente from the Netherlands, and Warsaw University of Technology from Poland. During his PhD, Sjoerd presented his work at several international conferences, including the 2014 World Congress of Biomechanics (organized once every four years), where he won the second prize in the PhD student paper competition for his innovative work on muscle activity during walking, measured with FDG-PET. Sjoerd now lives in Leuven, Belgium, where he works at Materialise as a Business Developer for the Mimics Innovation Suite.